WAVE-PARTICLE DYNAMICS IN A HOT INHOMOGENEOUS FUSION PLASMA

Michael Anthony Taylor

A Thesis Submitted for the Degree of PhD
at the
University of St Andrews

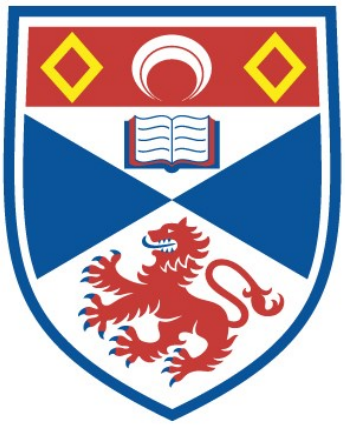

1996

WAVE-PARTICLE DYNAMICS IN A HOT INHOMOGENEOUS FUSION PLASMA

by

MICHAEL ANTHONY TAYLOR

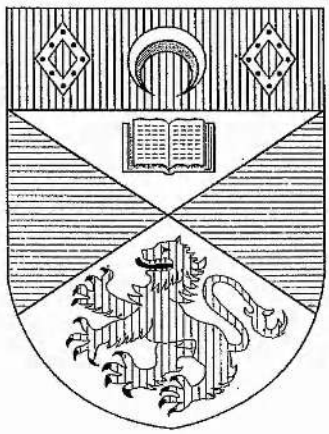

Thesis submitted for the degree of Doctor of Philosophy of the University of St. Andrews
March, 1996

Th C 24

ABSTRACT

An outstanding problem in the field of nuclear fusion research is the precise mechanism by which a hot, magnetically inhomogeneous plasma is heated when illuminated by a constant beam of small amplitude radio waves matched in frequency to harmonics of the ion Larmor frequency. An accurate model must include microscopic dynamics and inevitably a kinetic theory is required. Highly energetic ions($> 1MeV$) born from fusion reactions or powered by gyroresonance have large Larmor radii($> 10cm$) which are comparable in size to the wavelength of the incident radiation. In particular we will focus on fast magnetosonic waves.

Exact full wave equations describing a thermal plasma in a weakly inhomogeneous field are presently at least fourth order integro-differential equations(Sauter, 1992). These are computationally taxing. Recently a method was proposed to reduce the problem to a second order integro-differential equation at the expense of information related to the propagation of mode-converted waves(Holt, 1992). We present here a generalisation of the theory to allow for arbitrary velocity-dependent equilibria while at the same time retaining a general functional form for the field profile. We consider the specific case of a bi-Maxwellian plasma immmersed in a linearly inhomogenous magnetic field.

We find that thermal anisotropy produces resonance localisation when the perpendicular ion temperature is greater than that parallel to the ambient field. A study of the symmetry properties of the conductivity tensor reveals that the Onsager reciprocal relations are obeyed only for an isotropic plasma in an inhomogeneous field. This is a generalisation of the result obtained by Nambu(1995). We present a generalisation of the reduction method to include effects due to changes in wave amplitude. We find that we are able to include the odd-order field derivatives responsible for energy conservation.

Our numerical study of fundamental Helium-3 gyroresonance in a majority Deuterium plasma reveals that we have $> 99.9\%$ energy conservation in all cases. We show that locally-uniform theory can be very inaccurate($\simeq 70\%$ in one case presented in our recent paper, Cairns et al., 1995) particularly for higher energy ions whose non-locality is more extreme. We present a representative sample of results for minority heating and mode conversion heating schemes. We report the appearance of an unexpected cut-off on the low field side of the minority gyroresonance which may have important consequences for antennae presently placed on the outside of Tokamaks.

ACKNOWLEDGEMENTS

I began this work with a great love of physics which I owe to Tom Winderam(Chinese international school, Hong Kong), John Lowell and George Whiterod(both at UMIST), and to the great clarity of Richard Feynman. My study of Philosophy with Jo Marsh united my fragmented knowledge of science into a more cohesive whole.

My supervisor Alan Carins has shown me the beauty of theoretical analysis and his ingenuity and intuition are a source of continual inspiration. His kindness and understanding have smoothed my difficult road as did the companionship of my dear friends Nitisha, Mamun and Kurshida, Cesar and Beatriz Mendosa, Jair Mejia, Wang Lu, Lin Jun, Abil Aliev, Andy Lowe and Martin Thornton. I want to thank my workmates particularly Darren McDonald and Steven Decent for their patient and clear explanations of the complexities of applied maths.

The year I spent at Culham laboratory in Oxford was fruitful thanks to the patience and caring guidance of Chris Lashmore-Davies through whose eyes I saw the utility of applied physics. The kindness of Julie, Lisa, Terry and the other staff made my stay a happy and comfortable one. I want to thank especially Uma Bhattacharyya for being my mentor and close friend who, along with Martin Gregory, allowed me to see life through new windows.

As a child my parents taught me to question and I was fortunate to have lived in a vibrant family. They have given me unwaning support and have shown me the joy of life outside science. It is to them that I owe the greatest thanks of all.

DECLARATIONS

I, Michael Anthony Taylor, hereby certify that this thesis, which is approximately 25 000 words in length, has been written by me, that it is a record of work carried out by me and that it has not been submitted in any previous application for a higher degree.

Signature of Candidate Date 14/5/96

POSTGRADUATE CAREER

I was admitted to the Faculty of Science of the University of St. Andrews under Ordinance General No 12 in October 1992 and as a candidate for the degree of Doctor of Philosophy in the same year.

Signature of Candidate Date 14/5/96

COPYRIGHT

In submitting this thesis to the University of St. Andrews I understand that I am giving permission for it to be made available for use in accordance with the regulations of the University Library for the time being in force, subject to any copyright vested in the work not being affected thereby. I also understand that the title and abstract will be published and that a copy of the work may be made and supplied to any *bona fide* library or research worker.

Signature of Candidate Date 14/5/96

CERTIFICATE

I hereby certify that the candidate has fulfilled the conditions of the Resolution and Regulations appropriate for the degree of Doctor of Philosophy in the University of St. Andrews and that the candidate is qualified to submit this theis in application for that degree.

Signature of Supervisor Date 23/5/96.

Contents

Chapter 1

Introduction

1.1 The Energy Crisis

It was once said that, 'the sole motivation for scientific thought should be to ease the acquisition of our everyday needs through an understanding of nature through science'(Trotsky, 1925). However, the needs of our modern industrialised age have led to a rapid depletion of non-renewable natural resources, in particular the fossil fuels(coal, oil and gas), and although the theoretical achievements of nuclear physics in the first half of this century have helped to alleviate part of this problem by harnessing the power of the atom in the form of fission energy, we all live under the shadow of the catastrophic destruction of Nagasaki and Hiroshima by the atom bombs. In its more peaceful guise, the energy produced in controlled nuclear fission reactions accounts for a substantial proportion of the energy budgets of many European nations. The geological time scales associated with the isolation of the radioactive waste are of the order of 100 million years and, as such, are a major environmental threat. Widespread public concern(see for example Schumacher, 1973) has prompted a search for alternative, environmentally friendly renewable sources of energy and many nations presently ease their burdens by harnessing the natural power of the wind, water waves and the sun. Indeed Iceland receives 90% of its energy supply from the geothermal reservoir upon which it rests(Rusbridge, 1992). Despite this success, demographical studies have suggested that by the middle of the next century, population growth combined with economic development will at least double the global energy demand(see for example Eleizer, 1984) and furthermore, calculations of maximum energy flow by physicists(Jonas, 1991) have indicated that we will not be able to meet this demand from the renewable natural resources alone even if we could guarantee an energy conversion efficiency of 100%.

It has long been known that stars like our sun burn Hydrogen producing Helium generating the energy they need to sustain them against gravitational collapse. This process of fusing light nuclei to form heavier, more stable ones, is known as nuclear fusion. The most strongly bound nuclei are those in the middle of the Periodic Table such as Iron, accounting for its high occurrence in stable cosmic forms such as the planets of our solar

system. The complement process to fusion is fission whereby heavy nuclei are transformed(by spontaneous mutation) into lighter ones through the process of radioactive decay releasing their nuclear binding energy in the form of $1MeV$ neutrons and tending again towards their most stable existence in the form of Iron. Mankind has been able to recreate these processes which fuel the stars only in an uncontrollable fashion and sadly only for military uses. The inability to confine and control these processes is due to the intense temperatures of some 100 million degrees Centigrade required to overcome the electrostatic repulsion of the positively charged nuclei. The relaxation of conditions of secrecy in 1958 at the Geneva 2nd U.N. conference on the peaceful uses of atomic energy meant that various programmes were made public and a system known as a Tokamak(derived from the Russian, **tor**iodalnaya-**ka**mera- **mag**nitnaya, meaning toroidal-chamber-magnetic), was devised in the U.S.S.R.(the first device being built at the Kurchatov Institute in Moscow) to confine charged particles in closed magnetic fields. This triggered off an international programme of theoretical and experimental research into controlled nuclear fusion(see for example Berger, 1958, Bernstein, 1958 and Artsimovitch, 1972). This has had some recent success and it is envisaged that fusion power will be a significant contributor to the world's energy needs in the next century.

In addition to the adequacy of fusion to support our energy needs for the future, its greatest asset is its limited impact on the environment. Unlike the dwindling reserves of fossil fuels, its fuel comprises heavy isotopes of Hydrogen; Deuterium which is abundant and accessible through the electrolysis of sea water, and Tritium which may be produced *in situ* from a blanket of abundant Lithium in the reactor vessel. Fusion does not produce the large Carbon Dioxide and Sulphur Dioxide emissions created by burning fossil fuels and, although care must be taken with radioactive Tritium(due to its affinity to Oxygen producing radioactive water), its usage in minute quantities(miligrammes in comparison to kilogrammes of Uranium) and comparatively short half life of 12.3 years(Wesson, 1987), makes fusion energy a potentially effective and careful solution to the energy crisis which we may soon face if governments do not meet the long term needs of our planet. There are still a number of hurdles to be overcome before efficient fusion power stations can be built and it is the aim of this thesis to contribute in some small way to our understanding of the heating of the reactants to the high temperatures required for controlled nuclear fusion.

1.2 The Physics Of Controlled Nuclear Fusion

1.2.1 The Nature Of A Typical Fusion Plasma

The Hydrogen nuclei to be fused together are positively charged ions and are in an ionised state. An ionised gas consisting predominantly of ions and their constituent electrons, rather than neutral atoms or molecules, is a plasma and is affectionately known as the 4th state of matter(at the time of writing a 5th state has recently been discovered called the super-atom which is the Bose-Einstein condensate predicted theoretically over 70 years

ago). Although plasma is the prevalent form of matter in the universe($\simeq 99\%$), we live in a small corner where matter is mostly solid, liquid or a gas and our only contacts with plasma are when lightning strikes or when the Aurora Borealis(the northern lights) illuminates the sky. A typical fusion plasma consists of fully ionised Hydrogen(Deuterium and Tritium) and electrons.

The ionised nature of a plasma means that the inter-particle forces will be dominated by the weak, long range Coulomb force contrary to a neutral gas where strong, short range forces mean that the dynamics are dominated by collisions. Any individual charge(q) in the plasma will repel like charges away and attract opposite charges leading to an oppositely charged cloud forming around it. As a result, the electrostatic potential produced by the charge does not have the Coulomb $1/r$ dependence upon distance(r) but instead falls off faster as $e^{-\frac{r}{\lambda_D}}/r$ and the Debye length ($\lambda_D = \left(\frac{\epsilon_0 k_B T}{n_0 q^2}\right)^{1/2}$) is the distance over which the effect of the charge is screened off and is therefore the effective range of the inter-particle force(if we consider the JET parameters at the end of this chapter then for a Deuteron $\lambda_D \simeq 23.5\mu m$ and for an electron $\lambda_D \simeq 47.0\mu m$). Here T is the particle temperature, n_0 is the number density and ϵ_0 is the permittivity of free space.

A charged particle moving through a plasma interacts with all the charged particles surrounding it inside a sphere of radius equal to the Debye length(called the Debye sphere= $\frac{4}{3}\pi\lambda_D^3$). Any change in its velocity will then be due to a resultant force from the surrounding particles. If there are more particles in the Debye sphere then the surrounding particles will be more evenly distributed and the chance of a resultant force will be less. For a typical fusion plasma the number of charged particles in the Debye sphere($N = \frac{4}{3}\pi n_0 \lambda_D^3$) is large(the JET parameters predict that $N \simeq 2.7$ million for Deuterons!) and so the effects of collisions are very weak. Such conditions mean that particles are almost free-streaming through the plasma due to their long mean free paths.

An equilibrium charge in a lattice structure will undergo simple harmonic oscillations about its origin once displaced, due to the Coulomb attraction on one side and repulsion on the other. The characteristic frequency of oscillation will be proportional to the product of the charge of the displaced particle and the neighbouring charge(by the Coulomb force) and will be inversely proportional to mass(m) by inertia and is known as the plasma frequency ($\omega_p = \left(\frac{n_0 q^2}{\epsilon_0 m}\right)^{1/2}$). If we consider again the JET parameters, then typically $\frac{\omega_{pi}}{2\pi} \simeq 1GHz$ and $\frac{\omega_{pe}}{2\pi} \simeq 64GHz$.

A plasma may then be defined in terms of a typical length scale, the Debye length, and a typical time scale equal to the inverse of the plasma frequency. Their product provides yet another fundamental parameter of a plasma namely the equilibrium thermal velocity, $v_T = \left(\frac{2\kappa_B T}{m}\right)^{1/2}$(which for JET gives $v_{Ti} \simeq \frac{c}{10000}$(non-relativistic) and $v_{Te} \simeq \frac{c}{10}$(relativistic)). κ_B is Boltzmann's constant and c is the speed of light in a vacuum.

A further consideration is whether or not we need to use quantum mechanics rather than classical mechanics in our study of wave-particle dynamics. Quantum physics tells us(see for example Rae, 1988) that we may use a classical description whenever $\frac{n}{2}\kappa_B T \gg \hbar\omega$. Here, n is the number of degrees of freedom of a particle and $\hbar$ is Planck's constant. To check this we find that for JET, $\frac{3}{2}\kappa_B T_i \simeq 4.8 \times 10^{-16} J$. If we consider $\omega \simeq \omega_{pi}$ then we find $\hbar\omega \simeq 1.4 \times 10^{-24} J$ indicating that we are well within the classical world.

In terms of the Debye length, the plasma frequency and the thermal velocity we may classify a plasma as being collisional or collisionless, classical or quantum and even relativistic or non-relativistic. We have shown that the plasma in the core of a typical Tokamak is a classical, collisionless system containing relativistic electrons and non-relativistic ions.

1.2.2 Tokamak Physics

The existence of charged particles means that a plasma can carry electrical currents and the physics of Tokamak plasmas is therefore dominated by their interaction with electromagnetic(EM) fields. A charged particle in a magnetic field moves under the influence of the Lorentz force, travelling in a helical orbit centred along a line of constant magnetic induction(field line). A Tokamak is a device whereby external current carrying coils arranged around the circumference of a torus, produce a circular magnetic field(toroidal field) around which the charged particles of a plasma will orbit tied to the field lines. In practice this is not a perfect confinement system since the gradient of the toroidal field(which decreases radially from the centre) causes particles to drift in a direction perpendicular to the field gradient. The direction of the drift will be opposite for ions and electrons and so will result in the setting up of an electrical field between the displaced ions and electrons. It is the interaction of this electrical field with the toroidal field which causes the plasma to become unstable, expanding across the toroidal field along the direction of decreasing magnetic field gradient towards the walls of the Tokamak where the plasma will thermalize. The Tokamak overcomes this by inductively coupling a toroidal current to the plasma, generating a poloidal magnetic field. The resultant magnetic field structure is helical in nature being a hybrid of the toroidal and poloidal fields and has a cross-section which consists of nested flux surfaces. So the poloidal field compensates for the swelling of the plasma by limiting its radial motion.

The Tokamak concept consists then of a toroidal vessel surrounded by poloidal coils which generate toroidal magnetic fields, and toroidal coils for inducing the toroidal current in the plasma which generates the poloidal magnetic field as shown in figure 1.1.

Other confinement systems are being studied such as magnetic mirrors, theta pinches, Stellerators and inertial confinement devices and it is hoped that these will help unveil the physics needed for the most efficient scheme. Tokamaks have a simple field geometry making them the most favoured design at present. We will therefore tailor our theory of plasma heating to the toroidal geometry of a tokamak plasma, adopting the standard

coordinates: $\hat{\mathbf{x}}$ along the radial direction, $\hat{\mathbf{y}}$ along the poloidal direction and $\hat{\mathbf{z}}$ along the toroidal direction.

To achieve fusion we need to raise the bulk temperature of the plasma to temperatures of some 100 million degrees Centigrade(or about $10keV$) so that ions have velocities large enough to overcome their Coulomb repulsive forces, and in addition, we need to confine the plasma long enough(about 1s) for a significant amount of energy to be extracted from inside the vessel at a high enough density(about $2 \times 10^{20} m^{-3}$ so that the nuclei are sufficiently close together to have a reasonable probability of interaction(also known as the cross-section). The fusion reaction with the highest cross-section and therefore that which requires least heating is the D-T reaction,

$$D_1^2 + T_1^3 \rightarrow He_2^4 + n_0^1 + 17.56MeV. \tag{1.1}$$

This is illustrated in figure 1.2. Since Tritium is a radioisotope then D-D fusion,

$$D_1^2 + D_1^2 \rightarrow He_2^3 + n_0^1 + 3.3MeV, \tag{1.2}$$

which is the predominant reaction in the sun, is more desirable although its lower cross-section means that it requires a higher temperature to achieve fusion.

The product of the ion temperature(T_i), the ion density(n_{0i}) and the confinement time(τ_E) is known as the fusion product. The Lawson criterion says that it must be at least $3 \times 10^{21} m^{-3} keVs$ (Lawson, 1957). Under these extreme physical conditions we can recycle a sufficient fraction of the output power so as to maintain the temperature against radiation and diffusion losses. Heat generated in the surrounding Lithium blanket of the vessel is then used to drive generators in the usual fashion. At the present time, fusion experiments have succeeded in achieving these goals individually but no experiment has been able to reach the required temperature and density while maintaining a sufficiently long confinement time. Two notable experiments are the Tokamak Fusion Test Reactor(TFTR) and the Joint European Torus(JET) which have achieved about 20% of what is required for break-even in accordance with the Lawson criterion(for recent experimental progress see Phillips and the TFTR team, 1994 and Gormezano and the JET team, 1993).

The large number of experimental runs performed to date allow us to find correlations between experimental data and the physical parameters. From these we may deduce empirical scaling laws which offer predictions of the physical behaviour of future devices and allow us to determine, within certain error bounds, what physical parameters a fusion experiment must have for it to achieve the Lawson criterion and to be efficient enough to perform as a viable power station. For example, the confinement time has been found to scale according to the square of the minor radius of a Tokamak(Artsimovitch, 1972) and so the production of a break-even plasma should simply require the building of a large enough experiment. Such an experiment, the International Tokamak Experimental

Reactor(ITER), is currently being designed(see for example Post, 1991). We will be concerned here with the heating of the ions to the fusion temperature($T_i \simeq 10keV$).

1.3 Raising The Plasma Temperature

The inductively coupled toroidal current in the plasma, apart from creating the poloidal magnetic field needed to help confine the plasma, also results in Ohmic heating of the order of $2MW$ of power due to the resistance of the plasma to the current. It is well known that the collisional resistivity of a plasma varies as $T_e^{-3/2}$ (see for example Cairns, 1985) and ironically, such a heating scheme becomes less effective as the temperature rises. Temperatures of only around $T_i = 3keV$ can be achieved in this way and then we must seek to use some other auxiliary method of heating the plasma.

Neutral beam heating involves the bombarding of a plasma with a beam of high energy neutral atoms travelling across the toroidal field and which transfer their linear momentum predominantly into the perpendicular velocity of the ions through ionisation and then through subsequent binary Coulomb collisions. Present experiments like JET and TFTR couple about $10MW$ of power through this method to the plasma. Despite its apparent effectiveness, some highly energetic neutrals pass straight through the plasma and bombard the vessel wall recycling atomic fragments of the wall material back into the plasma. These higher atomic mass impurities have higher radiation losses(which scale with mass number) and degrade the energy confinement of the plasma. Hence there is an effective upper limit to the energy of the beams which are useful. Furthermore, the physical nature of the beams means that it is only possible to deposit energy locally in the plasma although the linear transfer of momentum may be used to provide toroidal current, also known as current drive. This may provide a valuable, steady state alternative to the inductively coupled toroidal current which relies on pulsed operation. The ability to actively and accurately deposit heat has a practical foundation since we first of all require maximal heating at the plasma core(where the density is highest and where the effect of recycled impurities from the wall is least), and also because systems of localised heating may provide a mechanism for stabilising the plasma.

Radio frequency heating involves the transfer of energy from an external source to the plasma by launching radio waves into the plasma from an antenna(for low frequencies) or from a waveguide(for high frequencies). These EM waves may then interact with the plasma through collisionless processes transferring energy to the charged particles. The power coupled to the plasma from radio waves is of the order of $15MW$ in current experiments. Typically, combinations of Ohmic heating, neutral beam heating and radio frequency heating schemes are used in present fusion experiments and it is predicted that ITER will operate using a combination of all three schemes.

Heating Schemes For JET	Power Coupled
Ohmic Heating	$\simeq 2MW$
Neutral Beam Injection	$\simeq 10MW$
Radio Frequency Heating	$\simeq 15MW$

1.3.1 Radio Frequency Heating

An extensive survey of this important topic has been done by Cairns(1991) and we present here a brief overview. The ability of a plasma to support a wide variety of waves(see for example Stix, 1992) means that we can selectively use different wave modes to heat the plasma through collisionless processes. As different wave modes have different frequencies(ω) and different wave-vectors(k), then, due to the existence of a number of resonant frequencies in the plasma, various heating schemes are available and, provided that these modes do not strongly couple(such as in mode conversion regions which we will discuss later), we can launch several waves into the plasma at any one time. The most successful of these are(Lashmore-Davies, 1995),

Radio Frequency Heating Schemes	Frequency Range
Ion Cyclotron Heating	$30 - 120MHz$
Lower Hybrid Heating	$1 - 8GHz$
Electron Cyclotron Heating	$100 - 200GHz$

Each scheme has the same general features: an efficient, high power generator remote from the plasma, a low loss transmission line and an efficient antenna (or waveguide) which couples EM energy to the plasma. Once coupled, the energy is required to propagate with negligible loss to a localised absorption zone whose spatial position is externally controllable.

In the next chapter we will obtain the resonances which are present in each of these frequency ranges and here we will simply state what these are for EM waves propagating radially towards the plasma core. The incident wave has a frequency(ω) which is fixed by the generator and a toroidal wavenumber spectrum($k_{||}$) which is determined by the antenna or waveguide. So we may tune these variables to match an internal natural resonant frequency. The lowest frequency scheme is ion cyclotron resonance heating(ICRH) for frequencies $\omega \simeq \Omega_i$(the cyclotron frequency is given by $\Omega_s = \frac{q_s B_0}{m_s}$ for a magnetic field strength(B_0) and for the JET parameters gives, $\frac{\Omega_D}{2\pi} \simeq 26MHz$ and $\frac{|\Omega_e|}{2\pi} \simeq 96GHz$). According to cold plasma theory, a resonant frequency occurs for radially propagating EM waves only when two or more ion species are present(Buchsbaum, 1960) at the 2-ion hybrid frequency(ω_{ii}),

$$\omega_{ii}^2 = \Omega_1 \Omega_2 \frac{X_1 \Omega_2 + X_2 \Omega_1}{X_1 \Omega_1 + X_2 \Omega_2}, \tag{1.3}$$

which lies between the cyclotron frequencies of either species. Here $X_i = n_{0i} m_i$ is the concentration of ion species i. The lower hybrid resonance frequency lies between Ω_i and

$|\Omega_e|$. For the high density regions of a Tokamak where $\omega_{pi}^2 \gg \Omega_i^2$ then neglecting terms of order $\simeq m_e/m_i$, the lower hybrid resonance frequency(ω_{LH}) is,

$$\omega_{LH}^2 \simeq \frac{\omega_{pi}^2 \Omega_e^2}{\omega_{pe}^2 + \Omega_e^2}. \tag{1.4}$$

Finally, the highest frequency scheme is electron cyclotron resonance heating for frequencies $\omega \simeq |\Omega_e|$. Again, cold plasma theory predicts a resonant frequency only for radially propagating EM waves at the upper hybrid frequency(ω_{UH}),

$$\omega_{UH}^2 \simeq \omega_{pe}^2 + \Omega_e^2. \tag{1.5}$$

Each of these is a linear wave-wave resonance whereby energy from an incident EM wave may be transferred reactively to the oscillatory EM fields associated with the collective, self-consistent plasma particle motions. Since all of the particles are involved in sustaining a natural wave in the plasma, these resonances are strong and any instabilities which may be present will also be strong. This is in contrast to wave-particle resonances where, typically, a much smaller number of particles (the resonant ones in the velocity distribution) contribute. Another important difference is that wave-particle interactions are dissipative in nature whereas wave-wave resonances by themselves are not. This will be shown to have an important bearing upon techniques for heating fusion plasmas by collisionless absorption.

Cold theory predicts wave-particle resonance interactions only at the fundamental of the ion or electron gyrofrequency as we shall show in chapter 2. We will show that wave-particle resonances at all harmonics of the gyrofrequency and for perpendicularly propagating EM waves are the province of kinetic theory.

1.3.2 Heating In The Ion Cyclotron Range Of Frequencies(ICRF)

We will focus most of our attention on ICRH in this thesis as it is in this range of frequencies that the interaction of EM waves with high energy ions(MeV) of large Larmor radius is least understood. The direct deposition of energy on the ions is crucial to raise the bulk temperature of the plasma to that required by the Lawson criterion. In essence the ions orbit the magnetic field lines with a natural angular frequency(the Larmor frequency or gyrofrequency $\Omega = qB_0/m$) determined by the strength of the magnetic field(B_0) on the field line at the guiding centre position of the ion, and also on the charge to mass ratio(q/m) of the ion. If a constant stream of circularly polarised EM waves propagate into the plasma matched to the ion gyrofrequency at some spatial value(say at the plasma core) with the electric field rotating in the same sense as the ions, then the ions at the resonance position in the core will see an effectively constant electric field in their frame of reference (their natural cyclotron frequency will be in phase with the driving frequency) and are accelerated, gaining energy in a direction tangential to their orbit. As mentioned

earlier in the context of neutral beam heating, this then leads to a distribution of ion velocities which is largely anisotropic due to a gain in perpendicular energy.

These high energy gyro-resonant ions then transfer energy through binary Coulomb collisions to other ions raising the energy of the ion population or equivalently the bulk ion temperature. Alternatively, we may think of ions as moving in to or out of resonance during their traversals of the torus, picking up energy each time they pass through the resonance layer. The ability to tune the EM wave frequency means that we can choose where we wish the resonance layer to be in the plasma due to the fact that the magnetic field is spatially non-uniform. This also means that the resonance will have a finite absorption width on the scale of a few times the ion Larmor radius(a few centimetres) and so we may selectively heat the plasma through localised power deposition allowing us to adjust the thermal profile of the plasma as previously mentioned. A review of the progress in ion cyclotron heating may be found in Swanson(1985). It is our ambition then to model the interaction of these high energy, large Larmor radius gyro-resonant ions with the incident EM waves. We will place particular emphasis on the effects of the thermal anisotropy of the ion velocity distribution and the spatial inhomogeneity of the toroidal magnetic field upon these processes.

Electron cyclotron resonance heating relies on much the same physics as ion cyclotron resonance heating but now the EM wave frequency(ω) is matched to the higher gyrofrequency of the electrons(now in the microwave range of frequencies) and rotating in the opposite sense to the ions. In addition we will need to take into account the effects of relativity as the velocity of gyro-resonant electrons is an appreciable fraction(0.1) of the speed of light. The smaller Larmor radius of the electrons(a few microns) means that power is deposited on a much shorter local length scale allowing for even more precise power deposition. For heating of the bulk ions the energy deposited must then be transferred to the ions through collisional processes. The high frequency EM waves can couple to the plasma(across the wall-plasma interface) without attenuation due to their ability to propagate in a vacuum. The recent development of gyrotrons has facilitated the delivery of larger power loads at these high frequencies, making electron cyclotron resonance heating a valuable accessory. An excellent review of this field has been compiled by Bornatici et al.(1983).

In addition to cyclotron resonance heating where energy is dissipated upon the resonant particles, there is another mechanism available for transferring energy from incident EM waves to the plasma. This involves the reactive loss of energy in an incident mode to a second wave mode in a region where the two waves are degenerate(having identical wave frequencies(ω) and wave-vectors($\mathbf{k}$)). This is known as linear mode conversion(see for example Cairns et al., 1982).

We have already remarked that a linear wave-wave resonance(the 2-ion hybrid resonance) exists for perpendicular propagation in the ICRF. The extensive work by Budden(1956)

on the propagation of EM waves in the ionosphere revealed that wave-resonances have associated with them cut-offs which are often in the same local neighbourhood(although isolated cut-offs can also occur). We will refer to the zones of the plasma where resonance and cut-offs occur(almost back to back) as interaction regions. In the next chapter we will show that a characteristic feature of resonance is that $\mathbf{k} \rightarrow \infty$(or equivalently that the phase velocity $\mathbf{v}_p = \frac{\omega}{\mathbf{k}} \rightarrow 0$). Conversely, the characteristic feature of a cut-off is that $\mathbf{k} \rightarrow 0$ (or equivalently $\mathbf{v}_p \rightarrow \infty$). Figure 1.3 illustrates these features for the propagation of the fast wave in the ICRF using a cold plasma theory.

A wave will only propagate when $\mathbf{k}^2 > 0$ and so the plasma conditions for which $\mathbf{k} \rightarrow \infty$ or $\mathbf{k} \rightarrow 0$ define absorption and cut-off surfaces respectively. We see that in the interaction regions of a hot, collisionless plasma the wave-vector can take on an infinite range of values. This means that an incident wave is likely to be mode converted to another mode which may be propagating in the interaction region.

In the next chapter we will describe how, within the framework of a kinetic theory, it is possible for the mode-converted waves to deliver energy through other dissipative processes such as Landau damping and magnetic pumping. Energy is mainly transferred to the electron population which then interacts with the ions through collisional processes. Heating in the ICRF relies then on both direct dissipation of energy on the ions through collisionless wave-particle interactions at gyro-resonances and also through dissipation of mode-converted waves. In chapter 2 we will go into more detail when describing these processes.

In regions where $\mathbf{k}^2 < 0$(called evanescent regions) then the plasma is unable to support the wave. We may classify the wave behaviour into four categories as follows,

Wave Propagation Characteristic	Wave-Number Behaviour
Resonance	$\mathbf{k} \rightarrow \infty$
Cut-off	$\mathbf{k} \rightarrow 0$
Propagation	$\mathbf{k}^2 > 0$
Evanescence	$\mathbf{k}^2 < 0$

However, if the region of evanescence is thin enough then there will be a finite probability that some of the wave can tunnel through to a region of propagation where $\mathbf{k}^2 > 0$ in a way analogous to quantum-mechanical scattering of wave-functions from potentials. If there is no dissipation in the evanescent region and if the wave energy is unable to be transferred to another mode, then there will be part of the wave energy reflected equal to the difference between the incident and transmitted energy. Constructive interference of these waves then gives a standing wave on the incident side of the cut-off as shown in figure 1.4 for an arbitrary potential.

For wide evanescent regions then the probability of transmission is slight and the reflected component will be greater. In the neighbourhood of a cut-off there will be a superposition

of incident and reflected waves meaning that we require a second order ODE to describe the underlying physics.

1.3.3 The Budden Model And Wave Interactions

The simplest ODE which is able to describe these processes is the Budden equation(Budden, 1956),

$$\frac{d^2\phi}{d\zeta^2} + k_0^2(\frac{\zeta - \zeta_c}{\zeta})\phi = 0, \tag{1.6}$$

which is a second order ODE of the Schrödinger type. ϕ is a normalised wave amplitude, ζ is a normalised spatial coordinate and k_0 is the asymptotic wave number when $|\zeta| \gg \zeta_c$. There is a resonance at $\zeta = 0$ and a cut-off at $\zeta = \zeta_c$. Budden showed how, by calculating the ratio of intensities($|\phi^2|$) of the transmitted and incident waves, the fractional power transmitted across an interaction region per unit incident power is given by the transmission coefficient,

$$T = e^{-\pi k_0 \zeta_c},$$

and depends only on the separation of the cut-off and the resonance(ζ_c). The transmission is independent of whether or not the wave encounters the cut-off or the resonance first and has a robust nature(since calculations performed by a WKB theory give similar results to the ODE as we will show in chapter 8). The symmetry in the transmission of energy is contrasted by an asymmetry regarding the reflection of energy.

If the wave is incident on the cut-off first, then the reflection coefficient (R) is related to the transmission coefficient(T) by, $R = (1 - T)^2$. If, however, the wave is incident on the resonance first then $R = 0$(Budden, 1956). Budden found that $R+T < 1$ indicating a lack of energy conservation. The missing energy can only be identified using a higher order ODE to model the physics because of mode conversion to a new wave mode(a hot plasma mode) The inclusion of the extra mode- converted wave means that the physics must be modelled by a fourth order ODE so that the propagation of energy in the new mode is included. In a hot plasma, kinetic theory gives additional dissipation due to wave-particle phenomena.

Let us consider the propagation of the fast magneto-sonic wave(compressional Alfvèn wave) or fast wave(FW) propagating perpendicularly through a 2-ion species plasma in the ICRF. In the next chapter we will show how, in this frequency range, there will be gyro-resonances at each harmonic of the gyrofrequency. There will also be the cold plasma 2- ion hybrid resonance and its associated cut-off, located spatially between the two gyro-resonances. Although there will be dissipation of the fast wave energy by wave-particle interactions at the gyro-resonances (chapter 2), we will concern ourselves here with the

transfer of energy due to a cold, 2-ion hybrid resonance(undamped) and cut-off so as to compare with the analysis of the Budden model described above.

In the neighbourhood of the 2-ion hybrid resonance, the incident fast wave bifurcates and couples to a hot plasma mode called the ion-hybrid wave(IHW) which is a predominantly electromagnetic wave propagating perpendicularly to the ambient, toroidal magnetic field. An incident fast wave can convert to two different branches of the ion-hybrid wave: one propagating to shorter perpendicular wavelengths($k_\perp \to \infty$) and the other propagating to longer perpendicular wavelengths($k_\perp \to 0$). The asymmetry of the reflection is due to the difference in physical behaviour of these two branches. The branch going to resonance does not meet a cut-off and represents a fast wave incident from the high magnetic field side as shown in figure 1.5.

The incident fast wave of unit amplitude has a fraction, T, transmitted and the remainder, $1-T$, is mode-converted at the 2-ion hybrid resonance to the ion-hybrid wave propagating to short wavelengths. The story is very different for a fast wave incident from the low magnetic field side as depicted in figure 1.6.

In the region of the 2-ion hybrid resonance, the incident fast wave of unit amplitude is partially transmitted, T, and partially mode-converted to the ion-hybrid wave, $1-T$. The ion-hybrid wave then propagates to its cut-off where a fraction, T, of the incident energy, $1-T$, is transmitted, $T(1-T)$, and the remainder, $(1-T)-T(1-T) \equiv (1-T)^2$, is mode-converted to the reflected fast wave.

For low field incidence, the net result is that a fraction, T, of the incident fast wave energy is transmitted, a fraction, $(1-T)^2$, is reflected and a fraction, $T(1-T)$, is mode-converted to the ion-hybrid wave. Since the ion-hybrid wave remains in the plasma, this accounts for the missing energy absorbed in the Budden model. Furthermore, standing waves, set up by the interference of incident and reflected waves on the low field side of a cut-off, are a common feature of wave phenomena in interaction regions as we shall show in chapter 8. The salient behaviour of a wave incident on a cut-off echoes the Airy function(Ai) and may be described simply by multiples of,

$$Ai(x) = \frac{1}{\pi}\int_0^\infty dt \cos(xt + \frac{1}{3}t^3).$$

In the region of positive x where the wave propagates, the asymptotic behaviour for large x is(Cairns, 1995),

$$Ai(x) \sim \frac{1}{\sqrt{\pi}}x^{-1/4}\sin(\frac{3}{2}x^{3/2} + \frac{\pi}{4}),$$

which, when expressed in terms of complex exponentials, gives a superposition of waves of equal amplitude propagating in opposite directions. The standing wave set up on the

incident side of the cut-off in figure 1.4 has this functional form.

For high field incidence, the net result is that a fraction, T, of the incident fast wave energy is transmitted, a fraction, $1-T$, is mode-converted to the ion-hybrid wave while none is reflected.

Most energy is transferred to the plasma for high field incidence but this scheme has the misfortune that an antenna is less easily placed on this side of the Tokamak due to space restrictions(the transformer yoke has to pass through the torus centre). This means that large Tokamaks such as JET or TFTR have low field antennae. All is not lost though as we shall see in chapter 2 since there is also dissipation at the gyro-resonances.

In addition to the ion-hybrid wave, which is present around the localised region of the 2-ion hybrid resonance, there are also ion Bernstein waves(IBW) which propagate between harmonics of the gyrofrequency as shown in dispersion diagram in figure 1.7.

There is also the possibility of mode-conversion of the fast wave to these waves but their coupling is much weaker due to the involvement of only a few particles in the velocity distribution in the wave-particle interactions at the gyro-resonances. At the 2-ion hybrid resonance the ion-hybrid wave is supported by the whole plasma and so coupling to the fast wave is strong.

In an early paper, Cairns et al.(1982) showed how, due to the degeneracy of two waves in a mode-conversion region, the local dispersion relation associated with the Budden equation,

$$k^2 = k_0^2(\frac{\zeta - \zeta_c}{\zeta}),$$

can be cast in the form,

$$(k-k_1)(k-k_2) = \mu.$$

Here k_1 and k_2 are the wave-numbers of the undamped modes and μ is a measure of the closest distance between the modes. This physical behaviour is portrayed in figure 1.8. Cairns et al.(1982) went on to show how such an approach is able to provide the same energy transmission and reflection as the Budden model while at the same time quantifying mode conversion. Furthermore, since they found that,

$$T \propto e^{-\mu},$$

there is a simple geometric relation between the closest approach of two waves and their coupling. The transmission is inversely proportional to the closest approach and so mode conversion is stronger for larger μ.

We are now able to provide an explanation of the behaviour of the fast wave near to the gyro-resonances and in the vicinity of the 2-ion hybrid resonance. Close to the gyro-resonances, μ is small and so the coupling is weak and mode conversion to ion cyclotron waves is negligible but at the 2-ion hybrid resonance, μ is much larger and the coupling and mode-conversion to ion-hybrid waves is much more significant. In figure 1.9 we present the dispersion diagram for these wave interactions.

In general, interaction regions of a Tokamak contain gyro-resonance layers(in addition to linear wave-wave resonances and their associated cut-offs) and so EM energy incident on an interaction region with unit amplitude will have fractions of energy partly transmitted (T), partly reflected(R), partly dissipated(D) upon resonant particles and partly mode-converted(C) to another wave mode which can carry energy away from the interaction region as portrayed in figure 1.10.

In the next chapter we will see how there is an intimate relationship between the amount of energy dissipated by the resonant particles and the occurrence of mode conversion regions. We will explain this effect by appealing to the polarisation of the EM waves. In a single ion species plasma the damping of the fast wave by gyro-resonant absorption is found to be weak at the fundamental of the gyrofrequency($\omega = \Omega_i$) but stronger at the first harmonic of the gyrofrequency($\omega = 2\Omega_i$). In a 2-ion species plasma, produced deliberately by injecting protons into the plasma or by the recycling of ions from the radio frequency antenna or the vessel Beryllium wall, then there can be strong damping of the fast wave at the fundamental of the minority gyrofrequency. This occurs because the majority ion species dictates the wave polarisation which is found to be favourable for gyro-resonance of the minority ions at the fundamental of the minority gyrofrequency. The strength of the damping increases proportionally with the concentration of the minority ions until the 2-ion hybrid resonance occurs at a critical minority ion density. The appearance of this linear wave-wave resonance affects the wave polarisation profoundly, making it less favourable for minority gyro-resonance, and setting an upper limit to the amount of energy which can be dissipated on the minority ions. Since energy will be deposited in a small fraction of the ion population, a tail will be produced on the ion velocity distribution which will remain if there are not enough Coulomb collisions to thermalize the distribution(to make it Maxwellian or isotropic). Since the Coulomb cross-section decreases with particle velocity, these high energy ions have a higher probability of losing energy to electrons than to other ions and can therefore lead to bulk electron heating. Further transfer of energy from the fast wave to the plasma may occur only as a result of mode conversion to a hot plasma mode which itself may be dissipated on the electrons. We will discuss this further in chapter 2.

Let us simply state here that there will be two regimes of heating in a two ion species plasma which are differentiated by the ratio of the densities of the ion species(η). In the first regime, known as minority heating, η is less than a critical value(η_C) and the 2-ion hybrid resonance is absent and fast wave energy is dissipated on the minority ions through

gyro-resonant absorption. In the second regime, known as the mode conversion regime, the 2-ion hybrid resonance is present when $\eta > \eta_C$ and fast wave energy is transferred to the ion-hybrid wave which damps on the electrons. Another complex scenario which will not be relevant to this thesis involves minority heating of pure Hydrogen in a Deuterium plasma since the fundamental gyro-resonance of Hydrogen coincides precisely with the first harmonic gyro-resonance of Deuterium allowing gyro-resonant absorption by *both* species. In chapter 8 we will apply our theory of non-local, large Larmor radius wave-ion interactions to the first two heating scenarios.

We will find that we would like to apply our theoretical investigations to a relevant fusion experiment. The JET experiment is currently the largest experiment capable of investigating the regime of high energy fusion products and we take our physical parameters as those of JET(Lashmore-Davies),

Physical Parameters Of JET	Range	Case Study
Major Radius(L)	$3.1m$	$3.1m$
Minor Radius	$1.25m$	
Toroidal Magnetic Field(B_0)	$1-4T$	$3.4T$
Poloidal Magnetic Field	$0.5-1T$	
Toroidal Plasma Current	$0.1-5MA$	
Plasma Mass	$0.1-1mg$	
Plasma Volume	$1-100m^3$	
Plasma Pressure	$0.1-1Atm$	
Central Ion Density(n_{0i})	$10^{19}-10^{20}m^{-3}$	$5\times10^{19}m^{-3}$
Central Ion Temperature(T_i)	$1-10keV$	$2keV$
Central Electron Density(n_{0e})	$10^{19}-10^{20}m^{-3}$	$5\times10^{19}m^{-3}$
Central Electron Temperature(T_e)	$1-10keV$	$2keV$
Ion Confinement Time	$0.1-1s$	
Parallel Wavenumber spectrum($k_{\|\|}$)	$2-7m^{-1}$	$2-7m^{-1}$

1.4 Overview Of The Thesis

The cornerstone of this work is the derivation of the non-local wave equations which will describe the propagation of EM waves through ion gyro-resonances in the presence of high energy, large Larmor radius ions and fusion products in a weakly inhomogeneous fusion plasma for a general equilibrium distribution function.

In chapter 2 we will discuss the merits of existing theories while at the same time arguing for an extension of locally non-uniform, guiding centre theory so as to include the effects of thermal anisotropy(which is a congenital feature of plasmas heated by auxiliary methods). In addition, we will introduce the tools of the trade which we will use in our study of wave-particle interactions such as ordering, analytic continuation and causality, and wave polarisation. On a more practical note we will discuss the conservation of energy

and the problem of accessibility of the resonances.

In chapter 3 we will present a generalisation of the guiding centre theory of Cairns et al.(1995) so as to cover a range of plasma equilibria in weakly inhomogeneous plasmas. We will follow the path integral method of Shafranov(1962) to derive the conductivity tensor of a hot, thermally anisotropic plasma immersed in an inhomogeneous magnetic field.

We then present in chapter 4 an application of the results of chapter 3 to the analytically tractable Tokamak scenario of a bi-Maxwellian plasma immersed in a linear magnetic field gradient. As a verification of our equations we show how we may reproduce the results obtained by other authors in certain limits of our equations. We then form the 2D non-local, integro-differential wave equation(IDE) describing the propagation of EM waves into a weakly inhomogeneous magnetic field gradient, which will be the pivot about which the remainder of the thesis will revolve.

In chapter 5 we review resonance broadening from the standpoint of statistics and covariance theory allowing us to determine a criterion for the absorption width of the ion gyro-resonances which we will show to be of the order of a few Larmor radii. We will also derive a criterion for their resolution. Covariance theory shows how resonance broadening effects simply sum as errors when they are uncorrelated. We will use the results born out from our statistical analysis to explain some of the qualitative features of the theoretical results of chapter 4. We present a new physical effect due to thermal anisotropy; namely a reduction in resonance broadening when the ion temperature parallel to the field is less than the perpendicular temperature(which is typically the case in auxiliarly heated plasmas). As a useful aside, we shall perform a short calculation which estimates the broadening of a cold plasma, linear wave-wave resonance due to thermal effects in a hot plasma.

In chapter 6 we discuss the relevance of the Onsager reciprocal relations to the microscopic time reversible dynamics of our theory, generalising the work of Nambu(1994) so as to include the effects of magnetic field inhomogeneity. We are able to reiterate Nambu's claims that Onsager symmetry is evident for an isotropic plasma but not for an anisotropic plasma. We also show that the Onsager relations are independent of their mathematical formulation revealing the covariant nature of the underlying physics.

Chapter 7 is devoted to a study of the IDE derived in chapter 4. We present a new approximation which formalises and extends the fast wave approximation(Kay et al., 1988 and Lashmore-Davies et al., 1988) so as to retain effects due to odd-order derivatives of the electric field which have been shown to be necessary for energy conservation(Swanson, 1985). This will be shown to be an extension of the work of Cairns et al.(1991) into the large Larmor radius regime. Indeed, we are able to recover their energy conserving O-mode equation from our general summation form for the plasma response by taking the

limit of small Larmor radius ions. We will then use our theory to deduce a second order, energy conserving ODE for the spatial variation of the fast wave electric field along with its conservation law. This is then extended to allow for a symmetrisation of the response function with respect to the incident wave-modes allowing odd-order derivatives of the field to enter the ODE in a simple way. In addition we offer a solution to the controversy surrounding the effective dielectric tensor of Beskin et al.(1987), clarifying some conflicting reports in the literature about the applicability of their theory to the study of inhomogeneous plasmas.

In chapter 8 we investigate numerically the behaviour of the fast wave for various heating scenarios in the ICRF. We will place particular emphasis upon the role of the magnetic field inhomogeneity in affecting the energy transport through a ion gyro-resonance region in the company of large Larmor radius ions or fusion products. We present a representative sample of results calculated from non-uniform and locally-uniform theories. We will show that the locally-uniform models of large Larmor radius ions can be very inaccurate(especially for high energy ions) suggesting that our theory may present a more efficient and energy conserving alternative. We report the appearance of a novel physical effect at high energies and high minority ion densities, namely a cut-off on the low magnetic field side of the minority gyroresonance. This may have important implications for ICRH in future experiments.

Finally we draw to a close in chapter 9 by bringing together the results of the first 8 chapters in the light of recent theoretical and experimental developments.

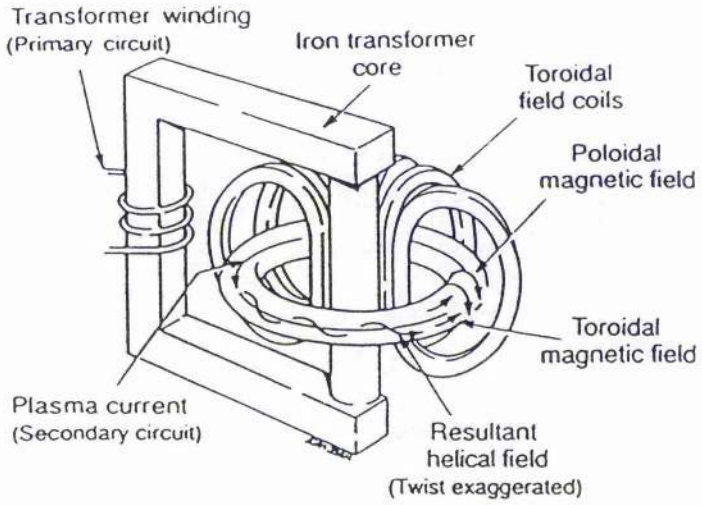

(Diagram courtesy of UKAEA Culham Laboratory)

Figure 1.1: Schematic representation of the magnetic field coils used to confine the plasma in a Tokamak.

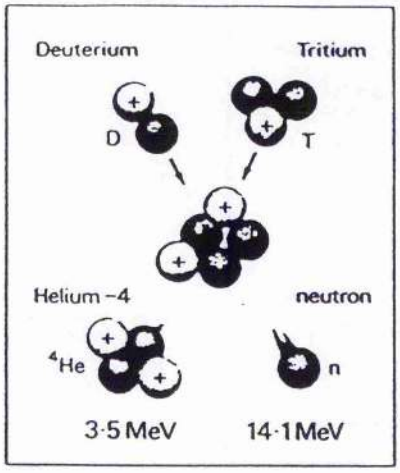

(Diagram courtesy of UKAEA – Culham Laboratory)

Figure 1.2: The Deuterium-Tritium fusion reaction.

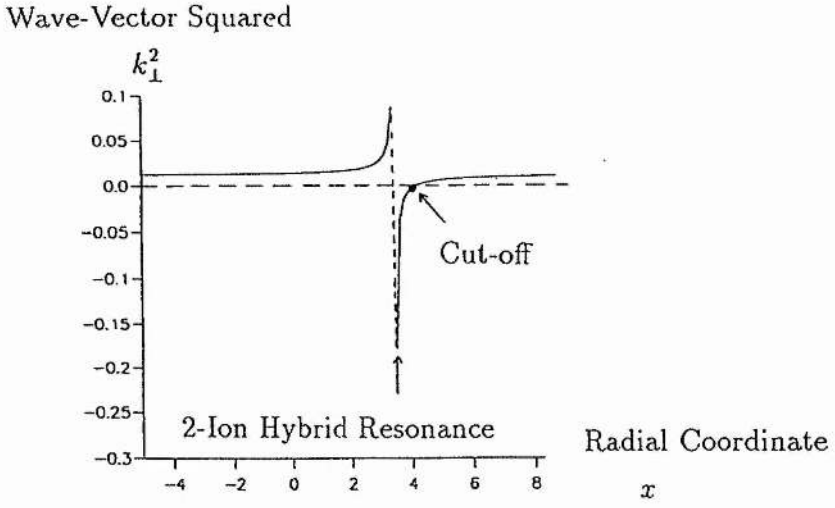

Figure 1.3: Fast wave radial propagation in the ICRF illustrating the 2-ion hybrid resonance and cut-off.

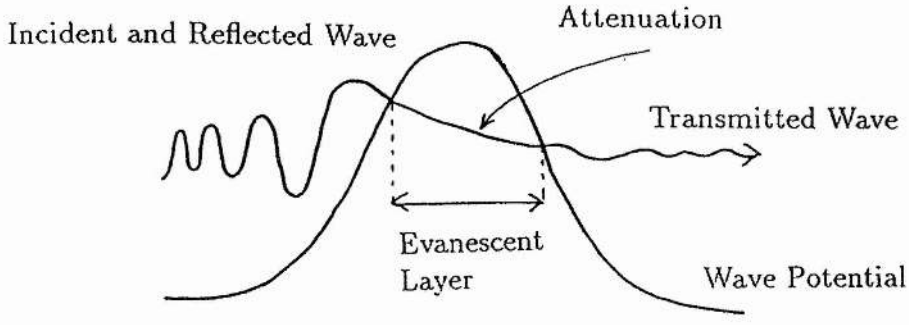

Figure 1.4: Wave tunneling through an evanescent layer illustrating transmission at the output and interference at the input (after Fröman, 1965).

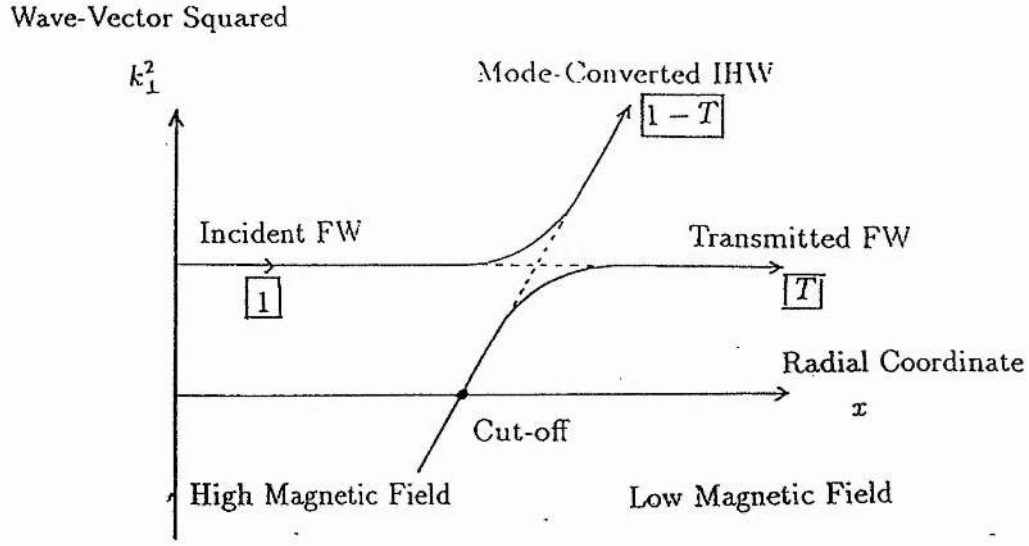

Figure 1.5: Mode conversion of the fast wave for high magnetic field incidence.

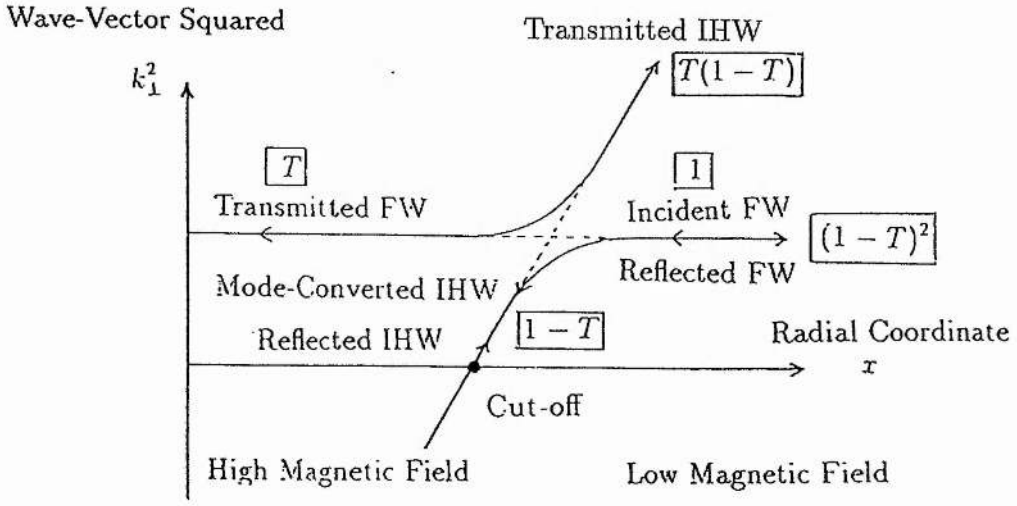

Figure 1.6: Mode conversion of the fast wave for low magnetic field incidence.

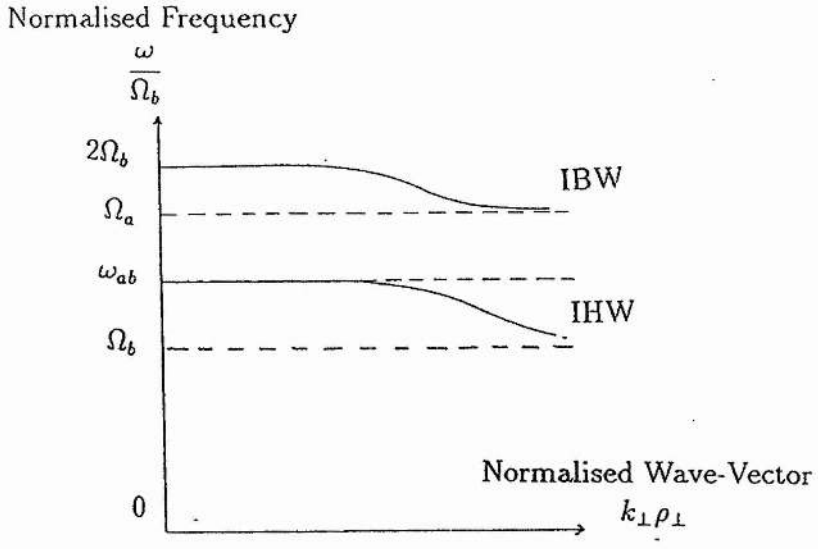

Figure 1.7: Electrostatic dispersion relation for the ion-Bernstein wave(IBW) and the ion-hybrid wave(IHW) in the ICRF(after Lashmore-Davies, 1995).

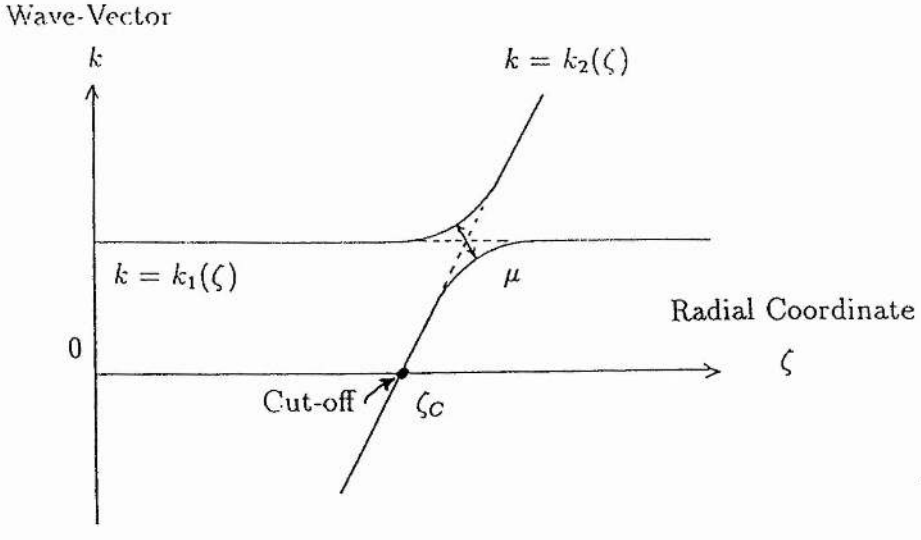

Figure 1.8: Schematic representation of a typical mode conversion event illustrating the coupling constant μ(after Cairns, 1982).

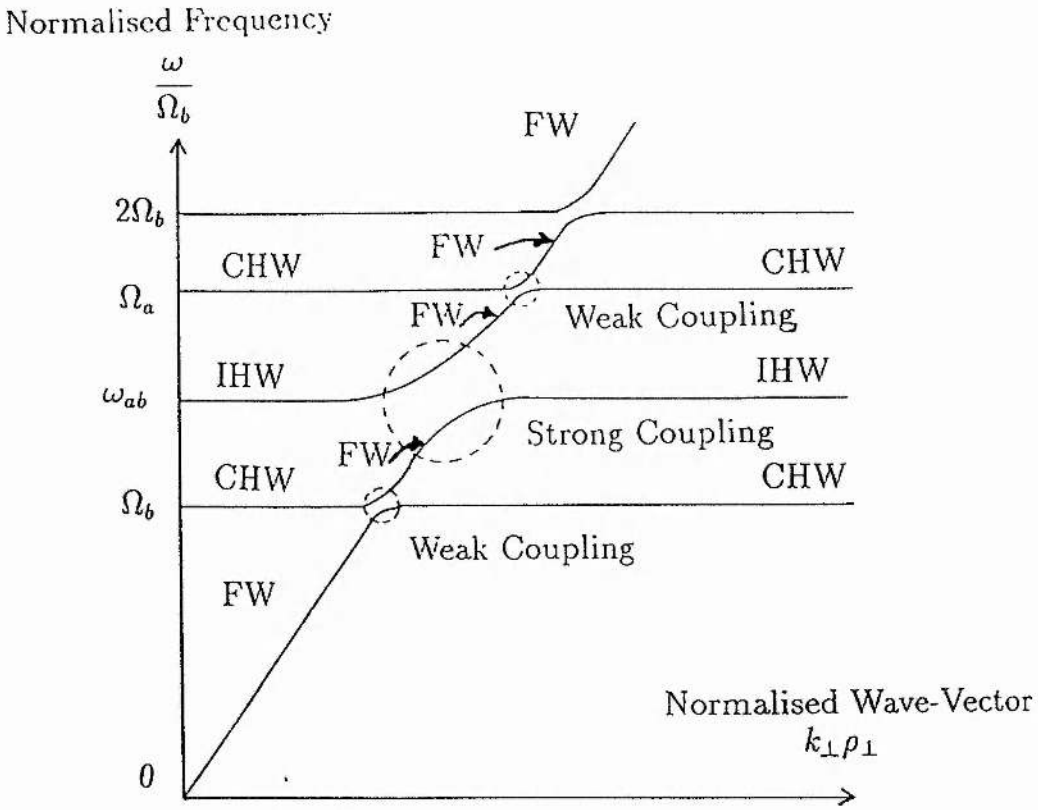

Figure 1.9: Electromagnetic dispersion relation illustrating the coupling of the fast wave(FW) to the ion-hybrid wave(IHW) and to the cyclotron harmonic waves(CHW) in the ICRF(after Lashmore-Davies, 1995).

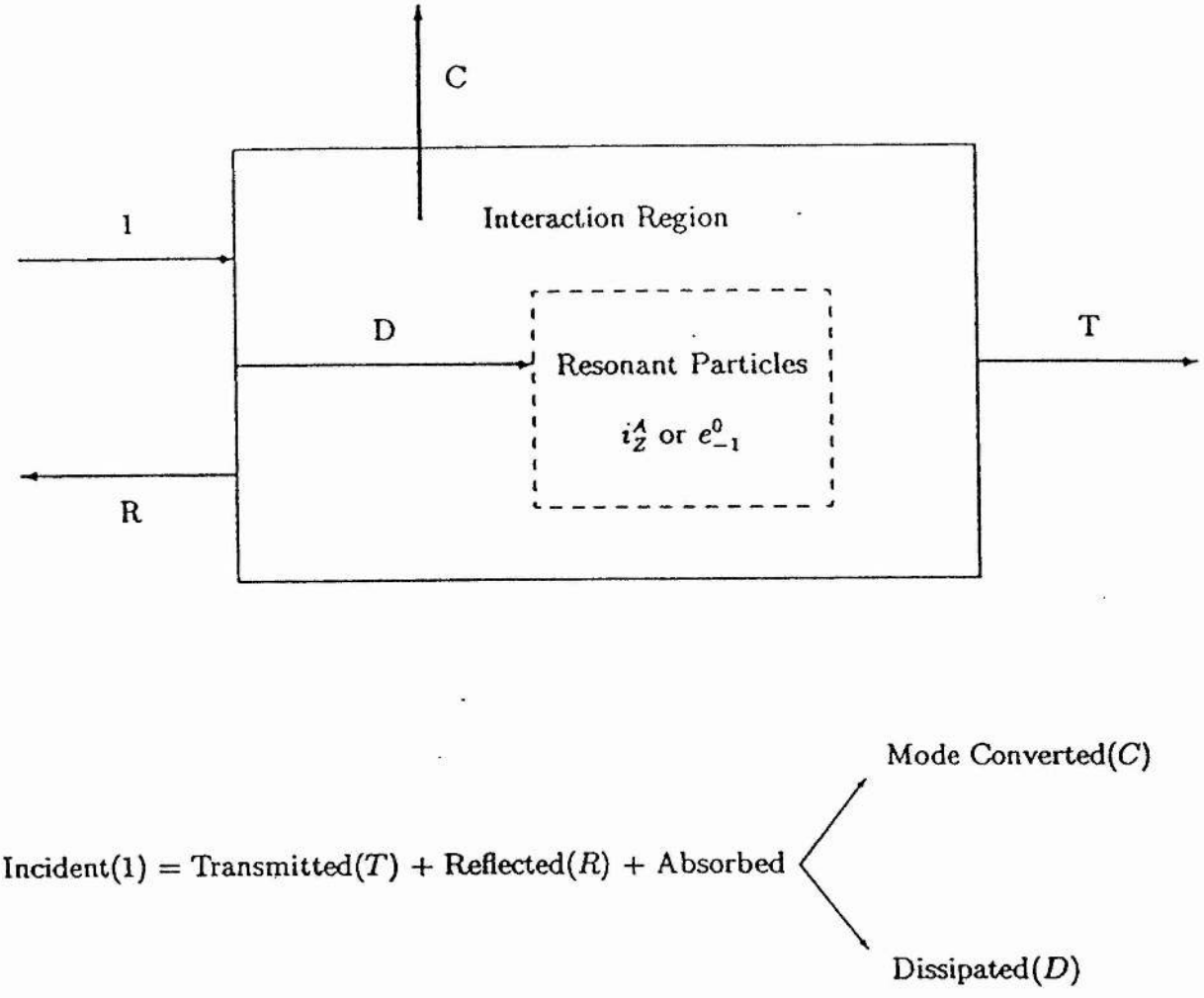

Figure 1.10: Schematic representation of the distribution of incident energy through an interaction region.

Chapter 2

Related Elements Of Plasma Wave Theory

Following the discovery by Appleton in 1925 of electrically conducting layers in what became known as the ionosphere, much of the theory of waves in a cold plasma was developed to help explain the propagation of radio waves. Astrophysicists such as Alfvèn then developed the theory of magnetohydrodynamics(MHD) in the early 1940's to study low frequency phenomena and, shortly after, a more thorough kinetic theory was devised to extrapolate to high temperature, high frequency phenomena culminating in the famous work of Landau in 1946 with a description of the collisionless damping of electrostatic waves. The onset of research into fusion in the early 1950's then further developed the zoo of plasma waves. As a result of this effort, there are now numerous works on this subject notable examples of which include Allis, Buchsbaum and Bers(1963), Chen(1987), Swanson(1989) and Stix(1992).

Although cold plasma theory is capable of describing some of the properties of plasma waves in homogeneous and weakly inhomogeneous magnetic fields, we will show that it does not predict the existence of gyroresonance at all harmonics of the gyrofrequency in the plasma and can not therefore describe EM wave propagation through them. For this we must use a kinetic theory. Furthermore, although the theory of Wentzl, Kramers and Brillouin (WKB) is able to describe the local EM wave amplitude changes(and hence can estimate absorption) due to wave-particle interactions, its single mode character means that it is incapable of describing linear wave-wave phenomena such as resonant reflection and linear mode-conversion. We will use the limitations of these various methods to argue for a simpler full wave kinetic theory which can describe multi-mode processes in addition to the microscopic dynamics of individual particles. Let us first of all set the scene by starting with a brief discussion of EM wave propagation in a homogeneous plasma.

2.1 Waves In A Homogeneous Plasma

By homogeneous we mean that the plasma is immersed in a uniform magnetic field which has no gradient in field strength. This may seem a rather crude model of a Tokamak plasma in a toroidal field but it does lead to an analytically tractable description housing some of the effects present in inhomogeneous fields, namely gyroresonance phenomena due to charged particle orbits in a magnetised plasma.

The basic analysis proceeds as follows. We take the equilibrium plasma state with zero order quantities such as the ambient magnetic field($\mathbf{B_0}$) and the ion density(n_0) static in time and uniform in space. Next, we perturb the plasma with a small amplitude EM wave which is harmonic in time and space so that all first order(perturbed) quantities vary as $e^{i\mathbf{k}\bullet\mathbf{r}-i\omega t}$. Fourier analysis then reveals that $\nabla \equiv i\mathbf{k}$ and $\partial/\partial t \equiv -i\omega$ so that Maxwell's equations for the EM field yield the following wave equation in momentum(Fourier) space,

$$\frac{c^2}{\omega^2}\mathbf{k}\times(\mathbf{k}\times\mathbf{E}(\omega,\mathbf{k}))+\mathbf{E}(\omega,\mathbf{k})+\frac{i}{\epsilon_0\omega}\mathbf{J}(\omega,\mathbf{k})=0. \tag{2.1}$$

We then solve the linearised equation of motion for the plasma(which is dependent upon the model being used) to write the perturbed current density($\mathbf{J}$) in terms of the perturbed wave electric field ($\mathbf{E}$). Substitution into (2.1) then yields a dispersion equation for $\mathbf{E}$ of the general form,

$$\mathcal{D}_{ij}(\omega,\mathbf{k})\bullet\mathbf{E}(\omega,\mathbf{k})=0. \tag{2.2}$$

The condition for non-trivial solutions of this equation is that the determinant of the dispersion tensor($\mathcal{D}$) be zero. This condition gives the dispersion relation $\omega=\omega(\mathbf{k})$. In general, for a given wave-vector($\mathbf{k}$), the dispersion relation can contain a multiple(and sometimes infinite) number of ω roots so that, $\omega=\omega_j(\mathbf{k})$ for $j=1,2,..n$. The roots of the dispersion relation then describe the natural(often named normal) modes of oscillation of the plasma and provide details of the group velocity(ω/k) and phase velocity($\partial\omega/\partial\mathbf{k}$) of each mode. Substitution of ω into (2.2) then enables us to determine the eigenvector($\mathbf{E}_j$) corresponding to each eigenvalue(ω_j). From $\mathbf{E}_j$, the polarisation of the perturbed electric(or magnetic) field for the j^{th} branch(normal mode) with respect to the direction of propagation along $\mathbf{k}$ or to the ambient magnetic field($\mathbf{B_0}$) is known. This provides the essential information required for phase synchronisation in resonance phenomena as we will describe in more detail later in this chapter. Let us begin by deducing the dispersion tensor for waves in a cold plasma and also for waves in a hot plasma.

2.1.1 Cold Plasma Waves

In the cold plasma model we treat each particle species(s) as a zero temperature, frictionless fluid having fluid velocity $\mathbf{u_s}(\mathbf{r},t)$. The motion of each plasma species is then determined by the momentum equation,

$$\frac{\partial \mathbf{u}_s}{\partial t} + (\mathbf{u}_s \bullet \nabla)\,\mathbf{u}_s = \frac{q_s}{m_s}\left(\mathbf{E} + \mathrm{u}_s \times \mathbf{B}\right), \tag{2.3}$$

which we linearise. The wave fields($\mathbf{E}$ and $\mathbf{B}$) are the same in each set of fluid equations and, being dependent upon the combined motion of all particles, provide the link between the separate equations for each species. Since $\mathbf{u}_s$ is a first order quantity representing the perturbed fluid velocity then, in a linear analysis, only the unperturbed ambient part of the magnetic field($\mathbf{B}_0$) will give any physical effect. Fourier-transforming over space and time and taking the vector and scalar products with $\mathbf{B}_0$, we obtain the solution of (2.3) for the fluid velocity. The perturbed current density is a function of this velocity,

$$\mathbf{J} = \sum_s n_{0s} q_s \mathbf{u}_s. \tag{2.4}$$

The dispersion tensor is found by inserting this expression for the current into the wave equation (2.1). Without loss of generality, we consider the ambient magnetic field($\mathbf{B}_0$) to be along the $\hat{\mathbf{z}}$ direction making an angle(θ) with the wave-vector ($\mathbf{k}$). For EM waves propagating in the $\hat{\mathbf{x}} - \hat{\mathbf{z}}$ plane(which is the equatorial plane of the Tokamak) then the dispersion tensor can be shown to be of the general form,

$$\mathcal{D}_{ij}\left(\omega, \mathbf{k}\right) = \epsilon_{ij}(\omega, \mathbf{k}) - n^2 \delta_{ij} + \mathbf{nn}, \tag{2.5}$$

with dielectric tensor(ϵ_{ij}),

$$\epsilon_{ij} = \delta_{ij} + \sum_s \chi_{ij(s)} = \begin{bmatrix} 1 - \sum_s \frac{\omega_{ps}^2}{\omega^2 - \Omega_s^2} & -i\sum_s \frac{\omega_{ps}^2 \Omega_s}{\omega(\omega^2 - \Omega_s^2)} & 0 \\ i\sum_s \frac{\omega_{ps}^2 \Omega_s}{\omega(\omega^2 - \Omega_s^2)} & 1 - \sum_s \frac{\omega_{ps}^2}{\omega^2 - \Omega_s^2} & 0 \\ 0 & 0 & 1 - \sum_s \frac{\omega_{ps}^2}{\omega^2} \end{bmatrix}. \tag{2.6}$$

The dispersion tensor may also be written in the following more transparent form(Stix, 1992),

$$\mathcal{D}_{ij}\left(\omega, \mathbf{k}\right) = \begin{bmatrix} S - n^2\cos^2\theta & -iD & n^2\cos\theta\sin\theta \\ iD & S - n^2 & 0 \\ n^2\cos\theta\sin\theta & 0 & P - n^2\sin^2\theta \end{bmatrix}, \tag{2.7}$$

with,

$$\begin{array}{llll} R = 1 + \sum_s \chi_s^- & = 1 - \sum_s \frac{\omega_{ps}^2}{\omega(\omega + \Omega_s)}, & & \\ L = 1 + \sum_s \chi_s^+ & = 1 - \sum_s \frac{\omega_{ps}^2}{\omega(\omega - \Omega_s)}, & & \\ S = \frac{1}{2}\left(R + L\right) & = 1 - \sum_s \frac{\omega_{ps}^2}{\omega^2 - \Omega_s^2} & = \epsilon_{xx} = \epsilon_{yy} & \equiv \epsilon_\perp, \\ D = \frac{1}{2}\left(R - L\right) & = \sum_s \frac{\omega_{ps}^2 \Omega_s}{\omega(\omega^2 - \Omega_s^2)} & = i\epsilon_{xy} = -i\epsilon_{yx} & \equiv \epsilon_/, \\ P = 1 + \sum_s \chi_{zz(s)} & = 1 - \sum_s \frac{\omega_{ps}^2}{\omega^2} & = \epsilon_{zz} & \equiv \epsilon_\parallel. \end{array} \tag{2.8}$$

Here, Ω_s is the particle gyro-frequency(which is negative for electrons with $q_e < 0$ and positive for ions with $q_i > 0$), ω_{ps} is the plasma frequency and $\mathbf{n} = \frac{c}{\omega}(k\sin\theta, 0, k\cos\theta)$

is the refractive index which gives a measure of the opacity of the plasma. In chapter 1 we defined the limiting behaviour of the refractive index. Cutoffs are present whenever the refractive index goes to zero and resonances are present whenever the refractive index goes to infinity. Harmonics of the gyrofrequency are absent from the dispersion tensor and so we see that the cold plasma description fails to predict gyroresonance at harmonics of the gyrofrequency although it does provide the framework for the basic properties of EM waves in a plasma away from such regions.

The determinant of the dispersion tensor, $Det|\mathcal{D}| = 0$, gives the following general dispersion relation which is quadratic in n^2(representing the propagation of two distinct wave modes),

$$An^4 + Bn^2 + C = 0,$$

with,

$$\begin{aligned} A &= S\sin^2\theta + P\cos^2\theta, \\ B &= RL\sin^2\theta + PS\left(1+\cos^2\theta\right), \\ C &= PRL. \end{aligned}$$

We may eliminate the $\sin\theta$ and $\cos\theta$ dependences giving,

$$\tan^2\theta = -\frac{P\left(n^2-R\right)\left(n^2-L\right)}{\left(Sn^2-RL\right)\left(n^2-P\right)}.$$

We may stress more strongly the difference between parallel and perpendicular propagation by introducing $n_{\|} = n\cos\theta$ and $n_{\perp} = n\sin\theta$. Let us first consider EM waves propagating along the magnetic field with $\mathbf{n} = \left(0,0,n_{\|}\right)$. Since $\theta = 0$ then $\tan\theta = 0$ and we have the solutions: $n_{\|}^2 = L$ and $n_{\|}^2 = R$ representing left and right-circularly polarised EM waves propagating along the magnetic field. A glimpse at the expressions for L and R above in (2.8) reveals that these represent ion and electron cyclotron resonance respectively. At high frequencies($\omega \simeq |\Omega_e|$) electron gyroresonance is possible with the R-wave(the 'whistler' mode) but not with the L-wave which rotates in the opposite sense to the electrons. At low frequencies($\omega \simeq \Omega_i$) ion gyroresonance is possible with only the L-wave. Both the L and R-waves become shear Alfvén waves($\omega = k_{\|}u_A$) in the low frequency limit flowing along the ambient magnetic field at the Alfvén speed($u_A = \frac{B_0}{\sqrt{(\mu_0\rho_i)}}$) rather like waves on mass-loaded strings. Cut-offs will be present when $R = 0$ or $L = 0$.

Now let us consider EM waves propagating perpendicularly across the magnetic field with $\mathbf{n} = (n_{\perp},0,0)$. Since $\theta = \frac{\pi}{2}$ then $\tan\theta = \infty$ and we have the solutions: $n_{\perp}^2 = \frac{RL}{S}$ and $n_{\perp}^2 = P$. There will be resonance when $S = 0$ and cutoffs when $R = 0$, $L = 0$ or $P = 0$.

We will be interested in the study of EM waves propagating radially across the toroidal magnetic field(as launched from an antenna or waveguide at the plasma edge in a Tokamak) and it will be useful to look at the dispersion relations which arise for perpendicular propagation. Returning for a moment to (2.7) and setting $\theta = \pi/2$ then we have,

$$\mathcal{D}_{ij}(\omega, \mathrm{k}) \bullet \mathbf{E}(\omega, \mathrm{k}) = \begin{bmatrix} S & -iD & 0 \\ iD & S - n_\perp^2 & 0 \\ 0 & 0 & P - n_\perp^2 \end{bmatrix} \begin{pmatrix} E_x \\ E_y \\ E_z \end{pmatrix} = 0.$$

We note that due to the disappearance of the x and y elements of the z-manifold in $\mathcal{D}$, the equations for E_x and E_y have decoupled from the equation for E_z giving two independent wave modes: the ordinary mode(O-mode) where $E_x = E_y = 0$ and the extra-ordinary mode(X-mode) where $E_z = 0$.

For the O-mode only E_z is non-zero and so we have a purely transverse mode with dispersion relation,

$$n_\perp^2 = P = 1 - \sum_s \frac{\omega_{ps}^2}{\omega^2}.$$

This is just the usual light wave(EM wave with $\omega^2 = c^2 k^2$ in a vacuum) modified by the presence of the plasma. For Tokamak plasmas the sum over all particle plasma frequencies is dominated by the electron plasma frequency by a factor m_i/m_e and so an electron wave will propagate in this mode only if $\omega \geq \omega_{pe}$ determined by a critical electron density n_{0e}.

For the X-mode, E_x and E_y are non-zero and so we have a partly transverse and partly longitudinal mode with dispersion relation,

$$n_\perp^2 = \frac{S^2 - D^2}{S} \equiv \frac{RL}{S}.$$

In a single ion species plasma we may neglect terms of order m_e/m_i giving the radial refractive index squared,

$$n_\perp^2 \simeq \frac{(\omega^2 - \omega_{pe}^2 + \Omega_i\Omega_e + \omega\Omega_e)(\omega^2 - \omega_{pe}^2 + \Omega_i\Omega_e - \omega\Omega_e)}{(\omega^2 - \omega_{LH}^2)(\omega^2 - \omega_{UH}^2)}.$$

There is a low frequency($\omega \ll \Omega_e$) resonance when $\omega = \omega_{LH}$ at the lower-hybrid frequency(equation (1.4)) and a high frequency($\omega \simeq \Omega_e$) resonance when $\omega = \omega_{UH}$ at the upper-hybrid frequency(equation (1.5)). Both of these resonances have arisen from the condition that $S = 0$ and, in a multiple-ion species plasma, this condition also gives rise to extra resonances (in addition to the lower and upper-hybrid resonances) due to interactions between any two ion species at the 2-ion hybrid resonance where $\omega = \omega_{ii}$(equation (1.3)). The terminology O and X are usually reserved for high frequency, electron dominated waves propagating through a static ion background. Low frequency oscillations

due to *both* electron and ion dynamics reveal a similar separation into instead the slow and fast magnetosonic waves(slow and fast waves) otherwise known as the compressional Alfvén waves. The slow wave is almost entirely linearly polarised with $\mathbf{E} \parallel \mathbf{B}_0$ while the fast wave is almost entirely elliptically polarised with $\mathbf{E} \perp \mathbf{B}_0$.

A more general dispersion relation allows for oblique angles of propagation. At the low frequencies($\omega \simeq \Omega_i$) considered here, the higher mobility of electrons compared to ions(due to smaller electron inertia) means that charge separation along the magnetic field is inevitable. The resulting electric field shorts out any pre-existing electric field meaning that effectively $E_z \simeq 0$. A valid approximation then is to neglect the z-manifold of $\mathcal{D}$ which is the coefficient of E_z. This effectively means that we are neglecting the propagation of the slow wave. The determinant of the remaining x, y-manifold in (2.7) then gives the fast wave dispersion relation,

$$n_\perp^2 = \frac{(S - n_\parallel^2) - D^2}{(S - n_\parallel^2)}. \tag{2.9}$$

The fast wave propagates across the ambient field and so is well suited to transport of EM energy radially to the centre of a Tokamak plasma subject to the cut-offs and resonances which may be encountered on the way. We will say more about this later at the end of the chapter when we discuss accessibility conditions. In this thesis we will focus on the wave-particle dynamics introduced by the fast wave. Using the definitions in (2.8), the fast wave dispersion relation of (2.9) can also be written as,

$$n_\perp^2 = \frac{(R - n_\parallel^2)(L - n_\parallel^2)}{(S - n_\parallel^2)}.$$

The 2-ion hybrid resonance occurs when $S - n_\parallel^2 = 0$ and the associated cut-off condition is $L - n_\parallel^2 = 0$. The cut-off associated with $R - n_\parallel^2 = 0$ is the low density cut-off of the fast wave, which, for $k_\parallel \simeq 5m^{-1}$ occurs around $n_e \simeq 2 \times 10^{18} m^{-3}$.

Away from a resonance layer in a Tokamak plasma, cold plasma fluid theory adequately describes wave propagation. Thermal(finite temperature) effects will add minor corrections to the basic wave behaviour which will be dominated by the cold plasma cut-offs and resonances. In these regions where the refractive index may vary substantially such that the plane wave approach used here is not reliable(the wavelength is no longer negligible in comparison to the Larmor radius), we need to use other levels of description such as a WKB theory or a full wave theory as we will describe a little later on. Furthermore, we have shown that cold plasma theory does not predict gyroresonance for perpendicular propagation or gyroresonance at harmonics of the gyrofrequency, which are known to exist experimentally (Stix, 1975). In order to describe EM waves passing through them we must use a kinetic theory which will include the dynamics of individual particles at a microscopic level.

2.1.2 Hot Plasma Waves

We may describe the dynamics of individual particles using a kinetic theory. In chapter 1 we showed that Tokamak plasmas typically have a large number of particles in their Debye sphere and in a magnetised plasma charged particles effectively free-stream along the toroidal magnetic field in helical orbits. This can be thought of as the equilibrium state(f_0) and, for an unperturbed plasma may be described by a Maxwellian velocity distribution,

$$f_{0s} = n_{os}\pi^{-3/2}u_{Ts}^{-3}e^{-u^2/u_{Ts}^2}, \tag{2.10}$$

which simply states that most particles will have the thermal velocity($u = u_T$). The equation of motion for each particle species in a hot, collisionless plasma is the Vlasov equation which describes the time evolution of a general particle distribution(F_s) of particle positions($\mathbf{r}$) and velocities($\mathbf{u}$),

$$\frac{\partial F_s}{\partial t} + \mathbf{u} \bullet \frac{\partial F_s}{\partial \mathbf{r}} + \frac{q_s}{m_s}(\mathbf{E} + \mathbf{u} \times \mathbf{B}) \bullet \frac{\partial F_s}{\partial \mathbf{u}} = 0. \tag{2.11}$$

We linearise and write $\mathbf{B}$ in terms of $\mathbf{E}$ using Maxwell's equation for Faraday induction. Integration along the equilibrium orbits then gives us an expression for the perturbed particle distribution(f_s) in terms of the equilibrium particle distribution(f_{0s}). The perturbed current density is then given by the first velocity moment of the perturbed distribution function(f_s),

$$\mathbf{J} = \sum_s q_s \int d\mathbf{u}\mathbf{u}f_s, \tag{2.12}$$

which, when inserted into the wave equation (2.1), gives us the following dispersion tensor(see for example Cairns, 1985 or Stix, 1992),

$$\mathcal{D}_{ij}(\omega, \mathbf{k}) = \epsilon_{ij}(\omega, \mathbf{k}) - n^2\delta_{ij} + \mathbf{nn},$$

with dielectric tensor,

$$\begin{aligned}
\epsilon_{ij} &= \delta_{ij} + \sum_s \sum_l \frac{\omega_{ps}^2}{\omega^2}\zeta_{0s}e^{-\lambda_s} \\
&\times \begin{bmatrix} \frac{l^2 I_l}{\lambda_s}Z & il\left[I_l' - I_l\right]Z & \frac{-lI_l}{\sqrt{2\lambda_s}}Z' \\ -il\left[I_l' - I_l\right]Z & \left[\left(\frac{l^2}{\lambda_s} + 2\lambda_s\right)I_l - 2\lambda_s I_l'\right]Z & i\sqrt{\frac{\lambda_s}{2}}\left[I_l' - I_l\right]Z' \\ \frac{-lI_l}{\sqrt{2\lambda_s}}Z' & -i\sqrt{\frac{\lambda_s}{2}}\left[I_l' - I_l\right]Z' & -I_l\zeta_{ls}Z' \end{bmatrix},
\end{aligned} \tag{2.13}$$

and,

$$\lambda_s = \frac{1}{2}k_\perp^2\rho_s^2, \quad \zeta_{ls} = \frac{\omega - l\Omega_s}{k_\parallel u_{Ts}}, \quad \rho_s = \frac{u_{Ts}}{\Omega_s}, \quad u_{Ts}^2 = \frac{2\kappa T_s}{m_s}.$$

Here ρ_s is the Larmor radius of the particle, $I_l = I_l(\lambda_s)$ is the modified Bessel function of order l and $Z = Z(\zeta_{ls})$ is the plasma dispersion function(Z-function) shown graphically in figure 2.1. Primes denote derivatives with respect to the argument. The Z-function was first tabulated by Fried and Conte(1962) and has the following equivalent definitions,

$$Z(\zeta) \equiv \frac{1}{\sqrt{\pi}} \int_L dt \frac{e^{-t^2}}{t-\zeta} \equiv i \int_0^\infty dt e^{it\zeta - \frac{1}{4}t^2} \equiv -2e^{-\zeta^2} \int_0^\zeta dt e^{t^2} + i\sqrt{\pi} e^{-\zeta^2}, \tag{2.14}$$

where L is known as the Landau contour in the complex plane, chosen as as to satisfy causality requirements(this notion will be expanded upon in a later section) by integrating around the simple pole on the real t-axis at $t = \zeta$. Note that the Z-function is complex even for real arguments. The Landau contour is such that there is no response of the plasma until the EM field is present ensuring that causes precede effects. The Z-function is a congenital feature of wave-particle phenomena in a hot plasma having a thermal(Maxwellian) velocity distribution function.

The hot plasma dispersion tensor contains a sum over all cyclotron harmonics(l). There will be collisionless dissipation of the EM wave by gyroresonant absorption. This resonance behaviour is embedded in the Z-function.
En route to the dielectric tensor of (2.13) it was necessary to evaluate velocity integrals of the form,

$$\epsilon_{ij} = \delta_{ij} + \sum_s \sum_l \frac{\epsilon_0 q_s^2}{m_s \omega^2} \int d\mathbf{u} \frac{S_{ij}(\mathbf{u})}{\omega - k_{||} u_{||} - l\Omega_s},$$

which, if S_{ij} is a function of a thermal velocity distribution, is seen to be the origin of the Z-functions by glancing back at (2.14). Ions will be in resonance with the incident EM waves whenever the following wave-particle condition is satisfied,

$$\omega = l\Omega_s + k_{||} u_{||} \quad or \quad u_{||} = \frac{\omega}{k_{||}} - \frac{l\Omega_s}{k_{||}}. \tag{2.15}$$

The Landau(or Cerenkov) resonance condition is given by $l = 0$. Wave energy in this resonance is transferred to the parallel degree of freedom of the resonant particles by the electric field component parallel to the ambient magnetic field. This is significant for the fast wave in the ICRF(Lashmore-Davies et al., 1995) and has the following physical interpretation. Particles with a velocity($u_{||}$) close to the wave phase velocity($\frac{\omega}{k_{||}}$) may 'surf' the wave. We may make some general comments about average gains or losses of energy by examining the slope of the equilibrium velocity distribution function(f_{0s}) so as to offer a physical interpretation. Let us consider first of all particles with an initial velocity slightly higher than the wave phase velocity. Those particles which gain energy move away from the resonant velocity while those that lose energy approach it, interacting more effectively with the wave and hence there is a net transfer of energy from particles to the wave. The opposite is true if we consider particles whose initial velocity is slightly slower than the wave phase velocity. For a Maxwellian(thermal) distribution there will be more particles

in the latter state, resulting in a net loss of energy from the wave by collisionless processes.

There is also another mechanism by which wave energy may be transferred under the Landau resonance condition known as magnetic pumping(or transit time damping). Essentially, magnetic field energy is transferred by the interaction of the component of the wave magnetic field parallel to the ambient magnetic field and is known to contribute to direct electron dissipation of the fast wave, being comparable to the dissipation due to Landau damping.

When $l \neq 0$ then gyroresonance occurs and, contrary to the Landau resonance, energy is fed into the perpendicular energy of the resonant particles. This can occur irrespective of whether or not the particle velocity is slow or fast compared to the wave phase velocity. Moreover, the Z-functions, having a Gaussian form for their imaginary part($\simeq e^{-\zeta_{ls}^2}$), introduce a smooth absorption profile at each gyroresonance(since the singularity arising from the pole is smoothed out by the imaginary part which moves the contour off the real t-axis). We see that there will be collisionless absorption of energy from the EM waves whenever gyroresonant particles, orbiting at harmonics of the gyrofrequency, see the Doppler-shifted incident wave frequency. In chapter 5 we will perform a detailed statistical analysis of resonance broadening.

For large ζ(in the limit of perpendicular propagation where $k_{\parallel} \to 0$ or in the limit of a cold plasma where $T \to 0$) then the asymptotic expansion of Z(Fried and Conte, 1962),

$$Z(\zeta) \simeq i\sqrt{\pi}\sigma e^{-\zeta^2} - \frac{1}{\zeta}\left[1 + \frac{1}{2\zeta^2} + \frac{3}{4\zeta^4} + \frac{15}{8\zeta^6} + ...\right], \quad \sigma = \begin{cases} 0 & Im\{\zeta\} > 0, \\ 1 & Im\{\zeta\} = 0, \\ 2 & Im\{\zeta\} < 0 \end{cases} \tag{2.16}$$

means that Z' is a negligibly small quantity. In this case the x and y parts of the z-manifold of $\mathcal{D}_{ij}$ vanish and we have the same block structure as was found for the cold plasma waves with independently propagating O and X-modes. Their dispersion relations are now modified by the introduction of thermal effects which are housed in the modified Bessel functions. Thermal effects introduce extra hot plasma modes (not described by cold plasma theory) which are associated with higher powers of k in the dispersion relation. If we expand the modified Bessel functions to order unity in the low temperature approximation($\lambda \to 0$) using the following series expansion for small λ(see Stix, 1992),

$$I_l(\lambda)\, e^{-\lambda} = \frac{1}{l!}\left(\frac{\lambda}{2}\right)^l \left[1 - \lambda + \left(\frac{\lambda}{2}\right)^2 \left(2 + \frac{1}{l+1}\right) + ...\right], \tag{2.17}$$

then the dispersion equations for the O-Mode and X-mode become order l polynomials in $\mathbf{k}$. These higher order terms in $\mathbf{k}$, which have arisen from the thermal effects of kinetic theory, correspond physically to extra modes of propagation. A polynomial of order l

in $\mathbf{k}^2$ will describe l non-degenerate wave modes. It has been known for some time that there is a family of hot plasma modes which propagate between the cyclotron resonances of the ions(there is a family for the electrons too), known as the ion Bernstein modes after Bernstein(1958). When different species of ions are present in the plasma then this family of waves bifurcates at the 2-ion hybrid frequency and we have another set of hot plasma modes known as ion-hybrid waves (Lashmore-Davies, 1995). The fact that these hot plasma modes propagate between harmonics of the gyrofrequency means that they will be present in the interaction regions described in chapter 1. Incident EM waves may then be mode-converted to these hot plasma modes in the neighbourhood of gyroresonances and cut-offs where the wave-vector has dramatic variation.

In recent years, investigations of wave-particle interactions in hot plasmas have used (2.17) to expand the modified Bessel functions so as to provide simple expressions for the plasma response correct to order λ(see for example Lashmore-Davies et al., 1988). Such expansions are known as, 'finite Larmor radius(FLR) expansions' and are amenable to analytic progress due to their simplified nature. In figure 2.2 we show the functional form of the first few orders of (2.17).

In the last chapter we described how thermal effects are weak for fundamental gyroresonance in a single ion species plasma along with other related effects. We are now in a position to say a little more about this. When we perform the FLR expansions(note that this is only possible when $\lambda \ll 1$ and will not be applicable to a study of large Larmor radius ions of high energy where $\lambda \geq 1$) then we see that thermal effects arise from the powers of λ. In a single ion species plasma then thermal effects at the fundamental of the gyrofrequency arise from the $l = 1$ terms. However, the order λ terms cancel leaving only thermal effects of order λ^2 which are negligible and hence gyroresonant absorption will be negligible at the fundamental. At twice the ion gyrofrequency(the first harmonic) then thermal effects arise from the $l = 2$ terms. The first order thermal terms of order λ no longer cancel and we find that there is strong gyroresonant absorption. In a 2-ion species plasma the picture is more complicated since thermal effects are distributed between the resonant response of the different ions and also propagating hot plasma modes. The strength of gyroresonant absorption is influenced by wave polarisation and we find that it is possible to have effective gyroresonant absorption at the fundamental of the minority ion gyrofrequency. We will discuss the role of wave polarisation in a later section.

Away from gyroresonances, most of the ions in the velocity distribution will be non-resonant, having velocities(u) which are non-thermal ($u/u_T \geq 3$) and will not contribute to resonant absorption which is scaled by a factor proportional to $e^{-u^2/u_T^2} \simeq 0.0001$. This will be true for particles some distance from the gyroresonance layer where ζ will be large. We may then replace the non-resonant particle response by its cold plasma counterpart. This is most easily done by retaining only the $l = 0, \pm 1$ terms in (2.17) and keeping only the leading order terms in the asymptotic series for Z.

We turn now to a study of the dispersion properties of an inhomogeneous plasma.

2.2 Waves In An Inhomogeneous Plasma

By inhomogeneous we mean to say that macroscopic quantities such as the ambient magnetic field($\mathbf{B_0}$), the plasma density(n_{0s}) and the plasma temperature(T) have a spatial variation. In a Tokamak, both the ion density and temperature profiles decrease almost parabolically from the centre to the plasma edge while the toroidal magnetic field profile falls off as $1/r$ with radial distance(r) from the centre. This is a direct consequence of Ampere's law($\oint \mathbf{B_0} \bullet d\mathbf{x} = \sum_N \mu_0 I_N$) which, for a circular loop of radius(r), gives $B = \frac{\mu_0 IN}{2\pi r}$.

We have seen in the last section that the dispersion properties of hot collisionless plasmas are dominated by the effects of wave-particle interactions at resonant magnetic field lines. Although spatial variations in plasma density and temperature will proportionately modify the values of plasma frequencies and thermal velocities, the dominant behaviour of charged particles is governed by gyroresonance and so will be markedly altered by small variations in magnetic field strength due to a field gradient. We will use this fact to simplify our analysis of the inhomogeneous plasma by including only the spatial variation of the ambient magnetic field, treating density and temperature profiles as constants.

We will consider a weakly inhomogeneous Tokamak plasma where the toroidal field is along $\hat{\mathbf{z}}$ and has a gradient in strength along the radial $\hat{\mathbf{x}}$ direction, varying slowly over a long length scale so that we may approximate the field variation by the first few terms of a Taylor series expanded about the resonance position(which we are free to choose at the origin),

$$\mathbf{B_0}(x) = B_0(1 + \epsilon x),$$

with $\epsilon = \frac{1}{B_0(0)} \frac{\partial B_0(0)}{\partial x}$. We ignore curvature effects due to the poloidal field(which is an order of magnitude weaker than the toroidal field) so that we have a 1D inhomogeneity. We note that there will now be a variation in the strength of the magnetic field across the Larmor orbits of the charged particles. Some models of inhomogeneous plasmas include only the spatial variations of macroscopic variables like the magnetic field in the dielectric tensor elements for a *homogeneous* plasma. While including the global variation of physical parameters due to the inhomogeneity, these models fail to include the local variation of the magnetic field across the Larmor orbits and are known as locally uniform models. They fail to produce energy conserving wave equations however as we shall see. Due to the lack of availability of a simple theory to describe large Larmor radius ions and fusion products in an inhomogeneous plasma, computer codes presently in use at JET are using precisely this type of locally uniform theory to model large Larmor radius ion gyroresonance and it will be our aim to devise an efficient and energy-conserving physical

model for this which is fully inclusive of the effects of inhomogeneity.

For most of the plasma in a Tokamak(away from resonance layers) the dielectric properties vary slowly over a length scale which we may associate with the major radius(a few metres) in contrast to the rapid variations of the incident waves on the much shorter length scale of the wavelength(a few centimetres in the ICRF). In this regime we may use a single mode WKB theory to obtain equations similar to those for a homogeneous plasma.

2.2.1 Single Mode Methods

In the derivation of the dispersion properties of waves in a homogeneous plasma, we considered perturbations which vary harmonically in time and space in the single mode form of plane waves. For example the wave electric field was chosen to vary as,

$$\mathbf{E} = \mathbf{E}_0 e^{i\mathbf{k}\bullet\mathbf{r}-i\omega t}.$$

This provided an easy way of obtaining the momentum space(k-space) variables from which we could derive the dispersion relation. In a weakly inhomogeneous plasma the plasma parameters are slowly varying functions of position and the dielectric tensor will also be a slowly varying function of position. When these slow changes in the plasma are accommodated by adiabatic changes in the wave-vector($\mathbf{k}$) then a single mode can continuously propagate throughout the plasma. In the case of our $1D$ inhomogeneity along $\hat{\mathbf{x}}$ we may model the perturbed quantities, for instance the wave electric field by,

$$\mathbf{E}(x) = \mathbf{E}_0(x)\, e^{i\int_0^x k_x(x)dx + ik_y y + ik_z z - i\omega t}, \tag{2.18}$$

with the values of k_y and k_z being pre-determined by the antenna spectrum. A fully $3D$ description requires the introduction of an eikonal (Ψ) such that $\nabla\Psi = \mathbf{k}$ with $\mathbf{k}$ satisfying the local dispersion relation. In accordance with this eikonal analysis we may approximate the electric field by,

$$\mathbf{E}(x) = E_0(x)e^{i\Psi-i\omega t}.$$

The group velocity gives the direction of energy flow,

$$\mathbf{v}_g = \frac{\partial\omega}{\partial\mathbf{k}} \equiv \frac{d\mathbf{r}}{dt}.$$

In a stationary plasma then the dispersion relation is given by,

$$K(\mathbf{r},\mathbf{k},\omega) = Det|\mathcal{D}| = 0,$$

with total derivative,

$$\frac{dK}{dt} = \frac{\partial K}{\partial\mathbf{k}} \bullet \frac{d\mathbf{k}}{dt} + \frac{\partial K}{\partial\mathbf{r}} \bullet \frac{d\mathbf{r}}{dt} = 0,$$

giving the relations,

$$\begin{aligned}\frac{d\mathbf{r}}{dt} &= -\frac{\partial K/\partial \mathbf{k}}{\partial K/\partial \omega} = \frac{\partial \omega}{\partial \mathbf{k}}, \\ \frac{d\mathbf{k}}{dt} &= \frac{\partial K/\partial \mathbf{r}}{\partial K/\partial \omega} = -\frac{\partial \omega}{\partial \mathbf{r}}.\end{aligned}$$

These are known as the ray tracing equations which are similar to Hamilton's equations in classical mechanics. A source at the plasma edge produces a wave-number spectrum and we integrate the ray tracing equations to find paths along which various components of the spectrum flow into the plasma (see for example Bhatnager et al., 1982).

The condition for validity of approximations like (2.18) is that $k_x(x)$ be slowly varying such that,

$$\frac{1}{k_x}\frac{dk_x}{dx} \ll k_x.$$

However, in the neighbourhood of gyroresonances and cut-offs then the dielectric response of the plasma varies instead on the short length scale of the absorption width which is comparable to the wavelength and so we expect WKB theory to be inaccurate. The theory also breaks down in mode conversion regions where two modes couple since it is unable to distinguish between them. A more elaborate multi-mode theory must be adopted in these regions.

2.2.2 Multi-Mode Methods

The essence of multi-mode theory is that we retain the full spectrum of wave modes in the description of perturbations. In the derivation of the full wave equations we will adopt the method of orbit integration(Shafranov, 1962) to work out the dielectric response. As outlined in the last section, we integrate the perturbed distribution along the equilibrium orbits of the charged particles but rather than assuming plane wave forms for the field quantities, we now express them as a complete sum over all Fourier modes. This complicates the analysis by introducing an extra integral but allows for wave-wave interactions which are crucial to a detailed understanding of the behaviour of interaction regions. We will perform this calculation for a general plasma equilibrium in a weakly inhomogeneous magnetic field in chapter 3.

In modelling the whole plasma what we do then is calculate the effect of resonances, cut-offs and mode-conversions using a multi-mode theory and we match asymptotically to solutions from the simpler WKB theory calculated outside these regions of extreme variation of the dielectric tensor. This provides a global picture of EM wave propagation

in the plasma.

There have been numerous approaches to the problem of describing wave-particle interactions in an inhomogeneous plasma apart from the path integral method of Shafranov(1962) which we will use(see for example the geometrical optics methods of Bernstein(1975), the contour integral methods of Swanson(1978) and also Antonsen and Manheimer(1978), the boundary layer analysis of Imre(1987), the Hamiltonian methods of Ye and Kaufman(1988), the gyrokinetic theory of Lashmore-Davies and Dendy(1989), the Lie transform methods of Littlejohn(1993) and more recently the guiding centre method of Cairns et al.(1991) and (1995)). In essence they are all either single mode(plane wave or wave packet) methods or multi-mode methods.

2.2.3 Locally Uniform And Locally Non-Uniform Theories And The Connection With Energy Conservation

Another distinction(in addition to that between single mode and multi-mode methods) is that between locally uniform and locally non-uniform treatments of the magnetic field variation on the short length scale of the Larmor radius(which can be of the same size as the wavelength). We have already described how, in an inhomogeneous plasma, the magnetic field strength varies across the Larmor orbits of the charged particles so that locally it is non-uniform. Only an accurate mathematical model of this phenomenon, taking into account the effects of non-uniformity, will lead to fully energy conserving wave equations. The inclusion of these effects is non-trivial however and it is only recently that energy conserving equations describing electron and ion gyroresonance have appeared in the literature (relativistic electron gyroresonance(Maroli, 1986) and ion gyroresonance (Lashmore-Davies and Dendy, 1989)). The basic reason is that in an inhomogeneous plasma no simple, closed form for the equilibrium orbits exists since the inhomogeneity transforms the nature of the orbits making them nonlinear(Beskin et al., 1987). We will discuss this in more detail in chapter 3.

A simple way of overcoming this problem has been proposed recently (Cairns et al., 1991). Essentially they realised that, due to the variation of the field strength across the Larmor radius, the gyrofrequency should be evaluated at the guiding centre $(x + \frac{u_y}{\Omega})$ rather than at the actual particle position (x). This correction to the gyrofrequency became known as, 'the gyrokinetic correction'. When all the spatially varying quantities are evaluated at the guiding centres a simplified form for the equilibrium orbits may be used. Cairns et al. then showed how this simple method leads to energy conserving wave equations. This fact was reiterated by an independent analysis(Lashmore-Davies and Dendy, 1989) using the rigorous gyrokinetic theory of Chen and Tsai(1983). Moreover, they showed that the inclusion of the gyrokinetic correction introduces an additional damping mechanism due entirely to the variation of the magnetic field strength felt by gyroresonant particles in different parts of their orbit. More recently still, the simplicity of the method of Cairns

et al. has allowed for a straight-forward extension so as to include weakly relativistic electron effects(McDonald et al., 1994).

In the work of Cairns et al.(1991) and of McDonald et al.(1994), energy conserving ordinary differential equations(ODEs) describing the propagation of EM waves through gyroresonances were obtained in the limit of small Larmor radius particles(small compared to the wavelength). Echoing the results obtained by other authors(Brambilla, 1991 and Sauter and Vaclavik, 1992), Cairns et al. remarked that for large Larmor radius particles, such as gyroresonant ions or fusion products produced by high temperature break-even fusion plasmas, the energy conserving wave equations are integro-differential equations(IDEs) rather than ODEs. We have shown in a recent paper(Cairns et al., 1995) how an approximation (called, 'the fast wave approximation'(Kay et al., 1988 and Lashmore-Davies et al., 1988), similar in spirit to the Born approximation of quantum-mechanical scattering theory(see for example Harding, 1968), allows us to reduce the IDEs to ODEs while retaining the non-local effects of the large Larmor radius particles. Let us describe briefly the physical basis for this approximation. In a linear mode conversion process two wave modes interact due to their degeneracy. The backward propagating modes play no role in the process and so we expect that a second order equation should provide the required information concerning the wave interactions. Essentially the mode converted wave(the ion-hybrid wave for hot EM waves in a multi-species plasma) exists as the driven response of the fast wave in the interaction region. Consideration of the fast wave alone, using the local value of the wave-number, then provides information of the degree of mode-coupling. There will not, however, be any information concerning the propagation of the mode-converted wave available. In chapter 7 we will formalise this reduction process and we will show how higher order corrections may be obtained in a simple way.

2.2.4 The Formulation Of Differential Wave Equations

Differential equations describing EM wave propagation through a plasma may be easily constructed using the method of Cairns et al.(1991) whereby we simply replace the wave-vectors by differential operators such that,

$$\mathcal{D}\left(\omega, \mathbf{k}\left(\mathbf{r}\right)\right) \rightarrow \mathcal{D}\left(\omega, -i\left(\frac{\partial}{\partial \mathbf{r}}\right)_{\mathbf{E}}\right).$$

In essence this is equivalent to an inversion of the Fourier transform. In a locally uniform theory the differential operators act only on the EM fields. Unfortunately the resultant equations only conserve energy for a homogeneous medium. The problem is that, due to the spatial variation of the physical parameters in an inhomogeneous medium, not only the EM fields vary spatially, the dielectric tensor will vary spatially too. The differential operators obtained by inverting the Fourier transform above act *only* on the field. It is the absence of differential operators acting on the dielectric tensor which ultimately leads

to a lack of energy conservation in a locally uniform model of an inhomogeneous medium. This was clearly demonstrated for the Budden form of the O-mode by Cairns et al.(1991).

The method of Cairns et al.(1991) which includes the gyrokinetic correction, gives an integral representation of the plasma response when applied to large Larmor radius particles in an inhomogeneous plasma(as opposed to the algebraic form obtained for a homogeneous plasma). It was shown how, in the low energy limit(small Larmor radius particles), the modified Bessel functions can be expanded to any order of their argument(λ) which is a simple function of the wave-vectors k and k_1. By differentiating under the remaining integral, which is of the form of the Z-function, they showed how each wave-vector k gives rise to a differential operator acting on the EM field($\mathbf{E}$) while each wave-vector k_1 gives rise to a differential operator acting on the response function(Z-function) so that,

$$\mathcal{D}\left(\omega, k\left(\mathrm{r}\right), k_1\right) \rightarrow \mathcal{D}\left(\omega, -i\left(\frac{\partial}{\partial \mathrm{r}}\right)_{\mathbf{E}}, -i\left(\frac{\partial}{\partial \mathrm{r}}\right)_{Z}\right).$$

The ODEs now include the odd order derivatives of the dielectric function required for energy conservation(Swanson, 1985). We will provide an example of this technique in chapter 4 and also in chapter 7 within the context of high energy, large Larmor radius ions.

However, in the high energy regime(large Larmor radius particles), λ becomes a large number(comparable to unity) and we cannot expand the modified Bessel functions using it as an expansion parameter. Instead, we must retain the full integrals(which are essentially modified Z-functions) leading to IDEs as we will show in chapter 4. Brambilla(1991) expressed the integral response in terms of a sum of polynomials and Sauter and Vaclavik(1992) used the integral representation of the modified Bessel functions to obtain a non-local real space($\mathbf{r}$-space) integral. More recently, Holt(1992) reproduced the result of Sauter and Vaclavik after considerable algebra, starting instead from the guiding centre method of Cairns et al.(1991). The equations obtained in each case did not have a closed analytical form and yielded only through elaborate and time consuming finite element methods of numerical computation.

In our recent publication(Cairns et al., 1995), we used the guiding centre method of Cairns et al.(1991) to describe the inhomogeneous plasma. We then applied the fast wave approximation to the IDE enabling us to reduce it to a second order ODE having a non-local potential function which housed the effects of large Larmor radius particles. In chapter 7 we will obtain a summation form for the response of the plasma and we will show that the fast wave approximation is simply the zero order case. The second order ODE is amenable to rapid and accurate solution using standard Runge-Kutta routines. Furthermore, Lashmore-Davies and Dendy(1993) have shown how such second order wave equations conserve energy in the low energy regime. We will show in chapter 8 that this is also the case for the high energy regime of large Larmor radius particles as we will

demonstrate for some topical Tokamak scenarios in chapter 8.

In the remainder of this chapter we will present the techniques which we will need in our study of the propagation of EM waves in inhomogeneous plasmas.

2.3 Techniques Used To Study Inhomogeneous Plasmas

2.3.1 Ordering

We will find that the full response of the plasma to perturbing EM waves will be of the form of an infinite summation picking up contributions due to EM wave interaction with each and every harmonic of the gyrofrequency. Fortunately, in practice, we are limited(by engineering constraints) to the launching into the plasma of just a couple of non-interacting waves matched perhaps to a single harmonic of the ion gyrofrequency or the electron gyrofrequency. This means that the response of the plasma will be dominated by those terms in the sum which are related to these harmonics. We may approximate the other non-resonant terms in some way(usually by their cold plasma counterparts).

As we have already remarked, cold plasma theory describes the salient behaviour of waves in a plasma. Finite temperature effects will, in general, add small corrections to the basic cold plasma behaviour. We need a way of quantifying the relative magnitudes of the terms and, moreover, we would like to describe other orderings which arise naturally in our mathematical model of the underlying physics.

One of the most fundamental properties of the plasma which is independent of EM wave characteristics and Tokamak device length scales, is the ratio of the masses of the constituent particles. The ratio of the mass of the electron to the proton is much smaller than unity. Let us assign the parameter η to be the order of quantities which are small compared to unity such that,

$$\frac{m_e}{m_i} \simeq \eta^2 \ll 1. \tag{2.19}$$

In our discussion of the production of ODEs we described how thermal effects are inherent in the argument λ_s of the modified Bessel functions. λ_s is dependent upon the perpendicular wavelength($k_\perp = 2\pi/\lambda_\perp$) and also the Larmor radius(ρ_s). In the ICRF the wavelength of the EM waves is typically a few centimetres. For low energy ions the Larmor radius is typically a few millimetres and so the ratio of the Larmor radius to the wavelength is a quantity small compared to unity and is of order η,

$$k_\perp \rho_i \simeq \frac{\rho_i}{\lambda_\perp} \simeq \eta < 1.$$

In the case of electrons, this is further reduced by the ratio,

$$\frac{\rho_e}{\rho_i} \simeq \sqrt{\frac{m_e}{m_i}} \simeq \eta < 1.$$

But λ_s is proportional to the square of $k_\perp \rho_s$ so that,

$$\lambda_i \simeq k_\perp^2 \rho_i^2 \simeq \eta^2 \ll 1,$$

and we are justified in using λ_i as a small expansion parameter in this regime. Moreover, apart from appearing explicitly as the perpendicular and parallel temperatures in an anisotropic plasma(as we shall see in chapter 4), thermal effects also appear through the thermal velocities($u_{Ts} \propto \sqrt{T_s}$) of the charged particles. As λ_s is dependent upon the thermal velocity through the Larmor radius, we see that thermal effects are at most of order λ_s in the low energy regime. The resonant terms in the dielectric response will then be small corrections to the order unity cold plasma terms(although they are found to be essential for the production of energy conserving wave equations).

For high energy ions($\simeq 1MeV$) and fusion products the Larmor radius can be comparable to or greater than the wavelength and so our ordering in this case is,

$$k_\perp \rho_i \simeq \frac{\rho_i}{\lambda_\perp} \simeq 1. \tag{2.20}$$

In this case λ_s is comparable to unity and we cannot expand the modified Bessel functions using this as an expansion parameter as now the resonance terms can be of the same order as the cold plasma terms. Although this has the disadvantage that we cannot expand the modified Bessel functions so as to produce ODEs according to the recipe of Cairns et al.(1991), we note that the non-resonant terms may simply be approximated by their cold plasma values with only the $n = 0, \pm 1$ terms in the sum contributing. This allows us to reduce the infinite sum to a finite one over just a few terms: the resonant term and the cold plasma terms.

In addition to these orderings, obtained through finite temperature considerations, there is another ordering related to the physical length scales inherent in the model. The wavelength(a few centimetres) is much smaller than the length scale over which the toroidal magnetic field varies(a few metres) and if we retain the constraint that the Larmor radius be comparable to the wavelength then we have the ordering,

$$\frac{\lambda_\perp}{L} \simeq \frac{\rho_i}{L} \simeq \eta^2 \ll 1. \tag{2.21}$$

The equilibrium orbits, which must be obtained iteratively in an inhomogeneous plasma, are presented to first order in this ratio in chapter 3.

Finally, we will mention in passing the order of the width of the resonances, scaled to an appropriate length scale. In (2.15) we showed that there was an error($\delta\omega / \Omega_s$) in

the cyclotron resonance condition $\omega = l\Omega_s$ due to the parallel motion of the charged particle guiding centres along the field lines(producing a Doppler shift). The parallel wave-number($k_{\|}$) is typically of the same order as the cold plasma asymptotic perpendicular wave-number($k_{\perp}$) so that in this case,

$$k_{\|}\rho_i \simeq \eta. \tag{2.22}$$

In our discussion of the effects of field inhomogeneity above, we indicated that there will now be an additional source of error in the resonance condition arising from the gyrokinetic correction. In this case the resonance condition will be,

$$\omega = l\Omega_s + k_{\|}u_{\|} - \frac{lu_y}{L}, \tag{2.23}$$

and if we ignore Doppler broadening effects($k_{\|} = 0$) for a moment so as to isolate the error due only to the gyrokinetic correction, we find that there is a symmetric absorption profile on the scale of,

$$\frac{\delta\omega}{l\Omega_s} \simeq \frac{\rho_i}{L} \simeq \eta^2. \tag{2.24}$$

Following this rather non-mathematical and heuristic discussion we turn now to a more involved study of some of the physical effects brought about by the long mean free path of free-streaming charged particles in a collisionless plasma.

2.3.2 Non-locality

In deriving the momentum space representations in our discussion of the dispersion properties of homogeneous plasmas, the electrical displacement($\mathbf{D}$) is related to the electric field($\mathbf{E}$) through the dielectric tensor(ϵ_{ij}) as follows,

$$\mathbf{D}(\omega, \mathbf{k}) = \epsilon_{ij}(\omega, \mathbf{k}) \bullet \mathbf{E}(\omega, \mathbf{k}), \tag{2.25}$$

so that they have a simple multiplicative relation in momentum space. There is a theorem of Fourier analysis called the convolution theorem which states that the convolution of two functions in real space is equivalent to the simple product of their Fourier transforms in momentum(Fourier) space. So we may equivalently relate the electrical displacement ($\mathbf{D}$) of a space-time point to the electric field ($\mathbf{E}$) at every other point in space-time via the correlation function which is the dielectric tensor (ϵ_{ij}),

$$\mathbf{D}(\mathbf{r}, t) = \frac{1}{(2\pi)^4} \int d\mathbf{r}' \int_{-\infty}^{t} dt' \epsilon_{ij}(\mathbf{r} - \mathbf{r}', t - t') \bullet \mathbf{E}(\mathbf{r}', t'). \tag{2.26}$$

The displacement at a point is then evaluated from the non-local interaction of the electric field at every other point. In practice, there are restraints due to specific plasma conditions which mean that the response at a point may be influenced by only a few

neighbouring points. We will show that this is the case for gyroresonance where the charged particles are confined to field lines(restricting their degrees of freedom as shown in figure 2.3) and effectively they sample the electric field of the plasma only within a few Larmor radii (for high energy particles this can be an appreciable distance typically several tens of centimetres).

The free-streaming of particles along the field in a collisionless plasma means that the particles have long mean free paths and an impulse at one point in space-time leads to responses not only later in time, but also at different positions in the plasma. We see that because the response of the plasma is in the form of a convolution integral, it is non-local in nature.

A question arises quite naturally here. If we consider the electric field as the stimulus of action(in the Hamiltonian sense) in the plasma and the current density as the response of the particles(such that the susceptibility is the response function), how do we incorporate into this description of impulses and non-local responses the fact that causes must precede effects? This requirement places a strong restriction on the mathematical character of the response functions and we will see that a correctly formulated dispersion relation will always obey causality.

2.3.3 Causality And Analytic Continuation

We have already remarked that we will follow Shafranov's path integral method(1962) for determining the perturbed current density(the response of the particles) whereby we integrate the equation of motion along the equilibrium orbits of the charged particles. In doing so we will use a multi-mode representation of the perturbing quantities such as the electric field.

For an inhomogeneous plasma whose equilibrium state is independent of the spatial co-ordinate, the plasma response will have the general form,

$$\mathbf{J}(\mathbf{r},\mathbf{k},\omega) = \int_{-\infty}^{0} d\tau e^{i\mathbf{k}\bullet R[\Omega(\mathbf{r}),\tau]-i\omega\tau} G_{ij}(\mathbf{k},\omega,\tau) \bullet \mathbf{E}(\mathbf{k},\omega). \tag{2.27}$$

For complex wave frequencies($\omega = \omega_r + i\omega_i$) then $e^{-i\omega\tau} = e^{-i\omega_r\tau}e^{\omega_i\tau}$. The addition of a positive infinitesimal imaginary part(ω_i) to ω ensures that $e^{-i\omega\tau}$ vanishes as $\tau \rightarrow -\infty$ guaranteeing causality so that we pick up contributions from the whole of the orbit up until the present time. This process of making ω complex so as to satisfy causality is an example of analytic continuation. To see more clearly what this means we will discuss it in the light of an example from the derivation which will be presented in chapter 3. In the course of the derivation of the plasma response we will encounter velocity integrals of the following singular form(a simple pole of order unity at $u_{\|} = u_0 = \frac{\omega}{|k|}$),

$$I(u_0) = \int du_{||} \frac{g\left(u_{||}\right)}{u_{||} - u_0}. \tag{2.28}$$

For integrals of this type we need to specify a contour of integration due to the vanishing of the denominator for real ω. The integral comprises a contribution from the pole and also the remaining line segment along the real $u_{||}$ axis. The addition of a positive, infinitesimal imaginary part(ω_i) to the real wave frequency(ω_r) in order to ensure causality, moves the singularity above the real axis. The integral for real ω is then obtained by letting $\omega_i \rightarrow 0$. Feynman showed that this prescription is equivalent to simply bypassing the pole on the real axis by an infinitesimal, semicircular excursion of radius $|\omega_i|$ below the axis. Contours avoiding the pole in this way for both negative and positive ω_i are shown in figure 2.4. We will be using contours like the one in the lower diagram in figure 2.4 since our causal arguments mean that we have added a positive ω_i to the real wave frequency. There will be a contribution from the pole equal to πi times the residue at u_0 which is $g(u_0)$. Physically the residue represents the initial conditions and we see that this is how the effects of causality are illustrated mathematically. The remainder of the real axis will provide the Cauchy principal value(P) such that,

$$P\int_{-\infty}^{\infty} du_{||} \frac{g\left(u_{||}\right)}{u_{||} - u_0} = \lim_{\omega_i \rightarrow 0} \left(\int_{-\infty}^{u_0 - \omega_i} du_{||} \frac{g\left(u_{||}\right)}{u_{||} - u_0} + \int_{u_0 + \omega_i}^{\infty} du_{||} \frac{g\left(u_{||}\right)}{u_{||} - u_0} \right).$$

If the imaginary part of ω is truly positive then there is no pole on the real axis and we may simply integrate along the entire axis without difficulty. If the imaginary part of ω is negative we can still use the above technique to obtain the integral. However we must now deform the contour of integration so that the contour always passes below the pole as shown in figure 2.5. The deformation of the contour of integration in this way provides the analytic continuation of the integral for all values of ω_i. This prescribed deformation of the contour by the pole is analogous to the way that a marble depresses(or warps) a rubber sheet when placed upon it. The use of contour integration to calculate the causal response of a hot, collisionless plasma was first described by Landau(1946) in a classic paper which revealed the collisionless damping of an electrostatic wave in an unmagnetised plasma. This work paved the way for the discovery of other damped waves and instabilities(see for example Mikhailovskii, 1968) and indeed the very understanding of the process of the resonance heating of Tokamak plasmas is a credit to Landau.

2.4 Practical Considerations

2.4.1 Spatial Dispersion

In chapter 1 we saw that there will be regions of the plasma where $\mathbf{k}^2 < 0$ and so $\mathbf{k}(\mathbf{r})$ can become complex. To see what effect a complex wave-vector has upon the dispersive

properties of the plasma let us write out $\mathbf{E}$ in complex form for a $1D$ inhomogeneity along the $\hat{\mathbf{x}}$-direction using (2.18),

$$\mathbf{E}(\mathbf{r}) = \mathbf{E}_0 e^{i\int Re\{k(x)\}dx - i\omega t} e^{-\int Im\{k(x)\}dx}.$$

The first exponent is oscillatory while the second is not and is responsible for field amplification or reduction and provides a measure of the spatial dispersion. This is often quantified by the so-called, 'optical depth' or 'opacity',

$$\tau = \int Im\{k(x)\}dx.$$

We see that it is the imaginary part of the wavevector which results in wave damping or growth. In our analysis of cold plasma waves earlier in this chapter we obtained expressions for the fast wave refractive index squared which, in figure 1.1 of chapter 1, can be seen to have negative values indicating wave evanescence on the high magnetic field side of the cut-off associated with the 2-ion hybrid resonance. In this region k is complex and the fast wave is attenuated or damped. However the dielectric tensor of a cold plasma(equation (2.5)) has no explicit dependence upon the wavevector and so the damping of the fast wave is a passive one arising from a whole plasma wave resonance rather than the active damping which due to wave-particle dynamics which occur in processes like gyroresonance. We see then that active damping by particles will enter through the dielectric tensor.

2.4.2 Energy Considerations

When an EM wave propagates in a plasma there will be energy associated with the oscillating electric field(U_E) and also the oscillating magnetic field(U_M) as in the case of light transit through the vacuum of space. The flow of this EM energy is known as the Poynting flux($\nabla \bullet \mathbf{S}$). There will also be energy associated with the particle motions caused by the oscillating fields. The coherent mechanical motion of the particles which carries the information connected with the EM wave is known as the acoustic flux or kinetic flux($\nabla \bullet \mathbf{T}$) and represents a reversible flow of acoustic(kinetic) energy(U_T) around the plasma. A hot plasma is a dispersive medium(since the dielectric response is a spatially varying function of $\mathbf{k}$. Any dispersive medium is also a dissipative medium as we demonstrated in the last section and so there will be dissipative energy(D) transferred between the EM field and the particles. Since we must have global conservation of energy there will, naturally, be a balance of energy between the fields and the particles whereby a decrease in energy in a local volume will be balanced by a flux of energy density in to or out of the volume boundary. Intuitively we may write down the following energy balance equation *a priori*,

$$\nabla \bullet (\mathbf{S} + \mathbf{T}) + \frac{\partial}{\partial t}(U_E + U_M + U_T) + D = 0. \tag{2.29}$$

The EM field related terms: U_E, U_M and $\mathbf{S}$ have a mathematical form which is independent of the properties of the medium. The remaining terms are dependent upon the dispersive properties of the plasma and are sensitive to the method of description(for example cold theory or kinetic theory).

Let us derive expressions for the various terms in the above energy balance equation whose interactions are represented schematically in figure 2.6. We begin with two postulates(see for example Feynman, 1965):

- Global Energy Conservation: All the energy in the universe is constant.
- Local Energy Conservation: If the amount of energy changes in a region then this is because energy is flowing through the boundaries of the region or works on matter.

If we let U represent the total energy density in the EM field, $\mathbf{S}$ represent the energy flux in the EM field and W be the rate at which work is done on matter then we may write down the following energy balance equation based solely upon the above postulates,

$$W = -\frac{\partial U}{\partial t} - \nabla \bullet \mathbf{S}. \tag{2.30}$$

In appendix A we use this formula to derive Poynting's energy conservation theorem,

$$\mathbf{E} \bullet \mathbf{J} = -\nabla \bullet (\frac{\mathbf{E} \times \mathbf{B}}{\mu_0}) - \frac{\partial}{\partial t}[\frac{\epsilon_0}{2}(\mathbf{E} \bullet \mathbf{E}) + \frac{1}{2\mu_0}(\mathbf{B} \bullet \mathbf{B})]. \tag{2.31}$$

The total EM energy density(U) is,

$$U = \frac{\epsilon_0}{2}(\mathbf{E} \bullet \mathbf{E}) + \frac{1}{2\mu_0}(\mathbf{B} \bullet \mathbf{B}) \equiv U_E + U_M, \tag{2.32}$$

and the EM energy flux($\mathbf{S}$) is,

$$\mathbf{S} = \frac{\mathbf{E} \times \mathbf{B}}{\mu_0}. \tag{2.33}$$

We see that the left hand side of (2.31) is the rate at which work is done by the EM fields on the plasma and has arisen naturally out of Maxwell's field equations. The fact that the current density is a source term is indicative of the properties of the medium supporting the EM wave. In a hot, collisionless plasma, the most accurate description of the plasma state is provided by the Vlasov equation. As the rate of work done involves the product of two first order(linearly perturbed) quantities then we need to consider the second order equation of state(the second order Vlasov equation). A single mode analysis(WKB or other) is able to provide lucid expressions for particle-related energy terms (see for example Shafranov, 1962, Landau and Lifshitz, 1980 or Stix, 1992) although there will be no information concerning linear wave-wave interactions (such as reflection or mode conversion). Here we write the current density in terms of the full dielectric tensor so as

to preserve the generality of a multi-mode analysis.

As energy enters kinetic theory through the second velocity moment of the distribution function, we may obtain the rate of work done by multiplying the second order Vlasov equation by the kinetic energy ($T = \frac{1}{2}m\mathbf{v}^2$) and then integrating over all velocity space (the second velocity moment inetgral). The resulting kinetic energy theorem is(Maroli, 1988),

$$\mathbf{E} \bullet \mathbf{J} = \frac{\partial}{\partial t} \int d\mathbf{v} T(\mathbf{v}) f_2(\mathbf{r}, \mathbf{v}, t) + \nabla \bullet \int d\mathbf{v} T(\mathbf{v}) \mathbf{v} f_2(\mathbf{r}, \mathbf{v}, t). \tag{2.34}$$

The first term on the right hand side is the power absorbed by the plasma from the EM fields and includes energy dissipated. When this term is negative then it represents a flow of power from the plasma back to the field.

The second term is the kinetic power flux(or sloshing flux) flowing reversibly around the plasma. Such terms have been shown to integrate to zero across the whole plasma(Maroli, 1988, Lashmore-Davies and Dendy, 1989 and McDonald et al., 1994) indicating conservation of kinetic energy within the plasma. The above authors worked entirely within the framework of small Larmor radius particles meaning that closed, algebraic forms for the plasma response functions could be obtained.

However, in an inhomogeneous plasma containing high energy, large Larmor radius ions we are unable to deduce closed analytic forms for the terms on the right hand side of (2.31) since the plasma response is described by non-local response integrals(which will be derived in chapters 3 and 4). Our priority in this work is to quantify the absorption of energy from EM waves through wave-particle interactions and, although we will not identify explicitly the mathematical forms of the kinetic flux, the kinetic energy of the particles and the dissipation, we will derive an energy conserving wave equation which is inclusive of all of these effects and which allows us to identify the fraction of incident energy absorbed. The absorbed energy is distributed between resonant particles(in the neighbourhood of gyro-resonances) and mode-converted hot plasma waves in interaction regions. In general it is impossible to separate these two effects and we will seek to quantify the total energy transferred to the plasma.

In chapter 7 we will derive an ODE describing the spatial variation of the electric field amplitude(E_y) in the neighbourhood of a gyroresonance region which will be shown to be of the form,

$$\frac{d^2}{dx^2} E_y(x) + V(x, k_0) E_y(x) = 0,$$

where $V(x, k_0)$ is the fast wave potential function and has, folded into it, the physical make-up of the wave-particle interactions. By this we mean that effects of non-locality, thermal anisotropy and magnetic field inhomogeneity are included. In addition, the coupling of the incident fast wave to the mode-converted, hot plasma modes present in

the interaction region is also described allowing a quantification of the degree of mode-conversion. However, as a 2^{nd} order ODE this describes only the spatial variation of the fast wave and cannot give any information concerning the *propagation* of the mode-converted modes.

We will show in chapter 7 that the fast wave ODE has, associated with it, the following conservation relation,

$$\frac{\partial}{\partial x}\left[Im\{E_y^*\frac{\partial E_y}{\partial x}\}\right] \equiv -Im\{V(x,k_0)\}|E_y|^2. \tag{2.35}$$

We now demonstrate that this does indeed satisfy the law of conservation of energy.

If we average the energy balance equation over a few oscillations of the field using the mean value theorem for the average of the product of two periodic complex quantities over a few cycles,

$$\overline{\mathbf{a}(x,t)\mathbf{b}(x,t)} \equiv \frac{1}{2}Re\{\mathbf{a}^*(x)\mathbf{b}(x)\},$$

and note that terms proportional to $e^{\pm 2i\omega t}$ average to zero, then the average rate of work done on the particles is equivalent to the average EM energy flux delivered to the particles,

$$\frac{1}{2}Re\{\mathbf{E}^* \bullet \mathbf{J}\} = \frac{1}{2}Re\{\nabla \bullet \left(\frac{\mathbf{E}\times\mathbf{B}^*}{\mu_0}\right)\}. \tag{2.36}$$

For the ambient magnetic field which we are modelling ($\mathbf{B}_0 = B_0(x)\,\hat{\mathbf{z}}$) then the left hand side of (2.36) can be shown to be equivalent to,

$$\frac{1}{2}Re\{\nabla \bullet \left(\frac{\mathbf{E}\times\mathbf{B}^*}{\mu_0}\right)\} \equiv -\frac{1}{2\omega\mu_0}\frac{\partial}{\partial x}\left[Im\{E_y^*\frac{\partial E_y}{\partial x}\}\right]. \tag{2.37}$$

If we compare (2.35), (2.36) and (2.37) then we have the relation,

$$\frac{1}{2}Re\{\mathbf{E}^* \bullet \mathbf{J}\} \equiv \frac{1}{2\omega\mu_0}\frac{\partial}{\partial x}\left[Im\{E_y^*\frac{\partial E_y}{\partial x}\}\right], \tag{2.38}$$

and we see that the time-averaged work done on the plasma by the EM fields is related to the average divergence of EM flux. The right hand side of the conservation law in (2.35) is then just the average work done in accordance with the energy balance required for energy conservation. We may now discuss our conservation law of (2.35) in the light of these results and also in the more general framework of the energy balance equation of (2.29). We have shown unambiguously how the conservation relation of (2.35) comprises a balance of the time-averaged field EM flux and the time-averaged work done on the plasma,

$$< \nabla \bullet \mathbf{S} > + < W >= 0.$$

If we look back at the general energy balance equation for the plasma given by (2.29) then we need to account for all of the terms when talking about the energy conserving nature of the conservation law. We have already remarked how the rate of work done upon the plasma is divided between the kinetic power flux within the plasma, the acoustic energy of the particles and also energy dissipated by the particles. When we average over time using the mean value theorem then the energy density terms average to zero over a cycle and the time-averaged energy balance equation becomes,

$$< \nabla \bullet (\mathbf{S} + \mathbf{T}) > + < D >= 0,$$

and so the time-averaged work done on the plasma(described by the right hand side of (2.35)) contains the combined effects of the kinetic power flux and energy dissipation. In chapter 8 we will present a numerical proof of the global conservation of energy represented by (2.35).

2.4.3 Wave Polarisation

We have already described how wave energy will be strongly absorbed at a gyroresonance if a large fraction of the wave energy resides in electric fields rotating in the same sense as the resonant particles. To quantify this let us return to the local wave equation of (2.2) written in terms of the dielectric tensor of equation(2.5) which, for EM waves in a cold plasma propagating in the equatorial plane of a Tokamak($\hat{\mathbf{x}} - \hat{\mathbf{z}}$ plane) is,

$$\begin{pmatrix} \epsilon_\perp - n_\parallel^2 & \epsilon_{xy} & n_\perp n_\parallel \\ -\epsilon_{xy} & \epsilon_\perp - n_\perp^2 - n_\parallel^2 & 0 \\ n_\perp n_\parallel & 0 & \epsilon_\perp - n_\perp^2 \end{pmatrix} \begin{pmatrix} E_x \\ E_y \\ E_z \end{pmatrix} = \begin{pmatrix} 0 \\ 0 \\ 0 \end{pmatrix}. \tag{2.39}$$

Here,

$$\epsilon_\perp = 1 - \sum_s \frac{\omega_{ps}^2}{(\omega^2 - \Omega_s^2)} \equiv \epsilon_{xx} \equiv \epsilon_{yy}, \quad \epsilon_\parallel = 1 - \sum_s \frac{\omega_{ps}^2}{\omega^2} \equiv \epsilon_{zz}$$

$$\epsilon_{xy} = i \sum_s \frac{\omega_{ps}^2 \Omega_s}{\omega(\omega^2 - \Omega_s^2)} \equiv -\epsilon_{yx} \quad n_\perp = \frac{ck_\perp}{\omega} \quad n_\parallel = \frac{ck_\parallel}{\omega}.$$

If we set to zero the determinant of the matrix which pre-multiplies the electric field vector then we obtain the following dispersion relation,

$$\epsilon_\perp n_\perp^4 - \left[(\epsilon_\perp - n_\parallel^2)(\epsilon_\perp + \epsilon_\parallel) + \epsilon_{xy}^2\right] n_\perp^2 + \epsilon_\parallel \left[(\epsilon_\perp - n_\parallel^2)^2 + \epsilon_{xy}^2\right] = 0. \tag{2.40}$$

Since this is a quadratic in $n_\perp^2$ it describes the propagation of two different wave modes in the context of cold plasma theory which are the fast and slow magnetosonic waves. As described earlier, the higher mobility of the electrons compared to the ions along the electric field means that the parallel electric field is effectively shorted out and so the conductivity($\epsilon_\parallel$) of particles along $\hat{\mathbf{z}}$ will be large compared to the conductivity of particles

in the equatorial plane($\epsilon_\perp, \quad \epsilon_{xy}$). If we retain only the coefficients of $\epsilon_\parallel$ in (2.40) then we recover the fast wave dispersion relation for oblique propagation,

$$n_\perp^2 \simeq \frac{(\epsilon_\perp - n_\parallel^2)^2 + \epsilon_{xy}^2}{(\epsilon_\perp - n_\parallel^2)}, \tag{2.41}$$

which is equivalent to (2.9) and gives the hybrid resonance surface $\epsilon_\perp - n_\parallel^2 = 0$. If we return to (2.39) and write out the first and third linear equations noting the effects of high electron mobility,

$$(\epsilon_\perp - n_\parallel^2)E_x + \epsilon_{xy}E_y \simeq 0, \tag{2.42}$$

$$n_\perp n_\parallel E_x + (\epsilon_\parallel - n_\perp^2)E_z = 0, \tag{2.43}$$

then we have the following relationships between the electric field components,

$$\frac{E_z}{E_x} \simeq -\frac{n_\perp n_\parallel}{\epsilon_\parallel} \ll 1, \tag{2.44}$$

$$\frac{E_y}{E_x} \simeq -\frac{(\epsilon_\perp - n_\parallel^2)}{\epsilon_{xy}}. \tag{2.45}$$

The first ratio simply reiterates the fact that the parallel electric field is effectively shorted out due to high electron mobility along the magnetic field. The second ratio needs more careful consideration of the behaviour of the surface $\epsilon_\perp - n_\parallel^2 = 0$. Near to the 2-ion hybrid resonance, $\epsilon_\perp - n_\parallel^2 \to 0$ and so $E_y \ll E_x$. This indicates that the fast wave polarisation is predominantly longitudinal($k_\perp \perp B_0$ and $k_\perp \parallel E_x$). This is the crucial piece of physics we need regarding gyroresonant absorption. A longitudinal wave can be decomposed into a mixture of right and left- circularly polarised waves,

$$E_\pm = E_x \pm iE_y, \tag{2.46}$$

which can interact with the ions(E_+) and electrons(E_-) respectively as shown in figure 2.7.

Since, in the region of the 2-ion resonance, $E_x \gg E_y$ the magnitudes of E_+ and E_- can be large leading to strong gyroresonant absorption. The longitudinal nature of the fast wave polarisation is responsible for the coupling to ion-Bernstein modes and ion-hybrid waves which are themselves longitudinally polarised. Far away from the interaction layer, $E_x \simeq E_y$ and and the fast wave is partly transverse(E_y) and partly longitudinal(E_x) and the circular polarisation is likely to be zero meaning that the electric field of the fast wave is polarised in exactly the opposite sense to the ions and electrons and therefore cannot interact with them through gyroresonant wave-particle interactions.

Let us return to the question of how the fast wave polarisation is affected by the presence of an extra ion species. First of all let us consider a single ion species plasma. The ratio

of the transverse and longitudinal polarisations expressed by (2.45) is, for perpendicular propagation in the ICRF,

$$\frac{E_y}{E_x} \simeq \frac{-(\frac{\omega_{pi}^2}{\omega^2-\Omega_i^2} + \frac{\omega_{pe}^2}{\omega^2-\Omega_e^2})}{i(\frac{\omega_{pi}^2\Omega_i}{\omega(\omega^2-\Omega_i^2)} + \frac{\omega_{pe}^2\Omega_e}{\omega(\omega^2-\Omega_e^2)})}, \tag{2.47}$$

and since $\omega \simeq \Omega_i$ we find that the singular ion terms dominate so that,

$$i\frac{E_y}{E_x} = \frac{-(\frac{\omega_{pi}^2}{\omega^2-\Omega_i^2})}{(\frac{\omega_{pi}^2\Omega_i}{\omega(\omega^2-\Omega_i^2)})}. \tag{2.48}$$

This gives us the polarisation,

$$E_+ = E_x + iE_y \equiv 0.$$

Hence there is identically no gyroresonance at the fundamental of the ion gyrofrequency in a single ion species plasma. In a two ion species plasma(majority ion(subscript 1) and minority ion(subscript 2)) the story is completely different. The ratio of transverse to longitudinal polarisations given by (2.45) is now,

$$\frac{E_y}{E_x} \simeq \frac{-(\frac{\omega_{p1}^2}{\omega^2-\Omega_1^2} + \frac{\omega_{p2}^2}{\omega^2-\Omega_2^2} + \frac{\omega_{pe}^2}{\omega^2-\Omega_e^2})}{i(\frac{\omega_{p1}^2\Omega_1}{\omega(\omega^2-\Omega_1^2)} + \frac{\omega_{p2}^2\Omega_2}{\omega(\omega^2-\Omega_2^2)} + \frac{\omega_{pe}^2\Omega_e}{\omega(\omega^2-\Omega_e^2)})}, \tag{2.49}$$

and at the fundamental of the minority gyrofrequency $\omega \simeq \Omega_2$, we must retain both of the ion terms since $\Omega_1 \simeq \Omega_2$ giving,

$$i\frac{E_y}{E_x} = \frac{-(\frac{\omega_{p1}^2}{\omega^2-\Omega_1^2} + \frac{\omega_{p2}^2}{\omega^2-\Omega_2^2})}{(\frac{\omega_{p1}^2}{\omega^2-\Omega_1^2} + \frac{\omega_{p2}^2}{\omega^2-\Omega_2^2}(\frac{\Omega_2}{\Omega_1}))}, \tag{2.50}$$

and this time there is no cancellation due to the ratio of the ion gyrofrequencies in the denominator which cannot equal unity in a plasma containing two different ion species by definition. The degree of ion gyroresonant absorption is now dictated by the ratio of the ion species densities(due to ratios of the ion plasma frequencies) which allows E_+ to take on a large range of values. We find that there is now the possibility of gyroresonant absorption at the fundamental of the minority gyrofrequency. A kinetic treatment of wave polarisation extends this analysis so as to include the effects of additional hot plasma modes on the polarisation of the fast wave at the ion gyroresonances. The appearance of the 2-ion hybrid resonance at large minority to majority ion density ratios has destructive effects on the value of E_+ near to the minority fundamental reducing absorption. We will show this to be the case in our numerical studies in chapter 8.

Although the cold plasma analysis performed here does not include the damping of the fast wave at higher harmonics of the gyrofrequency(since these are the province of a kinetic theory), the principles are equivalent. Detailed calculations identifying the terms related to thermal effects on the wave polarisation are beyond the scope of this thesis(due to time restraints) although all of the thermal effects are included in our theoretical investigations in the following chapters.

Finally, having presented some of the basic phenomena associated with EM wave propagation in plasmas, we need to check that such waves are able to propagate under the extreme physical conditions required to achieve fusion in a Tokamak plasma. In chapter 8 we will apply our model equations to the problem of ion heating. For this an EM wave, matched to the fundamental gyrofrequency of the minority ion species(for our study we consider a $D_1^2(He_2^3)e_{-1}^0$ plasma with He_2^3 being the minority), is assumed to resonate with the minority ions in some layer of the plasma preferably in the hot, dense core.

2.4.4 Accessibility

To see this let us look more closely at the dispersion relation of the fast wave whose dispersion relation was presented in (2.9). Since resonance is a localised phenomenon(recall that $\frac{\rho}{L} \ll 1$) then we can use cold plasma theory to consider the approach of EM waves to such regions.

We have shown that the fast wave will have a low density cut-off at around $n_e \simeq 2 \times 10^{18} m^{-3}$. The density in a large Tokamak like JET falls off parabolically from a maximum of around $n_e \simeq 2 \times 10^{20} m^{-3}$ in the hot plasma core to around $n_e \simeq 1 \times 10^{17} m^{-3}$ near the plasma edge(Wesson, 1987). The fast wave will be cut-off near the plasma edge in the low density region. Provided the radio frequency antenna is situated close to the location of the cut-off, the fast wave can tunnel through to a region of propagation without much attenuation. However, we have described how, in a 2-ion species plasma, the 2-ion hybrid resonance may occur for a minority ion densities above a critical value($n_2 \leq 0.1 n_1$). We have shown how the hybrid resonance has associated with it a cut-off and so the fast wave will also have a high density cut-off near the hybrid resonance. Figure 2.8 shows the locations of the resonance and cut-off surfaces in the JET plasma. It is the hybrid cut-off which will govern the accessibility of the fast wave.

The disparity in the fast wave propagation behaviour in the minority heating regime and also the mode conversion regime is revealed in figure 2.9 and some experimental evidence of the effect of the hybrid resonance on fast wave heating from the TFTR Tokamak(which has an antenna on the high magnetic field side) is shown in figure 2.10.

The neutron counting rate gives a measure of the degree of ion heating. The counting rate is high when the hybrid resonance is situated in the plasma centre as in (a) and (c).

The counting rate is low when the proton resonance is situated in the plasma centre and the hybrid resonance is at the plasma edge as in (b). This indicates that heating is predominantly due to mode conversion rather than minority heating. Furthermore, it is clear that mode conversion is stronger in the plasma core where the density and temperature are several orders of magnitude higher than at the edge.

The Budden model, described in chapter 1, has shown how fast wave energy is distributed after crossing the interaction region. If fast wave energy is to be deposited on the resonant ions by minority heating then we must launch the fast wave from the low magnetic field where it has an unimpeded path to the minority gyroresonance. Furthermore, if the undamped fraction of fast wave energy(calculated to be at most 75%(Jacquinot, 1987)) is to be absorbed in the interaction region, the fast wave incident on the low field side must tunnel through the evanescent layer which exists on the low field side of the 2-ion hybrid resonance before being mode converted and subsequently damped on electrons. Alternatively, if the mode conversion heating scheme is to be used, the fast wave should be launched from the high magnetic field side where all of the incident energy can be mode converted. Presently, JET has only a low field side radio frequency antenna as can be seen in figure 2.11. For optimal heating, a combination of low and high field side antennae would allow efficient deposition of fast wave energy on the ions(through minority heating for low field launch) and on the electrons(through mode conversion for high field launch). In chapter 8 we will present numerical results relevant to both of these schemes. We will report our finding of a new cut-off at the low field side of the minority gyroresonance which may have profound consequences for the accessibility of the fast wave from the low field antenna.

Following this rather lengthy overview of the underlying physics of wave-particle interactions in a Tokamak in the ICRF let us now build upon this foundation by deriving a new theory which is capable of describing the interaction of radio waves with large Larmor radius ions and fusion products in a thermally anisotropic plasma immersed in an inhomogeneous magnetic field.

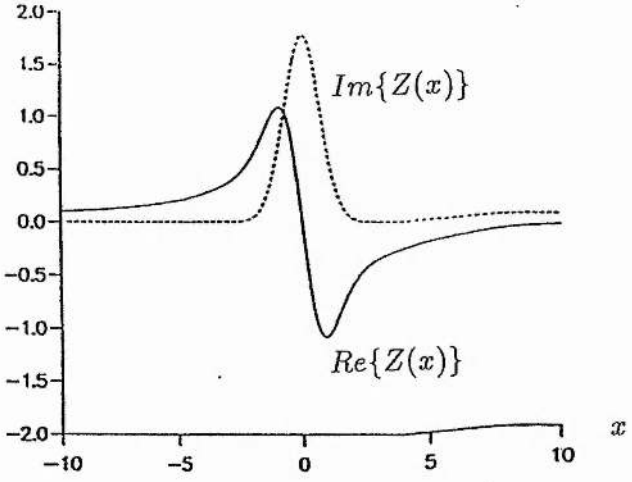

Figure 2.1: Graphical representation of the plasma dispersion function $Z(x)$ for real argument(x)(After Fried and Conte, 1961).

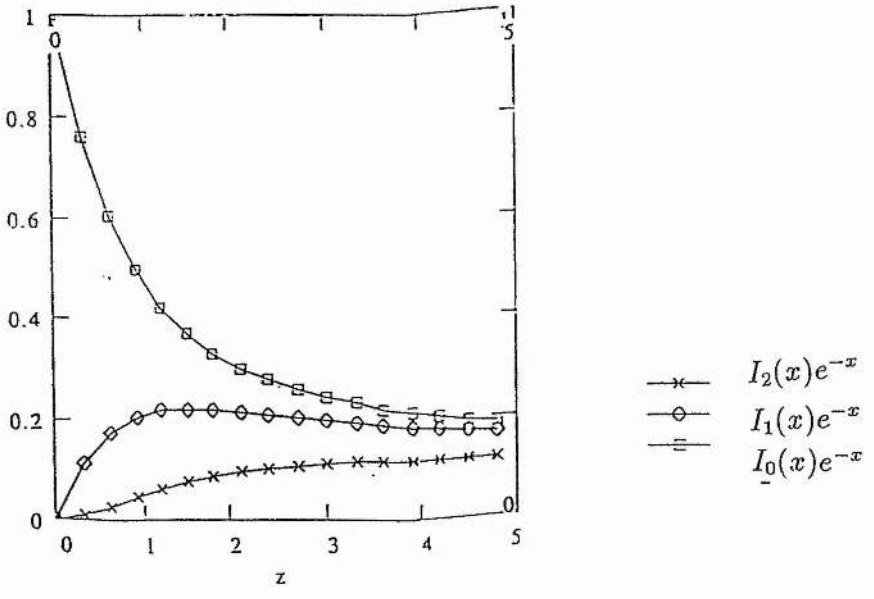

Figure 2.2: Graphical representation of the Modified Bessel function $I_n(x)$ scaled by e^{-x} for real argument(x).

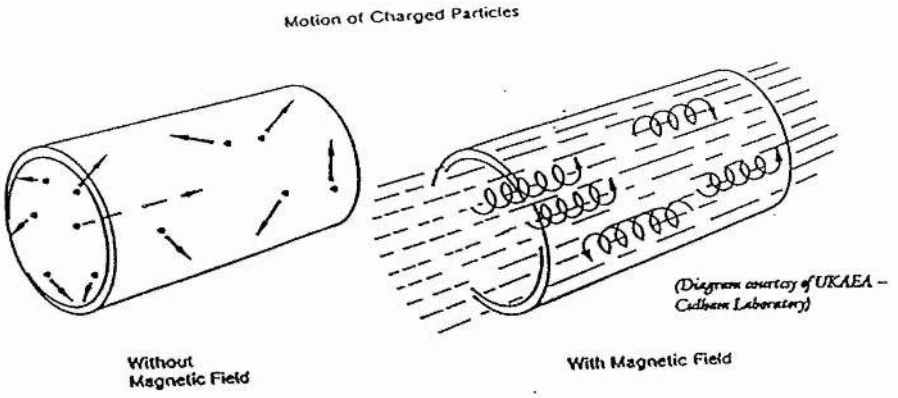

Figure 2.3: Schematic representation of the reduction of the degrees of freedom of plasma particles when immersed in a magnetic field.

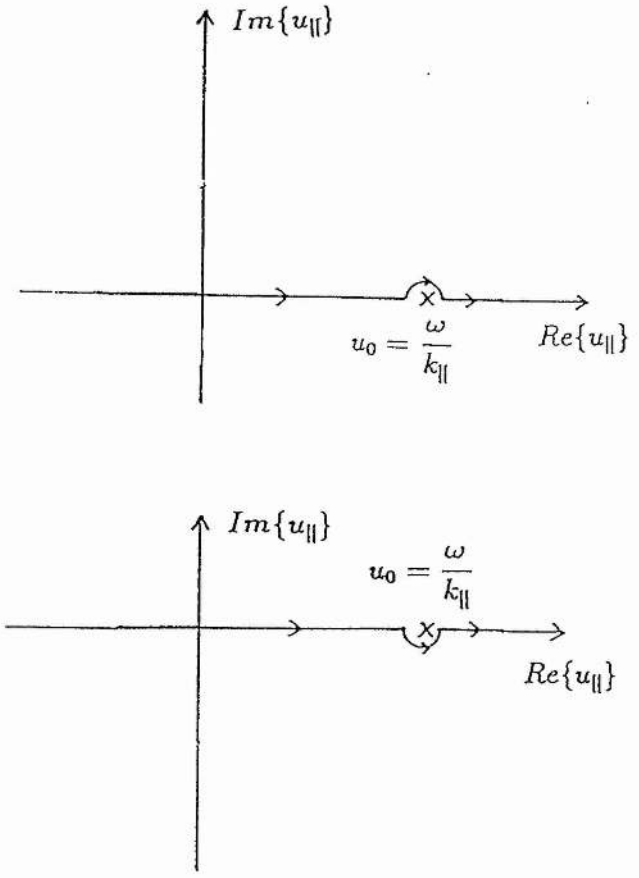

Figure 2.4: Contours of integration for the integral $I(u_0)$ in (2.28) which avoid the pole at $Re\{u_{\|}\} = u_0$.

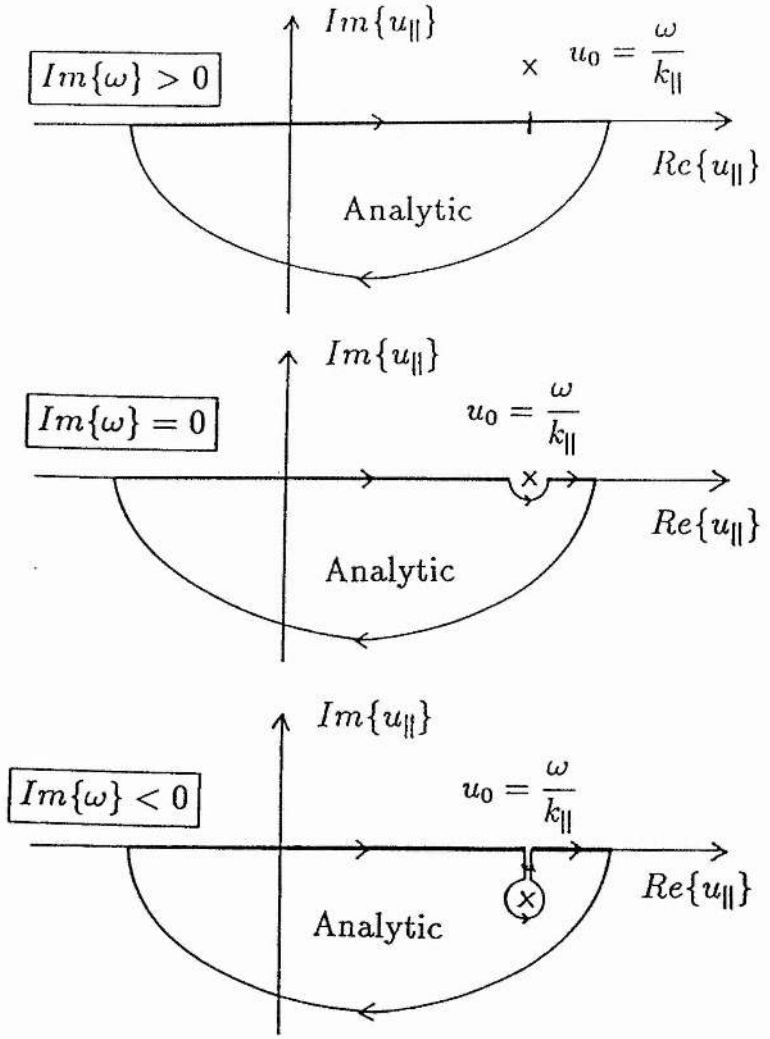

Figure 2.5: Analytic continuity for different values of $Im\{\omega\}$.

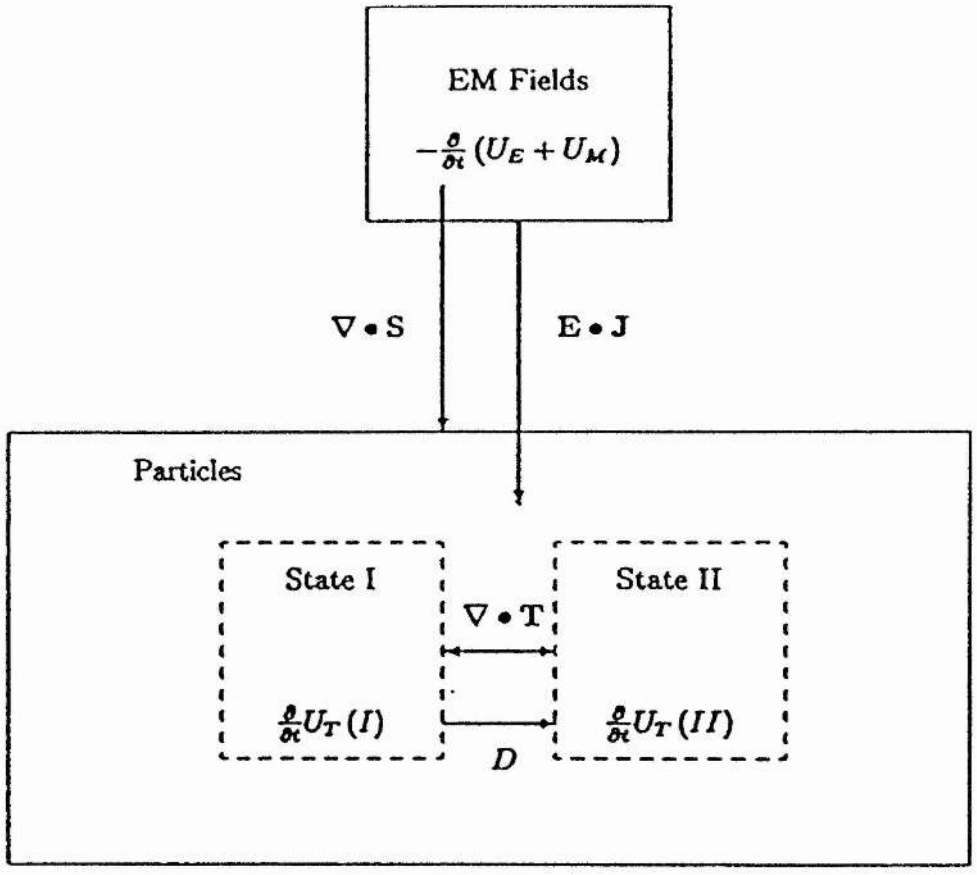

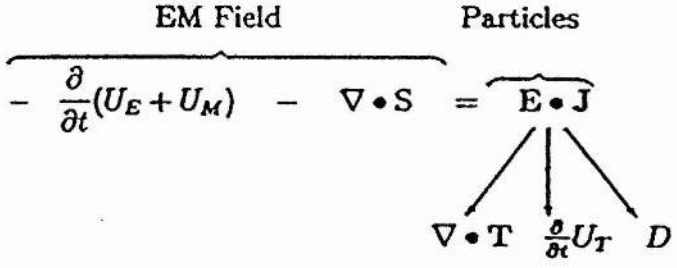

Figure 2.6: Schematic representation of the distribution of EM field energy density in the plasma.

Figure 2.7: Schematic representation of ion and electron(e^-) gyroresonance.

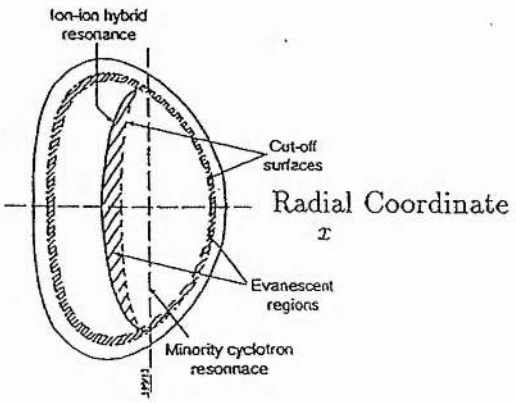

(Diagram courtesy of UKAEA – Culham Laboratory)

Figure 2.8: Schematic representation of resonance and cut-off surfaces in the JET plasma in the ICRF indicating regions of evanescence.

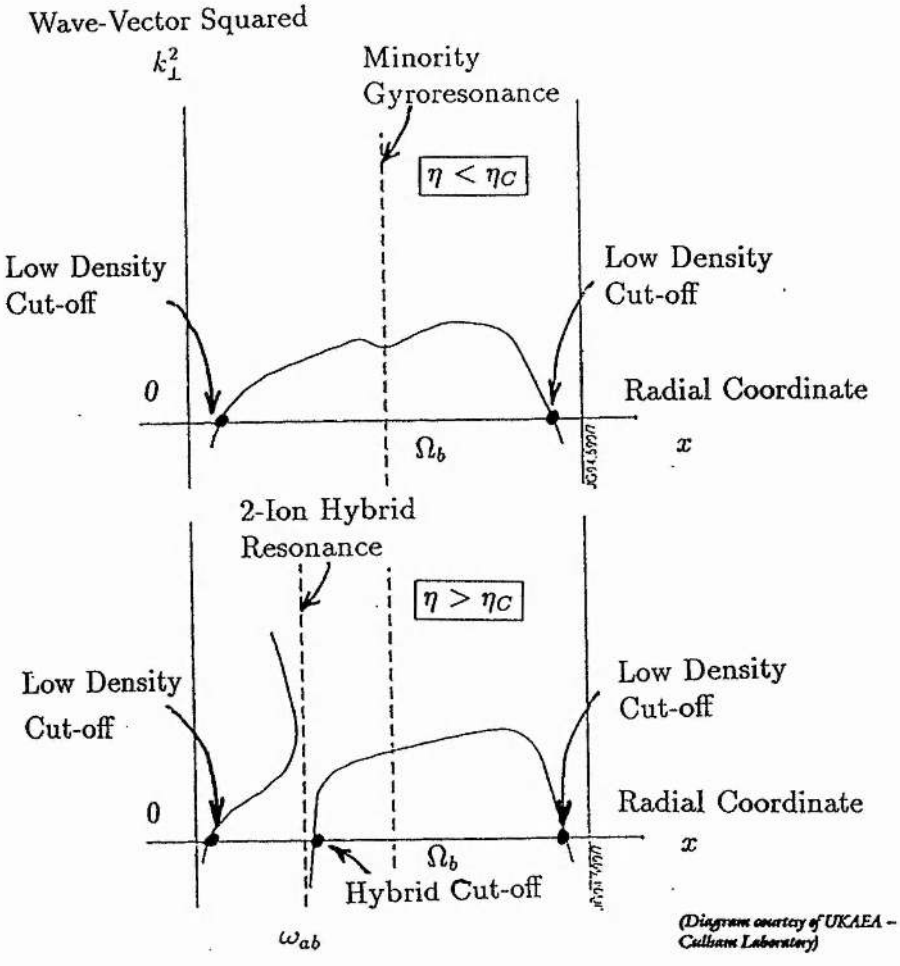

Figure 2.9: Schematic representation of the sensitivity of the 2-ion hybrid resonance to the ratio of the minority(b) to majority(a) ion density ratio(η).

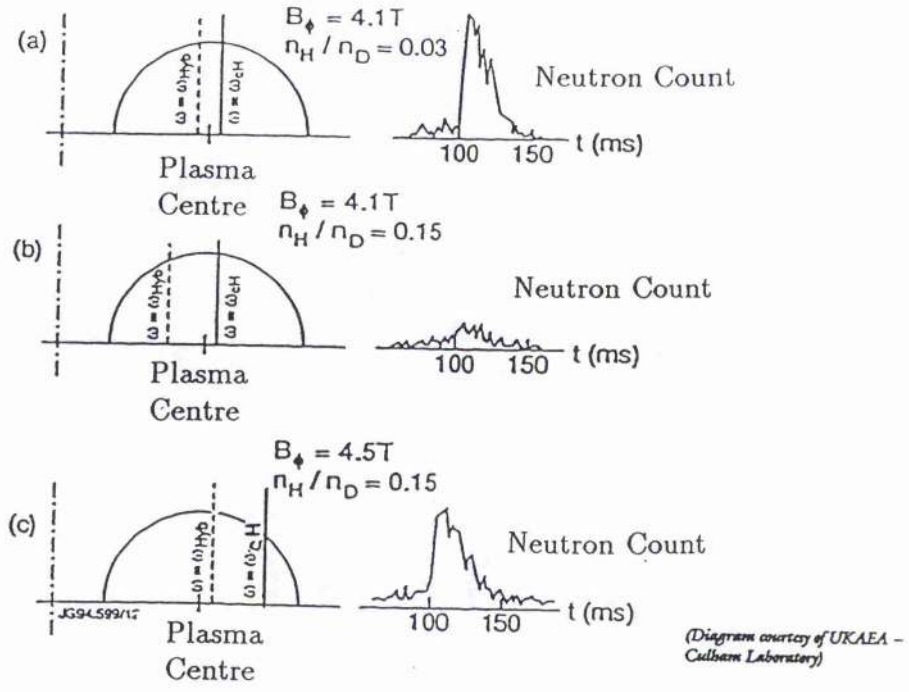

Figure 2.10: Experimental evidence of the sensitivity of ion heating ($\propto$ neutron count) to the spatial position of the 2-ion hybrid resonance(ω_{Hyb}) and to the minority gyroresonance (ω_{cH}).

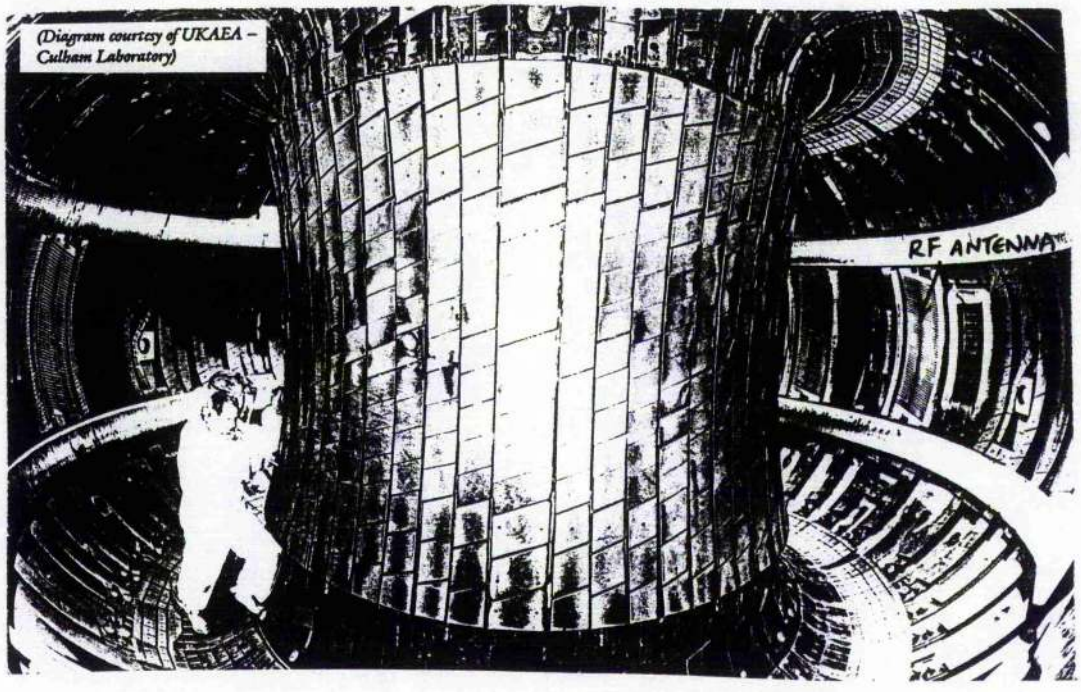

Figure 2.11: Internal view of the JET Tokamak indicating the low magnetic field side RF antenna.

Chapter 3

Waves In A Generalised Inhomogeneous Plasma

In the previous chapter we remarked that only a kinetic theory of plasma waves is fully able to describe the perpendicular gyroresonances which are present in a hot, collisionless plasma when immersed in a uniform magnetic field. We will now describe a theory which enables us to introduce into the analysis a gradient in this magnetic field and which, contrary to existing models, allows a general field profile to be used while retaining the generality of the equilibrium plasma state.

3.1 Vlasov Theory For An Inhomogeneous Plasma

Let us now work out the response of a hot anisotropic plasma to small amplitude electromagnetic waves (EM waves) when immersed in an inhomogeneous magnetic field($\mathbf{B}_0$). We will use the Vlasov theory whereby the evolution of the particle distribution(f), is governed by the Vlasov equation with the Lorentz force directing the motion of the charged particles. In essence, EM waves perturb an equilibrium state(f_0) and the response of the plasma f_1 is obtained by integrating the Vlasov equation along the unperturbed orbits of the particles. The perturbed current density and other measurable macroscopic variables are then found by taking moments of f_1. Maxwell's field equations, with the sources of charge and current density obtained in this way from the Vlasov equation, then give a self-consistent description of EM waves in the plasma.

For EM waves that are harmonic in time, varying as $e^{-i\omega t}$ with the wave frequency(ω) having an infinitessimal positive imaginary part so as to satisfy causality, then Maxwell's electromagnetic field equations may be rearranged to give the following wave equation,

$$-\frac{c^2}{\omega^2}\nabla \times (\nabla \times \mathbf{E}) + \mathbf{E} + \frac{i}{\epsilon_0 \omega}\mathbf{J} = 0. \tag{3.1}$$

We need to solve this self-consistently with the response of the plasma, in the form of the perturbed current density($\mathbf{J}$), being calculated from the first velocity moment of the

perturbed particle distribution(f) as follows,

$$\mathbf{J} = q \int d\mathbf{u} \mathbf{u} f_1. \tag{3.2}$$

The particle distribution itself is calculated from the equation of state which, for a hot collisionless plasma, is the Vlasov equation,

$$\frac{df}{dt} \equiv \{\frac{\partial}{\partial t} + \mathbf{u} \bullet \frac{\partial}{\partial \mathbf{r}} + \frac{q}{m} (\mathbf{E}(\mathbf{r},t) + \mathbf{u} \times \mathbf{B}(\mathbf{r},t)) \bullet \frac{\partial}{\partial \mathbf{u}}\} f(\mathbf{r},\mathbf{u},t) = 0, \tag{3.3}$$

describing the temporal evolution of the particle distribution f. Here $\mathbf{r}$ and $\mathbf{u}$ are points in $(\mathbf{r},\mathbf{u})$ phase space, and the velocity($\mathbf{u}$) may be written in polar coordinates with θ being the angle between $u_\perp$ and the $\hat{\mathbf{x}}$ direction so that,

$$\mathbf{u} = \hat{\mathbf{x}} u_\perp \cos\theta + \hat{\mathbf{y}} u_\perp \sin\theta + \hat{\mathbf{z}} u_{||}. \tag{3.4}$$

In the presence of small amplitude, perturbing EM waves, we may linearise with the following ordering,

$$f = f_0 + \epsilon f_1, \qquad \mathbf{E} = \epsilon \mathbf{E}, \qquad \mathbf{B} = \mathbf{B}_0 + \epsilon \mathbf{B}, \qquad \mathbf{J} = \epsilon \mathbf{J}, \tag{3.5}$$

and ϵ is a small parameter related to the scale-length of the magnetic field inhomogeneity. The ambient magnetic field($\mathbf{B}_0$) is assumed to be in the $\hat{\mathbf{z}}$ direction with a gradient in field strength along the $\hat{\mathbf{x}}$ direction, that is, $\mathbf{B}_0 = B_0(x)\,\hat{\mathbf{z}}$. In the case of weak inhomogeneities, the magnetic field can be expanded in a Taylor series and may be approximated by the first two terms,

$$\mathbf{B}_0 = \left[\sum_{n=0}^{\infty} \frac{1}{n!} (x - x_0)^n \frac{d^n B_0(x_0)}{dx^n}\right] \hat{\mathbf{z}} \simeq B_0(x_0)\,(1 + \epsilon\,(x - x_0))\,\hat{\mathbf{z}}, \tag{3.6}$$

with $\epsilon = \left(\frac{1}{B_0}\frac{dB_0}{dx}\right)_{x=x_0}$. Our plasma can be thought of as being restrained in a finite inhomogeneous slab geometry as portrayed in figure 3.1.

The plasma particle charge(q) and mass(m) will, in general, be different for different particle species in the plasma and there will be a Vlasov equation of the form of (3.3) associated with each species. In what follows we shall assume summation over contributions from all species of charged particles in the plasma.

It is well known that the Onsager reciprocal relations arise from the time reversal invariance of many microscopic phenomena in thermodynamic systems. If one reverses time in (3.3) then the Vlasov equation returns to its original form if one also changes the signs of $\mathbf{u}$ and also of $\mathbf{B}$. Thus, the Vlasov equation is invariant under the transformation,

$$t \to -t, \qquad \mathbf{u} \to -\mathbf{u}, \qquad \mathbf{B} \to -\mathbf{B}, \qquad \mathbf{r} \to \mathbf{r}, \qquad \mathbf{E} \to \mathbf{E}. \tag{3.7}$$

We shall return to these properties later on. We will show that the time reversal invariance of the microscopic plasma dynamics is lost when we use non-thermal distributions

in the macroscopic averaging process associated with taking moments.

The zero order solution of (3.3) is just the equilibrium solution,

$$\frac{q}{m}(\mathbf{u}\times\mathbf{B}_0)\bullet\frac{\partial f_0}{\partial \mathbf{u}}=0. \tag{3.8}$$

There are many possible solutions of (3.8) but they are subject to the requirement that the equilibrium distribution f_0 be constructed from the constants of the motion, which for a plasma immersed in an inhomogeneous magnetic field are: the perpendicular kinetic energy $W = mu_\perp^2/2$, the parallel momentum $p_\parallel = mu_\parallel$ and the canonical momenta: $\zeta_x = m\{u_x - \int \Omega(\mathbf{r})\,dy\}$ and $\zeta_y = m\{u_y + \int \Omega(\mathbf{r})\,dx\}$ which when divided by $m\Omega$ give the coordinates of the guiding centre. The plasma state we wish to describe has a gradient only in the $\hat{\mathbf{x}}$ direction and so the most general equilibrium distribution will be a function of $u_\perp^2, u_\parallel$ and ζ_y. In the plasma equilibrium we expect there to be a balance of magnetic pressure $\frac{B_0^2}{2\mu_0}$ and plasma pressure $2neT$. Magnetic pressure arising from a magnetic field inhomogeneity along $\hat{\mathbf{x}}$ should then be balanced by an equal and opposite plasma pressure arising from a density inhomogeneity along $\hat{\mathbf{x}}$. We wish to study the wave-particle interactions in a low β plasma, one in which the ratio of the plasma to magnetic pressures is small, and so we may approximate the density variation by a constant since its effects will not be pronounced in comparison with effects due to the magnetic field variation. To this end we may consider equilibrium distributions which are independent of the spatial coordinates ζ_x and ζ_y so that $f_0 = f_0\left(u_\perp^2, u_\parallel\right) \equiv f_0(\mathbf{u})$.

The order ϵ solution arising from (3.3) is,

$$\left(\frac{d}{dt}f_1(\mathbf{r},t,\mathbf{u})\right)_0 = -\frac{q}{m}\{\mathbf{u}\times\mathbf{B}(\mathbf{r},t)\}\bullet\frac{\partial f_0(\mathbf{u})}{\partial \mathbf{u}}. \tag{3.9}$$

The left hand side is a total time derivative along the equilibrium orbit and represents the rate of change of f_1 along the zero order trajectory in phase space. Since (3.9) is an exact differential then it may be integrated from $t' = -\infty$ to $t' = t$ along a path in $(\mathbf{r},\mathbf{u})$ phase space which coincides with the orbit of a charged particle in the equilibrium state. This method of solving differential equations is often referred to as, 'the method of characteristics' and the resultant integral is known in the literature as the Shafranov path integral(Shafranov, 1967),

$$\begin{aligned} f_1(\mathbf{r},t,\mathbf{u}) = & -\frac{q}{m}\int_{-\infty}^{t} dt'\{\mathbf{E}(\mathbf{r}',t')+\mathbf{u}'\times\mathbf{B}(\mathbf{r}',t')\}\bullet\frac{\partial f_0(\mathbf{u})}{\partial \mathbf{u}'} \\ & + f_1\{\mathbf{r}'(-\infty),\mathbf{u}'(-\infty),t'(-\infty)\}, \end{aligned} \tag{3.10}$$

and gives the development of the perturbed distribution f_1 in terms of the particle orbits in the unperturbed fields which are denoted by primes. We have replaced $f_0(\mathbf{u}')$ by $f_0(\mathbf{u})$ since these are equivalent in the equilibrium state. We will seek the time asymptotic result

when the last term in (3.10) vanishes so that we can neglect the effect of initial conditions. We follow a method, first proposed by Antonsen and Manheimer(1978), whereby we express the EM fields in terms of their Fourier modes with amplitudes equal to the Fourier coefficients(indicated by a bar),

$$\mathbf{E}(\mathbf{r}',t') = \int d\mathrm{k}\overline{\mathbf{E}}(\mathrm{k})\, e^{i\mathbf{k}\bullet\mathbf{r}-i\omega t} e^{i\mathbf{k}\bullet(\mathbf{r}'-\mathbf{r})-i\omega(t'-t)}, \tag{3.11}$$

so that the charged particle orbits undergo a Fourier transformation.

For generality we would like to describe EM waves propagating in arbitrary directions, making an angle ϕ with $\mathbf{B}_0$ and an angle ψ with the direction of the inhomogeneity along $\hat{\mathbf{x}}$. A suitable choice of wavevector is then,

$$\mathrm{k} = \hat{\mathbf{x}}k_\perp \cos\psi + \hat{\mathbf{y}}k_\perp \sin\psi + \hat{\mathbf{z}}k_{||}, \tag{3.12}$$

having the geometry represented in figure 3.2.

Maxwell's induction equation conveniently allows us to express $\mathbf{B}$ in terms of $\mathbf{E}$ as follows,

$$\mathbf{B}(\mathbf{r}',t') = \frac{1}{\omega}\mathrm{k}\times\mathbf{E}(\mathbf{r}',t'), \tag{3.13}$$

which, by virtue of an identity from vector analysis: $\mathbf{A}\times(\mathbf{B}\times\mathbf{C}) \equiv \mathbf{B}(\mathbf{A}\bullet\mathbf{C}) - \mathbf{C}(\mathbf{A}\bullet\mathbf{B})$, enables us to rewrite the Lorentz force as a sole function of the electric field. The perturbed distribution may then be written as,

$$\begin{aligned} f_1(\mathbf{r},t,\mathbf{u}) = \; & -\frac{q}{m}\int d\mathrm{k} e^{i\mathbf{k}\bullet\mathbf{r}-i\omega t}\int_{-\infty}^{t} dt' e^{i\mathbf{k}\bullet(\mathbf{r}'-\mathbf{r})-i\omega(t'-t)} \\ & \times \left(\left[\delta_{ij}\left(1-\frac{\mathbf{u}'\bullet\mathrm{k}}{\omega}\right)+\frac{\mathbf{u}'\mathrm{k}}{\omega}\right]\bullet\overline{\mathbf{E}}(\mathrm{k})\right)\bullet\frac{\partial f_0(\mathbf{u})}{\partial\mathbf{u}'}. \end{aligned} \tag{3.14}$$

The perturbed distribution f_1 therefore arises naturally as the space-time correlation of the charged particle motion and the guiding centre. We have a vector quantity in the large bracket of (3.14) since we have the product of a tensor(square bracket) and a vector($\overline{\mathbf{E}}$). We identify the tensor as the Lorentz force tensor(L_{ij}). If we rewrite (3.14) in terms of the time $\tau = t'-t$ and introduce the quantity $\mathbf{R} = \mathbf{r}'-\mathbf{r}$ then the Fourier coefficient is,

$$\overline{f}_1(\mathrm{k},t,\mathbf{u}) = -\frac{q}{m}\int_{-\infty}^{0} d\tau e^{i\mathbf{k}\bullet\mathbf{R}-i\omega\tau}\left(L_{ij}(\mathrm{k},\mathbf{u}')\bullet\frac{\partial f_0(\mathbf{u})}{\partial\mathbf{u}'}\right)\bullet\overline{\mathbf{E}}(\mathrm{k}). \tag{3.15}$$

To proceed further we need to specify the orbit equations for charged particles in the equilibrium state of an inhomogeneous plasma.

3.2 Particle Orbits In The Equilibrium State

In the equilibrium state we know that charged particles move under the influence of the Lorentz force, winding around the magnetic field in helical orbits with gyrofrequency $\Omega(x) = qB_0(x)/m$. This physical situation is the equilibrium, unperturbed state and is described by the solutions of the following equations of motion,

$$\frac{\partial \mathbf{r}'}{\partial t'} = \mathbf{u}', \tag{3.16}$$

$$\frac{\partial \mathbf{u}'}{\partial t'} = \frac{q}{m}\{\mathbf{u}' \times \mathbf{B}_0(\mathbf{r}')\} \equiv \mathbf{u}' \times \Omega(\mathbf{r}')\hat{\mathbf{z}}, \tag{3.17}$$

with boundary conditions,

$$\mathbf{r}'(t' = t) = \mathbf{r}, \qquad \mathbf{u}'(t' = t) = \mathbf{u}. \tag{3.18}$$

If we recall the form of the weakly inhomogeneous magnetic field given in (3.6) then we see that the gyrofrequency can be represented by,

$$\Omega(x') \simeq \Omega(x)[1 + \epsilon(x' - x)]. \tag{3.19}$$

The particle orbit equations are then found by iterating (3.16) and (3.17) in the small parameter ϵ. To order ϵ, we obtain the following orbit equations as solutions when we utilise the above approximation to the gyrofrequency,

$$x' = x + \frac{u_\perp}{\Omega}\{\sin(\Omega\tau - \theta) + \sin\theta\}, \tag{3.20}$$

$$y' = y + \frac{u_\perp}{\Omega}\{\cos(\Omega\tau - \theta) - \cos\theta\} - \epsilon\frac{u_\perp^2\tau}{2\Omega}, \tag{3.21}$$

$$z' = z + u_\parallel\tau, \tag{3.22}$$

$$t' = t + \tau, \tag{3.23}$$

$$u_x' = u_\perp\cos(\Omega\tau - \theta), \tag{3.24}$$

$$u_y' = -u_\perp\sin(\Omega\tau - \theta) - \epsilon\frac{u_\perp^2}{2\Omega}, \tag{3.25}$$

$$u_z' = u_\parallel. \tag{3.26}$$

The constants of integration were chosen so that at time $t' = t$ then $\mathbf{u}' \to \mathbf{u}$ and $\mathbf{r}' \to \mathbf{r}$. Since $\epsilon \propto 1/L$ and the Larmor radius $\rho \simeq u_\perp/\Omega$ then these orbit equations are correct to order ρ/L with the ordering of (2.21).

In a weakly inhomogeneous magnetic field we see that the particle orbits are still helical in nature as is the case for a homogeneous field. The orbits are, however, subjected to drifts proportional to ϵ. The equilibrium orbits are inherently nonlinear since, in the inhomogeneous magnetic field, the gyrofrequency(Ω) is a function of x' which is itself

a function of Ω so that the orbit equations are built up iteratively. As a next step, instead of taking the charged particle orbits correct to order ϵ, we now consider only the most important contribution of the inhomogeneity to the orbits namely the nonlinear correction to the gyrofrequency $\Omega(x')$. Elsewhere than in the rapidly varying phase factors, $\Omega(x')$ can be approximated by $\Omega(x)$ where, $\Omega(x) = \Omega_0(x_0)(1 + \epsilon(x - x_0))$. We may choose the coordinate system in order to write our expressions around the position $x_0 = 0$ so that in the non-rapidly varying terms we put, $\Omega_0(x) = \Omega_0(0)(1 + \epsilon x)$, with $\Omega_0(0) = qB_0(0)/m$. If we evaluate the gyrofrequency $\Omega(x')$ at the $\hat{\mathbf{x}}$ coordinate of the guiding centre position(x_g),

$$x_g(x) = x + \frac{u_\perp}{\Omega_0(x)} \sin\theta, \tag{3.27}$$

then we may define,

$$\Omega_g(x) = \Omega\{x' = x_g(x)\} = \Omega_0(x) + \epsilon u_\perp \sin\theta. \tag{3.28}$$

The nonlinear correction arising from the magnetic field gradient is seen to be $\epsilon u_\perp \sin\theta$.

We are performing a linear perturbative analysis and it will be shown in a later chapter that this first iteration is both necessary and sufficient to provide energy conserving wave equations. If $\epsilon = 0$ then the orbit equations reduce to the traditional orbits in a homogeneous magnetic field. We note here that there is a secular term in the $\hat{\mathbf{y}}$ direction which arises from the macroscopic drift motion of charged particles in an inhomogeneous magnetic field, commonly known as, 'the grad **B** drift'. Since we are primarily interested in the non-local nature of wave-particle interactions arising from thermal anisotropy and magnetic field inhomogeneity, let us consider the less general case of EM waves propagating directly into the magnetic field gradient in the $\hat{\mathbf{x}} - \hat{\mathbf{z}}$ plane so that drift effects are not included. This does not mean that they are negligible. Indeed it is well known how drift terms affect the dispersion properties of low frequency EM waves in a homogeneous plasma. The drift effects are most easily filtered out by setting $\psi = 0$ in (3.12) so that,

$$\mathrm{k} = \left(k_\perp, 0, k_\parallel\right)^T, \tag{3.29}$$

and the orbits in the absence of drift effects are,

$$\mathbf{r}' = \mathbf{r} + \hat{\mathbf{x}}\frac{u_\perp}{\Omega_0}\{\sin(\Omega_g\tau - \theta) + \sin\theta\} + \hat{\mathbf{y}}\frac{u_\perp}{\Omega_0}\{\cos(\Omega_g\tau - \theta) - \cos\theta\} + \hat{\mathbf{z}}u_\parallel\tau, \tag{3.30}$$

$$t' = t + \tau, \tag{3.31}$$

$$\mathrm{u}' = \hat{\mathbf{x}}u_\perp\cos(\Omega_g\tau - \theta) - \hat{\mathbf{y}}u_\perp\sin(\Omega_g\tau - \theta) + \hat{\mathbf{z}}u_\parallel, \tag{3.32}$$

It is these orbit equations which we must use in the calculation of the perturbed distribution $\overline{f}_1$ given by (3.15).

3.3 Calculation Of The Generalised Conductivity Tensor

We may now use the orbit equations (3.29) up to (3.32) to write the perturbed distribution explicitly. If we define the argument $b = \frac{k_\perp u_\perp}{\Omega_0}$ then in (3.15),

$$e^{i\mathbf{k}\bullet\mathbf{R}-i\omega\tau} = e^{ib\{\sin(\Omega_g\tau-\theta)+\sin\theta\}-i\left(\omega-k_\parallel u_\parallel\right)\tau}. \tag{3.33}$$

We see that the Fourier transformation of the particle orbits in (3.11) has produced a $\sin(\Omega_g\tau-\theta)$ term in the exponential, oscillating rapidly on the timescale of the gyrofrequency. This will ultimately be responsible for the appearance of gyroresonances.

The constants of the motion from which f_0 is constructed are, $u_\perp = \sqrt{u_x'^2+u_y'^2}$ and $u_\parallel = u_z'$, and the gradient of the equilibrium distribution is calculated from them to be,

$$\frac{\partial f_0}{\partial \mathbf{u}'} = \left(\frac{\partial f_0}{\partial u_\perp}\frac{u_x'}{u_\perp}, \frac{\partial f_0}{\partial u_\perp}\frac{u_y'}{u_\perp}, \frac{\partial f_0}{\partial u_\parallel}\right)^T. \tag{3.34}$$

In addition, the Lorentz force tensor L_{ij} has the following explicit form,

$$L_{ij} = \begin{bmatrix} 1-\frac{k_\parallel u_\parallel}{\omega} & 0 & \frac{k_\parallel u_x'}{\omega} \\ \frac{k_\perp u_y'}{\omega} & 1-\frac{\left(k_\perp u_x'+k_\parallel u_\parallel\right)}{\omega} & \frac{k_\parallel u_y'}{\omega} \\ \frac{k_\perp u_\parallel}{\omega} & 0 & 1-\frac{k_\perp u_x'}{\omega} \end{bmatrix}. \tag{3.35}$$

We may now write down the Fourier coefficient of the perturbed distribution,

$$\begin{aligned} \overline{f}_1(\mathbf{k},t,\mathbf{u}) = \; & -\frac{q}{m}\int_{-\infty}^{0} d\tau e^{ib\{\sin(\Omega_g(x)\tau-\theta)+\sin\theta\}-i\left(\omega-k_\parallel u_\parallel\right)\tau} \\ & \times \begin{pmatrix} \frac{u_x'}{u_\perp}\frac{\partial f_0}{\partial u_\perp} + \frac{k_\parallel u_x'}{\omega}\left(\frac{\partial f_0}{\partial u_\parallel} - \frac{u_\parallel}{u_\perp}\frac{\partial f_0}{\partial u_\perp}\right) \\ \frac{u_y'}{u_\perp}\frac{\partial f_0}{\partial u_\perp} + \frac{k_\parallel u_y'}{\omega}\left(\frac{\partial f_0}{\partial u_\parallel} - \frac{u_\parallel}{u_\perp}\frac{\partial f_0}{\partial u_\perp}\right) \\ \frac{\partial f_0}{\partial u_\parallel} - \frac{k_\perp u_x'}{\omega}\left(\frac{\partial f_0}{\partial u_\parallel} - \frac{u_\parallel}{u_\perp}\frac{\partial f_0}{\partial u_\perp}\right) \end{pmatrix} \bullet \begin{pmatrix} \overline{E}_x(\mathbf{k}) \\ \overline{E}_y(\mathbf{k}) \\ \overline{E}_z(\mathbf{k}) \end{pmatrix}. \end{aligned} \tag{3.36}$$

The helical motion of the charged particles motivates a coordinate transformation from Cartesian to cylindrical velocity coordinates where the volume element is $du_\perp u_\perp d\theta du_\parallel$. The Jacobian is identified as $u_\perp$ and in this system of coordinates, the current density is from (1.2),

$$\mathbf{J}(\mathbf{r}) = -\frac{q^2}{m}\int d\mathbf{k} e^{i\mathbf{k}\bullet\mathbf{r}-i\omega t}\int_0^\infty du_\perp u_\perp \int_0^{2\pi} d\theta \int_L du_\parallel \int_{-\infty}^{0} d\tau e^{ib\{\sin(\Omega_g\tau-\theta)+\sin\theta\}-i\left(\omega-k_\parallel u_\parallel\right)\tau}$$

$$\times \left[\begin{pmatrix} u_x \\ u_y \\ u_z \end{pmatrix} \begin{pmatrix} \frac{u'_x}{u_\perp}\frac{\partial f_0}{\partial u_\perp} + \frac{k_\parallel u'_x}{\omega}\left(\frac{\partial f_0}{\partial u_\parallel} - \frac{u_\parallel}{u_\perp}\frac{\partial f_0}{\partial u_\perp}\right) \\ \frac{u'_y}{u_\perp}\frac{\partial f_0}{\partial u_\perp} + \frac{k_\parallel u'_y}{\omega}\left(\frac{\partial f_0}{\partial u_\parallel} - \frac{u_\parallel}{u_\perp}\frac{\partial f_0}{\partial u_\perp}\right) \\ \frac{\partial f_0}{\partial u_\parallel} - \frac{k_\perp u'_x}{\omega}\left(\frac{\partial f_0}{\partial u_\parallel} - \frac{u_\parallel}{u_\perp}\frac{\partial f_0}{\partial u_\perp}\right) \end{pmatrix} \right] \bullet \begin{pmatrix} \overline{E}_x(\mathbf{k}) \\ \overline{E}_y(\mathbf{k}) \\ \overline{E}_z(\mathbf{k}) \end{pmatrix}, \tag{3.37}$$

and here L is the Landau contour described in chapter 2. The Jacobian $u_\perp$ may be included in the square bracket of (3.37) which is now of tensorial form and we may associate the new bracket with a velocity tensor $V_{ij}(\mathbf{k}, \mathbf{u}, \mathbf{u}')$. $\mathbf{J}$ can now be written as follows,

$$\mathbf{J}(\mathbf{r}) = \int d\mathbf{k} e^{i\mathbf{k}\bullet\mathbf{r} - i\omega t} \sigma_{ij}(x, \mathbf{k}) \bullet \overline{\mathbf{E}}(\mathbf{k}), \tag{3.38}$$

and σ_{ij} is the conductivity tensor defined by,

$$\sigma_{ij}(x, \mathbf{k}) = -\frac{q^2}{m} \int_0^\infty du_\perp \int_0^{2\pi} d\theta \int_L du_\parallel \int_{-\infty}^0 d\tau e^{ib\{\sin(\Omega_g(x)\tau - \theta) + \sin\theta\} - i\left(\omega - k_\parallel u_\parallel\right)\tau} V_{ij}(\mathbf{k}, \mathbf{u}, \mathbf{u}'). \tag{3.39}$$

Equation (3.38) may be thought of as the continuous analogue of Ohm's law.

We may now write out the elements of V_{ij} in full if we express $\mathbf{u}$ and $\mathbf{u}'$ in cylindrical coordinates using (3.4) and (3.32),

$$V_{ij} = \begin{bmatrix} u_\perp^2 \cos\theta \cos(\Omega_g\tau - \theta) F_1 & -u_\perp^2 \cos\theta \sin(\Omega_g\tau - \theta) F_1 & u_\perp^2 \cos\theta F_2 \\ u_\perp^2 \sin\theta \cos(\Omega_g\tau - \theta) F_1 & -u_\perp^2 \sin\theta \sin(\Omega_g\tau - \theta) F_1 & u_\perp^2 \sin\theta F_2 \\ u_\perp u_\parallel \cos(\Omega_g\tau - \theta) F_1 & -u_\perp u_\parallel \sin(\Omega_g\tau - \theta) F_1 & u_\perp u_\parallel F_2 \end{bmatrix}, \tag{3.40}$$

and here we have introduced the following functional dependences on f_0,

$$F_1 = \frac{\partial f_0}{\partial u_\perp} + \frac{k_\parallel u_\perp}{\omega}\left(\frac{\partial f_0}{\partial u_\parallel} - \frac{u_\parallel}{u_\perp}\frac{\partial f_0}{\partial u_\perp}\right), \tag{3.41}$$

$$F_2 = \frac{\partial f_0}{\partial u_\parallel} - \frac{k_\perp u_\perp}{\omega}\cos(\Omega_g\tau - \theta)\left(\frac{\partial f_0}{\partial u_\parallel} - \frac{u_\parallel}{u_\perp}\frac{\partial f_0}{\partial u_\perp}\right). \tag{3.42}$$

The integrations appear formidable but, thanks to the Fourier Bessel identities from the theory of Bessel functions, we may remove the trigonometric dependence upon θ in the exponentials of (3.39) as follows,

$$e^{iX\sin Y} \equiv \sum_n J_n(X) e^{inY}, \tag{3.43}$$

$$\cos Y e^{iX\sin Y} \equiv \sum_n \frac{n}{X} J_n(X) e^{inY}, \tag{3.44}$$

$$\sin Y e^{iX\sin Y} \equiv -i\sum_n J'_n(X) e^{inY}, \tag{3.45}$$

enabling us to identify the following relations,

$$A\left(\Omega_g\tau-\theta,\theta\right)e^{ib\{\sin(\Omega_g\tau-\theta)+\sin\theta\}}=\sum_l\sum_m A_{l,m}\left(b\right)e^{il\Omega_g\tau}e^{i(m-l)\theta}, \tag{3.46}$$

with $A\left(\Omega_g\tau-\theta,\theta\right)$ representing combinations of trigonometric functions which have arisen from the particle velocity when expressed in cylindrical coordinates, and $A_{l,m}\left(b\right)$ being the resulting combination of Bessel functions and their derivatives. We may summarize these forms in the following table,

$A\left(\Omega_g\tau-\theta,\theta\right)$	$A_{l,m}\left(b\right)$
1	J_lJ_m
$\sin\theta$	$-iJ_lJ'_m$
$\cos\theta$	$\frac{m}{b}J_lJ_m$
$\sin\left(\Omega_g\tau-\theta\right)$	$-iJ'_lJ_m$
$\cos\left(\Omega_g\tau-\theta\right)$	$\frac{l}{b}J_lJ_m$
$\sin\left(\Omega_g\tau-\theta\right)\sin\theta$	$-J'_lJ'_m$
$\sin\left(\Omega_g\tau-\theta\right)\cos\theta$	$-\frac{im}{b}J'_lJ_m$
$\cos\left(\Omega_g\tau-\theta\right)\sin\theta$	$-\frac{il}{b}J_lJ'_m$
$\cos\left(\Omega_g\tau-\theta\right)\cos\theta$	$\frac{lm}{b^2}J_lJ_m$

In this way Bessel functions arise naturally from the orbit equations of a plasma immersed in an inhomogeneous magnetic field. In addition, we see that a summation over all harmonics(l) of the gyrofrequency $\Omega_g\left(x\right)$ is intrinsic to this analysis arising naturally from the Fourier transform of the orbits. The conductivity tensor of (3.39) may then be expressed in a form independent of trigonometric functions,

$$\sigma_{ij}\left(x,\mathbf{k}\right)=-\frac{q^2}{m}\sum_l\sum_m\int_0^\infty du_\perp\int_0^{2\pi}d\theta e^{i(m-l)\theta}\int_L du_\parallel\int_{-\infty}^0 d\tau e^{-i\left(\omega-l\Omega_g(x)-k_\parallel u_\parallel\right)\tau}V_{ij}\left(\mathbf{k},\mathbf{u}\right), \tag{3.47}$$

where,

$$V_{ij}=\begin{bmatrix} u_\perp^2\frac{lm}{b^2}J_lJ_mF_1 & iu_\perp^2\frac{m}{b}J'_lJ_mF_1 & u_\perp^2\frac{m}{b}J_lJ_mF_2 \\ -iu_\perp^2\frac{l}{b}J_lJ'_mF_1 & u_\perp^2J'_lJ'_mF_1 & -iu_\perp^2J_lJ'_mF_2 \\ u_\perp u_\parallel\frac{l}{b}J_lJ_mF_1 & iu_\perp u_\parallel J'_lJ_mF_1 & u_\perp u_\parallel J_lJ_mF_2 \end{bmatrix}, \tag{3.48}$$

and if we note that $\frac{k_\perp u_\perp}{\omega}\frac{l}{b}=\frac{l\Omega_0}{\omega}$ then,

$$F_1 = \frac{\partial f_0}{\partial u_\perp}+\frac{k_\parallel u_\perp}{\omega}\left(\frac{\partial f_0}{\partial u_\parallel}-\frac{u_\parallel}{u_\perp}\frac{\partial f_0}{\partial u_\perp}\right)\equiv\left(\frac{\omega-k_\parallel u_\parallel}{\omega}\right)\frac{\partial f_0}{\partial u_\perp}+\frac{k_\parallel u_\parallel}{\omega}\frac{u_\perp}{u_\parallel}\frac{\partial f_0}{\partial u_\parallel}, \tag{3.49}$$

$$F_2 = \frac{\partial f_0}{\partial u_\parallel}-\frac{l\Omega_0}{\omega}\left(\frac{\partial f_0}{\partial u_\parallel}-\frac{u_\parallel}{u_\perp}\frac{\partial f_0}{\partial u_\perp}\right)\equiv\left(\frac{\omega-l\Omega_g}{\omega}\right)\frac{\partial f_0}{\partial u_\parallel}+\frac{l\Omega_0}{\omega}\frac{u_\parallel}{u_\perp}\frac{\partial f_0}{\partial u_\perp}. \tag{3.50}$$

The first term on the right hand sides of (3.49) and (3.50) comes from the wave electric field while the other terms are from the wave magnetic field and vanish in the limit of an isotropic plasma when $\frac{\partial f_0}{\partial u_\perp} - \frac{u_\perp}{u_\parallel}\frac{\partial f_0}{\partial u_\parallel} \equiv 0$ so that $F_1 \to \frac{\partial f_0}{\partial u_\perp}$ and $F_2 \to \frac{\partial f_0}{\partial u_\parallel}$.

It will be instructive to compare the terms coming from the wave electric field with those coming from the wave magnetic field. We may perform a back of the envelope calculation to get an idea of their relative magnitudes. Using (3.13) we may write the magnetic field in terms of the electric field so that the Lorentz force may be written as,

$$\mathbf{E} + \mathbf{u} \times \mathbf{B} \equiv \mathbf{E} + \frac{1}{\omega}\mathbf{u} \times \mathbf{k} \times \mathbf{E} \simeq 1 : \frac{k_\perp u_\perp}{\omega} \simeq 1 : \frac{u_T}{c}\frac{c}{c_A}. \tag{3.51}$$

Now for a classical nonrelativistic plasma then $u_T \ll c$ and c can be large compared to c_A and so, in general, we cannot say that the wave electric field term is dominant over the additional terms in an anisotropic plasma associated with the wave magnetic field.

We are now able to perform the τ-integral which, if we note that the wave frequency has a positive, infinitesimal imaginary part by causality then we find,

$$\sigma_{ij}(x, \mathbf{k}) = -i\frac{q^2}{m}\sum_l \sum_m \int_0^\infty du_\perp \int_0^{2\pi} d\theta e^{i(m-l)\theta} \int_L du_\parallel \frac{V_{ij}(\mathbf{k}, \mathbf{u})}{\left(\omega - l\Omega_g(x) - k_\parallel u_\parallel + i0\right)}. \tag{3.52}$$

In (3.52), the denominator is often referred to as the 'resonant denominator' since its zero leads to a simple pole type of singularity. Fortunately for us, the values of the physical parameters which bring about this interesting, and indeed important, resonant behaviour lie within the parameter range of application of our theory to hot thermonuclear fusion plasmas. As the singularity arises from a zero of a function, small differences in quantities around the zero value of the denominator will lead to important corrections. It is at this point that the order ϵ correction to the gyrofrequency, arising from the magnetic field inhomogeneity, shows its true colours. The resonance condition is given by,

$$\omega - l\Omega_g(x) - k_\parallel u_\parallel = 0. \tag{3.53}$$

If an EM wave of frequency ω is launched into the plasma, matched to the l^{th} harmonic of the gyrofrequency at a position x then, since the gyrofrequency is $\Omega_g(x) = \Omega_0(x) + \epsilon u_\perp \sin\theta$, the resonance condition may be satisfied over a range of values of x and may be written explicitly as,

$$\omega - l\Omega_0(x) - k_\parallel u_\parallel - l\epsilon u_\perp \sin\theta = 0, \tag{3.54}$$

differing from locally uniform models by the nonlinear correction $-l\epsilon u_\perp \sin\theta$. We will show in chapter 7 how this correction, often named, 'the gyrokinetic(GK) correction', is absolutely necessary for the creation of energy conserving wave equations.

The GK correction is also present in $F_2(3.50)$ and greatly complicates the form of the velocity tensor. We may circumvent this by a neat trick proposed by Stix(1992). We use the difference $u_\perp F_2 - u_\parallel F_1$ to eliminate F_2 in favour of F_1,

$$u_\perp F_2 = u_\parallel F_1 + \frac{\left(\omega - l\Omega_g - k_\parallel u_\parallel\right)}{\omega}\left(u_\perp \frac{\partial f_0}{\partial u_\parallel} - u_\parallel \frac{\partial f_0}{\partial u_\perp}\right). \tag{3.55}$$

The pre-multiplying velocity components are crucial since only this combination leads to a cancellation of the resonant denominator and the GK correction which it possesses. The conductivity may now be expressed as,

$$\sigma_{ij}(x,\mathbf{k}) = -i\frac{q^2}{m}\sum_l \sum_m \int_0^\infty du_\perp \int_0^{2\pi} d\theta e^{i(m-l)\theta} \int_L du_\parallel \{\frac{F_1 V_{ij}(\mathbf{k},\mathbf{u})}{D_l(x)} + N_{3j}(\mathbf{k},\mathbf{u})\}, \tag{3.56}$$

and if we note that $b = \frac{k_\perp u_\perp}{\Omega_0}$ then,

$$V_{ij} = \begin{bmatrix} \frac{lm\Omega_0^2}{k_\perp^2} J_l J_m & iu_\perp \frac{m\Omega_0}{k_\perp} J_l' J_m & u_\parallel \frac{m\Omega_0}{k_\perp} J_l J_m \\ -iu_\perp \frac{l\Omega_0}{k_\perp} J_l J_m' & u_\perp^2 J_l' J_m' & -iu_\perp u_\parallel J_l J_m' \\ u_\parallel \frac{l\Omega_0}{k_\perp} J_l J_m & iu_\perp u_\parallel J_l' J_m & u_\parallel^2 J_l J_m \end{bmatrix}. \tag{3.57}$$

The resonant denominator is,

$$D_l(x) = \omega - l\Omega_g(x) - k_\parallel u_\parallel + i0, \tag{3.58}$$

and we identify the non-resonant remainder in (3.36) as,

$$N_{3j} = \frac{\left(u_\perp \frac{\partial f_0}{\partial u_\parallel} - u_\parallel \frac{\partial f_0}{\partial u_\perp}\right)}{\omega} \begin{bmatrix} \frac{m\Omega_0}{k_\perp} J_l J_m \\ -iu_\perp J_l J_m' \\ u_\parallel J_l J_m \end{bmatrix}. \tag{3.59}$$

In a homogeneous plasma then the gyrofrequency is independent of the angle θ and the orthogonality integral over θ is usually performed at this point. If we note the following identities,

$$\sum_m \int_0^{2\pi} d\theta e^{i(m-l)\theta} J_m \equiv \begin{cases} 2\pi \sum_l J_l, & m = l, \\ 0, & m \neq l, \end{cases} \tag{3.60}$$

$$\sum_l l J_l^2 \equiv 0, \tag{3.61}$$

$$\sum_l J_l J_l' \equiv 0, \tag{3.62}$$

$$\sum_l J_l^2 \equiv 1, \tag{3.63}$$

then we arrive at the conductivity tensor for a plasma immersed in a homogeneous(h) magnetic field,

$$\begin{aligned}\sigma_{ij}^{h}(x,\mathbf{k}) = & - 2\pi i\frac{q^2}{m}\int_0^\infty du_\perp \int_L du_\parallel \frac{u_\parallel\left(u_\perp\frac{\partial f_0}{\partial u_\parallel} - u_\parallel\frac{\partial f_0}{\partial u_\perp}\right)}{\omega}\hat{\mathbf{e}}_{33} \\ & - 2\pi i\frac{q^2}{m}\sum_l \int_0^\infty du_\perp \int_L du_\parallel \frac{F_1 V_{ij}^{h}(\mathbf{k},\mathbf{u})}{D_l^{h}(x)},\end{aligned} \tag{3.64}$$

with,

$$V_{ij}^{h} = \begin{bmatrix} \frac{l^2\Omega_0^2}{k_\perp^2}J_l^2 & iu_\perp\frac{l\Omega_0}{k_\perp}J_l'J_l & u_\parallel\frac{l\Omega_0}{k_\perp}J_l^2 \\ -iu_\perp\frac{l\Omega_0}{k_\perp}J_lJ_l' & u_\perp^2 J_l'J_l' & -iu_\perp u_\parallel J_lJ_l' \\ u_\parallel\frac{l\Omega_0}{k_\perp}J_l^2 & iu_\perp u_\parallel J_l'J_l & u_\parallel^2 J_l^2 \end{bmatrix}, \tag{3.65}$$

and,

$$D_l^{h}(x) = \omega - l\Omega_0(x) - k_\parallel u_\parallel + i0. \tag{3.66}$$

We note here that the velocity tensor for a homogeneous plasma is Hermitian.

In an inhomogeneous magnetic field however, we have shown that the gyrofrequency(Ω) is a function of the guiding centre position(x_g) and therefore has a θ dependence which must be addressed prior to evaluation of the velocity integrals. For a self-consistent analysis, we must also evaluate all other spatially varying quantities such as the particle density and temperature at the guiding centre rather than at the final position x of the particles. Earlier, we said that the GK correction will only be important in the resonant part of the integral. In the non-resonant parts of the integral, we may use the terms appropriate to a homogeneous plasma. The explicit spatial dependence on the guiding centre in the resonant terms may be included using a delta function,

$$\sigma_{ij}(x_g) = \int dx''\sigma_{ij}(x')\,\delta(x'' - x_g), \tag{3.67}$$

so that the conductivity tensor for an inhomogeneous plasma, (3.36), becomes,

$$\begin{aligned}\sigma_{ij}(x,\mathbf{k}) = & - 2\pi i\frac{q^2}{m}\int_0^\infty du_\perp \int_L du_\parallel \frac{u_\parallel\left(u_\perp\frac{\partial f_0}{\partial u_\parallel} - u_\parallel\frac{\partial f_0}{\partial u_\perp}\right)}{\omega}\hat{\mathbf{e}}_{33} \\ & - i\frac{q^2}{m}\sum_l\sum_m \int dx'' \int_0^\infty du_\perp \int_0^{2\pi} d\theta e^{i(m-l)\theta}\int_L du_\parallel \\ & \times \frac{F_1 V_{ij}(\mathbf{k},\mathbf{u})\,\delta\left(x'' - x - \frac{u_\perp}{\Omega_0}\sin\theta\right)}{D_l(x'')},\end{aligned} \tag{3.68}$$

with,

$$D_l\left(x''\right) = \omega - l\Omega\left(x''\right) - k_{\|}u_{\|} + i0. \tag{3.69}$$

The subscript g has been dropped from Ω since our delta function takes into account the evaluation of the gyrofrequency at the guiding centre.

It is clear now that the orthogonality integral over θ cannot be evaluated as for the homogeneous plasma since the GK correction has introduced a $\sin\theta$. Fortunately there is a nice property of the Fourier Bessel identities which allows us to continue unhindered. To see this, we first express the delta function as a Fourier integral with $b'' = \frac{k''u_\perp}{\Omega_0}$,

$$\delta\left(x'' - x - \frac{u_\perp}{\Omega_0}\sin\theta\right) \equiv \frac{1}{2\pi}\int dk'' e^{ik''(x''-x)-ib''\sin\theta}, \tag{3.70}$$

and, since the summation index m is associated with angles θ, then we see that changing the coefficient of $\sin\theta$ is equivalent to changing the argument of the Bessel functions through the relation,

$$\sum_m J_m\left(b\right)e^{im\theta}e^{-ib''\sin\theta} \equiv e^{i(b-b'')\sin\theta} = \sum_m J_m\left(b-b''\right)e^{im\theta}. \tag{3.71}$$

Related to this change is the factor $\frac{m\Omega_0}{k_\perp}$ originating from $\cos\theta$ in (3.45). The modification to the argument $b \to b - b''$ is followed by a subsequent change $\frac{m\Omega_0}{k_\perp} \to \frac{m\Omega_0}{k_\perp - k''}$. Having extracted all trigonometric dependences upon the angle θ, we are now able to perform the orthogonality integral over θ. The conductivity tensor may now be written as,

$$\begin{aligned}\sigma_{ij}\left(x,\mathbf{k}\right) = & - 2\pi i\frac{q^2}{m}\int_0^\infty du_\perp\int_L du_{\|}\frac{u_{\|}\left(u_\perp\frac{\partial f_0}{\partial u_{\|}} - u_{\|}\frac{\partial f_0}{\partial u_\perp}\right)}{\omega}\hat{\mathbf{e}}_{33} \\ & - i\frac{q^2}{m}\sum_l\int dx''\int dk'' e^{ik''(x''-x)}\int_0^\infty du_\perp\int_L du_{\|}\frac{F_1 V_{ij}\left(\mathbf{k},\mathbf{u}\right)}{D_l\left(x''\right)},\end{aligned} \tag{3.72}$$

with,

$$V_{ij} = \begin{bmatrix} \frac{l^2\Omega_0^2}{k_\perp(k_\perp-k'')}J_lJ_l & iu_\perp\frac{l\Omega_0}{(k_\perp-k'')}J_l'J_l & u_{\|}\frac{l\Omega_0}{(k_\perp-k'')}J_lJ_l \\ -iu_\perp\frac{l\Omega_0}{k_\perp}J_lJ_l' & u_\perp^2J_l'J_l' & -iu_\perp u_{\|}J_lJ_l' \\ u_{\|}\frac{l\Omega_0}{k_\perp}J_lJ_l & iu_\perp u_{\|}J_l'J_l & u_{\|}^2J_lJ_l \end{bmatrix}, \tag{3.73}$$

and the Bessel functions have arguments $b = \frac{k_\perp u_\perp}{\Omega_0}$ and $b - b'' = \frac{(k_\perp - k'')u_\perp}{\Omega_0}$ respectively. F_1 and D_l are given by equations (3.50) and (3.69) respectively.

This is a generalised result for an unspecified plasma equilibrium f_0 constructed from the constants of the motion $u_\perp^2$ and $u_{\|}$ when immersed in a weakly inhomogeneous magnetic field $\mathbf{B_0}$ whose precise spatial variation is unspecified due to the general parameter

$\epsilon = \left(\frac{1}{B_0(0)}\frac{\partial B_0}{\partial x}\right)_{x=0}$.

The conductivity tensor of a hot, non-uniform plasma is seen to consist of a set of spatially varying coefficients of the electric field components. In the general case considered here, these are non-local, being made up of kernel functions which multiply the unknown electric field components inside integrals. In the next chapter we will provide a theoretical basis for the scale-length of the non-locality and we will show that for a thermally anisotropic plasma in a linear field gradient that this is of the order of a few Larmor radii.

In the intensive amount of literature dedicated to the discussion of EM waves in inhomogeneous plasmas, either the explicit form for the equilibrium distribution was intrinsic to the evaluation of the conductivity tensor such as in recent papers by Caldela et al.(1989 and 1990) or else the explicit form for the spatial variation of the magnetic field was specified as in the calculations of McDonald et al.(1994), Cairns et al.(1991) and Lashmore-Davies et al.(1989) We have illustrated a method whereby we can preserve the generality of the model while enabling further progress to be made without added difficulty. In the next chapter we calculate the response to EM waves of an anisotropic Bi-Maxwellian plasma immersed in an inhomogeneous magnetic field with a linear gradient profile. This choice, while breaking new theoretical ground due to the inclusion of thermal anisotropy terms, allows us to make a comparison with well trodden paths since in the limit of an isotropic plasma we may compare directly our results with numerous other works in the field.

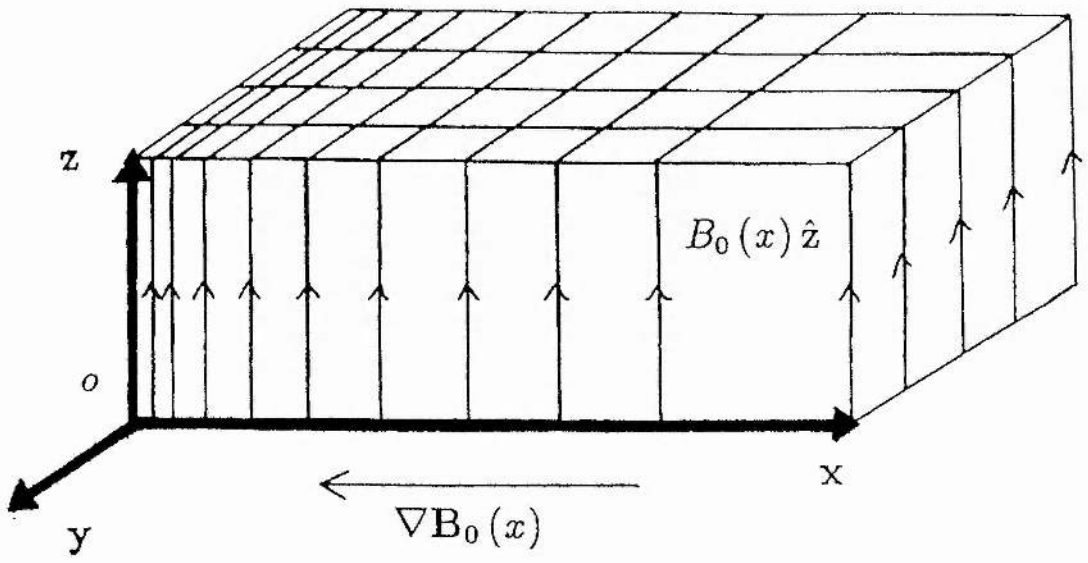

Figure 3.1: A schematic representation of the $1D$ inhomogeneous magnetic field in slab geometry.

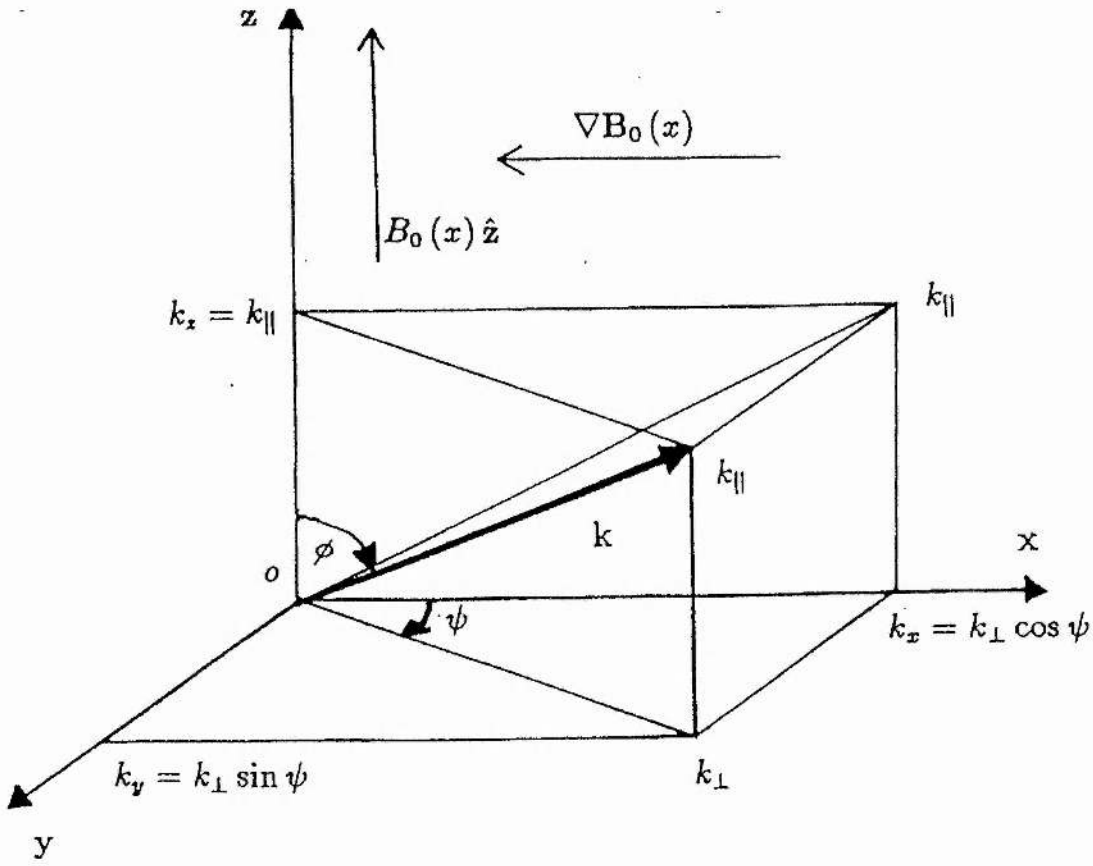

Figure 3.2: A schematic representation of the propagation wavevector geometry.

Chapter 4

Inclusion Of Thermal Anisotropic Effects

In the previous chapter we derived the response of an inhomogeneous plasma expressed in terms of a generalised conductivity tensor. Here we throw caution to the wind and specify the functional form of the spatial variation of Ω and, in addition, we specify an equilibrium distribution f_0.

4.1 A Bi-Maxwellian Plasma In A Linear Gradient

We would like to find a practical application for our generalised conductivity tensor. Of topical interest is the use of high frequency EM waves matched resonantly to natural frequencies of the charged particle gyrofrequencies in hot thermonuclear fusion plasmas so as to produce collisionless transport of energy to the bulk plasma. Our analysis has been non-relativistic but may be easily extended to include the relativistic effects of very high energy charged particles. Indeed, McDonald et al.(1994) have performed a relativistic calculation for an isotropic plasma in a linear field gradient.

In magnetically confined plasmas, such as in tokamak devices like the Joint European Torus(JET), the toroidal magnetic field $B_0(x)\,\hat{\mathbf{z}}$ has a gradient in field strength in the radial $\hat{\mathbf{x}}$ direction. In a tokamak scenario we may identify the radial, poloidal and toroidal directions as $\hat{\mathbf{x}}$, $\hat{\mathbf{y}}$ and $\hat{\mathbf{z}}$ respectively as depicted in figure 4.1. The functional form of the weakly varying magnetic field given by (3.6) may be approximated by a linear gradient with a scale-length L,

$$\mathbf{B}_0(x) \simeq B_0(0)\,(1+\epsilon x)\,\hat{\mathbf{z}} = B_0(0)\left(1-\frac{x}{L}\right)\hat{\mathbf{z}}, \tag{4.1}$$

This is illustrated in figure 4.2. The small parameter used in our model is $\epsilon = -1/L$ and we may associate L with the major radius of a Tokamak.

The effect of $\mathbf{B_0}$ is housed in the gyrofrequency(Ω) which, for a linear field gradient has the following form,

$$\Omega\left(x''\right) = \Omega_0\left(0\right)\left(1 - \frac{x''}{L}\right). \tag{4.2}$$

Further calculations are most easily done by reinstating the resonant denominator as a Fourier integral,

$$\frac{i}{D_l} \equiv \int\limits_{-\infty}^{0} d\tau e^{-iD_l\tau}, \tag{4.3}$$

with,

$$D_l\left(x''\right) = \omega - l\Omega_0\left(0\right) + \frac{l\Omega_0\left(0\right)x''}{L} - k_{\|}u_{\|} + i0, \tag{4.4}$$

so that the conductivity tensor in (3.72) becomes,

$$\begin{aligned}
\sigma_{ij}\left(x,\mathbf{k}\right) = & - 2\pi i\frac{q^2}{m}\int\limits_0^{\infty} du_{\perp}\int_L du_{\|}\frac{u_{\|}\left(u_{\perp}\frac{\partial f_0}{\partial u_{\|}} - u_{\|}\frac{\partial f_0}{\partial u_{\perp}}\right)}{\omega}\hat{\mathbf{e}}_{33} \\
& - \frac{q^2}{m}\sum_l\int dx''\int dk''e^{ik''(x''-x)}\int\limits_0^{\infty} du_{\perp}\int_L du_{\|} \\
& \times \int\limits_{-\infty}^{0} d\tau e^{-iD_l(x'')\tau}F_1V_{ij}\left(\mathbf{k},\mathbf{u}\right).
\end{aligned} \tag{4.5}$$

The x''-integral gives a δ-function,

$$\int dx''e^{ix''\left(k''-\frac{l\Omega_0(0)\tau}{L}\right)} = 2\pi\delta\left(k'' - \frac{l\Omega_0\left(0\right)\tau}{L}\right), \tag{4.6}$$

so that,

$$\begin{aligned}
\sigma_{ij}\left(x,\mathbf{k}\right) = & - 2\pi i\frac{q^2}{m}\int\limits_0^{\infty} du_{\perp}\int_L du_{\|}\frac{u_{\|}\left(u_{\perp}\frac{\partial f_0}{\partial u_{\|}} - u_{\|}\frac{\partial f_0}{\partial u_{\perp}}\right)}{\omega}\hat{\mathbf{e}}_{33} \\
& - 2\pi\frac{q^2}{m}\sum_l\int dk''e^{-ik''x}\int\limits_0^{\infty} du_{\perp}\int_L du_{\|} \\
& \times \int\limits_{-\infty}^{0} d\tau e^{-i\tau\left(\omega - l\Omega_0(0) - k_{\|}u_{\|}\right)}F_1V_{ij}\delta\left(k'' - \frac{l\Omega_0\left(0\right)\tau}{L}\right).
\end{aligned} \tag{4.7}$$

The delta function lets us easily work out the k'' -integral and if we recall the definition $\Omega_0(x) = \Omega_0(0)(1 - x/L)$ then we obtain,

$$\sigma_{ij}(x,\mathbf{k}) = - 2\pi i \frac{q^2}{m} \int_0^\infty du_\perp \int_L du_\parallel \frac{u_\parallel \left(u_\perp \frac{\partial f_0}{\partial u_\parallel} - u_\parallel \frac{\partial f_0}{\partial u_\perp} \right)}{\omega} \hat{\mathbf{e}}_{33}$$
$$- 2\pi \frac{q^2}{m} \sum_l \int_0^\infty du_\perp \int_L du_\parallel \int_{-\infty}^0 d\tau e^{-i\tau(\omega - l\Omega_0(x) - k_\parallel u_\parallel)} F_1 V_{ij}(k_\perp, \tau, \mathbf{u}), \quad (4.8)$$

with,

$$V_{ij} = \begin{bmatrix} \frac{l^2\Omega_0^2}{k_\perp\left(k_\perp - \frac{l\Omega_0\tau}{L}\right)} J_l J_l & iu_\perp \frac{l\Omega_0}{\left(k_\perp - \frac{l\Omega_0\tau}{L}\right)} J_l' J_l & u_\parallel \frac{l\Omega_0}{\left(k_\perp - \frac{l\Omega_0\tau}{L}\right)} J_l J_l \\ -iu_\perp \frac{l\Omega_0}{k_\perp} J_l J_l' & u_\perp^2 J_l' J_l' & -iu_\perp u_\parallel J_l J_l' \\ u_\parallel \frac{l\Omega_0}{k_\perp} J_l J_l & iu_\perp u_\parallel J_l' J_l & u_\parallel^2 J_l J_l \end{bmatrix}. \quad (4.9)$$

The Bessel functions have arguments $\frac{k_\perp u_\perp}{\Omega_0}$ and $\frac{k_\perp u_\perp}{\Omega_0} - \frac{lu_\perp \tau}{L}$ respectively.

We now need to specify the last vestige of generality, the equilibrium, f_0. In line with our plasma physics model, we note that due to gyroresonance when $\omega - l\Omega_0 - k_\parallel u_\parallel = 0$, charged particles receive a boost to their perpendicular velocity component $u_\perp$ and inevitably, in the time asymptote, the steady state distribution will have an anisotropy between perpendicular and parallel temperature. In addition, many magnetically confined plasmas also receive an input beam of high energy neutrals which transfer energy into the perpendicular component $u_\perp$ of the ions making this thermal anisotropy all the more pronounced.

We choose perhaps the simplest of anisotropic distributions, a bi-Maxwellian,

$$f_0 = n_0 \pi^{-3/2} u_{T\perp}^{-2} u_{T\parallel}^{-1} e^{-\frac{u_\perp^2}{u_{T\perp}^2} - \frac{u_\parallel^2}{u_{T\parallel}^2}}, \quad (4.10)$$

and for substitution into F_1 and $\hat{\mathbf{e}}_{33}$ we also need the derivatives,

$$\frac{\partial f_0}{\partial u_\perp} = -2u_\perp u_{T\perp}^{-2} f_0, \quad (4.11)$$
$$\frac{\partial f_0}{\partial u_\parallel} = -2u_\parallel u_{T\parallel}^{-2} f_0. \quad (4.12)$$

We may now write F_1 of (3.50) explicitly as,

$$F_1 = -2n_0 \pi^{-3/2} u_\perp u_{T\perp}^{-2} u_{T\parallel}^{-1} e^{-\frac{u_\perp^2}{u_{T\perp}^2} - \frac{u_\parallel^2}{u_{T\parallel}^2}} \{u_{T\perp}^{-2} + \frac{k_\parallel u_\parallel}{\omega}\left(u_{T\parallel}^{-2} - u_{T\perp}^{-2}\right)\}, \quad (4.13)$$

and similarly $\hat{\mathbf{e}}_{33}$ of (4.8) is,

$$\frac{u_\parallel\left(u_\perp\frac{\partial f_0}{\partial u_\parallel}-u_\parallel\frac{\partial f_0}{\partial u_\perp}\right)}{\omega}=-2n_0\pi^{-3/2}\frac{u_\parallel^2u_\perp}{\omega}u_{T\perp}^{-2}u_{T\parallel}^{-1}e^{-\frac{u_\perp^2}{u_{T\perp}^2}-\frac{u_\parallel^2}{u_{T\parallel}^2}}\{u_{T\parallel}^{-2}-u_{T\perp}^{-2}\}. \tag{4.14}$$

If we note that the plasma frequency is $\omega_p^2=\frac{n_0q^2}{\epsilon_0m}$ then the conductivity tensor of (4.8) becomes,

$$\begin{aligned}\sigma_{ij}(x,\mathrm{k}) &= \frac{4i\epsilon_0\omega_p^2}{\sqrt{\pi}\omega u_{T\perp}^2u_{T\parallel}}\left(u_{T\parallel}^{-2}-u_{T\perp}^{-2}\right)\int_0^\infty du_\perp u_\perp e^{-\frac{u_\perp^2}{u_{T\perp}^2}}\int_L du_\parallel u_\parallel^2e^{-\frac{u_\parallel^2}{u_{T\parallel}^2}}\hat{\mathbf{e}}_{33}\\ &+ \frac{4\epsilon_0\omega_p^2}{\sqrt{\pi}u_{T\perp}^2u_{T\parallel}}\sum_l\int_{-\infty}^0 d\tau e^{-i\tau(\omega-l\Omega_0)}\int_0^\infty du_\perp u_\perp e^{-\frac{u_\perp^2}{u_{T\perp}^2}}\int_L du_\parallel e^{-\frac{u_\parallel^2}{u_{T\parallel}^2}+ik_\parallel u_\parallel\tau}\\ &\times \{u_{T\perp}^{-2}+\frac{k_\parallel u_\parallel}{\omega}\left(u_{T\parallel}^{-2}-u_{T\perp}^{-2}\right)\}V_{ij}\left(k_\perp,\tau,u_\perp,u_\parallel\right).\end{aligned} \tag{4.15}$$

We need only work out the velocity integrals now to complete our analysis. In order to ease the algebra we rescale the velocity components to their thermal values as follows,

$$U=\frac{u_\perp}{u_{T\perp}}, \tag{4.16}$$

$$W=\frac{u_\parallel}{u_{T\parallel}}, \tag{4.17}$$

so that,

$$\begin{aligned}\sigma_{ij}(x,\mathrm{k}) = &+ \frac{4i\epsilon_0\omega_p^2}{\sqrt{\pi}\omega}u_{T\parallel}^2\left(u_{T\parallel}^{-2}-u_{T\perp}^{-2}\right)\int_0^\infty dUUe^{-U^2}\int_L dWW^2e^{-W^2}\hat{\mathbf{e}}_{33}\\ &+ \frac{4\epsilon_0\omega_p^2}{\sqrt{\pi}}\sum_l\int_{-\infty}^0 d\tau e^{-i\tau(\omega-l\Omega_0)}\int_0^\infty dUUe^{-U^2}\int_L dWe^{-W^2+ik_\parallel u_{T\parallel}\tau W}\\ &\times \{u_{T\perp}^{-2}+\frac{k_\parallel u_{T\parallel}}{\omega}W\left(u_{T\parallel}^{-2}-u_{T\perp}^{-2}\right)\}V_{ij}\left(k_\perp,\tau,U,W\right),\end{aligned} \tag{4.18}$$

and,

$$V_{ij}=\begin{bmatrix}\frac{l^2\Omega_0^2}{k_\perp\left(k_\perp-\frac{l\Omega_0\tau}{L}\right)}J_lJ_l & i\frac{l\Omega_0}{\left(k_\perp-\frac{l\Omega_0\tau}{L}\right)}u_{T\perp}UJ_l'J_l & \frac{l\Omega_0}{\left(k_\perp-\frac{l\Omega_0\tau}{L}\right)}u_{T\parallel}WJ_lJ_l\\ -i\frac{l\Omega_0}{k_\perp}u_{T\perp}UJ_lJ_l' & u_{T\perp}^2U^2J_l'J_l' & -iu_{T\perp}u_{T\parallel}UWJ_lJ_l'\\ \frac{l\Omega_0}{k_\perp}u_{T\parallel}WJ_lJ_l & iu_{T\perp}u_{T\parallel}UWJ_l'J_l & u_{T\parallel}^2W^2J_lJ_l\end{bmatrix}. \tag{4.19}$$

The Bessel functions have arguments $\left(\frac{k_\perp u_{T\perp}}{\Omega_0}\right)U$ and $\left(\frac{k_\perp u_{T\perp}}{\Omega_0}-\frac{lu_{T\perp}\tau}{L}\right)U$ respectively.

To evaluate the $u_\perp$-integrals we are blessed by an apt and beautiful identity of Watson(1922),

$$\int_0^\infty dx x e^{-p^2x^2} J_n(\alpha x) J_n(\beta x) \equiv \frac{1}{2p^2} e^{-\mu} I_n(\lambda), \tag{4.20}$$

which, together with combinations of partial derivatives with respect to α,β and p, give the set of formulae we need to cope with the various permutations of Bessel function products appearing in the U-integral,

$$\begin{aligned}
\int_0^\infty dx x^2 e^{-p^2x^2} J_n'(\alpha x) J_n(\beta x) &\equiv \frac{\partial}{\partial\alpha}\left[\frac{1}{p^2} e^{-\mu} I_n(\lambda)\right] \\
&\equiv \frac{1}{4p^4} e^{-\mu}\left[\beta I_n'(\lambda) - \alpha I_n(\lambda)\right], \qquad (4.21) \\
\int_0^\infty dx x^2 e^{-p^2x^2} J_n(\alpha x) J_n'(\beta x) &\equiv \frac{\partial}{\partial\beta}\left[\frac{1}{p^2} e^{-\mu} I_n(\lambda)\right] \\
&\equiv \frac{1}{4p^4} e^{-\mu}\left[\alpha I_n'(\lambda) - \beta I_n(\lambda)\right], \qquad (4.22) \\
\int_0^\infty dx x^3 e^{-p^2x^2} J_n(\alpha x) J_n(\beta x) &\equiv -\frac{1}{2p}\frac{\partial}{\partial p}\left[\frac{1}{p^2} e^{-\mu} I_n(\lambda)\right] \\
&\equiv \frac{1}{2p^4} e^{-\mu}\left[(1-\mu) I_n(\lambda) + \lambda I_n'(\lambda)\right], \qquad (4.23) \\
\int_0^\infty dx x^3 e^{-p^2x^2} J_n'(\alpha x) J_n'(\beta x) &\equiv \frac{\partial^2}{\partial\alpha\beta}\left[\frac{1}{p^2} e^{-\mu} I_n(\lambda)\right] \\
&\equiv \frac{1}{2p^4} e^{-\mu}\left[\left(\lambda + \frac{n^2}{2\lambda}\right) I_n(\lambda) - \mu I_n'(\lambda)\right]. \qquad (4.24)
\end{aligned}$$

Here I_n is the modified Bessel function with argument $\lambda = \frac{1}{2p^2}(\alpha\beta)$ and $\mu = \frac{1}{4p^2}(\alpha^2+\beta^2)$. We note here that in a homogeneous(h) plasma then α appears in the argument of both Bessel functions and we may identify $\lambda^h = \frac{1}{2p^2}\alpha^2$. In each case above a prime indicates a derivative with respect to the argument. For the non-resonant term will also need the identity,

$$\int_0^\infty dx x^{2n+1} e^{-px^2} \equiv \frac{n!}{2p^{n+1}}. \tag{4.25}$$

Setting, $x = U$, $p = 1$, $\alpha = \frac{k_\perp u_{T\perp}}{\Omega_0}$ and $\beta = \left(k_\perp - \frac{l\Omega_0\tau}{L}\right)\frac{u_{T\perp}}{\Omega_0}$ then the U-integral may be performed to give,

$$\begin{aligned}\sigma_{ij}(x,\mathbf{k}) = &+ \frac{4i\epsilon_0\omega_p^2}{\sqrt{\pi}\omega}u_{T\|}^2\left(u_{T\|}^{-2}-u_{T\perp}^{-2}\right)\frac{1}{2}\int_L dW W^2 e^{-W^2}\hat{\mathbf{e}}_{33}\\ &+ \frac{4\epsilon_0\omega_p^2}{\sqrt{\pi}}\sum_l\int_{-\infty}^{0}d\tau e^{-i\tau(\omega-l\Omega_0)}\int_L dW e^{-W^2+ik_\|u_{T\|}\tau W}\\ &\times \left\{u_{T\perp}^{-2}+\frac{k_\|u_{T\|}}{\omega}W\left(u_{T\|}^{-2}-u_{T\perp}^{-2}\right)\right\}V_{ij}(k_\perp,\tau,W), \qquad (4.26)\end{aligned}$$

and,

$$V_{ij}=\frac{1}{2}e^{-\mu}\begin{bmatrix}\frac{l^2\Omega_0^2}{k_\perp\left(k_\perp-\frac{l\Omega_0\tau}{L}\right)}I_l & i\frac{l\Omega_0}{\left(k_\perp-\frac{l\Omega_0\tau}{L}\right)}u_{T\perp}\frac{1}{2}\left[\beta I_l'-\alpha I_l\right] & \frac{l\Omega_0}{\left(k_\perp-\frac{l\Omega_0\tau}{L}\right)}u_{T\|}WI_l\\ -i\frac{l\Omega_0}{k_\perp}u_{T\perp}\frac{1}{2}\left[\alpha I_l'-\beta I_l\right] & u_{T\perp}^2\left[\left(\lambda+\frac{l^2}{2\lambda}\right)I_l-\mu I_l'\right] & -iu_{T\perp}u_{T\|}W\frac{1}{2}\left[\alpha I_l'-\beta I_l\right]\\ \frac{l\Omega_0}{k_\perp}u_{T\|}WI_l & iu_{T\perp}u_{T\|}W\frac{1}{2}\left[\beta I_l'-\alpha I_l\right] & u_{T\|}^2W^2I_l\end{bmatrix}. \qquad (4.27)$$

To perform the W-integral, we complete the square in the exponential containing a quadratic in W through the substitution,

$$W' = W-\frac{1}{2}i\psi, \qquad (4.28)$$

allowing us to note the following forms,

$$\begin{aligned}dW' &= dW, &(4.29)\\ -W'^2-\frac{1}{4}\psi^2 &= -W^2+i\psi W, &(4.30)\\ W &= W'+\frac{1}{2}i\psi, &(4.31)\\ W^2 &= W'^2+i\psi W'-\frac{1}{4}\psi^2, &(4.32)\end{aligned}$$

with, $\psi = k_\|u_{T\|}\tau$. We can factor out $u_{T\perp}^{-2}$ from the curly bracket in (4.26) and transfer it into the velocity tensor. If in addition, we note that $\frac{u_{T\|}^2}{u_{T\perp}^2}=\frac{T_\|}{T_\perp}$, then the conductivity tensor may be written as,

$$\begin{aligned}\sigma_{ij}(x,\mathbf{k}) = &- \frac{2i\epsilon_0\omega_p^2}{\sqrt{\pi}\omega}\frac{T_\|}{T_\perp}\left(1-\frac{T_\perp}{T_\|}\right)\int_L dW W^2 e^{-W^2}\hat{\mathbf{e}}_{33}\\ &+ \frac{\epsilon_0\omega_p^2}{\sqrt{\pi}}\sum_l\int_{-\infty}^{0}d\tau e^{-i\tau(\omega-l\Omega_0)-\mu-\frac{1}{4}\psi^2}\\ &\times \int_L dW' e^{-W'^2}L(W')V_{ij}(\mathbf{k},\tau,W'). \qquad (4.33)\end{aligned}$$

Here,

$$L\left(W'\right)=\{1-\frac{k_{\|}u_{T\|}}{\omega}\left(1-\frac{T_{\perp}}{T_{\|}}\right)\left(W'+\frac{1}{2}i\psi\right)\}, \tag{4.34}$$

and,

$$V_{ij}=\begin{bmatrix} \frac{2l^2\Omega_0^2}{k_{\perp}\left(k_{\perp}-\frac{l\Omega_0\tau}{L}\right)u_{T\perp}^2}I_lA_1 & i\frac{l\Omega_0}{\left(k_{\perp}-\frac{l\Omega_0\tau}{L}\right)u_{T\perp}}\left[\beta I_l'-\alpha I_l\right]A_1 & \frac{2l\Omega_0}{\left(k_{\perp}-\frac{l\Omega_0\tau}{L}\right)u_{T\perp}}I_lA_2 \\ -i\frac{l\Omega_0}{k_{\perp}u_{T\perp}}\left[\alpha I_l'-\beta I_l\right]A_1 & \left[\left(2\lambda+\frac{l^2}{\lambda}\right)I_l-2\mu I_l'\right]A_1 & -i\left[\alpha I_l'-\beta I_l\right]A_2 \\ \frac{2l\Omega_0}{k_{\perp}u_{T\perp}}I_lA_2 & i\left[\beta I_l'-\alpha I_l\right]A_2 & 2I_lA_3 \end{bmatrix}. \tag{4.35}$$

We have defined the following factors A_j which are associated with the thermal anisotropy and we name them the anisotropy factors,

$$A_1 = 1, \tag{4.36}$$

$$A_2 = \sqrt{\frac{T_{\|}}{T_{\perp}}}\left(W'+\frac{1}{2}i\psi\right), \tag{4.37}$$

$$A_3 = \frac{T_{\|}}{T_{\perp}}\left(W'^2+i\psi W'-\frac{1}{4}\psi^2\right). \tag{4.38}$$

If we absorb L into the anisotropy factors A_1, A_2 and A_3 such that,

$$A_1 = \{1-\frac{k_{\|}u_{T\|}}{\omega}\left(1-\frac{T_{\perp}}{T_{\|}}\right)\left(W'+\frac{1}{2}i\psi\right)\}, \tag{4.39}$$

$$A_2 = \sqrt{\frac{T_{\|}}{T_{\perp}}}\{\left(W'+\frac{1}{2}i\psi\right)-\frac{k_{\|}u_{T\|}}{\omega}\left(1-\frac{T_{\perp}}{T_{\|}}\right)\left(W'^2+i\psi W'-\frac{1}{4}\psi^2\right)\}, \tag{4.40}$$

$$\begin{aligned} A_3 = {} & \frac{T_{\|}}{T_{\perp}}\{\left(W'^2+i\psi W'-\frac{1}{4}\psi^2\right) \\ & -\frac{k_{\|}u_{T\|}}{\omega}\left(1-\frac{T_{\perp}}{T_{\|}}\right)\left(W'^3+\frac{3}{2}i\psi W'^2-\frac{3}{4}\psi^2W'-\frac{1}{8}i\psi^3\right)\}, \end{aligned} \tag{4.41}$$

then we may perform the W and W'-integrals with the aid of the following identities,

$$\int_{-\infty}^{\infty}dxe^{-px^2} \equiv \sqrt{\frac{\pi}{p}}, \tag{4.42}$$

$$\int_{-\infty}^{\infty}dxx^{2n+1}e^{-px^2} \equiv 0, \tag{4.43}$$

$$\int_{-\infty}^{\infty}dxx^2e^{-px^2} \equiv \frac{1}{2p}\sqrt{\frac{\pi}{p}}, \tag{4.44}$$

giving the conductivity,

$$\sigma_{ij}(x,\mathbf{k}) = -\frac{2i\epsilon_0\omega_p^2}{\sqrt{\pi}\omega}\frac{T_{\|}}{T_{\perp}}\left(1-\frac{T_{\perp}}{T_{\|}}\right)\left(\frac{\sqrt{\pi}}{2}\right)\hat{\mathbf{e}}_{33} + \frac{\epsilon_0\omega_p^2}{\sqrt{\pi}}\sum_l\int_{-\infty}^{0} d\tau e^{-i\tau(\omega-l\Omega_0)-\mu-\frac{1}{4}\psi^2}V_{ij}(\mathbf{k},\tau). \quad (4.45)$$

The velocity tensor is as in (4.35) but with,

$$A_1 = \sqrt{\pi}\{1-i\psi\frac{k_{\|}u_{T\|}}{2\omega}\left(1-\frac{T_{\perp}}{T_{\|}}\right)\}, \quad (4.46)$$

$$A_2 = \sqrt{\frac{T_{\|}}{T_{\perp}}}\frac{1}{2}\sqrt{\pi}\{i\psi-\frac{k_{\|}u_{T\|}}{\omega}\left(1-\frac{T_{\perp}}{T_{\|}}\right)\left(1-\frac{1}{2}\psi^2\right)\}, \quad (4.47)$$

$$A_3 = \frac{T_{\|}}{T_{\perp}}\frac{1}{2}\sqrt{\pi}\{1-\frac{1}{2}\psi^2-\frac{k_{\|}u_{T\|}}{2\omega}\left(1-\frac{T_{\perp}}{T_{\|}}\right)\left(3i\psi-\frac{1}{2}i\psi^3\right)\}. \quad (4.48)$$

So we have,

$$\sigma_{ij}(x,\mathbf{k}) = -\frac{i\epsilon_0\omega_p^2}{\omega}\frac{T_{\|}}{T_{\perp}}\left(1-\frac{T_{\perp}}{T_{\|}}\right)\hat{\mathbf{e}}_{33} + \epsilon_0\omega_p^2\sum_l\int_{-\infty}^{0} d\tau e^{-i\tau(\omega-l\Omega_0)-\mu-\frac{1}{4}\psi^2}V_{ij}(\mathbf{k},\tau), \quad (4.49)$$

where,

$$V_{ij} = \begin{bmatrix} \frac{l^2}{\lambda}I_lA_1 & il\left[I_l'-\frac{\alpha}{\beta}I_l\right]A_1 & \frac{l}{\beta}I_lA_2 \\ -il\left[I_l'-\frac{\beta}{\alpha}I_l\right]A_1 & \left[\left(2\lambda+\frac{l^2}{\lambda}\right)I_l-2\mu I_l'\right]A_1 & -i\frac{\alpha}{2}\left[I_l'-\frac{\beta}{\alpha}I_l\right]A_2 \\ \frac{l}{\alpha}I_lA_2 & i\frac{\beta}{2}\left[I_l'-\frac{\alpha}{\beta}I_l\right]A_2 & I_lA_3 \end{bmatrix}, \quad (4.50)$$

and,

$$A_1 = 1-\frac{i\psi}{2\zeta_0}\left(1-\frac{T_{\perp}}{T_{\|}}\right), \quad (4.51)$$

$$A_2 = \sqrt{\frac{T_{\|}}{T_{\perp}}}\left[i\psi-\frac{\left(1-\frac{1}{2}\psi^2\right)}{\zeta_0}\left(1-\frac{T_{\perp}}{T_{\|}}\right)\right], \quad (4.52)$$

$$A_3 = \frac{T_{\|}}{T_{\perp}}\left[\left(1-\frac{1}{2}\psi^2\right)-\frac{\left(3i\psi-\frac{1}{2}\psi^3\right)}{2\zeta_0}\left(1-\frac{T_{\perp}}{T_{\|}}\right)\right]. \quad (4.53)$$

There are a number of variables in (4.49) and for ease of reference we write them out here,

$$\alpha = \frac{k_\perp u_{T\perp}}{\Omega_0}, \quad \beta = \left(k_\perp - \frac{l\Omega_0\tau}{L}\right)\rho_\perp, \quad \lambda^h = \frac{1}{2}\alpha^2, \quad \lambda = \frac{1}{2}\alpha\beta, \quad \mu = \frac{1}{4}\left(\alpha^2+\beta^2\right),$$

$$\psi = k_\parallel u_{T\parallel}\tau, \quad \zeta_0 = \frac{\omega}{k_\parallel u_{T\parallel}}, \quad u_T^2 = \frac{2\kappa T}{m}, \quad \omega_p^2 = \frac{n_0 q^2}{\epsilon_0 m},$$

$$\Omega_0(x) = \Omega_0(0)\left(1-\frac{x}{L}\right), \quad \Omega_0(0) = \frac{qB_0(0)}{m}, \quad \rho_\perp = \frac{u_{T\perp}}{\Omega(0)}, \quad \tau = t'-t \quad (4.54)$$

The existence of terms containing the integration variable τ in the velocity tensor mean that the τ-integral cannot be performed and so a closed analytic form for the conductivity cannot be obtained. In addition, as an infinite sum over all the harmonics l the conductivity is not very amenable to further calculation. In chapter 7 we will present an approximation which will allow us to proceed further with our analysis. We note that the velocity tensor does not have the same Hermitian form as its homogeneous plasma counterpart given in (3.64). In chapter 6 we will show that the plasma response written in terms of the conductivity tensor obeys the Onsager reciprocal relations for an isotropic plasma in a homogeneous magnetic field and also in an inhomogeneous magnetic field. We will go further and demonstrate that the Onsager reciprocal relations are not obeyed for an anisotropic plasma.

In order to compare our theoretical results with those of other authors, it will be convenient to express the conductivity tensor in forms which allow an easy recovery of well known limiting cases.

4.1.1 Alternative Representations

We may rewrite the conductivity tensor solely in terms of λ and λ_h so as to facilitate expansions of the modified Bessel functions with λ as an expansion parameter as discussed in chapter 2. We do this as follows. Since, from (4.54), $\alpha = \sqrt{2\lambda^h}$ and $\beta = 2\lambda/\alpha$, then we can deduce the following,

$$\beta = \frac{2\lambda}{\sqrt{2\lambda^h}}, \quad \frac{\beta}{\alpha} = \frac{\lambda}{\lambda^h}, \quad \frac{\alpha}{\beta} = \frac{\lambda^h}{\lambda}, \quad \mu = \frac{1}{2}\left(\lambda^h + \frac{\lambda^2}{\lambda^h}\right) \equiv \lambda + \frac{1}{4}(\beta-\alpha)^2, \quad (4.55)$$

and in the last identity we have made use of the fact that $(\alpha^2+\beta^2) = (\beta-\alpha)^2 + 2\alpha\beta$. In terms of these variables we may write,

$$\begin{aligned}\sigma_{ij}(x,\mathbf{k}) = & -\frac{i\epsilon_0\omega_p^2}{\omega}\frac{T_\parallel}{T_\perp}\left(1-\frac{T_\perp}{T_\parallel}\right)\hat{\mathbf{e}}_{33} \\ & + \epsilon_0\omega_p^2\sum_l \int_{-\infty}^{0} d\tau e^{-i\tau(\omega-l\Omega_0)-\frac{1}{4}\left[\psi^2+(\beta-\alpha)^2\right]}e^{-\lambda}V_{ij}(\mathbf{k},\tau), \quad (4.56)\end{aligned}$$

with,

$$\begin{bmatrix} \frac{l^2}{\lambda} I_l A_1 & il\left[I_l' - \frac{\lambda^h}{\lambda} I_l\right] A_1 & l\frac{\sqrt{2\lambda^h}}{2\lambda} I_l A_2 \\ -il\left[I_l' - \frac{\lambda}{\lambda^h} I_l\right] A_1 & \left[\left(2\lambda + \frac{l^2}{\lambda}\right) I_l - \left(\lambda^h + \frac{\lambda^2}{\lambda^h}\right) I_l'\right] A_1 & -i\sqrt{\frac{\lambda^h}{2}}\left[I_l' - \frac{\lambda}{\lambda^h} I_l\right] A_2 \\ l\frac{1}{\sqrt{2\lambda^h}} I_l A_2 & i\frac{\lambda}{\sqrt{2\lambda^h}}\left[I_l' - \frac{\lambda^h}{\lambda} I_l\right] A_2 & I_l A_3 \end{bmatrix}, \quad (4.57)$$

and the anisotropy factors A_j are as before. The algebraic representation of the conductivity tensor in terms of α,β and μ is useful for symmetry considerations but in order to compare with results obtained by other authors in the field, it will be more practical to write out the terms explicitly. We do this by noting the following,

$$\psi^2 + (\beta - \alpha)^2 \equiv \frac{l^2 u_{T\perp}^2 \tau^2}{L^2}\left[1 + \frac{k_\parallel^2 L^2}{l^2}\frac{T_\parallel}{T_\perp}\right], \quad \lambda = \frac{1}{2} k_\perp \left(k_\perp - l\Omega_0 \tau / L\right) \rho_\perp^2$$
$$\frac{\alpha}{\beta} = \frac{k_\perp}{k_\perp - l\Omega_0 \tau / L}, \quad \frac{\beta}{\alpha} = \frac{k_\perp - l\Omega_0 \tau / L}{k_\perp}. \quad (4.58)$$

The conductivity is then,

$$\sigma_{ij}(x, \mathbf{k}) = - \frac{i\epsilon_0 \omega_p^2}{\omega}\frac{T_\parallel}{T_\perp}\left(1 - \frac{T_\perp}{T_\parallel}\right)\hat{\mathbf{e}}_{33}$$
$$+ \epsilon_0 \omega_p^2 \sum_l \int_{-\infty}^{0} d\tau e^{-i\tau(\omega - l\Omega_0) - \frac{\tau^2 l^2 u_{T\perp}^2}{4L^2}\left[1 + k_\parallel^2 L^2 \left(\frac{T_\parallel}{T_\perp}\right)/l^2\right] - \lambda} V_{ij}(\mathbf{k}, \tau), \quad (4.59)$$

with,

$$\begin{bmatrix} V_{xx} = & \frac{l^2}{\lambda} I_l A_1, \\ V_{xy} = & il\left[I_l' - \left(\frac{k_\perp}{k_\perp - \frac{l\Omega_0\tau}{L}}\right) I_l\right] A_1, \\ V_{xz} = & \frac{l}{(k_\perp - l\Omega_0\tau/L)\rho_\perp} I_l A_2, \\ V_{yx} = & -il\left[I_l' - \left(\frac{k_\perp - \frac{l\Omega_0\tau}{L}}{k_\perp}\right) I_l\right] A_1, \\ V_{yy} = & \left[\left(2\lambda + \frac{l^2}{\lambda}\right) I_l - \left(2\lambda + \frac{l^2 u_{T\perp}^2 \tau^2}{2L^2}\right) I_l'\right] A_1, \\ V_{yz} = & -i\frac{k_\perp \rho_\perp}{2}\left[I_l' - \left(\frac{k_\perp - \frac{l\Omega_0\tau}{L}}{k_\perp}\right) I_l\right] A_2, \\ V_{zx} = & \frac{l}{k_\perp \rho_\perp} I_l A_2, \\ V_{zy} = & i\frac{(k_\perp - l\Omega_0\tau/L)\rho_\perp}{2}\left[I_l' - \left(\frac{k_\perp}{k_\perp - \frac{l\Omega_0\tau}{L}}\right) I_l\right] A_2, \\ V_{zz} = & I_l A_3 \end{bmatrix}. \quad (4.60)$$

Or, alternatively, we may introduce a new variable k_1 having the same dimensions as a wavenumber such that $k_1 = \frac{-l\Omega_0(0)\tau}{L}$. Apart from a modification of the integration

range, this also results in the slight changes: $\beta \rightarrow (k_\perp + k_1)\,\rho_\perp$, $\lambda \rightarrow \frac{1}{2}k_\perp\,(k_\perp + k_1)\,\rho_\perp^2$ and $\psi \rightarrow -\frac{k_\parallel u_{T\parallel} k_1 L}{l\Omega_0(0)}$. If, in addition, we write out the x-dependence of Ω_0,

$$\omega - l\Omega_0\,(x) = \omega - l\Omega_0\,(0) + \frac{l\Omega_0\,(0)}{L}x, \tag{4.61}$$

then we find that the conductivity tensor of (4.59) takes the following form,

$$\begin{aligned}\sigma_{ij}\,(x,\mathbf{k}) = & - \frac{i\epsilon_0\omega_p^2}{\omega}\frac{T_\parallel}{T_\perp}\left(1-\frac{T_\perp}{T_\parallel}\right)\hat{\mathbf{e}}_{33} \\ & + \frac{\epsilon_0\omega_p^2 L}{l\Omega_0\,(0)}\sum_l \\ & \times \int_0^\infty dk_1 e^{ik_1 x + ik_1[\omega - l\Omega_0(0)]\frac{L}{l\Omega_0(0)} - \frac{1}{4}k_1^2\rho_\perp^2\left[1+k_\parallel^2 L^2\left(\frac{T_\parallel}{T_\perp}\right)/l^2\right]-\lambda} V_{ij}\,(\mathbf{k},k_1)\,,\end{aligned} \tag{4.62}$$

with,

$$\left[\begin{array}{lll} V_{xx} &=& \frac{l^2}{\lambda}I_l A_1, \\ V_{xy} &=& il\left[I_l' - \frac{k_\perp}{k_\perp+k_1}I_l\right]A_1, \\ V_{xz} &=& \frac{l}{(k_\perp+k_1)\rho_\perp}I_l A_2, \\ V_{yx} &=& -il\left[I_l' - \frac{k_\perp+k_1}{k_\perp}I_l\right]A_1, \\ V_{yy} &=& \left[\left(2\lambda+\frac{l^2}{\lambda}\right)I_l - \left(2\lambda+\frac{1}{2}k_1^2\rho_\perp^2\right)I_l'\right]A_1, \\ V_{yz} &=& -i\frac{k_\perp\rho_\perp}{2}\left[I_l' - \frac{k_\perp+k_1}{k_\perp}I_l\right]A_2, \\ V_{zx} &=& \frac{l}{k_\perp\rho_\perp}I_l A_2, \\ V_{zy} &=& i\frac{(k_\perp+k_1)\rho_\perp}{2}\left[I_l' - \frac{k_\perp}{k_\perp+k_1}I_l\right]A_2, \\ V_{zz} &=& I_l A_3 \end{array}\right]. \tag{4.63}$$

As a check on the validity of our theoretical results let us compare with those obtained by some other authors for models which we may aspire to by taking certain limits.

4.2 Comparison With Other Related Work

We would ideally like to have a means of checking both the effects of nonuniformity which are presented in the form of the integrals and also the terms which have arisen due to thermal anisotropy. McDonald et al.(1994) have presented tensor elements for a relativistic isotropic plasma in an inhomogeneous magnetic field and so, in the limit of non-relativistic particle energies, we may compare the non-local integrals although we cannot check our anisotropic terms. Stix(1992) has presented tensor elements for a bi-Maxwellian plasma immersed in a uniform magnetic field and so we can compare our anisotropic terms although, in this case, our non-local integrals will be approximated by

their plasma dispersion functions (Z-functions) and so their more general form cannot be checked. In what follows we will show that we recover the results of the above authors in the limiting cases for which their theory applies. We hope that the numerical results of chapter 8 combined with the qualitative insights presented in the next chapter will add more credence to our theory.

4.2.1 A Non-Relativistic Thermally Isotropic But Magnetically Inhomogeneous Plasma

We begin by quoting equation (3.23) of McDonald et al.(1994),

$$i\omega\mu_0\mathbf{J}_1(x) = \frac{i\mu\omega_p^2}{c^2}\sum_n \int_{-\infty}^{\infty} dk_x e^{ik_x x}\int_0^{\infty} dt \frac{e^{i\zeta_n t - \frac{a_n t^2}{(1-it)}}}{(1-it)^{5/2}} C_n(k_x,t) \bullet \mathbf{E}_1(k_x), \tag{4.64}$$

from which we may identify the conductivity tensor,

$$\sigma_n(x,k_x,t) = \frac{\mu\epsilon_0\omega_p^2}{\omega}\sum_n \int_0^{\infty} dt \frac{e^{i\zeta_n t - \frac{a_n t^2}{(1-it)}}}{(1-it)^{5/2}} C_n(k_x,t), \tag{4.65}$$

with,

$$C_n(k_x,t) = e^{-\lambda} C_{ij}(k_x,t), \tag{4.66}$$

$$\left[\begin{array}{rcl} C_{xx} &=& \frac{n^2}{\lambda} I_n, \\ C_{xy} &=& in\left[I_n' - \frac{k_x}{k_x+h_n t} I_n\right], \\ C_{xz} &=& -\frac{2i\alpha n t}{(k_x+h_n t)\rho} I_n, \\ C_{yx} &=& -in\left[I_n' - \frac{k_x+h_n t}{k_x} I_n\right], \\ C_{yy} &=& \left(2\lambda + \frac{n^2}{\lambda}\right) I_n - \left(2\lambda + \frac{h_n^2\rho^2}{2(1-it)}\right) I_n', \\ C_{yz} &=& -\frac{\alpha\rho t}{(1-it)}\left[k_x I_n' - (k_x + h_n t) I_n\right], \\ C_{zx} &=& -\frac{2i\alpha n t}{k_x\rho} I_n, \\ C_{zy} &=& \frac{\alpha\rho t}{(1-it)}\left[(k_x + h_n t) I_n' - k_x I_n\right], \\ C_{zz} &=& \left(1 - \frac{2\alpha^2 t^2}{(1-it)}\right) I_n. \end{array}\right] . \tag{4.67}$$

The definitions of the variables used are,

$$\begin{gathered} \zeta_n = \mu\frac{\omega - n\Omega_0}{\omega}, \quad \alpha = n_z\frac{c}{u_t}, \quad h_n = \frac{n\Omega_0\mu}{\omega L}, \quad \mu = 2\frac{c^2}{u_t^2}, \quad t = -\frac{\omega\tau}{\mu\gamma}, \\ n_z = \frac{ck_z}{\omega}, \quad a_n = \alpha^2 + \left(\frac{h_n\rho}{2}\right)^2, \quad \lambda = \frac{\frac{1}{2}k_x(k_x + h_n t)\rho^2}{(1-it)}, \end{gathered} \tag{4.68}$$

allowing us to write,

$$dt = -\frac{\omega}{\mu\gamma}d\tau, \quad \zeta t = -\frac{(\omega - n\Omega_0)\tau}{\gamma}, \quad h_n t = -\frac{n\Omega_0}{\gamma L}\tau, \quad \alpha t = -\frac{k_z u_t}{2\gamma}\tau, \alpha\rho t = -\frac{k_z u_t^2}{2\gamma\Omega_0}\tau,$$
$$1 - it = 1 + \frac{i\omega}{\mu\gamma}\tau, \quad \lambda = \frac{1}{2}k_x\left(k_x - \frac{n\Omega_0}{\gamma L}\tau\right)\rho^2, \quad a_n t^2 = \frac{n^2 u_t^2}{4\gamma^2 L^2}\tau^2\left(1 + k_z^2 L^2 n^2\right) \quad (4.69)$$

In the limit of a non-relativistic plasma we have the following behaviour,

$$\left.\begin{array}{c} \mu = 2\frac{c^2}{u_t^2} \to \infty \\ \gamma = \frac{1}{\sqrt{1-u_t^2/c^2}} \to 1 \end{array}\right\} as \quad \frac{u_t^2}{c^2} \to 0. \quad (4.70)$$

If we substitute expressions (4.69) into (4.65) and (4.66), while at the same time bearing in mind the non-relativistic limits of (4.70) then we obtain the non-relativistic conductivity tensor for an isotropic plasma immersed in an inhomogeneous magnetic field,

$$\sigma_n(x, k_x, \tau) = -\epsilon_0\omega_p^2 \sum_n \int_0^{-\infty} d\tau e^{-i\tau(\omega - n\Omega_0) - \frac{1}{4}\tau^2\frac{n^2 u_t^2}{L^2}\left(1 + k_z^2 L^2/n^2\right)} C_n(k_x, \tau), \quad (4.71)$$

with,

$$C_n(k_x, \tau) = e^{-\lambda} C_{ij}(k_x, \tau), \quad (4.72)$$

$$\left[\begin{array}{rcl} C_{xx} & = & \frac{n^2}{\lambda} I_n, \\ C_{xy} & = & in\left[I_n' - \frac{k_x}{k_x - n\Omega_0\tau/L} I_n\right], \\ C_{xz} & = & \frac{ink_z\Omega_0\tau}{k_x - n\Omega_0\tau/L} I_n, \\ C_{yx} & = & -in\left[I_n' - \frac{k_x - n\Omega_0\tau/L}{k_x} I_n\right], \\ C_{yy} & = & \left(2\lambda + \frac{n^2}{\lambda}\right) I_n - \left(2\lambda + \frac{n^2 u_t^2\tau^2}{2L^2}\right) I_n', \\ C_{yz} & = & \frac{k_z u_t^2\tau}{2\Omega_0}\left[k_x I_n' - \left(k_x - n\Omega_0\tau/L\right) I_n\right], \\ C_{zx} & = & \frac{ink_z\Omega_0\tau}{k_x} I_n, \\ C_{zy} & = & -\frac{k_z u_t^2\tau}{2\Omega_0}\left[\left(k_x - n\Omega_0\tau/L\right) I_n' - k_x I_n\right], \\ C_{zz} & = & \left(1 - \frac{k_z^2 u_t^2\tau^2}{2}\right) I_n \end{array}\right], \quad (4.73)$$

and here, $\lambda = \frac{1}{2}k_x\left(k_x - n\Omega_0\tau/L\right)\rho^2$, reproducing our result in (4.59) for an isotropic plasma with $T_\perp = T_\parallel \equiv T$.

4.2.2 A Non-Relativistic Thermally Anisotropic And Homogeneous Plasma

This calculation is most easily performed if we use the conductivity tensor for a thermally anisotropic plasma in an inhomogeneous magnetic field, expressed in terms of τ as in

(4.59). If we separate out the uniform and the non-uniform parts of λ in the exponential then we may write,

$$\begin{aligned}\sigma_{ij}(x,\mathbf{k}) = & - \frac{i\epsilon_0\omega_p^2}{\omega}\frac{T_\parallel}{T_\perp}\left(1-\frac{T_\perp}{T_\parallel}\right)\hat{\mathbf{e}}_{33} \\ & - \epsilon_0\omega_p^2 e^{-\lambda^h}\sum_l \int_0^{-\infty} d\tau e^{-i\tau X-\frac{1}{4}\tau^2Y^2}V_{ij}(\mathbf{k},\tau), \end{aligned} \tag{4.74}$$

and we have defined,

$$X = \omega - l\Omega_0 + \frac{1}{2}ik_\perp\frac{lu_{T\perp}^2}{\Omega_0 L}, \tag{4.75}$$

$$Y^2 = \frac{l^2u_{T\perp}^2}{L^2}\left[1+\frac{k_\parallel^2L^2}{l^2}\left(T_\parallel/T_\perp\right)\right]. \tag{4.76}$$

Let us now take the limit of a locally uniform plasma whereby $L\to\infty$ so that we have,

$$\left.\begin{array}{l} X\to\omega-l\Omega_0 \\ Y\to k_\parallel u_{T\parallel} \\ \lambda\to\lambda^h \end{array}\right\} as \quad L\to\infty, \tag{4.77}$$

and,

$$\left[\begin{array}{rcl} V_{xx} &=& \frac{l^2}{\lambda^h}I_lA_1, \\ V_{xy} &=& il\left(I_l'-I_l\right)A_1, \\ V_{xz} &=& l\frac{1}{\sqrt{2\lambda^h}}I_lA_2, \\ V_{yx} &=& -il\left(I_l'-I_l\right)A_1, \\ V_{yy} &=& \left[\frac{l^2}{\lambda^h}I_l+2\lambda^h\left(I_l-I_l'\right)\right]A_1, \\ V_{yz} &=& -i\sqrt{\frac{\lambda^h}{2}}\left(I_l'-I_l\right)A_2, \\ V_{zx} &=& l\frac{1}{\sqrt{2\lambda^h}}I_lA_2, \\ V_{zy} &=& i\sqrt{\frac{\lambda^h}{2}}\left(I_l'-I_l\right)A_2, \\ V_{zz} &=& I_lA_3 \end{array}\right], \tag{4.78}$$

with A_j defined by (4.52) to (4.53). Since the argument of the modified Bessel functions is now λ^h then they are independent of the variable of integration-τ. If we recall that the plasma dispersion function(Z-function) can be written as,

$$Z\left(\frac{X}{Y}\right) \equiv -iY\int_0^{-\infty} d\tau e^{-i\tau X-\frac{1}{4}\tau^2Y^2}, \tag{4.79}$$

and that differentiation under the integral sign gives us the generalisation,

$$\int_0^{-\infty} d\tau \left[-i\tau\right]^n e^{-i\tau X - \frac{1}{4}\tau^2 Y^2} \equiv \frac{i}{Y}\left[\frac{\partial^n}{\partial X^n}\right] Z\left(\frac{X}{Y}\right) \equiv \frac{i}{Y}\left[\frac{1}{Y^n}\right] Z^{[n]}(\zeta)\,, \tag{4.80}$$

then the homogeneous plasma form becomes,

$$\begin{aligned} \sigma_{ij}^h(x,\mathbf{k}) = & - \frac{i\epsilon_0\omega_p^2}{\omega}\frac{T_\parallel}{T_\perp}\left(1-\frac{T_\perp}{T_\parallel}\right)\hat{\mathbf{e}}_{33} \\ & - \frac{i\epsilon_0\omega_p^2}{k_\parallel u_{T\parallel}} e^{-\lambda^h} V_{ij}^h\left(\mathrm{k}, \overrightarrow{\partial}_\zeta\right) Z(\zeta)\,. \end{aligned} \tag{4.81}$$

The operator terms $\overrightarrow{\partial}_\zeta$ arise from the anisotropic tail factors A_j of V_{ij} which, noting that from (4.80) $\psi \equiv i\partial_\zeta$, become

$$\overrightarrow{A}_1 = \{1 + \frac{k_\parallel u_{T\parallel}}{2\omega}\left(1-\frac{T_\perp}{T_\parallel}\right)\frac{\partial}{\partial\zeta}\}, \tag{4.82}$$

$$\overrightarrow{A}_2 = \sqrt{\frac{T_\parallel}{T_\perp}}\{-\frac{\partial}{\partial\zeta} - \frac{k_\parallel u_{T\parallel}}{\omega}\left(1-\frac{T_\perp}{T_\parallel}\right)\left(1+\frac{1}{2}\frac{\partial^2}{\partial\zeta^2}\right)\}, \tag{4.83}$$

$$\overrightarrow{A}_3 = \frac{T_\parallel}{T_\perp}\{1 + \frac{1}{2}\frac{\partial^2}{\partial\zeta^2} + \frac{k_\parallel u_{T\parallel}}{2\omega}\left(1-\frac{T_\perp}{T_\parallel}\right)\left(3\frac{\partial}{\partial\zeta} + \frac{1}{2}\frac{\partial^3}{\partial\zeta^3}\right)\}. \tag{4.84}$$

If we introduce the argument for the fundamental $\zeta_0 = \omega \big/ k_\parallel u_{T\parallel}$ then we have,

$$\overrightarrow{A}_1 Z = \{Z + \frac{1}{2\zeta_0}\left(1-\frac{T_\perp}{T_\parallel}\right)Z'\}, \tag{4.85}$$

$$\overrightarrow{A}_2 Z = \sqrt{\frac{T_\parallel}{T_\perp}}\{-Z' - \frac{1}{\zeta_0}\left(1-\frac{T_\perp}{T_\parallel}\right)\left(Z+\frac{1}{2}Z''\right)\}, \tag{4.86}$$

$$\overrightarrow{A}_3 Z = \frac{T_\parallel}{T_\perp}\{Z + \frac{1}{2}Z'' + \frac{1}{2\zeta_0}\left(1-\frac{T_\perp}{T_\parallel}\right)\left(3Z' + \frac{1}{2}Z'''\right)\}. \tag{4.87}$$

These may be further simplified through the use of the recurrence relations for higher derivatives of Z,

$$Z'(\zeta) = -2\left[1 + \zeta Z(\zeta)\right], \tag{4.88}$$

$$Z''(\zeta) = -2\left[Z(\zeta) + \zeta Z'(\zeta)\right], \tag{4.89}$$

$$Z'''(\zeta) = -4\left[\left(1-\zeta^2\right)Z'(\zeta) - \zeta Z(\zeta)\right], \tag{4.90}$$

so that we can derive the results,

$$Z(\zeta)+\frac{1}{2}Z''(\zeta) = -\zeta Z'(\zeta), \tag{4.91}$$

$$3Z'(\zeta)+\frac{1}{2}Z'''(\zeta) = -2\left(1-\zeta^2\right)Z'(\zeta). \tag{4.92}$$

The conductivity tensor may now be written as,

$$\begin{aligned}\sigma_{ij}^h(x,\mathbf{k}) = & -\frac{i\epsilon_0\omega_p^2}{\omega}\frac{T_\parallel}{T_\perp}\left(1-\frac{T_\perp}{T_\parallel}\right)\hat{\mathbf{e}}_{33} \\ & -\frac{i\epsilon_0\omega_p^2}{\omega}\zeta_0 e^{-\lambda^h}V_{ij}^h(\mathbf{k}),\end{aligned} \tag{4.93}$$

and the velocity tensor is as before in (4.78) but now we have absorbed the Z-functions into the anisotropic tail factors,

$$A_1 = Z+\frac{1}{2\zeta_0}\left(1-\frac{T_\perp}{T_\parallel}\right)Z', \tag{4.94}$$

$$A_2 = -\sqrt{\frac{T_\parallel}{T_\perp}}\left[1-\frac{\zeta}{\zeta_0}\left(1-\frac{T_\perp}{T_\parallel}\right)\right]Z', \tag{4.95}$$

$$A_3 = -\frac{T_\parallel}{T_\perp}\zeta\left[1+\frac{(1-\zeta^2)}{\zeta_0\zeta}\left(1-\frac{T_\perp}{T_\parallel}\right)\right]\zeta Z'. \tag{4.96}$$

We note the existence of terms involving $\left(1-T_\perp/T_\parallel\right)$. These have arisen from the thermal anisotropy in the bi-Maxwellian distribution and may be traced back to their embryological origin in the magnetic component $(\mathbf{u}\times\mathbf{B}_0)$ of the Lorentz force. These naturally disappear in the limit of an isotropic plasma where $T_\perp \equiv T_\parallel$ giving the following isotropic plasma result,

$$\begin{aligned}\sigma_{ij}^h(x,\mathbf{k}) = & -\frac{i\epsilon_0\omega_p^2}{\omega}\zeta_0 e^{-\lambda^h} \\ & \times\begin{bmatrix} \frac{l^2}{\lambda^h}I_l Z & il\left(I_l'-I_l\right)Z & -l\frac{1}{\sqrt{2\lambda^h}}I_l Z' \\ -il\left(I_l'-I_l\right)Z & \left[\frac{l^2}{\lambda^h}I_l+2\lambda^h\left(I_l-I_l'\right)\right]Z & i\sqrt{\frac{\lambda^h}{2}}\left(I_l'-I_l\right)Z' \\ -l\frac{1}{\sqrt{2\lambda^h}}I_l Z' & -i\sqrt{\frac{\lambda^h}{2}}\left(I_l'-I_l\right) & -I_l\zeta Z'\end{bmatrix}.\end{aligned} \tag{4.97}$$

Our isotropic plasma result here is exactly equivalent to that obtained in equation (58) of chapter 10 of Stix(1992). To see this we note that for an isotropic plasma then we use (66) and (67) of Stix with $V=0$. Then if we write the coefficients of the z elements in (57) in terms of λ we may obtain the required agreement.

4.3 The Non-Local Integro-Differential Wave Equation(IDE)

The conductivity tensor(σ_{ij}) is a non-local response function, comprising a set of coefficients which multiply the electric field($\mathbf{E}$) so as to give the response of the plasma in the form of the current density ($\mathbf{J}$). If we introduce the susceptibility tensor,

$$\chi_{ij} \equiv \frac{i}{\epsilon_0 \omega} \sigma_{ij}, \tag{4.98}$$

then the current density described by (3.38) may be written,

$$\frac{i}{\epsilon_0 \omega} \mathbf{J}(\mathbf{r}) = \int d\mathbf{k} e^{i\mathbf{k}\bullet\mathbf{r} - i\omega t} \chi_{ij}(\mathbf{r}) \bullet \overline{\mathbf{E}}(\mathbf{k}). \tag{4.99}$$

This then, is the required term in Maxwell's wave equation (3.1). If we note the vector identity,

$$\mathbf{A} \times (\mathbf{B} \times \mathbf{C}) \equiv \mathbf{B}(\mathbf{A} \bullet \mathbf{C}) - \mathbf{C}(\mathbf{A} \bullet \mathbf{B}),$$

we may identify the wave equation,

$$\frac{c^2}{\omega^2} \nabla^2 \mathbf{E}(\mathbf{r}) - \frac{c^2}{\omega^2} \nabla(\nabla \bullet \mathbf{E}(\mathbf{r})) + \mathbf{E}(\mathbf{r}) + \int d\mathbf{k} e^{i\mathbf{k}\bullet\mathbf{r} - i\omega t} \chi_{ij}(\mathbf{r}) \bullet \overline{\mathbf{E}}(\mathbf{k}) = 0. \tag{4.100}$$

This is an integro-differential equation(IDE) for the electric field although, in this form, it appears confusing since the plasma response integral involves Fourier components of the electric field($\overline{\mathbf{E}}(\mathbf{k})$) in momentum(k)-space while the vacuum part(the first two terms) involves the electric field in real(r)-space. We shall resolve this in chapter 6. Before doing so, let us perform a qualitative analysis of the conductivity tensor so as to get an insight into its physical properties.

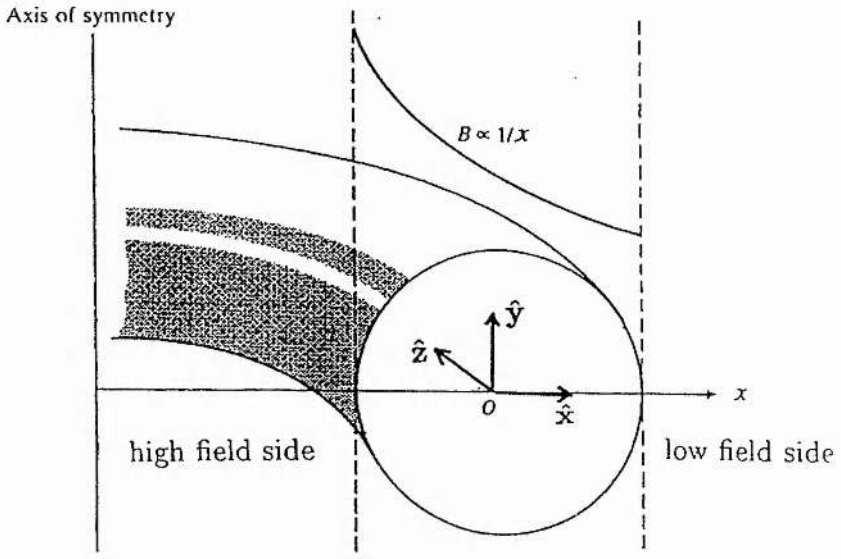

Figure 4.1: Cartesian coordinates in the context of tokamak geometry.

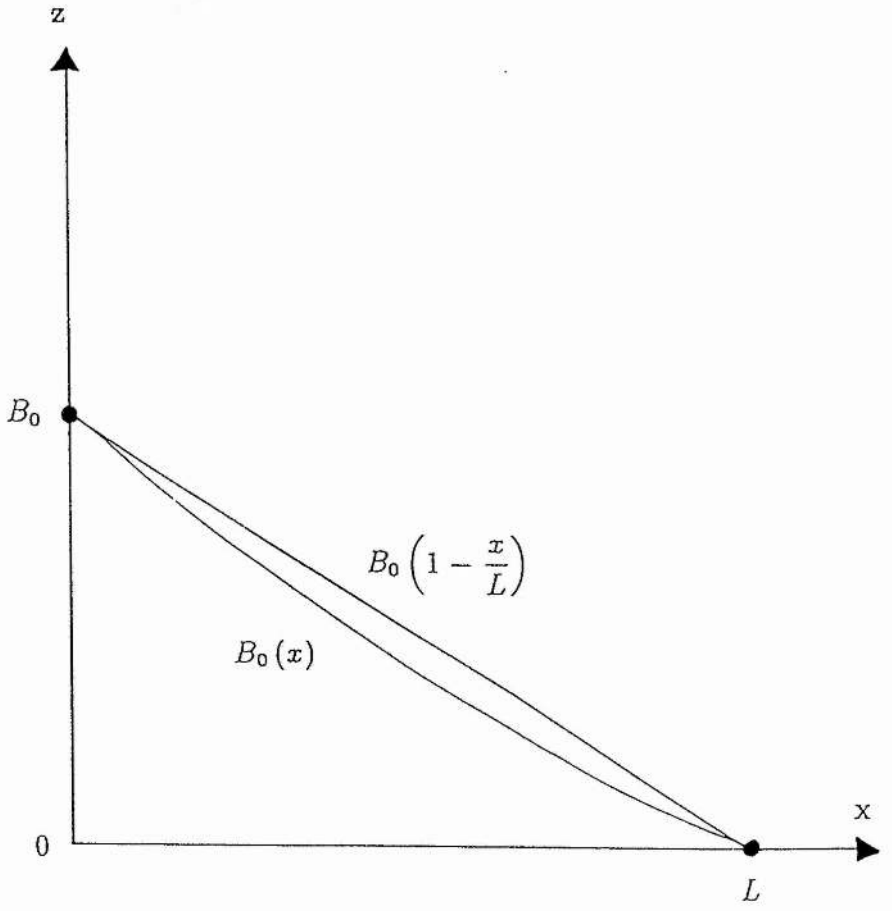

Figure 4.2: The linear gradient model of the magnetic field.

Chapter 5

A Statistical Approach To Resonance

In this chapter we will look carefully at the qualitative effects introduced by our analysis in comparison with existing theory. We can consider the insights we obtain, through a qualitative analysis, as a type of data. Indeed we obtain a crucial bit of knowledge about the resolution of the harmonics which allows us to handle the infinite summation over all harmonics in the response function of the previous chapter. A quote seems appropriate here,

> *It is a capital mistake to theorise before one has data. Inevitably one begins to twist the facts to suit theories instead of theories to suit facts.*
>
> *-Sir Arthur Conan Doyle.*

5.1 Resonance Broadening Described By A Standard Deviation

Since the object of any description is to convey an idea in a way that is effective, easy to grasp and honest, we present here an alternative study of the effects of thermal anisotropy and magnetic field inhomogeneity upon the conductivity with the hope of achieving this aim.

We have shown how a simple pole in the denominator of the conductivity tensor is responsible for resonance phenomena in hot magnetised plasmas. The resonance condition for a bi-Maxwellian plasma in a linearly inhomogeneous magnetic field is,

$$\omega + \delta\omega = l\Omega_0, \tag{5.1}$$

with,

$$\delta\omega = k_{\|}u_{\|} - lu_{\perp}\sin\theta\,/L\,, \tag{5.2}$$

and $\delta\omega$ is the frequency spread about the resonant harmonic of the gyrofrequency due to resonance broadening effects. The first term in (5.2) may be associated with the Doppler frequency shift due to motion of the resonant particles along the magnetic field while the second term is a frequency shift associated with the variation of the magnetic field across the orbit of the resonant particles. Each of these terms contribute uncertainties to the value of the frequency ω. We may construct a simple error analysis using the equilibrium distribution(f_0) as a continuous probability distribution function since the error in this case $\delta\omega$ is a function of the independent variable in the distribution, the particle velocity.

If we recall that the gyrofrequency varies as, $\Omega_0(x) = \Omega_0(0)(1 - x/L)$ then (5.1) gives us the condition,

$$\frac{x}{L} = \frac{\delta\omega}{l\Omega_0}. \tag{5.3}$$

Here x/L is a physical distance measure of the spread of frequencies $\delta\omega$ about the resonant harmonic of the gyrofrequency. The velocity dependence of $\delta\omega$ means that the resonance will be spread effectively by the velocity distribution.

We may now exploit the statistical nature of f_0 to calculate the actual absorption width of resonances in a hot magnetised plasma through a little knowledge of statistics,

> *...only by understanding the ways distributions give rise to data can we go on to use the particular behaviour of the data to produce general statements about the processes that produced them in the first place- or,as Holmes puts it, to twist your theory to suit your observed facts.*
>
> *-R. J. Barlow*

Our equilibrium distribution function f_0 is a continuous Gaussian probability distribution whose mean velocity is centred at the origin so that contours of constant f_0 are curves for which the quadratic exponent is a constant. This gives ellipses centred on the origin and whose minor and major axes are determined by the degree of thermal anisotropy being equal to $u_\parallel^2/u_{T\parallel}^2$ and $u_\perp^2/u_{T\perp}^2$. In the limit of an isotropic distribution then the ellipses becomes circles.

The Gaussian nature of the distribution means that most of the particles in the plasma will have a velocity approximately equal to the mean velocity which is, for our equilibrium, u_T. These particles will not contribute to $\delta\omega$ and so will not be responsible for spreading the resonance. However, particles with velocities comparable with their thermal values so that $u_\perp^2 \simeq u_{T\perp}^2$ and $u_\parallel^2 \simeq u_{T\parallel}^2$, will have a pronounced effect on the resonance width contributing to both the Doppler shifting and GK correction parts of $\delta\omega$, although they will number only about $1/e$ of those particles with the mean velocity. Similarly, particles of

even higher energies will contribute more, on an individual level, to the resonance broadening but their cumulative effect will be less than at the thermal velocity since they are fewer in number. In this way, we can see physically how exactly an equilibrium distribution function, constructed from the constants of the motion, is responsible for resonance broadening when their exist terms in the resonance condition which are also dependent on the constants of the motion of charged particles in an inhomogeneous magnetic field. We now replace this physically meaningful, though rather heuristic, thought process with one which has a more rigorous mathematical basis.

As a first step, we may normalise the distribution function to the total particle density n_o such that,

$$\int f_0(\mathbf{u})\, d\mathbf{u} = 1, \tag{5.4}$$

expressing the fact that a real-valued random velocity must certainly lie between $-\infty$ and ∞. The expectation value($\mathcal{E}$) of any quantity(g) which, since velocity is the independent variable in the distribution, must also be a function of velocity, is given by,

$$\mathcal{E}[g(\mathbf{u})] \equiv < g(\mathbf{u}) > = \int g(\mathbf{u})\, f_0(\mathbf{u})\, d\mathbf{u}. \tag{5.5}$$

In particular, the mean, $\overline{\mathbf{u}}$ is just the expectation value of $\mathbf{u}$. .It should be mentioned that this is a special property of Gaussians and is not true in general. We will be interested in calculating the expectation value of the frequency spread about a gyroresonance. Since the frequency spread arises from velocity dependent physics as described above in (5.2) then it may be thought of as introducing errors. For a systematic and thorough study of these errors we need to introduce some other statistical quantities.

A sensible measure of the spread of the frequency about the gyroresonance (equivalent to a spread of data about the mean) is the average squared deviation from the mean, the variance($\mathcal{V}$),

$$\mathcal{V}(\mathbf{u}) \equiv < (\mathbf{u} - < \mathbf{u} >)^2 > = \int (\mathbf{u} - < \mathbf{u} >)^2 f_0(\mathbf{u})\, d\mathbf{u} = < \mathbf{u}^2 > - < \mathbf{u} >^2 . \tag{5.6}$$

So the variance is the mean square minus the squared mean! We use the average squared deviation and not the average deviation since positive and negative deviations cancel. A more physically useful form which has the same dimensions as the independent variable is the root mean squared deviation or standard deviation($\mathcal{S}$),

$$\mathcal{S}(\mathbf{u}) \equiv \sqrt{\mathcal{V}(\mathbf{u})} = \sqrt{< \mathbf{u}^2 > - < \mathbf{u} >^2}. \tag{5.7}$$

One problem with using $\mathcal{S}$ as a measure of the spread is that its value can be dominated by a few extreme values out in the tails of the distribution (although a Gaussian decays monotonically to zero in the tails and hence is well behaved in this respect). An alternative measure often quoted is the full width at half maximum(FWHM) which is determined from the region around the central maximum and is related to the standard deviation.

For a Gaussian then $FWHM \simeq 2.35\mathcal{S}$.

We have seen how the mean and the standard deviation were calculated from the first and second powers(termed moments) of $\mathbf{u}$. Other useful quantities can be obtained from higher moments.

The skew is a way of describing the asymmetry($\mathcal{A}$) of the distribution. It is made from the third power of $\mathbf{u}$,

$$\mathcal{A}(\mathbf{u}) = \frac{<(\mathbf{u}- <\mathbf{u}>)^3>}{\mathcal{S}^3}. \tag{5.8}$$

Symmetric distributions like our Gaussian f_0 have $\mathcal{A} = 0$. This may easily be shown mathematically by a little knowledge of even and odd functions. The Gaussian is a symmetric function and since, in calculating the skew, we must integrate the third moment(cubic=odd function) times the distribution over all space then positive and negative regions exactly cancel reflecting the fact that an odd function integrates to zero over a symmetric interval.

In addition to the skew, the curtosis($\mathcal{C}$) is a way of describing the peakedness of a distribution and is made from the fourth power of $\mathbf{u}$,

$$\mathcal{C}(\mathbf{u}) = \frac{<(\mathbf{u}- <\mathbf{u}>)^4>}{\mathcal{S}^4} - 3. \tag{5.9}$$

For a Gaussian then $\mathcal{C} = 0$. The 3 in the definition is brought in specifically to ensure this! These latter two definitions allow us to compare quantitatively the equilibrium plasma state described by the equilibrium distribution f_0 with the response of the plasma in the form of the perturbed distribution f_1. We have shown how qualitative information may be found by investigating the moments of the distribution which for a general r^{th} moment($\mathcal{M}$) is,

$$\mathcal{M}_r \equiv <(\mathbf{u}- <\mathbf{u}>)^r> = \int (\mathbf{u}- <\mathbf{u}>)^r f_0(\mathbf{u})\, d\mathbf{u}, \tag{5.10}$$

and so,

$$\mathcal{M}_0 = 1, \tag{5.11}$$
$$\mathcal{M}_1 = 0, \tag{5.12}$$
$$\mathcal{M}_2 = \mathcal{S}^2, \tag{5.13}$$
$$\mathcal{M}_3 = \mathcal{A}, \tag{5.14}$$
$$\mathcal{M}_4 = \mathcal{C}. \tag{5.15}$$
$$\tag{5.16}$$

Our measure of the resonance width is given by (5.3) and, since it is velocity dependent, then from (5.5) we define,

$$g(\mathbf{u}) \equiv \frac{\delta\omega}{l\Omega_0} = \frac{k_{||}}{l\Omega_0}u_{||} - \frac{\sin\theta}{\Omega_0 L}u_{\perp}. \tag{5.17}$$

We may go ahead and work out the variance of this and obtain the absorption width in terms of the resultant standard deviation. However, f_0 is not simply an explicit function of $\mathbf{u}$ and is instead a function of the components of $\mathbf{u}$. So we must consider the effect of a distribution which is a function of more than one variable. Indeed these variables may be connected in some way and the variance should not be expected to have the $1D$ form proposed by (5.6).

A measure of the interdependence of variables in a distribution is the covariance, which for a 2D distribution comprising the variables X and Y is,

$$\begin{aligned} Cov(X,Y) &\equiv < (X- < X >)(Y- < Y >) > \\ &= \int\int (X- < X >)(Y- < Y >) f_0(X,Y)\, dXdY \\ &\equiv < XY > - < X >< Y > \equiv \sigma_{XY}. \end{aligned} \tag{5.18}$$

- Positive covariance means that above-average values of X have a tendency to occur together with above-average Y values, similarly for below-average values.
- Negative covariance means that large X tend to pair with small Y.
- Zero covariance occurs when X and Y are unconnected so that a positive $(X- < X >)$ has an equal chance of being multiplied by a positive or negative $(Y- < Y >)$ leading to a net cancellation.

There is a statistical theorem which allows us to combine variances,

$$V(X \pm Y) \equiv V(X) + V(Y) \pm 2Cov(X,Y). \tag{5.19}$$

So, for independent variables then we simply add the errors in quadrature. We will not go into a proof of why this is so. Instead, we quote a corollary of another statistical theorem- the central limit theorem which says that any quantity produced by the cumulative effect of many independent variables will be approximately Gaussian as the number of variables tends to ∞. This reflects the fact that the expectation value of a sum is equal to the sum of the expectation values.

The covariance is a dimensional quantity and so as a measure of the interdependence is not so useful just as a probability defined in metres would not make so much sense. A better measure is the correlation coefficient,

$$Corr \equiv \frac{Cov(X,Y)}{\mathcal{S}_X\mathcal{S}_Y} = \frac{< XY > - < X >< Y >}{\mathcal{S}_X\mathcal{S}_Y}, \tag{5.20}$$

so that $|Corr| = 1$.

- If $Corr > 0$ then $X > \overline{X}$ guarantees that $Y > \overline{Y}$.
- If $Corr < 0$ then $X > \overline{X}$ guarantees that $Y < \overline{Y}$.
- If $Corr = 0$ then X and Y are uncorrelated.
- If $Corr = \pm 1$ then X and Y are correlated and knowing the value of one precisely specifies the other. This is rather like collapsing the wave function in quantum theory and is responsible for the results born out of the infamous EPR experiment.

We will now see how all of this fits into a calculation of the resonance absorption width.

First of all let us write,

$$g(\mathbf{u}) \equiv g(u_\perp) + g\left(u_\parallel\right), \tag{5.21}$$

so that we can identify the separate contributions from each of the resonance broadening terms. From (5.18) we know that the covariance is,

$$Cov\left[g(u_\perp), g\left(u_\parallel\right)\right] \equiv < g(u_\perp) g\left(u_\parallel\right) > - < g(u_\perp) >< g\left(u_\parallel\right) > . \tag{5.22}$$

and if we set $g(u_\perp) = -(\sin\theta / \Omega_0 L) u_\perp$ and $g\left(u_\parallel\right) = \left(k_\parallel / l\Omega_0\right) u_\parallel$ in (5.21) and note the following set of identities,

$$\int_{-\infty}^{\infty} dx e^{-px^2} \equiv \sqrt{\frac{\pi}{p}}, \tag{5.23}$$

$$\int_{-\infty}^{\infty} dx x^{2n+1} e^{-px^2} \equiv 0, \tag{5.24}$$

$$\int_{-\infty}^{\infty} dx x^2 e^{-px^2} \equiv \frac{1}{2p}\sqrt{\frac{\pi}{p}}, \tag{5.25}$$

$$\int_{0}^{\infty} dx e^{-px^2} \equiv \frac{1}{2}\sqrt{\frac{\pi}{p}}, \tag{5.26}$$

$$\int_{0}^{\infty} dx x^{2n+1} e^{-px^2} \equiv \frac{n!}{2(p)^{n+1}}, \tag{5.27}$$

$$\int_{0}^{\infty} dx x^{2n} e^{-px^2} \equiv \frac{1.3.5...(2n-1)}{2(2p)^n}\sqrt{\frac{\pi}{p}}, \tag{5.28}$$

$$\int_0^{2\pi} d\theta \sin\theta \equiv 0, \tag{5.29}$$

$$\int_0^{2\pi} d\theta \sin^2\theta \equiv \pi, \tag{5.30}$$

then we find,

$$Cov\left[g\left(u_\perp\right), g\left(u_\parallel\right)\right] \equiv 0. \tag{5.31}$$

The contributions to $g(\mathbf{u})$ from the velocity components are uncorrelated. Physically we expect this as each component lies along an orthogonal axes and their dot product is zero. From the way variances combine in (5.19) we expect the velocity dependent errors $g\left(u_\perp\right)$ and $g\left(u_\parallel\right)$ to add in quadrature. As a matter of interest the inclusion of order ϵ drift terms proportional to $u_\perp^2/2\Omega_0 L$ means that there will, in this particular case, be a correlation between the resonance broadening due to the GK correction and that due to guiding centre drifts in an inhomogeneous magnetic field and there will be an extra term in the variance due to the covariance of these. If we use our distribution function f_0 of (4.10), the measure of the broadening of the resonance is,

$$\begin{aligned}
\mathcal{V}\left[g\left(\mathbf{u}\right)\right] \equiv \sigma^2\left[g\left(\mathbf{u}\right)\right] &\equiv < g\left(\mathbf{u}\right)^2 > - < g\left(\mathbf{u}\right) >^2 \\
&= \int d\mathbf{u} f_0\left(\mathbf{u}\right)\left[g\left(\mathbf{u}\right)\right]^2 - \left[\int d\mathbf{u} f_0\left(\mathbf{u}\right) g\left(\mathbf{u}\right)\right]^2 \\
&= \pi^{-3/2} u_{T\perp}^{-2} u_{T\parallel}^{-1} \int_0^\infty du_\perp u_\perp e^{-\frac{u_\perp^2}{u_{T\perp}^2}} \int_0^{2\pi} d\theta \int_{-\infty}^\infty du_\parallel e^{-\frac{u_\parallel^2}{u_{T\parallel}^2}} \\
&\times \left[\frac{k_\parallel^2 u_\parallel^2}{l^2\Omega_0^2} + \frac{u_\perp^2 \sin^2\theta}{\Omega_0^2 L^2} - \frac{2k_\parallel u_\parallel u_\perp \sin\theta}{l\Omega_0^2 L}\right] \\
&- \left[\pi^{-3/2} u_{T\perp}^{-2} u_{T\parallel}^{-1} \int_0^\infty du_\perp u_\perp e^{-\frac{u_\perp^2}{u_{T\perp}^2}} \int_0^{2\pi} d\theta \int_{-\infty}^\infty du_\parallel e^{-\frac{u_\parallel^2}{u_{T\parallel}^2}}\right. \\
&\times \left.\left(\frac{k_\parallel u_\parallel}{l\Omega_0} - \frac{u_\perp \sin\theta}{\Omega_0 L}\right)\right]^2 .
\end{aligned} \tag{5.32}$$

Our identities for the velocity integrals then give a simple result for the variance $\mathcal{V}\left[g\left(\mathbf{u}\right)\right]$ since $< g\left(\mathbf{u}\right) >^2$ is identically zero reflecting the symmetry of the gyroresonances about $l\Omega_0\left(0\right)$. This is not the case for a relativistic plasma though. The absorption profile obtained by McDonald et al.(1994) for a Maxwellian relativistic plasma in an linearly inhomogeneous magnetic field gradient is clearly asymmetric. An elegant piece of mathematical analysis was performed by the authors, providing a good foundation for the work presented in this thesis, although no account was given as to the physical mechanism responsible for the asymmetry. We know that gyroresonance at the l^{th} harmonic will occur

when $\omega - \delta\omega = l\Omega_0$. However, the gyrofrequency varies as the inhomogeneous magnetic field and so the resonance condition is satisfied over a range of values of x as revealed by (5.3). Furthermore, we know that relativistic particles behave differently from classical particles by the Lorentz factor $\gamma = 1/\sqrt{1 - \frac{u^2}{c^2}}$. The relativistic gyrofrequency, for example, becomes $\Omega_0(x) = qB_0(x)/m_0\gamma$ with m_0 being the classical rest mass. So relativistic charged particles with u being an appreciable fraction of c will require stronger magnetic fields to bring them into resonance. In an isotropic distribution of particles then there will be fewer resonant particles on the low magnetic field of the gyroresonance than on the high field side, and the resonance profile will be asymmetrically skewed towards the low magnetic field side. For our classical analysis which is perfectly valid for the ions in a thermonuclear fusion experiment such as JET since their thermal velocities are of the order of $c/1000$, then the gyrofrequency is non-relativistic and our resonance profile is nicely symmetric with variance,

$$\mathcal{V}[g(\mathbf{u})] \equiv \frac{1}{2}\left(\frac{u_{T\perp}^2}{\Omega_0^2 L^2} + \frac{k_\parallel^2 u_{T\parallel}^2}{l^2\Omega_0^2}\right). \tag{5.33}$$

The first term is just the variance of the error due to the GK correction while the second is the variance of the error arising from Doppler frequency shifting and so we have shown explicitly that the errors add in quadrature,

$$\mathcal{S}^2\left(\frac{\delta\omega}{l\Omega_0}\right) = \mathcal{S}^2\left(\frac{\delta\omega_\perp}{l\Omega_0}\right) + \mathcal{S}^2\left(\frac{\delta\omega_\parallel}{l\Omega_0}\right). \tag{5.34}$$

The Larmor radius is defined to be $\rho_\perp = u_{T\perp}/\Omega_0$ and so the standard deviation is found from (5.33) by taking the square root and may be written as,

$$\mathcal{S}\left(\frac{\delta\omega}{l\Omega_0}\right) = \frac{\rho_\perp}{L\sqrt{2}}\sqrt{1 + \frac{k_\parallel^2 L^2\left(T_\parallel/T_\perp\right)}{l^2}} \equiv \mathcal{S}\left(\frac{x}{L}\right) = \frac{x}{L}. \tag{5.35}$$

We may now come to the following conclusion. The number of charged particles which are resonant in a bi-Maxwellian plasma are symmetrically distributed about the gyroresonance and their standard deviation from the gyroresonance is equal to $1/\sqrt{2}$ times their perpendicular Larmor radius scaled by a factor differing from unity only by the amount of Doppler shifting and the thermal anisotropy of the distribution.

We may also make the following deductions.

- The resonance is broadened even for perpendicular propagation($k_\parallel = 0$). This is in agreement with a result obtained by Lashmore-Davies et al.(1989) which revealed EM wave damping on resonant particles due to resonance broadening by solely GK effects.

- Resonance broadening is greatest when there is Doppler shifting in conjunction with thermal anisotropy of the type $T_{\|} > T_{\perp}$.
- Gyroresonance feeds energy into the perpendicular direction and so usually we have the case of thermal anisotropy with $T_{\|} < T_{\perp}$ countering the effects of Doppler broadening.

A typical gyroresonance scenario in present day fusion experiments such as JET has the following values: $k_{\|} \simeq 5m^{-1}$, $L \simeq 3m$, $l = 1$ and $T_{\perp} \simeq 3T_{\|}$ giving a standard deviation of $\rho_{\perp}\sqrt{38/9} \simeq 2\rho_{\perp}$ which is about 9 times that of an isotropic plasma perturbed by perpendicularly propagating EM waves.

When the incident wave frequency(ω) is matched to the l^{th} harmonic of the gyrofrequency with $\omega \equiv l\Omega_0(0)$ then we may equate this to the spatially varying expression for the gyrofrequency such that $l\Omega_0(0) = \Omega_0(x) = \Omega_0(0)(1 - x/L)$, enabling us to to obtain the following expression for the locations of the gyroresonances,

$$x_l = (1 - l)\, L. \tag{5.36}$$

Furthermore, the separation of the n^{th} and the l^{th} gyroresonances will be,

$$\Delta x = |x_l - x_n| = |(l - n)|L. \tag{5.37}$$

This allows us to obtain a criterion for the resolution of the gyroresonances as follows. The standard deviation of (5.35) gives a measure of the width of the resonances which we can write as,

$$x = \mathcal{S}L = \frac{\rho_{\perp}}{\sqrt{2}}\sqrt{1 + \frac{k_{\|}^2 L^2 \left(T_{\|}/T_{\perp}\right)}{l^2}}. \tag{5.38}$$

The way we define the resolution is quite arbitrary. We take the lead of Lord Rayleigh who defined two similar profiles to be resolved when the maximum of one is commensurate with the adjacent minimum of the other. Two equivalent Gaussian distributions, separated by the $FWHM \equiv 2\sqrt{2\ln 2}\mathcal{S} \simeq 2.35\mathcal{S}$ will have clearly resolved peaks. When their peaks are $\left(2\sqrt{2}\right)\mathcal{S} \simeq 2.82\mathcal{S}$ apart then the resolution will be excellent. The choice of the factor $2\sqrt{2}$ is quite arbitrary. We were guided by the fact that since it is larger than the $FWHM$ it guarantees resolution and also leads to an aesthetically pleasing form for the resolving distance x_r which we define to be,

$$x_r \simeq \left(2\sqrt{2}\right)\mathcal{S}L = 2\rho_{\perp}\sqrt{1 + \frac{k_{\|}^2 L^2 \left(T_{\|}/T_{\perp}\right)}{l^2}}. \tag{5.39}$$

The gyroresonances will be resolved according to this criterion provided,

$$\Delta x > x_r, \tag{5.40}$$

or equivalently,

$$|l-n| > 2\frac{\rho_\perp}{L}\sqrt{1+\frac{k_\parallel^2 L^2\left(T_\parallel/T_\perp\right)}{l^2}}. \tag{5.41}$$

For the JET parameters quoted earlier we find for ions of Larmor radius of the order of about $3cm$ that,

$$l|l-n| \geq 0.17. \tag{5.42}$$

So the resonances will be resolved according to the above condition provided that they exist($l > 0$) and are non-degenerate($l \neq n$). We note that the gyroresonances should not be considered as an independent set of discrete lines. Rather, there is a degree of overlap and under certain physical conditions they can merge into a continuous spectrum. Fortunately, there is a strong line structure in the radio frequency range meaning that we are able to control where we would like to deposit energy in the plasma. A further consequence of this is that in calculating the conductivity tensor we may separate out the resonant harmonic from the summation over l and treat it independently from the remaining sum which will contain non-resonant terms, since for a JET plasma the resonances are well resolved. The contribution to the conductivity from the non-resonant thermal terms will be small in comparison to the resonant terms and so the effects of magnetic field inhomogeneity will add only minor corrections. This allows us to approximate the non-resonant terms by their uniform plasma equivalents or by their cold plasma values, making the analysis more tractable.

In the next section we will perform a calculation of the broadening of a cold plasma resonance by the introduction of thermal effects.

5.2 Broadening Of A Cold Plasma Resonance By Thermal Effects

In chapter 2 we described the cold plasma dispersion relations for EM waves (the O-mode and the X-mode) propagating perpendicularly across an ambient magnetic field. We showed that there is an additional wave resonance in a two-ion species plasma(such as the JET $D_1^2\left(He_2^3\right)e_{-1}^0$ plasma) due to the phase matching of oscillations of the ion space charge giving rise to the 2-ion hybrid resonance. Being a purely cold plasma resonance, the wave potential($V(x)$) is singular in nature(a simple pole) and has a zero absorption width. Thermal effects however move this pole off the real(x) axis by introducing an imaginary part to the singularity. In chapter 2 we have shown how the imaginary part of the potential($Im\{V(x)\}$) is responsible for the power lost by the wave to resonant particles(near a gyroresonance) or to another wave mode(mode conversion at the hybrid resonance). Lashmore-Davies et al.(1993) presented a calculation to determine

the asymptotic form of the imaginary part of the wave potential at the hybrid resonance which was shown to depend on the sign of the incident wavevector. For loss of power as a wave crosses the resonance then ($Im\{V(x)\} > 0$) and the sign of the incident wavevector must be chosen to be positive for waves propagating towards positive x. Here we will use their result, calculated in the regime of low energy ions(small Larmor radius), to provide an approximation to the thermal width of the hybrid resonance which we will use in our numerical studies in chapter 8.

Lashmore-Davies et al.(1993) expanded the Z-functions asymptotically by noting that for large minority ion(b) to majority ion(a) density ratios, the hybrid resonance is well separated from the minority ion gyroresonance so that the argument($\zeta = \frac{\omega - l\Omega_b(x)}{k_z v_{Tb}}$) of the Z-function will be large when $\frac{|x|}{\rho_b} > \frac{l}{k_z L}$. Let us begin by writing the asymptotic expression for the fast wave potential (their equation (26))in the following algebraic form with $X = \frac{x}{\rho_b}$ as a normalised variable,

$$V(X) = \frac{\omega^2}{c_A^2}\{\frac{a + \frac{b}{X} - \frac{ic}{X^2}}{d - \frac{e}{X} + \frac{if}{X^2}}\}. \tag{5.43}$$

If we rationalise the denominator then we find that the imaginary part is,

$$Im\{V(X)\} = -\frac{\omega^2}{c_A^2}\{\frac{\frac{c}{X^2}\left(d - \frac{e}{X}\right) + \frac{f}{X^2}\left(a + \frac{b}{X}\right)}{\left(d - \frac{e}{X}\right)^2 + \frac{f^2}{X^4}}\}. \tag{5.44}$$

In determining the width of the resonance, we will use the value of the imaginary part at the resonance position(X_R) as a reference value. To find the half width at half maximum we need to know at what X is $Im\{V(X)\}$ equal to $\frac{1}{2}Im\{V(X_R)\}$. Before doing this, we need an expression for the position of the resonance (X_R) which we can determine from equation(28) of Lashmore-Davies et al.(1993),

$$X_R = \frac{r_2\left(r_1^2 - 1\right) q\tau c_A}{2r_1 N_z v_{Tb}}, \tag{5.45}$$

providing the imaginary part of the potential at the resonance as given by their equation(31),

$$Im\{V(X_R)\} = \frac{\omega^2}{c_A^2}\frac{\left(r_1 - 1\right)^2 r_2 L}{r_1 k_x \rho_b^2}. \tag{5.46}$$

We want to know at what value of X this halves. Let us denote,

$$g = \frac{c_A^2}{\omega^2}\frac{Im\{V(X_R)\}}{2} \equiv \frac{\left(r_1 - 1\right)^2 r_2 L}{2r_1 k_x \rho_b^2}. \tag{5.47}$$

We must solve the condition $Im\{V(X)\} = \frac{1}{2}Im\{V(X_R)\}$ for X or equivalently,

$$g = -\{\frac{\frac{c}{X^2}\left(d - \frac{e}{X}\right) + \frac{f}{X^2}\left(a + \frac{b}{X}\right)}{\left(d - \frac{e}{X}\right)^2 + \frac{f^2}{X^4}}\}. \tag{5.48}$$

If we divide through by X^2 and rearrange then we obtain,

$$\{d^2X^2 - 2deX + e^2 + \frac{f^2}{X^2}\}g = -\{c\left(d - \frac{e}{X}\right) + f\left(a + \frac{b}{X}\right)\}. \tag{5.49}$$

Since we are in the asymptotic regime for large X then inverse powers of X may be neglected allowing us to write down the following quadratic equation in X,

$$d^2X^2 - 2deX + \left(e^2 + \frac{cd + af}{g}\right) = 0, \tag{5.50}$$

with solution,

$$X = \frac{e}{d} \pm \frac{\sqrt{-\frac{cd+af}{g}}}{d}. \tag{5.51}$$

Returning now to our expression for $V(X)$ in (5.43) (which is equation(26) of Lashmore-Davies et al., 1993) we need to identify all of the constants $a - f$ and also g. If we note that $q\tau\nu = 1$, $q\tau = \frac{1}{\nu} \equiv k_z L$ and $N_z v_{Tb} = c_A k_z \rho_b$ then we find,

$$\begin{aligned}
a &= -d = -\frac{1}{r_1^2 - 1}, \\
e &= \frac{r_2 L}{2 r_1 \rho_b}, \\
b &= e\frac{1}{r_1 + 1}\{1 + \tau^2\left(1 + \nu^2\right) - \frac{1}{2}k_x^2\rho_b^2\left(1 - \nu^4\tau^4\right)\}, \\
c &= e\frac{k_x\rho_b}{2\left(r_1 + 1\right)}\{3 + \tau^2\left(1 + \nu^2\right)\}, \\
f &= e\frac{k_x\rho_b}{2}, \\
g &= e\frac{\left(r_1 - 1\right)^2}{k_x\rho_b}.
\end{aligned} \tag{5.52}$$

If we substitute all of these into the expression we have for the position at which the imaginary part of the potential is half the value at the resonance given by (5.51), then we obtain after a little algebra,

$$X = \frac{r_2\left(r_1^2 - 1\right)L}{2 r_1 \rho_b} \pm \frac{k_x\rho_b}{2\left(r_1 - 1\right)}\sqrt{\left(r_1^2 - 1\right)\left[1 - \frac{3 + \tau^2\left(1 + \nu^2\right)}{2\left(r_1 + 1\right)}\right]}, \tag{5.53}$$

or,

$$X_{\pm} = X_R \pm \Delta. \tag{5.54}$$

The first term is the position of the hybrid resonance of (5.45), $X_R = \frac{r_2\left(r_1^2-1\right)q\tau c_A}{2r_1 N_z v_{Tb}} = e\left(r_1^2-1\right) \equiv \frac{r_2\left(r_1^2-1\right)L}{2r_1\rho_b}$. The second term is then the half width at half maximum which we were seeking. We shall use this result in our numerical calculations in chapter 8. This takes on a particularly simple form for perpendicular propagation. Since,

$$\begin{aligned} \tau = \frac{k_z L}{\left(1+k_z^2 L^2\right)^{1/2}} &\rightarrow 0 \quad as \quad k_z \rightarrow 0, \\ \nu = \frac{1}{k_z L} &\rightarrow \infty \quad as \quad k_z \rightarrow 0, \\ \tau\nu = \frac{1}{\left(1+k_z^2 L^2\right)^{1/2}} &\rightarrow 1 \quad as \quad k_z \rightarrow 0, \end{aligned} \tag{5.55}$$

then,

$$\sqrt{\left(r_1^2-1\right)\left[1-\frac{3+\tau^2\left(1+\nu^2\right)}{2\left(r_1+1\right)}\right]} \rightarrow \left(r_1-1\right) \quad as \quad k_z \rightarrow 0, \tag{5.56}$$

and so,

$$\Delta \rightarrow \frac{1}{2}k_x\rho_b \quad as \quad k_z \rightarrow 0. \tag{5.57}$$

We see that in the limit of a cold plasma($T \rightarrow 0$ therefore $\rho_b \rightarrow 0$) then we recover the singular form for the hybrid resonance.

5.3 A Qualitative Analysis Of The Conductivity

We have derived the response to small amplitude EM waves of an anisotropic bi-Maxwellian plasma immersed in a inhomogeneous magnetic field aligned along $\hat{\mathbf{z}}$ with a linear gradient in strength along $\hat{\mathbf{x}}$. It is the aim of the present chapter to identify the terms which have arisen from the thermal anisotropy of the plasma and to attach some physical meaning to them. The open form of the conductivity tensor means that we may only give here a qualitative analysis of the physical effects and we defer a quantitative analysis until later on when we have introduced the tools which will better able us to handle our rather elusive result.

In chapter 2 we showed how, in a cold magnetised plasma, resonances are singular in nature. We then described the gyroresonances of hot, isotropic and collisionless plasmas immersed in homogeneous and inhomogeneous magnetic fields and drew attention to their

well defined absorption profiles attributable to the resemblance of their resonance integrals to the plasma dispersion function(Z-function) which may be written in the form,

$$Z\left(\frac{\Gamma}{\Delta}\right) \equiv i\Delta \int_0^\infty dy e^{iy\Gamma - \frac{1}{4}y^2\Delta^2}. \tag{5.58}$$

If we recall the conductivity tensor obtained above in (4.62) then we may make the following deductions,

- The integral over k' is of the form of a scaled Z-function plus other terms which will effectively comprise derivatives of Z-functions. We know this because the velocity tensor V is a function of k' and from the method of Cairns et al.(1991) described in Chapter 2, we know that powers of k' act as spatial derivative operators upon the Z-function integral.

- The measure of the resonance broadening as given by (5.35), appears explicitly in the k'-integral. This is intimately linked to the factor Δ in (5.58) above as follows,

$$\Delta = \sqrt{2}SL\left(\frac{\delta\omega}{\omega}\right) \equiv \rho_\perp \sqrt{1 + \frac{k_\parallel^2 L^2 \left(T_\parallel / T_\perp\right)}{l^2}}. \tag{5.59}$$

  The quadratic nature of the exponent containing this means that when $k'^2\Delta^2$ is greater than a couple of times unity then this term dominates the behaviour of the k'-integral causing it rapidly to tend to zero, ensuring convergence for large k'. When $k'^2\Delta^2$ is of the order of a few times unity then the integrals will converge rapidly. So a typical length-scale over which the integrals have a appreciable effect is a couple of Δ. For the JET parameters quoted above Δ is of the order of about $9\rho_\perp \simeq 26cm$. This then means that the interaction of the resonant particles is substantially non-local sampling the EM fields over an appreciable section of the tokamak radius.

- A corollary of this is also an estimate of the validity of our slab model. The assumption of a plane stratified geometry is not strictly correct in a tokamak where the magnetic field gradient is not exactly perpendicular to the ambient field $\nabla \mathbf{B}_0 \bullet \mathbf{B}_0 \neq 0$. It is this quality which is responsible for trapped particle effects for example. If we allow the field to vary along $\hat{\mathbf{z}}$ with a length-scale L_z as well as along $\hat{\mathbf{x}}$ then the shift in the gyrofrequency Ω_0 after the particle has moved a distance z along the field is,

$$\delta\omega = \Omega_0 \frac{z}{L_z}. \tag{5.60}$$

  The time needed to produce this shift for a thermal particle with velocity $u_{T\parallel}$ is,

$$t = \frac{z}{u_{T\parallel}} \equiv \frac{\delta\omega L_z}{\Omega_0 u_{T\parallel}}. \tag{5.61}$$

There is also a frequency shift due to resonance broadening effects which is given by (5.2). We know from the previous section that this quantity appears explicitly in the resonance integral as the standard deviation. The time for this frequency shift may be found from our last deduction since the time τ is related to k' by $k' = -(l\Omega_0/L)\tau$ and so,

$$\tau \simeq \frac{L}{l\Omega_0\rho_\perp\sqrt{1+\frac{k_\parallel^2L^2\left(T_\parallel/T_\perp\right)}{l^2}}} \simeq \frac{\left(T_\perp/T_\parallel\right)}{k_\parallel u_{T\parallel}}, \tag{5.62}$$

for the regime of oblique propagation where GK effects are negligible. The time τ is a measure of how long it takes the integral back along the particle orbit to determine effectively its response. If the frequency shift along the field is approximately equal to the frequency shift due to broadening effects then we can also substitute (5.2) for $\delta\omega$ in (5.61) so that, again in the limit of negligible GK effects,

$$t \simeq \frac{k_\parallel L_z}{\Omega_0}. \tag{5.63}$$

We now impose the condition that the time for the generation of the particle response τ is much less than the time for the frequency shift due to parallel motion t so that,

$$L_z \gg \frac{\Omega_0\left(T_\perp/T_\parallel\right)^{1/2}}{k_\parallel^2 u_{T\perp}}. \tag{5.64}$$

For a Deuterium fundamental gyroresonance $\Omega_0 \simeq 10^8 s^{-1}$ and $u_{T\perp} \simeq 10^5 ms^{-1}$. The JET parameters then give $L_z \gg 10m$. This means that in a large tokamak such as JET our slab model is justified since the particle response occurs in a time substantially less than the time for any frequency shifts due to toroidal effects which vary slowly over a long distance.

- Doppler shifting with a finite $k_\parallel$ broadens the resonance but may be countered by thermal anisotropy when $T_\parallel < T_\perp$.

- The standard tensor elements for a Maxwellian plasma in a linearly varying inhomogeneous field are scaled by the following factors which arise from thermal anisotropy,

$$\begin{bmatrix} 1 & 1 & \sqrt{\frac{T_\parallel}{T_\perp}} \\ 1 & 1 & \sqrt{\frac{T_\parallel}{T_\perp}} \\ \sqrt{\frac{T_\parallel}{T_\perp}} & \sqrt{\frac{T_\parallel}{T_\perp}} & \frac{T_\parallel}{T_\perp} \end{bmatrix}.$$

- There are now additional terms in the anisotropic tail factors A_j which arise from the $\mathbf{u}\times\mathbf{B}_0$ term of the Lorentz force. In chapter 3 we did a back of an envelope calculation to compare the relative magnitudes of those terms arising from the electric

field of the wave with those terms arising from the wave magnetic field and we commented that they may be comparable. An interesting quality of these magnetic field terms is that they not only disappear in the limit of an isotropic plasma, they also disappear at perpendicular propagation when $k_{\parallel} = 0$. This may be explained again from our statistical approach to resonance. In the absence of Doppler terms then resonance broadening will only occur from the GK correction and hence will only be dependent upon the $u_{\perp}$ velocity component. In the presence of finite Doppler effects then the difference between velocities along and perpendicular to the ambient magnetic field will become important since resonance broadening will be due to contributions from both the $u_{\perp}$ and $u_{\parallel}$ velocity components.

Later on in chapter 8 we will present a numerical study of the interaction of EM waves propagating obliquely to an ambient and linearly varying inhomogeneous magnetic field in a thermally anisotropic bi-Maxwellian plasma, and we will reveal exactly how the qualitative effects predicted above are borne out.

Having studied in some detail the qualitative effects of thermal anisotropy upon the conductivity tensor, we turn now to the question of the symmetry.

Chapter 6

Symmetry Laws And Spatial Representations

In chapter 1 we remarked that the Vlasov equation, which governs the microscopic dynamics of the charged particles in a hot collisionless plasma, is invariant under time-reversal. That is, the laws of physics are the same if we reverse the arrow of time. Onsager(1931) has shown that this is reflected in the symmetry of a transport matrix relating thermodynamic fluxes to the forces which drive them. We will show here that the conductivity tensor for a thermal equilibrium obeys this symmetry even in the presence of an inhomogeneous magnetic field. More importantly we show that thermal anisotropy destroys this symmetry.

6.1 General Theory Of Onsager Symmetries

We know that a voltage gradient(∇V) will drive an electric current density($\mathbf{J}$) through a conducting medium, and the ratio of $\mathbf{J}$ to $-\nabla V$ is the electric conductivity tensor(σ_{ij}). The aim of transport theory is to relate the dissipative fluxes (of heat, particles and current) to the corresponding thermodynamic forces driving them (pressure gradients, temperature gradients and electric field). The latter quantities, which depend on the spatial gradients and the externally applied forces, are a measure of the departure of the system from equilibrium since the fluxes represent the response to this non-equilibrium situation. We may express the transport phenomena by a set of linear, algebraic, phenomenological relations of the general type,

$$\Gamma_i = \sum_{j=1}^{n} L_{ij} F_j, \quad (i = 1, 2, 3, ..., n), \tag{6.1}$$

where Γ_i and F_j are the fluxes and forces. The whole physics of the problem is contained within the transport coefficients L_{ij}. The existence of non-zero off-diagonal elements in this matrix expresses a coupling between various irreversible processes occurring in the system. Onsager(1931) showed that a general class of reciprocal relations could be

derived from the principle of microscopic reversibility by relating macroscopic irreversible processes to spontaneous fluctuations in the equilibrium state. The cornerstone of his work was the following symmetry property of the transport coefficients,

$$L(\Lambda) = L^{\dagger}(\Lambda). \tag{6.2}$$

The dagger represents Hermitian conjugation whereby we transpose the matrix($ij \rightarrow ji$) and take the complex conjugate (which we will denote by a $*$), and Λ represents a set of time-dependent quantities which change sign under time reversal.

So as to generalise the results of Onsager's original work, Krommes and Hu(1993) introduced the parity matrix(ϵ) so as to allow for variables which may be either odd or even under time reversal so that $F \rightarrow \epsilon F$. ϵ has the important property that it is idempotent: $\epsilon \bullet \epsilon = I$. With this in mind they derived the following result, relating the properties of fluctuations and transport in the time-reversed state $\overline{L}$ and the original steady state L,

$$L(\Lambda) = \epsilon \bullet \overline{L}^{\dagger}(-\Lambda) \bullet \epsilon^{\dagger},$$

or, upon defining $\mathcal{L} = \epsilon \bullet L$ we have the more symmetrical form,

$$\mathcal{L}(\Lambda) = \overline{\mathcal{L}}^{\dagger}(-\Lambda). \tag{6.3}$$

For a thermal equilibrium such as with Maxwellian velocity distributions then the particle dynamics are Hamiltonian and the time-reversed state coincides with the equilibrium state itself so that L and $\overline{L}$ are identical. In this case we recover the original Onsager symmetry.

We have already shown in chapter 3 that, at the microscopic level of description, the Vlasov equation is invariant under time reversal. So we must address the question of how exactly the irreversible nature appears. The perturbed current density($\mathbf{J}$) is calculated from the first velocity moment of the perturbed distribution function as in (3.2). We expanded on this in the last chapter where we presented the intimate relation between the first moment and the mean. So we see that essentially we are averaging over all the particle velocities. Although we may calculate the mean from a sample of data we cannot reconstruct our original data set from a knowledge of only the mean value. This then is the source of the irreversibility in our equations which, we have shown, have a definite basis in time reversible microdynamics as required by the prescription used by Onsager. Another intrinsic element of Onsager's celebrated work was that he considered fluctuations about an equilibrium state which regressed monotonically according to some hydrodynamical law. In our analysis we are perturbing a plasma equilibrium by harmonic EM waves and we expect the plasma response to similarly regress. Krommes and Hu(1993) further generalised Onsager's work so as to describe fluctuations about a non-equilibrium state and indicated that, providing the regression law is of Markovian form, then there is Onsager symmetry of the transport coefficients.

Nambu(1995) remarked that the forces(F_j) in (6.1) should not be mixed up with forces in the Newtonian sense. If we take fluxes(Γ_i) as the electric current density($\mathbf{J}$) then the forces(F_j) in this case are not simply electric fields($\mathbf{E}_j$), but $\mathbf{E}_j/T_j$, where T_j is the temperature in the j^{th} direction. If we define the electrical conductivity tensor σ_{ij} by,

$$\mathbf{J}_i = \sum_{j=1}^{n} \sigma_{ij} \mathbf{E}_j, \quad (i = 1, 2, 3, ..., n), \tag{6.4}$$

then we find that the transport coefficient L_{ij} defined in (6.1) is given by,

$$L_{ij} = T_j \sigma_{ij}, \tag{6.5}$$

such that,

$$\mathbf{J}_i = \sum_{j=1}^{n} (T_j \sigma_{ij}) \left(\frac{\mathbf{E}_j}{T_j} \right), \quad (i = 1, 2, 3, ..., n). \tag{6.6}$$

Onsager symmetry is then guaranteed by the property,

$$T_j \sigma_{ij} (\Lambda) = T_i \sigma^*_{ji} (-\Lambda). \tag{6.7}$$

This result has been overlooked by a number of recent authors in the field who have simply equated the transport coefficient to the conductivity tensor(see for example Beskin et al., 1986, Stix, 1992 and Caetano et al., 1992) without including the directional temperature components. Their claims of Onsager symmetry as pertaining to the symmetry of the conductivity tensor are purely a coincidence with the true thermodynamic form of (6.7) in the limit of an isotropic plasma when $T_i \equiv T_j$. As Nambu(1995) rightly pointed out, the temperature dependence of the transport coefficients is unimportant for thermally isotropic plasmas where there is no distinction between temperatures in different directions and Onsager symmetry reveals itself in this case. However in thermally anisotropic plasmas the temperature dependence of the transport coefficients is crucial to symmetry properties. As is well known the definition of fluxes and forces is not unique. The other choice that is consistent with (6.1) is that fluxes are given by $\mathbf{J}_i/T_i$ and forces are the electric field $\mathbf{E}_j$ so that in this case the transport matrix is $L_{ij} = \sigma_{ij}/T_i$ which is in fact equivalent to (6.4). We see that the same physics is preserved independent of the formulation which it must be of course.

In the time reversed state for charged particles in a magnetic field ($\mathbf{B_0}$), all velocities are reversed and the symmetry is assured by the change $\mathbf{B_0} \rightarrow -\mathbf{B_0}$. The wave vector k must also be reversed if the transport coefficients are Fourier transforms. If the medium is invariant under spatial inversion then we have even functions of k. For this we must bear in mind the reality condition:

$$L(\omega, \mathrm{k}) = L^*(-\omega, -\mathrm{k}), \tag{6.8}$$

Since the equilibrium distribution function is constructed from the constants of the motion then it too should be reversed with respect to the velocity component parallel to the ambient magnetic field. According to Onsager's principle we then have the following symmetry if we note the reality condition of (6.8),

$$L\left(\mathbf{k},\omega,\mathbf{u},\mathbf{B}_0;f_0\left(\mathbf{u}\right)\right)=L^{\dagger}\left(\mathbf{k},-\omega,-\mathbf{u},-\mathbf{B}_0;f_0\left(-\mathbf{u}\right)\right),$$

or equivalently from (6.7),

$$T_j\sigma_{ij}\left(\mathbf{k},\omega,\mathbf{u},\mathbf{B}_0;f_0\left(\mathbf{u}\right)\right)=T_i\sigma_{ji}^{*}\left(\mathbf{k},-\omega,-\mathbf{u},-\mathbf{B}_0;f_0\left(-\mathbf{u}\right)\right).$$

Having discussed the underlying symmetry engrained in the physics of our model we will show how these predictions are borne out by our theoretical analyses of the previous two chapters. Before doing that we will say a few words about how symmetries can be affected by different coordinate representations.

6.2 Spatial Forms For The Plasma Response

We have outlined the symmetry law suitable for our physical situation in terms of an abstract tensor notation representing sets of numbers identifying components in one particular coordinate system. However, as Krommes and Hu(1993) point out, which is the 'right' coordinate system for displaying Onsager symmetry? Several authors have claimed that failure to make the correct choice can lead to a violation. This is contrary to one of the most fundamental principles of physics, that of covariance, meaning that the physical content of an appropriately formulated theorem must be independent of the coordinate system used to represent it. Covariance and Geometry are deeply intertwined. Krommes and Hu(1993) introduced a fully covariant theory whereby the Weinhold metric was chosen to geometrise the thermodynamical basis of Onsager symmetry. This led to a tensor formalism which showed their generalised Onsager symmetry to be covariant under arbitrary transformations of the state variables. Although our aim is to present and discuss the Onsager symmetries pertinent to the electrical properties of a hot anisotropic plasma, we forego the more generalised formalism of Krommes and Hu(1993) and instead, for simplicity, we will present the Onsager symmetries of various spatial representations of the transport equations given by (6.4). This section is a collection of ideas formulated and clarified by work done by myself and D. C. McDonald.

6.2.1 Derivation Of The k-Space Form

In deriving the perturbed current density $\mathbf{J}\left(\mathbf{r}\right)$ of (4.99), we expressed the Electric field $\mathbf{E}\left(\mathbf{r}\right)$ in terms of its Fourier transform $\overline{\mathbf{E}}\left(\mathbf{k}\right)$ leading to an explicit form for the conductivity in mixed $\left(\mathbf{r},\mathbf{k}\right)$-space which we will call the simple form, and in terms of the dummy variable $\mathbf{k}'$ this is,

$$\mathbf{J}(\mathbf{r}) = \int d\mathbf{k}' e^{i\mathbf{k}'\bullet\mathbf{r}} \sigma_{ij}(\mathbf{r}, \mathbf{k}') \bullet \overline{\mathbf{E}}(\mathbf{k}'). \tag{6.9}$$

The wave equation of (4.100) is expressed in **r**-space but with χ_{ij} expressed in the mixed space. If we Fourier transform the **r**-dependence then we obtain,

$$\mathbf{J}(\mathbf{r}) = \int d\mathbf{k}' e^{i\mathbf{k}'\bullet\mathbf{r}} \int d\mathbf{k}'' e^{i\mathbf{k}''\bullet\mathbf{r}} \overline{\sigma}_{ij}(\mathbf{k}'', \mathbf{k}') \bullet \overline{\mathbf{E}}(\mathbf{k}'). \tag{6.10}$$

We may obtain the Fourier transform of the current density $\overline{\mathbf{J}}(\mathbf{k})$ through the inverse relation,

$$\overline{\mathbf{J}}(\mathbf{k}) = \frac{1}{(2\pi)^3} \int d\mathbf{r} e^{-i\mathbf{k}\bullet\mathbf{r}} \mathbf{J}(\mathbf{r}), \tag{6.11}$$

giving,

$$\overline{\mathbf{J}}(\mathbf{k}) = \frac{1}{(2\pi)^3} \int d\mathbf{r} e^{-\mathbf{k}\bullet\mathbf{r}} \int d\mathbf{k}' \int d\mathbf{k}'' e^{i(\mathbf{k}'+\mathbf{k}'')\bullet\mathbf{r}} \overline{\sigma}_{ij}(\mathbf{k}'', \mathbf{k}') \bullet \overline{\mathbf{E}}(\mathbf{k}'). \tag{6.12}$$

The **r** integral gives a delta function allowing us to write down a purely **k**-space form for the Fourier coefficient of the perturbed current,

$$\overline{\mathbf{J}}(\mathbf{k}) = \int d\mathbf{k}' \int d\mathbf{k}'' \delta(\mathbf{k}' + \mathbf{k}'' - \mathbf{k}) \overline{\sigma}_{ij}(\mathbf{k}'', \mathbf{k}') \bullet \overline{\mathbf{E}}(\mathbf{k}'). \tag{6.13}$$

Fortunately the δ-function allows us to perform the $d\mathbf{k}''$ integral without difficulty,

$$\overline{\mathbf{J}}(\mathbf{k}) = \int d\mathbf{k}' \overline{\sigma}_{ij}(\mathbf{k} - \mathbf{k}', \mathbf{k}') \bullet \overline{\mathbf{E}}(\mathbf{k}'). \tag{6.14}$$

We may think of **k** as the wave mode we are measuring and **k**′ as the mode which is causing the response and so we see that even in Fourier space the plasma response is non-local.

6.2.2 Derivation Of The r-Space Form

Returning to the current density expressed in mixed space given by (6.9), we may invert the Fourier transform,

$$\mathbf{J}(\mathbf{r}) = \frac{1}{(2\pi)^3} \int d\mathbf{r}' e^{-i\mathbf{k}'\bullet(\mathbf{r}-\mathbf{r}')} \int d\mathbf{k}' e^{i\mathbf{k}'\bullet\mathbf{r}} \sigma_{ij}(\mathbf{r}, \mathbf{r} - \mathbf{r}') \bullet \overline{\mathbf{E}}(\mathbf{k}'), \tag{6.15}$$

and if we recall that the electric field has been expressed as a sum over its Fourier modes then we see that the integral over **k**′ is simply the Fourier transform of the electric field. The **r**-space form for the current is then,

$$\mathbf{J}(\mathbf{r}) = \frac{1}{(2\pi)^3} \int d\mathbf{r}' \sigma_{ij}(\mathbf{r}, \mathbf{r} - \mathbf{r}') \bullet \mathbf{E}(\mathbf{r}'). \tag{6.16}$$

Here **r** is the point in space where the response is measured and **r**′ is the position of the point where the response is from, in other words, the stimulus. This brings about the

non-local nature of the plasma to perturbing small amplitude EM waves.

6.2.3 Other Forms Used In The Literature

In addition to the non-local **r**-space form derived above, it is conceivable that we could have postulated other forms which are sensitive to the choice of coordinate system since our response tensor or transport matrix is not of the covariant Weinhold kind. Two notable forms which come to mind are the Cartesian form,

$$\mathbf{J}(\mathbf{r}) = \frac{1}{(2\pi)^3} \int d\mathbf{r}' \sigma^c_{ij}(\mathbf{r}, \mathbf{r}') \bullet \mathbf{E}(\mathbf{r}'), \tag{6.17}$$

and the Symmetric form,

$$\mathbf{J}(\mathbf{r}) = \frac{1}{(2\pi)^3} \int d\mathbf{r}' \sigma^s_{ij}\left(\frac{1}{2}(\mathbf{r}+\mathbf{r}'), \mathbf{r}-\mathbf{r}'\right) \bullet \mathbf{E}(\mathbf{r}'). \tag{6.18}$$

Following steps similar to those presented above we may derive the associated $\mathbf{r}-\mathbf{k}$ and **k**-space forms allowing us to construct the following table of spatial representations of the plasma response,

Space	Tensor Space	Plasma Response
r	Cartesian	$\mathbf{J}(\mathbf{r}) = \frac{1}{(2\pi)^3}\int d\mathbf{r}' \sigma^c_{ij}(\mathbf{r}, \mathbf{r}') \bullet \mathbf{E}(\mathbf{r}')$
	Simple	$\mathbf{J}(\mathbf{r}) = \frac{1}{(2\pi)^3}\int d\mathbf{r}' \sigma_{ij}(\mathbf{r}, \mathbf{r}-\mathbf{r}') \bullet \mathbf{E}(\mathbf{r}')$
	Symmetric	$\mathbf{J}(\mathbf{r}) = \frac{1}{(2\pi)^3}\int d\mathbf{r}' \sigma^s_{ij}\left(\frac{\mathbf{r}+\mathbf{r}'}{2}, \mathbf{r}-\mathbf{r}'\right) \bullet \mathbf{E}(\mathbf{r}')$
$\mathbf{r}-\mathbf{k}$	Cartesian	$\mathbf{J}(\mathbf{r}) = \int d\mathbf{k}' \sigma^c_{ij}(\mathbf{r}, -\mathbf{k}') \bullet \overline{\mathbf{E}}(\mathbf{k}')$
	Simple	$\mathbf{J}(\mathbf{r}) = \int d\mathbf{k}' e^{i\mathbf{k}'\bullet\mathbf{r}} \sigma_{ij}(\mathbf{r}, \mathbf{k}') \bullet \overline{\mathbf{E}}(\mathbf{k}')$
	Symmetric	$\mathbf{J}(\mathbf{r}) = \int d\mathbf{k} e^{i\mathbf{k}\bullet\mathbf{r}} \overline{\mathbf{J}}(\mathbf{k})$
k	Cartesian	$\overline{\mathbf{J}}(\mathbf{k}) = \int d\mathbf{k}' \overline{\sigma}^c_{ij}(\mathbf{k}, -\mathbf{k}') \bullet \overline{\mathbf{E}}(\mathbf{k}')$
	Simple	$\overline{\mathbf{J}}(\mathbf{k}) = \int d\mathbf{k}' \overline{\sigma}_{ij}(\mathbf{k}-\mathbf{k}', \mathbf{k}') \bullet \overline{\mathbf{E}}(\mathbf{k}')$
	Symmetric	$\overline{\mathbf{J}}(\mathbf{k}) = \int d\mathbf{k}' \overline{\sigma}^s_{ij}\left(\mathbf{k}-\mathbf{k}', \frac{\mathbf{k}+\mathbf{k}'}{2}\right) \bullet \overline{\mathbf{E}}(\mathbf{k}')$

This will be shown to be of essence in deducing the symmetry properties of the response tensor and for clarifying conflicting reports in the literature. Note that we have not been able to obtain a clear expression of the plasma response in mixed space for the symmetric

tensor. This is due to the appearance of $\mathbf{r}$ in both of the arguments of the associated real space($\mathbf{r}$ space) form.

6.3 Onsager Symmetries Of The Transport Matrix

We want to look at the symmetries of the transport matrix in each space. We will separate out the spatial variables $\mathbf{r}$ and $\mathbf{k}$ from the set of variables $\Lambda = \{\omega, \mathbf{u}, \Omega; f_0\left(u_{\|}\right)\}$ which reverse sign in the time reversed state. Onsager symmetry is most conveniently expressed in Cartesian form,

$$L^c(\mathbf{r}, \mathbf{r}'; \Lambda) = L^{c\dagger}(\mathbf{r}', \mathbf{r}; -\Lambda). \tag{6.19}$$

A look at the table of spatial forms reveals the following connections between $\mathbf{r}$-space expressions,

$$L^c(\mathbf{r}, \mathbf{r}'; \Lambda) \equiv L(\mathbf{r}, \mathbf{r} - \mathbf{r}'; \Lambda) \equiv L^s\left(\frac{\mathbf{r} + \mathbf{r}'}{2}, \mathbf{r} - \mathbf{r}'; \Lambda\right). \tag{6.20}$$

So as to convert to the Cartesian form we introduce the variable,

$$\mathbf{r}_D = \mathbf{r} - \mathbf{r}' \tag{6.21}$$

such that,

$$L(\mathbf{r}, \mathbf{r}_D; \Lambda) \equiv L^c(\mathbf{r}, \mathbf{r} - \mathbf{r}_D; \Lambda) \equiv L^s\left(\mathbf{r} - \frac{\mathbf{r}_D}{2}, \mathbf{r}_D; \Lambda\right). \tag{6.22}$$

Similarly if we introduce the variables,

$$\begin{aligned} \mathbf{r}_D &= \mathbf{r} - \mathbf{r}', \\ \overline{\mathbf{r}} &= \frac{\mathbf{r} + \mathbf{r}'}{2}, \end{aligned} \tag{6.23}$$

then,

$$L^s(\overline{\mathbf{r}}, \mathbf{r}_D; \Lambda) \equiv L\left(\overline{\mathbf{r}} + \frac{\mathbf{r}_D}{2}, \mathbf{r}_D; \Lambda\right) \equiv L^c\left(\overline{\mathbf{r}} + \frac{\mathbf{r}_D}{2}, \overline{\mathbf{r}} - \frac{\mathbf{r}_D}{2}; \Lambda\right). \tag{6.24}$$

Now to obtain the symmetry law for each spatial form we may follow a simple prescription. We will illustrate this with the simple form of the transport matrix. First of all we equate the simple form with the Cartesian form of the tensor,

$$L(\mathbf{r}, \mathbf{r} - \mathbf{r}'; \Lambda) = L^c(\mathbf{r}, \mathbf{r}'; \Lambda). \tag{6.25}$$

As a second step we introduce the variables given by (6.23) so as to convert the chosen tensor to Cartesian form,

$$L(\mathbf{r}, \mathbf{r}_D; \Lambda) = L^c(\mathbf{r}, \mathbf{r} - \mathbf{r}_D; \Lambda). \tag{6.26}$$

Next we apply the Onsager symmetry law of (6.19),

$$L(\mathbf{r}, \mathbf{r}_D; \Lambda) = L^{c\dagger}(\mathbf{r} - \mathbf{r}_D, \mathbf{r}; -\Lambda). \tag{6.27}$$

Finally we convert the time reversed result back to simple form by letting $\mathbf{r} = \mathbf{r} - \mathbf{r}_D$ and $\mathbf{r}' = \mathbf{r}$ giving the Onsager symmetry law for the simple form in $\mathbf{r}$-space,

$$L(\mathbf{r}, \mathbf{r}_D; \Lambda) = L^{\dagger}(\mathbf{r} - \mathbf{r}_D, -\mathbf{r}_D; -\Lambda). \tag{6.28}$$

Following the same procedure we may arrive at the Onsager symmetry law for the symmetric form in $\mathbf{r}$-space,

$$L^s(\overline{\mathbf{r}}, \mathbf{r}_D; \Lambda) = L^{s\dagger}(\overline{\mathbf{r}}, -\mathbf{r}_D; -\Lambda). \tag{6.29}$$

To find the symmetry laws in $\mathbf{k}$-space there is another simple recipe. We need only Fourier transform the symmetry law expressed in $\mathbf{r}$-space and find a suitable change of variables which will equate the Fourier integrals. Again, we will use the simple form as an example.

So, Fourier transforming both sides of (6.28) we have,

$$\begin{aligned} \int d\mathbf{k} e^{i\mathbf{k}\bullet\mathbf{r}} \int d\mathbf{k}_D e^{i\mathbf{k}_D\bullet\mathbf{r}_D} L(\mathbf{k}, \mathbf{k}_D; \Lambda) &= \int d\kappa e^{i\kappa\bullet(\mathbf{r}-\mathbf{r}_D)} \int d\kappa' e^{-i\kappa'\bullet\mathbf{r}_D} L^{\dagger}(\kappa, \kappa'; -\Lambda), \\ &= \int d\kappa e^{i\kappa\bullet\mathbf{r}} \int d\kappa' e^{-i(\kappa+\kappa')\bullet\mathbf{r}_D} L^{\dagger}(\kappa, \kappa'; -\Lambda) \end{aligned} \tag{6.30}$$

We may make the left and right hand sides identically equal by the choice of variables,

$$\begin{aligned} \mathbf{k} &= \kappa \\ \mathbf{k}_D &= -\kappa - \kappa', \end{aligned} \tag{6.31}$$

and so the Onsager symmetry law in $\mathbf{k}$-space is,

$$L(\mathbf{k}, \mathbf{k}_D; \Lambda) = -L^{\dagger}(\mathbf{k}, -\mathbf{k} - \mathbf{k}_D; -\Lambda). \tag{6.32}$$

Following the same procedure we may arrive at the Onsager symmetry law for the symmetric form in $\mathbf{r}$-space,

$$L^s\left(\overline{\mathbf{k}}, \mathbf{k}_D; \Lambda\right) = -L^{s\dagger}\left(\overline{\mathbf{k}}, -\mathbf{k}_D; -\Lambda\right), \tag{6.33}$$

and for the Cartesian form,

$$L^c(\mathbf{k}, \mathbf{k}'; \Lambda) = L^{c\dagger}(\mathbf{k}', \mathbf{k}; -\Lambda). \tag{6.34}$$

We may now sum up the Onsager symmetry laws in the following table,

Space	Tensor Space	Onsager Symmetry Law
$\mathbf{r}$	Cartesian Simple Symmetric	$L^c(\mathbf{r},\mathbf{r}';\Lambda) = L^{c\dagger}(\mathbf{r}',\mathbf{r};-\Lambda)$ $L(\mathbf{r},\mathbf{r}_D;\Lambda) = L^{\dagger}(\mathbf{r}-\mathbf{r}_D,-\mathbf{r}_D;-\Lambda)$ $L^s(\overline{\mathbf{r}},\mathbf{r}_D;\Lambda) = L^{s\dagger}(\overline{\mathbf{r}},-\mathbf{r}_D;-\Lambda)$
$\mathbf{k}$	Cartesian Simple Symmetric	$L^c(\mathbf{k},\mathbf{k}';\Lambda) = L^{c\dagger}(\mathbf{k}',\mathbf{k};-\Lambda)$ $L(\mathbf{k},\mathbf{k}_D;\Lambda) = -L^{\dagger}(\mathbf{k},-\mathbf{k}-\mathbf{k}_D;-\Lambda)$ $L^s\left(\overline{\mathbf{k}},\mathbf{k}_D;\Lambda\right) = -L^{s\dagger}\left(\overline{\mathbf{k}},-\mathbf{k}_D;-\Lambda\right)$

In essence, each of these symmetry laws is equivalent in that they are simply different spatial representations of (6.7). Onsager symmetry is then invariant under arbitrary transformations of the coordinates revealing the covariant nature of the underlying physics.

We are now in a position to investigate the symmetry properties of our mixed space plasma response for the simple form of the conductivity tensor.

6.4 Demonstration Of Onsager Symmetry For Our Conductivity Tensor

In the previous section we derived the Onsager reciprocal relations for the thermodynamic transport matrix in real space and in momentum space. However, when we calculated the response of the plasma in chapters 3 and 4, we obtained a mixed space form for the conductivity tensor. In order to investigate the thermodynamic properties of our result using the symmetry laws of the last section, we first need to transform our transport matrix to real space or to momentum space. If we look at the form of the conductivity tensor in (4.49) we see that it has the general form,

$$\sigma_{ij}(x,\mathrm{k}) = \int_0^\infty dk_1 e^{ik_1 x} f_{ij}(k_1,\mathrm{k}), \tag{6.35}$$

with,

$$f_{ij}(k_1,\mathrm{k}) = -\frac{i\epsilon_0\omega_p^2}{\omega}\frac{T_{\|}}{T_{\perp}}\left(1-\frac{T_{\perp}}{T_{\|}}\right)\hat{\mathrm{e}}_{33}$$

$$+ \quad \frac{\epsilon_0 \omega_p^2 L}{l\Omega_0(0)} \sum_l e^{ik_1[\omega - l\Omega_0(0)]\frac{L}{l\Omega_0(0)} - \mu - \frac{1}{4}\psi^2} V_{ij}(k_1, \mathbf{k}). \tag{6.36}$$

If we introduce the Heaviside step function,

$$\Phi(k_1) = \begin{cases} 0 & for \quad k_1 < 0, \\ 1 & for \quad k_1 \geq 0, \end{cases} \tag{6.37}$$

then we may write,

$$\sigma_{ij}(x, \mathbf{k}) = \int_{-\infty}^{\infty} dk_1 e^{ik_1 x} \sigma_{ij}(k_1, \mathbf{k}), \tag{6.38}$$

and here,

$$\sigma_{ij}(k_1, \mathbf{k}) = f_{ij}(k_1, \mathbf{k}) \Phi(k_1). \tag{6.39}$$

This is the momentum space form of the conductivity tensor. Onsager symmetry is most easily demonstrated using the form of the conductivity tensor expressed algebraically in terms of α, β and μ in (4.49),

$$\begin{aligned} \sigma_{ij}(k_1, \mathbf{k}) &= -\frac{i\epsilon_0 \omega_p^2}{\omega} \frac{T_\parallel}{T_\perp} \left(1 - \frac{T_\perp}{T_\parallel}\right) \hat{\mathbf{e}}_{33} \\ &+ \frac{\epsilon_0 \omega_p^2 L}{l\Omega_0(0)} \sum_l e^{ik_1[\omega - l\Omega_0(0)]\frac{L}{l\Omega_0(0)} - \mu - \frac{1}{4}\psi^2} V_{ij}(k_1, \mathbf{k}) \Phi(k_1), \end{aligned} \tag{6.40}$$

with,

$$V_{ij} = \begin{bmatrix} \frac{l^2}{\lambda} I_l A_1 & il\left[I_l' - \frac{\alpha}{\beta} I_l\right] A_1 & \frac{l}{\beta} I_l A_2 \\ -il\left[I_l' - \frac{\beta}{\alpha} I_l\right] A_1 & \left[\left(2\lambda + \frac{l^2}{\lambda}\right) I_l - 2\mu I_l'\right] A_1 & -i\frac{\alpha}{2}\left[I_l' - \frac{\beta}{\alpha} I_l\right] A_2 \\ \frac{l}{\alpha} I_l A_2 & i\frac{\beta}{2}\left[I_l' - \frac{\alpha}{\beta} I_l\right] A_2 & I_l A_3 \end{bmatrix}. \tag{6.41}$$

For the simple form of the conductivity tensor, then the symmetry relation in $\mathbf{k}$-space is,

$$L(\mathbf{k}, \mathbf{k}_D; \Lambda) = -L^\dagger(\mathbf{k}, -\mathbf{k} - \mathbf{k}_D; -\Lambda).$$

When applying this to (6.39) then we need to also consider that k_1 itself changes sign under time reversal as it is a function of the gyrofrequency(Ω_0). Our symmetry relation is then,

$$T_j \sigma_{ij}[k_1(\Omega_0), k_\perp; \Lambda] = -T_i \sigma_{ji}^*[k_1(-\Omega_0), -k_\perp - k_1(-\Omega_0); -\Lambda]. \tag{6.42}$$

So the procedure for obtaining the right hand side involves the following four steps:

- Firstly, take $\sigma_{ij}\left[k_1(\Omega_0), k_\perp\right]$ and perform the coordinate transformation,

$$\begin{aligned} k_1(\Omega_0) &\rightarrow k_1(-\Omega_0), \\ k_\perp &\rightarrow -k_\perp - k_1(-\Omega_0). \end{aligned}$$

- Secondly, perform the time reversal transformation,

$$t \rightarrow -t, \quad \mathbf{B}_0 \rightarrow -\mathbf{B}_0, \quad \omega \rightarrow -\omega.$$

- Thirdly, we take the complex conjugate $i \rightarrow -i$.

- Finally transpose the elements of the resulting tensor.

We may clarify the steps in the analysis by introducing $\overrightarrow{C}$ as a coordinate transform operator and $\overrightarrow{T}$ as a time reversal transform operator so that,

$$\overrightarrow{C}\left\{\sigma_{ij}\left[k_1(\Omega_0), k_\perp; \Lambda\right]\right\} \equiv \sigma_{ij}\left[k_1(-\Omega_0), -k_\perp - k_1(-\Omega_0); \Lambda\right], \tag{6.43}$$

and,

$$\overrightarrow{T}\left\{\sigma_{ij}\left[k_1(\Omega_0), k_\perp; \Lambda\right]\right\} \equiv \sigma_{ij}\left[k_1(-\Omega_0), k_\perp; -\Lambda\right]. \tag{6.44}$$

Let us make the coordinate transform first. Now $k_\perp$ appears only in α and β which are themselves constituents of λ and μ. They transform as follows,

$$\begin{aligned} \overrightarrow{C}\{\alpha\} &= \left[-k_\perp - k_1(-\Omega_0)\right]\rho_\perp, \\ \overrightarrow{C}\{\beta\} &= -k_\perp \rho_\perp. \end{aligned}$$

The second operation has the following effect,

$$\begin{aligned} \overrightarrow{T}\left[\omega\right] &= -\omega, \\ \overrightarrow{T}\left[\Omega_0\right] &= -\Omega_0, \\ \overrightarrow{T}\left[\rho_\perp\right] &= -\rho_\perp, \\ \overrightarrow{T}\left[\zeta_0\right] &= -\zeta_0, \\ \overrightarrow{T}\left[k_1\right] &= -k_1, \\ \overrightarrow{T}\left[\psi\right] &= \psi, \\ \overrightarrow{T}\left[\tau\right] &= \tau. \end{aligned} \tag{6.45}$$

The anisotropic factors have the following properties under time reversal and subsequent complex conjugation,

$$\begin{aligned}\overrightarrow{T}\,[A_1^*] &= A_1,\\ \overrightarrow{T}\,[A_2^*] &= -A_2,\\ \overrightarrow{T}\,[A_3^*] &= A_3.\end{aligned} \tag{6.46}$$

The combined operations of coordinate transformation and also time reversal give the pleasing symmetry property,

$$\begin{aligned}\overrightarrow{T}\,\overrightarrow{C}\,\{\alpha\} &= \beta,\\ \overrightarrow{T}\,\overrightarrow{C}\,\{\beta\} &= \alpha,\\ \overrightarrow{T}\,\overrightarrow{C}\,\{\lambda\} &= \lambda,\\ \overrightarrow{T}\,\overrightarrow{C}\,\{\mu\} &= \mu.\end{aligned} \tag{6.47}$$

As λ and μ are left unchanged by the transforms, then only the elements of the velocity tensor are affected by the coordinate and time-reversal transformations.

We may now write down,

$$\begin{aligned}\overrightarrow{T}\,\overrightarrow{C}\,\{\sigma_{ij}^*\,[k_1(\Omega_0),k_\perp;\Lambda]\} \equiv\ & -\ \frac{i\epsilon_0\omega_p^2}{\omega}\frac{T_\parallel}{T_\perp}\left(1-\frac{T_\perp}{T_\parallel}\right)\hat{\mathbf{e}}_{33}\\ & -\ \frac{\epsilon_0\omega_p^2 L}{l\Omega_0\,(0)}\sum_l e^{ik_1[\omega-l\Omega_0(0)]\frac{L}{l\Omega_0(0)}-\mu-\frac{1}{4}\psi^2} \qquad (6.48)\\ & \times\ \overrightarrow{T}\,\overrightarrow{C}\,\{V_{ij}^*\,[k_1(\Omega_0),k_\perp]\}, \qquad (6.49)\end{aligned}$$

with,

$$\overrightarrow{T}\,\overrightarrow{C}\,\{V_{ij}^*\} = \begin{bmatrix} \frac{l^2}{\lambda}I_lA_1 & -il\left[I_l'-\frac{\beta}{\alpha}I_l\right]A_1 & \frac{l}{\alpha}I_lA_2\\ il\left[I_l'-\frac{\alpha}{\beta}I_l\right]A_1 & \left[\left(2\lambda+\frac{l^2}{\lambda}\right)I_l-2\mu I_l'\right]A_1 & i\frac{\beta}{2}\left[I_l'-\frac{\alpha}{\beta}I_l\right]A_2\\ \frac{l}{\beta}I_lA_2 & -i\frac{\alpha}{2}\left[I_l'-\frac{\beta}{\alpha}I_l\right]A_2 & I_lA_3 \end{bmatrix}. \tag{6.50}$$

Comparison of σ_{ij} in (4.49) with $\overrightarrow{T}\,\overrightarrow{C}\,\{\sigma_{ij}^*\}$ reveals the relation,

$$\sigma_{ij}\,[k_1(\Omega_0),k_\perp;\Lambda] = -\sigma_{ji}^*\,[k_1(-\Omega_0),-k_\perp-k_1(-\Omega_0);-\Lambda]\,. \tag{6.51}$$

Note that this is not the same as the original Onsager symmetry relation of (6.42) as we need to prefix both sides of (6.51) by directional temperature components. However, the fact that the above relation holds, independent of the effects of thermal anisotropy, means that an isotropic plasma($T_i = T_j$), supporting EM waves in an inhomogeneous magnetic field, obeys the Onsager reciprocal relations. This property appears not to have been reported in the literature within the present context of thermodynamic fluxes and forces in an *inhomogeneous* magnetic field. The most recent investigation of the thermodynamic properties of a thermally anisotropic but homogeneous plasma was undertaken by Nambu(1995) who reported that the Onsager reciprocal relations are violated for an anisotropic plasma supporting EM waves.

We have revealed a novel aspect of EM wave propagation in inhomogeneous plasmas. Onsager symmetry is still present for an inhomogeneous plasma provided it is in thermal equilibrium(having an isotropic Maxwellian distribution). An anisotropic plasma will violate Onsager symmetry since there will be a directional dependence on temperature ($T_i \neq T_j$).

Chapter 7

A Study Of The Integro-Differential Wave Equation(IDE)

In chapter 4 we derived the non-local IDE for small amplitude EM waves propagating through a hot, thermally anisotropic plasma immersed in a linearly inhomogeneous magnetic field. The response of the plasma is expressed through the current density($\mathbf{J}$) which is related to the electric field($\mathbf{E}$) by the response function, the plasma conductivity(σ_{ij}). In chapter 6 we indicated that the plasma response may be written in various spatial forms each with its own associated Onsager symmetry law. In this chapter we will present a study of the IDE in both real($\mathbf{r}$) space and momentum($\mathbf{k}$) space, indicating various methods of solution.

7.1 The IDE And Reduction To ODEs

In essence (4.100) is an integro-differential equation for the local electric field in real space(although in terms of the non-local electric field it is not very amenable to analytic solution). If we are able to obtain a solution to the IDE then we will have a global treatment of wave-wave and wave-particle interactions in the plasma from which we may extract information related to energy transport. This is vital for a comparison with experimental measurements.

In the last chapter we obtained an expression for the non-local response of the plasma in terms of the conductivity tensor in real space (6.16). We may now write down the wave equation (4.100) solely in real space,

$$\frac{c^2}{\omega^2}\nabla^2\mathbf{E}(\mathbf{r}) - \frac{c^2}{\omega^2}\nabla(\nabla \bullet \mathbf{E}(\mathbf{r})) + \mathbf{E}(\mathbf{r}) + \frac{1}{(2\pi)^3}\int d\mathbf{r}'\chi_{ij}(\mathbf{r}, \mathbf{r}-\mathbf{r}') \bullet \mathbf{E}(\mathbf{r}') = 0. \qquad (7.1)$$

7.1.1 Motivation For A New Approximation

A few years ago Sauter and Vaclavik(1992) presented a numerical solution of (7.1) using an elaborate finite element code. In order to obtain the non-local, real space response, they derived the conductivity tensor for a multiple ion species, isotropic plasma immersed in a linear magnetic field gradient and with spatially varying density and temperature profiles. In order to give a flavour of the mathematical form of the non-local response function in (7.1) we reproduce here a small excerpt from a recent publication which can be found at the end of this chapter.

The z-component of the current density arising from the $\hat{\mathbf{e}}_{zz}$ component of the conductivity tensor is,

$$J_z(x) = \int dk' e^{ik'x} \sigma_{zz}(x, k') \overline{E}_z(k'). \tag{7.2}$$

Inversion of the Fourier transform of the electric field gives the following $1D$ analogue of (7.11),

$$J_z(x) = \frac{1}{2\pi} \int dx' \int dk' e^{ik'(x-x')} \sigma_{zz}(x, k') E_z(x') \equiv \frac{1}{2\pi} \int dx' \sigma_{zz}(x, x - x') E_z(x'). \tag{7.3}$$

With reference to (4.62) we may identify the non-local, real space resonant response of an *isotropic* plasma at the *fundamental*($n = 1$) of the gyrofrequency in a linearly inhomogeneous magnetic field,

$$\begin{aligned} \sigma_{zz}(x, x - x') &= \int dk' e^{ik'(x-x')} \sigma_{zz}(x, k'), \\ &= \frac{\epsilon_0 \omega_p^2 L}{\Omega_0(0)} \int dk' e^{ik'(x-x')} \int_0^\infty dk_1 e^{ik_1 x - \frac{1}{4}k_1^2 \rho_\perp^2 (1 + k_\parallel^2 L^2)} \\ &\times \left(1 - \frac{1}{2} k_1^2 \rho_\perp^2 k_\parallel^2 L^2\right) I_1 \left[\frac{k_\perp (k_\perp + k_1) \rho_\perp^2}{2}\right] e^{-\frac{1}{2}k_\perp (k_\perp + k_1)\rho_\perp^2}. \end{aligned} \tag{7.4}$$

As a double integral over an infinite half-plane, this is not a very suitable form for numerical solution or for further analysis. In this thesis we will be concerned with approximations to the *non-local* electric field which allow a reduction in the complexity of the IDEs resulting from non-local response functions of the above form. Sauter and Vaclavik(1992) took a different path and pursued the theory a little further using the integral representation of the modified Bessel function, which for the fundamental is,

$$I_1(z) = \frac{1}{\pi} \int_0^\pi e^{z \cos\theta} \cos\theta d\theta.$$

The response function then involves the exponential of a quadratic in k' and k_1. The transformation $k' = K - \frac{1}{2}k_1$ switches to the principle axes of this quadratic, separating

the resulting K and k_1-integrals. This, combined with the generalised recurrence relation for the Z-function,

$$\frac{d^n Z(\zeta)}{d\zeta^n} = i\int_0^\infty (ik_1)^n e^{ik_1\zeta - \frac{1}{4}k_1^2} dk_1,$$

gives us the non-local, real space response function,

$$\begin{aligned}\sigma_{zz}(x, x-x') &= \frac{\epsilon_0\omega_p^2 L\rho_\perp}{i\omega\sqrt{2\pi}}\frac{1}{\pi}\int_0^\pi d\theta\cos\theta \\ &\times \frac{e^{-(x-x')^2/2\rho_\perp^2(1-\cos\theta)}}{\sqrt{1-\cos\theta}} \\ &\times \left[\frac{1}{a}Z(\frac{x+x'}{a\rho_\perp}) + \frac{k_\parallel^2 L^2}{a^3}Z''(\frac{x+x'}{a\rho_\perp})\right], \end{aligned} \tag{7.5}$$

with $a = \sqrt{2+2\cos\theta+4k_\parallel^2L^2}$. This expression for the non-local, real space response function is a specialisation of the result of Sauter and Vaclavik(1992) to the less general case of a linearly inhomogeneous plasma with constant density and temperature profiles. We have reduced the response function from a double integral over an infinite half-plane to a single, finite integral. We see that the plasma response described by (6.18) now involves a double integral rather than the triple integral which we would have in the case of the plasma response calculated from the mixed form of the response function (6.17). Although, on the surface, it appears that progress has been made, in practice it is difficult to see how use can be made of further approximations. For example it is not obvious how small Larmor radius expansions may be developed here whereas a simple procedure is available for expanding the modified Bessel functions to any order in the mixed space form of the response function(Cairns et al., 1991). In addition, a more complex scenario such as a thermally anisotropic plasma will introduce new terms into the mixed space response function which is unlikely to reduce in the simple way described above.

For these reasons, we will develop a more general form of an existing approximation to the wave behaviour, known as, 'the fast wave approximation' (Kay et al., 1988, and Lashmore-Davies et al., 1988). The fast wave approximation retains all of the information associated with the propagation of the fast wave even in the presence of mode conversion layers since it utilises the fact that interacting wave modes are degenerate in a linear mode conversion process. We hope this will provide more insight into the physics of the non-local interactions of EM waves with high energy, large Larmor radius particles.

7.2 The IDE, Dispersion Relations And The Effective Conductivity Tensor

We may Fourier transform the IDE(4.100) so as to obtain a dispersion relation(in momentum space) whose roots give the modes of oscillation of the plasma. We may then

infer the group velocity and phase velocity of these modes so as to describe the spatial and temporal dispersion characteristics of the plasma.

As a first step we express the electric field $\mathbf{E}(\mathbf{r})$ in the wave equation in terms of its Fourier modes as we did in (3.11) so that $\nabla \equiv i\mathbf{k}$. If, in addition, we use the momentum space representation of the plasma response (6.14) and note the definitions of the refractive index and the dielectric tensor in chapter 2, then we may write down the fully Fourier-transformed wave equation,

$$\int d\mathrm{k} e^{i\mathbf{k}\bullet\mathbf{r}} \left\{ \left[\mathbf{nn} - n^2 \delta_{ij} \right] \bullet \overline{\mathbf{E}}(\mathrm{k}) + \int d\mathrm{k}' \epsilon_{ij}(\omega, \mathrm{k} - \mathrm{k}', \mathrm{k}') \bullet \overline{\mathbf{E}}(\mathrm{k}') \right\} = 0. \qquad (7.6)$$

This may be solved to give a local dispersion relation which describes the modes of oscillation of the inhomogeneous plasma. We note that the coefficients of the electric field appear as kernels inside integrals and so plane waves are not the eigenfunctions of the linear problem. We will show that this is indeed the case when we come to a numerical study of our theory in chapter 8. Generally, integral equations like the one above require numerical solution since it is a non-algebraic integral equation. Furthermore, the convolution theorem of (2.25), valid for a *homogeneous* plasma, is now not the case. This is a direct consequence of the introduction of plasma inhomogeneity which transforms the nature of the wave-particle interactions meaning that the response function becomes spatially dependent, $\sigma_{ij}(\omega, \mathbf{k}) \rightarrow \sigma_{ij}(\mathbf{r}, \omega, \mathbf{k})$. It has been shown(Beskin et al., 1986) that, even in this case, the following modified convolution theorem may be used,

$$\overline{\mathbf{D}}(k) = \epsilon_{ij}^{eff}(x, k) \bullet \overline{\mathbf{E}}(k),$$

for a single mode k propagating through a plasma with a $1D$ inhomogeneity along $\hat{x}$. In terms of the effective dielectric tensor(ϵ^{eff}), the following algebraic dispersion relation,

$$Det|k_i k_j - k^2 \delta_{ij} + \frac{\omega^2}{c^2} \epsilon_{ij}^{eff}(x, k)| = 0, \qquad (7.7)$$

can be obtained(Beskin et al., 1986) within the framework of the geometrical optics approximation(Bernstein, 1975). This approach is able to give us information about the attenuation of an incident EM wave when passing through a volume of plasma since we may deduce the change in the wave-vector with position. Integration of the imaginary part of the wave-vector across a section of the plasma then gives an estimate of the opacity or optical depth(τ) of the plasma,

$$\tau = \int Im\{k(x)\} dx, \qquad (7.8)$$

from which we may quantify the wave transmission($T \simeq e^{-2\tau}$).

7.2.1 A Critique Of The Effective Tensor

In recent years a number of authors have discussed at length the relevance of the effective dielectric tensor in the study of inhomogeneous plasmas(see for example Beskin(1986), Nambu(1989), Michabeli(1991) and Istomin(1993)). Reports have often been conflicting and this is not surprising when one considers the complexity of the problem. Beskin et al.(1986) have presented a method of obtaining the effective conductivity tensor. They showed that the effective tensor(σ^{eff}) is seen to comprise an infinite sum of corrections to the standard conductivity tensor(σ) obtained as the response of a plasma to a plane wave,

$$\sigma_{ij}^{eff}(\mathbf{r},\mathbf{k}) = \sum_{n=0}^{\infty} \frac{1}{n!} \left(\frac{i}{2}\right)^n \left(\frac{\partial^2}{\partial \mathbf{r} \bullet \partial \mathbf{k}}\right)^n \sigma_{ij}(\mathbf{r},\mathbf{k}), \tag{7.9}$$

We have included the dot product in the denominator which Beskin et al.(1986) left out(they forgot to include the cross terms in the sum). In addition, we have noted Michabeli's correction(1991) which notes that,

$$\left(\frac{\partial^2}{\partial \mathbf{r} \bullet \partial \mathbf{k}}\right)^n \sigma_{ij}(\mathbf{r},\mathbf{k}) \neq \left(\frac{\partial^n}{\partial \mathbf{r}^n \bullet \partial \mathbf{k}^n}\right) \sigma_{ij}(\mathbf{r},\mathbf{k}).$$

Beskin et al.(1986) quoted the right hand side and then went on to claim(erroneously) that all orders of corrections are required in the dispersion relation (7.7) for a study of an inhomogeneous plasma due to extreme variations of the conductivity(on the scale of the wavelength) which arise in the neighbourhood of resonance and cut-off surfaces. However, as Nambu(1989) demonstrated, the standard WKB treatment(Bernstein, 1975) of a weak inhomogeneity utilises only the first two terms of the expansion,

$$\sigma_{ij}^{eff}(\mathbf{r},\mathbf{k}) \simeq \sigma_{ij}(\mathbf{r},\mathbf{k}) + \frac{i}{2} \frac{\partial^2 \sigma_{ij}(\mathbf{r},\mathbf{k})}{\partial \mathbf{r} \bullet \partial \mathbf{k}}. \tag{7.10}$$

Higher order terms are not included since they lead to a violation of the geometrical optics approximation. For more strenuous variations of the conductivity tensor we need to use a multi-mode theory to determine the plasma response. Furthermore, Nambu(1989) reiterated Bernstein's observations that first order corrections to the standard response are related to changes in the ray path in the inhomogeneous plasma and are not directly related to wave growth or damping as claimed by Beskin et al.(1986) and also by Istomin(1993). In contrast, true dissipation is due to the anti-Hermitian part of the conductivity tensor (see for example Shafranov, 1962 or Stix, 1992).

The effective tensor has recently been derived in a more concise way by Michabeli(1991). We will repeat a part of his calculation so as to bring to light some of the properties of the mixed form of the conductivity tensor which we have derived in chapter 4.

As our starting point let us take the simple form for the non-local response of the plasma in real space as given by (6.16). If we Fourier transform the non-local second argument of the conductivity tensor,

$$\sigma_{ij}(\mathbf{r},\mathbf{r}-\mathbf{r}') = \int d\mathbf{k}' e^{i\mathbf{k}'\bullet(\mathbf{r}-\mathbf{r}')}\sigma_{ij}(\mathbf{r},\mathbf{k}'),$$

then we may express the real space current density in terms of the mixed tensor as follows,

$$\mathbf{J}(\mathbf{r}) = \frac{1}{(2\pi)^3}\int d\mathbf{r}' \int d\mathbf{k}' e^{i\mathbf{k}'\bullet(\mathbf{r}-\mathbf{r}')}\sigma_{ij}(\mathbf{r},\mathbf{k}')\bullet\mathbf{E}(\mathbf{r}'). \tag{7.11}$$

We may then write the non-local electric field in terms of its Fourier modes as we did in chapter 3 using (3.11) so that,

$$\mathbf{J}(\mathbf{r}) = \frac{1}{(2\pi)^3}\int d\mathbf{r}' \int d\mathbf{k} e^{i\mathbf{k}\bullet\mathbf{r}} \int d\mathbf{k}' e^{i(\mathbf{k}'-\mathbf{k})\bullet(\mathbf{r}-\mathbf{r}')}\sigma_{ij}(\mathbf{r},\mathbf{k}')\bullet\overline{\mathbf{E}}(\mathbf{k}).$$

A key theme is the symmetrisation of the position vectors about a point ζ. This is most easily achieved through the change of variables,

$$\left.\begin{array}{l}\eta = \mathbf{r}'-\mathbf{r},\\ \zeta = \frac{\mathbf{r}+\mathbf{r}'}{2},\end{array}\right\} \rightarrow \left\{\begin{array}{l}\mathbf{r} = \zeta - \eta/2,\\ \mathbf{r}' = \zeta + \eta/2.\end{array}\right.$$

In this symmetric form, the plasma response at a point $\zeta = \mathbf{r}$ is,

$$\mathbf{J}(\mathbf{r}) = \frac{1}{(2\pi)^3}\int d\eta \int d\mathbf{k} e^{i\mathbf{k}\bullet\mathbf{r}} \int d\mathbf{k}' e^{i(\mathbf{k}-\mathbf{k}')\bullet\eta}\sigma_{ij}\left(\mathbf{r}-\frac{\eta}{2},\mathbf{k}'\right)\bullet\overline{\mathbf{E}}(\mathbf{k}).$$

Writing the plasma response in the familiar form of (3.38), we may identify the effective tensor as,

$$\sigma_{ij}^{eff}(\mathbf{r},\mathbf{k}) \equiv \frac{1}{(2\pi)^3}\int d\eta \int d\mathbf{k}' e^{i(\mathbf{k}-\mathbf{k}')\bullet\eta}\sigma_{ij}\left(\mathbf{r}-\frac{\eta}{2},\mathbf{k}'\right), \tag{7.12}$$

in agreement with equation (21) of Beskin et al.(1986). We see that this representation of the effective tensor is simply an integral transform which symmetrises the standard response of the plasma and has nothing at all to do with the inclusion of extra energy-related terms as claimed by Beskin et al.(1986).

We now use this integral transform to symmetrise our mixed space representation of the conductivity tensor to see how its symmetry properties are affected. This is most easily done by writing our response function (4.62) in the following symbolic form,

$$\sigma_{ij}(x,k') = C\hat{\mathbf{e}}_{33} + D\int_0^\infty dk_1 e^{ik_1 x} g_{ij}(k_1,k'),$$

where $C = -\frac{i\epsilon_0\omega_p^2}{\omega}\frac{T_\parallel}{T\perp}\left(1-\frac{T_\parallel}{T\perp}\right)$ and $D = \frac{\epsilon_0\omega_p^2 L}{l\Omega_0(0)}$. Note that we are using a dummy variable for the wave-vector and also that we are considering a $1D$ inhomogeneity along $\hat{x}$. Now,

$$\sigma_{ij}\left(x-\frac{\eta}{2},k'\right) = C\hat{\mathbf{e}}_{33} + D\int_0^\infty dk_1 e^{ik_1\left(x-\frac{\eta}{2}\right)} g_{ij}(k_1,k'),$$

and so we may construct the effective tensor using (7.12)

$$\begin{aligned}
\sigma_{ij}^{eff}(x,k_\perp) &= \frac{C}{2\pi}\int d\eta \int dk' e^{i(k_\perp-k')\eta}\hat{\mathbf{e}}_{33} \\
&+ \frac{D}{2\pi}\int d\eta \int dk' \int_0^\infty dk_1 e^{ik_1 x} g_{ij}(k_1,k')\, e^{i\left(k_\perp-k'-\frac{k_1}{2}\right)\eta}, \\
&= C\hat{\mathbf{e}}_{33} + D\int dk' \int_0^\infty dk_1 e^{ik_1 x} g_{ij}(k_1,k')\,\delta\left(k_\perp - k' - \frac{k_1}{2}\right), \\
&= C\hat{\mathbf{e}}_{33} + D\int_0^\infty dk_1 e^{ik_1 x} g_{ij}\left(k_1, k_\perp - \frac{k_1}{2}\right), \\
&\equiv \sigma_{ij}(x, k_\perp - \frac{k_1}{2}). \qquad (7.13)
\end{aligned}$$

If we make this change in our mixed space form for the response function in (4.62) then,

$$\begin{aligned}
\sigma_{ij}^{eff}(x,k_\perp) = &- \frac{i\epsilon_0\omega_p^2}{\omega}\frac{T_\parallel}{T_\perp}\left(1-\frac{T_\perp}{T_\parallel}\right)\hat{\mathbf{e}}_{33} \\
&+ \frac{\epsilon_0\omega_p^2 L}{l\Omega_0(0)}\sum_l \int_0^\infty dk_1 e^{ik_1 x + ik_1[\omega - l\Omega_0(0)]\frac{L}{l\Omega_0(0)} - \frac{1}{4}k_1^2\rho_\perp^2\left[1+k_\parallel^2 L^2\left(\frac{T_\parallel}{T_\perp}\right)/l^2\right]-\lambda} \\
&\times \begin{bmatrix}
V_{xx} = & \frac{l^2}{\lambda} I_l A_1, \\
V_{xy} = & il\left[I_l' - \left(\frac{k_\perp-\frac{k_1}{2}}{k_\perp+\frac{k_1}{2}}\right) I_l\right] A_1, \\
V_{xz} = & \frac{l}{\left(k_\perp+\frac{k_1}{2}\right)\rho_\perp} I_l A_2, \\
V_{yx} = & -il\left[I_l' - \left(\frac{k_\perp+\frac{k_1}{2}}{k_\perp-\frac{k_1}{2}}\right) I_l\right] A_1, \\
V_{yy} = & \left[\left(2\lambda+\frac{l^2}{\lambda}\right) I_l - \left(2\lambda+\frac{1}{2}k_1^2\rho_\perp^2\right) I_l'\right] A_1, \\
V_{yz} = & -i\frac{\left(k_\perp-\frac{k_1}{2}\right)\rho_\perp}{2}\left[I_l' - \left(\frac{k_\perp+\frac{k_1}{2}}{k_\perp-\frac{k_1}{2}}\right) I_l\right] A_2, \\
V_{zx} = & \frac{l}{\left(k_\perp-\frac{k_1}{2}\right)\rho_\perp} I_l A_2, \\
V_{zy} = & i\frac{\left(k_\perp+\frac{k_1}{2}\right)\rho_\perp}{2}\left[I_l' - \left(\frac{k_\perp-\frac{k_1}{2}}{k_\perp+\frac{k_1}{2}}\right) I_l\right] A_2, \\
V_{zz} = & I_l A_3
\end{bmatrix}, \qquad (7.14)
\end{aligned}$$

and here, $\lambda \equiv \frac{1}{2}\left(k_\perp^2 - \frac{1}{4}k_1^2\right)\rho_\perp^2$. The effective tensor is then simply the symmetrised with respect to x form of the mixed space tensor. In other words, the integral transform of (7.12) does not alter the physics of the wave-particle interaction(it does not separate out resonant particle effects for example), and instead simply re-expresses the conductivity in terms of a different (symmetrised) coordinate system. We note that under the time reversal transformation, $t \to -t$, it may be shown(with reference to chapter 6) that the symmetrised tensor, derived in the above manner, does indeed satisfy Onsager symmetry for an isotropic plasma but not in an anisotropic plasma for reasons described in the last

chapter. This provides yet another example of the invariance of Onsager symmetry to arbitrary changes of the coordinate system.

It will prove to be instructive to expand the conductivity tensor of (7.13) in a Taylor series about a local mode k,

$$\sigma_{ij}\left(x, k-\frac{k_1}{2}\right)=\sum_{n=0}^{\infty}\frac{1}{n!}\left(-\frac{k_1}{2}\right)^n\frac{\partial^n}{\partial k^n}\sigma_{ij}\left(x,k\right),$$

so that we consider only the perturbative effects of a single mode. If we notice that in (7.14) each $ik_1 \equiv \frac{\partial}{\partial x}$ then we may equivalently express the effective tensor as,

$$\sigma_{ij}^{eff}\left(x,k\right)=\sum_{n=0}^{\infty}\frac{1}{n!}\left(\frac{i}{2}\right)^n\left(\frac{\partial^2}{\partial x\partial k}\right)^n\sigma_{ij}\left(x,k\right).$$

This is precisely the summation form of the effective tensor quoted by Beskin et al.(1986) and is the $1D$ analogue of (7.9). As we have already mentioned, the usual geometric optics approximation is valid for the first two terms of the series. Higher order terms are irrelevant to a discussion of a weak inhomogeneity. This lies at the heart of many of the misconceptions in the literature(in particular Beskin et al.(1986) and Istomin et al.(1994)). The effective tensor obtained by the Beskin prescription is then just a symmetric representation of the plasma response to a single local wave mode.

A fundamental problem with writing the effective tensor in terms of the response to a single mode as above is that the single mode character of WKB theory excludes the possibility of studying resonant reflection and linear mode conversion phenomena since these require the existence of more than one wave. So WKB theories are generally only able to describe wave absorption effects. A global treatment of the wave-particle and linear wave-wave interactions in the plasma requires a full wave(multi-mode) description. In the next section we will present a study of the full IDE.

7.2.2 The Non-Local Response As An n^{th} Order Summation

As mentioned in chapter 2, Cairns et al.(1991) have shown how energy-conserving ODEs may be constructed from a multi-mode theory by constructing spatial derivatives of the field($\mathbf{E}$) and of the response function(Z). In what follows, we will derive an effective dielectric tensor comprising derivatives of the response function(like Beskin et al., 1986) but one which also provides the field derivatives which are known to be vital for energy conservation(Swanson, 1985).

In an interaction region, the electric field will have a phase angle which will not vary appreciably but an amplitude which is predicted to have substantial variation due to collisionless absorption from wave-particle and linear wave-wave energy exchanges. We

now make an approximation to the unknown, non-local electric field guided by the above *a priori* physics which is similar in spirit to the Born approximation of quantum-mechanical scattering theory(see for example Harding, 1968). We will let the phase angle be equal to the product of the local wave-vector($\mathbf{k}_0$) which may be evaluated from a cold plasma model and the non-local position vector($\mathbf{r}'$). We will express the amplitude as a Taylor series expansion,

$$f(x) = \sum_{n=0}^{\infty} \frac{1}{n!}(x - x_0)^n \frac{d^n f(x_0)}{dx^n}. \tag{7.15}$$

Let us expand about a local position vector $\mathbf{r}$. A suitable form for the non-local electric field is then,

$$\mathbf{E}(\mathbf{r}') = \left[\sum_{n=0}^{\infty} \frac{1}{n!}(\mathbf{r}' - \mathbf{r})^n \frac{d^n \mathbf{E}_0(\mathbf{r})}{d\mathbf{r}^n}\right] e^{i\mathbf{k}_0 \bullet \mathbf{r}'}. \tag{7.16}$$

The zero order case($n = 0$) is the fast wave approximation which we have used in a recent publication(Cairns et al., 1995). Equation (7.16) represents a generalisation of the approximation to include effects due to amplitude variation. We will show how these effects bring about the odd-order derivatives of the electric field which are required for energy conservation.

We may substitute this form for the electric field into our expression for the non-local response of the plasma given by (7.11),

$$\mathbf{J}_n(\mathbf{r}) = \sum_{n=0}^{\infty} \frac{1}{(2\pi)^3 n!} \int d\mathbf{r}' (\mathbf{r}' - \mathbf{r})^n \int d\mathbf{k}' e^{i\mathbf{k}' \bullet \mathbf{r}} e^{i(\mathbf{k}_0 - \mathbf{k}') \bullet \mathbf{r}'} \sigma_{ij}(\mathbf{r}, \mathbf{k}') \bullet \frac{d^n \mathbf{E}_0(\mathbf{r})}{d\mathbf{r}^n}.$$

If we note that we can identify each $i\mathbf{r}'$ with an operator $\partial_{\mathbf{k}_0}$ by differentiating under the integral sign, then we may take the term $(\mathbf{r}' - \mathbf{r})^n$ outside the integrals as follows,

$$\mathbf{J}_n(\mathbf{r}) = \sum_{n=0}^{\infty} \frac{1}{(2\pi)^3 n!} (-i\partial_{\mathbf{k}_0} - \mathbf{r})^n \int d\mathbf{r}' \int d\mathbf{k}' e^{i\mathbf{k}' \bullet \mathbf{r}} e^{i(\mathbf{k}_0 - \mathbf{k}') \bullet \mathbf{r}'} \sigma_{ij}(\mathbf{r}, \mathbf{k}') \bullet \frac{d^n \mathbf{E}_0(\mathbf{r})}{d\mathbf{r}^n}.$$

The $\mathbf{r}'$-integral is $2\pi\delta(\mathbf{k}_0 - \mathbf{k}')$ and the delta function allows us to easily perform the $\mathbf{k}'$-integral giving,

$$\mathbf{J}_n(\mathbf{r}) = \sum_{n=0}^{\infty} \frac{1}{n!} (-i\partial_{\mathbf{k}_0} - \mathbf{r})^n \sigma_{ij}(\mathbf{r}, \mathbf{k}_0) \bullet \frac{d^n \mathbf{E}_0(\mathbf{r})}{d\mathbf{r}^n} e^{i\mathbf{k}_0 \bullet \mathbf{r}}.$$

We may use Leibnitz' theorem for n^{th} order differentiation of a product,

$$\frac{d^n}{dx^n}[u(x)v(x)] = \sum_{k=0}^{n} \binom{n}{k} \frac{d^{n-k}}{dx^{n-k}}[u(x)] \frac{d^k}{dx^k}[v(x)], \quad \left\{ \binom{n}{k} = \frac{n!}{(n-k)!k!}, \right. \tag{7.17}$$

to obtain the following identity,

$$(-i\partial_{\mathbf{k}_0} - \mathbf{r})^n \left[\sigma_{ij}(\mathbf{r}, \mathbf{k}_0) e^{i\mathbf{k}_0 \bullet \mathbf{r}}\right] \equiv (-i)^n \frac{\partial^n \sigma_{ij}(\mathbf{r}, \mathbf{k}_0)}{\partial {\mathbf{k}_0}^n} e^{i\mathbf{k}_0 \bullet \mathbf{r}}.$$

The plasma response is then,

$$\mathbf{J}_n(\mathbf{r}) = \sum_{n=0}^{\infty} \frac{(-i)^n}{n!} \frac{\partial^n \sigma_{ij}(\mathbf{r}, \mathbf{k}_0)}{\partial {\mathbf{k}_0}^n} \bullet \frac{d^n \mathbf{E}_0(\mathbf{r})}{d\mathbf{r}^n} e^{i\mathbf{k}_0 \bullet \mathbf{r}}. \tag{7.18}$$

In the spirit of the approximation to the unknown non-local electric field in (7.16) we approximate the *local* electric field by,

$$\mathbf{E}(\mathbf{r}) = \mathbf{E}_0(\mathbf{r}) e^{i\mathbf{k}_0 \bullet \mathbf{r}}, \tag{7.19}$$

such that,

$$\mathbf{E}_0(\mathbf{r}) = \mathbf{E}(\mathbf{r}) e^{-i\mathbf{k}_0 \bullet \mathbf{r}}. \tag{7.20}$$

Leibnitz' theorem(7.17) then gives us,

$$\frac{\partial^n \mathbf{E}_0(\mathbf{r})}{\partial \mathbf{r}^n} = \sum_{k=0}^{n} \binom{n}{k} (-i\mathbf{k}_0)^k e^{-i\mathbf{k}_0 \bullet \mathbf{r}} \frac{\partial^{n-k} \mathbf{E}(\mathbf{r})}{\partial \mathbf{r}^{n-k}}.$$

Finally if we substitute this into our expression for the non-local response given by (7.18) then we obtain the following summation form for the non-local response,

$$\mathbf{J}_n(\mathbf{r}) = \sum_{n=0}^{\infty} \frac{(-i)^n}{n!} \frac{\partial^n \sigma_{ij}(\mathbf{r}, \mathbf{k}_0)}{\partial {\mathbf{k}_0}^n} \bullet \left[\sum_{k=0}^{n} \binom{n}{k} (-i\mathbf{k}_0)^k \frac{d^{n-k} \mathbf{E}(\mathbf{r})}{d\mathbf{r}^{n-k}}\right]. \tag{7.21}$$

Let us write down the non-local response to second order($n = 2$) in the corrections to the unknown electric field amplitude,

$$\begin{aligned} \mathbf{J}_2(\mathbf{r}) &= \sigma_{ij}(\mathbf{r}, \mathbf{k}_0) \bullet \mathbf{E}(\mathbf{r}) \\ &- i \frac{\partial \sigma_{ij}(\mathbf{r}, \mathbf{k}_0)}{\partial \mathbf{k}_0} \bullet \left[\frac{d\mathbf{E}(\mathbf{r})}{d\mathbf{r}} - i\mathbf{k}_0 \mathbf{E}(\mathbf{r})\right] \\ &- \frac{1}{2} \frac{\partial^2 \sigma_{ij}(\mathbf{r}, \mathbf{k}_0)}{\partial {\mathbf{k}_0}^2} \bullet \left[\frac{d^2\mathbf{E}(\mathbf{r})}{d\mathbf{r}^2} - 2i\mathbf{k}_0 \frac{d\mathbf{E}(\mathbf{r})}{d\mathbf{r}} - \mathbf{k}_0^2 \mathbf{E}(\mathbf{r})\right]. \end{aligned} \tag{7.22}$$

We see that the method provided above gives us an easy way of obtaining the non-local response of the plasma up to an n^{th} order correction of the field amplitude. In the n^{th} order we note that we recover the exact behaviour of the electric field amplitude although we are approximating its phase behaviour since we are considering only a single mode($\mathbf{k}_0$). Note also that our approximation provides the derivatives of the field as well as of the

response function. As we mentioned briefly in chapter 2 the odd-order derivatives of the electric field have been shown to be necessary for energy conservation(Swanson, 1985) and these appear naturally from this method.

An alternative view may be taken so as to retain the exact nature of the unknown non-local electric field behaviour while approximating the phase. Returning then to the exact non-local response in real space given by (7.11), we may expand the conductivity tensor in a Taylor series about a local wave-mode($\mathbf{k}_0$),

$$\sigma_{ij}(\mathbf{r},\mathbf{k}') = \sum_{n=0}^{\infty} \frac{1}{n!} (\mathbf{k}' - \mathbf{k}_0)^n \frac{\partial^n \sigma_{ij}(\mathbf{r},\mathbf{k}_0)}{\partial \mathbf{k}_0{}^n}. \tag{7.23}$$

The non-local response is then,

$$\mathbf{J}_n(\mathbf{r}) = \sum_{n=0}^{\infty} \frac{1}{(2\pi)^3 n!} \int d\mathbf{r}' \int d\mathbf{k}' (\mathbf{k}' - \mathbf{k}_0)^n e^{i\mathbf{k}'\bullet(\mathbf{r}-\mathbf{r}')} \frac{\partial^n \sigma_{ij}(\mathbf{r},\mathbf{k}_0)}{\partial \mathbf{k}_0{}^n} \bullet \mathbf{E}(\mathbf{r}').$$

If we now introduce the change of variable $\mathbf{k}_1 = \mathbf{k}' - \mathbf{k}_0$ and also associate each $i(\mathbf{k}_1 + \mathbf{k}_0)$ with an operator $\partial_{\mathbf{r}}$ by differentiating under the integral, then we are able to write the response as,

$$\mathbf{J}_n(\mathbf{r}) = \sum_{n=0}^{\infty} \frac{1}{(2\pi)^3 n!} \int d\mathbf{r}' \frac{\partial^n \sigma_{ij}(\mathbf{r},\mathbf{k}_0)}{\partial \mathbf{k}_0{}^n} \bullet [(-i\partial_{\mathbf{r}} - \mathbf{k}_0)^n \mathbf{E}(\mathbf{r}')] e^{i\mathbf{k}_0\bullet(\mathbf{r}-\mathbf{r}')} \int d\mathbf{k}_1 e^{i\mathbf{k}_1\bullet(\mathbf{r}-\mathbf{r}')}.$$

The $\mathbf{k}_1$-integral is $2\pi\delta(\mathbf{r}-\mathbf{r}')$ and again the $\mathbf{r}'$-integral may be performed in a straightforward way to give,

$$\mathbf{J}_n(\mathbf{r}) = \sum_{n=}^{\infty} \frac{1}{n!} \frac{\partial^n \sigma_{ij}(\mathbf{r},\mathbf{k}_0)}{\partial \mathbf{k}_0{}^n} \bullet [(-i\partial \mathbf{r} - \mathbf{k}_0)^n \mathbf{E}(\mathbf{r})].$$

The Binomial theorem,

$$(a+b)^n = \sum_{k=0}^{n} \binom{n}{k} a^{n-k} b^k, \quad \left\{ \binom{n}{k} = \frac{n!}{(n-k)!k!}, \right. \tag{7.24}$$

allows us to write,

$$(-i\partial_{\mathbf{r}} - \mathbf{k}_0)^n \equiv (-i)^n \sum_{k=0}^{n} \binom{n}{k} (-i\mathbf{k}_0)^k \partial_{\mathbf{r}}^{n-k} \mathbf{E}(\mathbf{r}),$$

and so the plasma response becomes,

$$\mathbf{J}_n(\mathbf{r}) = \sum_{n=0}^{\infty} \frac{(-i)^n}{n!} \frac{\partial^n \sigma_{ij}(\mathbf{r},\mathbf{k}_0)}{\partial \mathbf{k}_0{}^n} \bullet \left[\sum_{k=0}^{n} \binom{n}{k} (-i\mathbf{k}_0)^k \frac{d^{n-k}\mathbf{E}(\mathbf{r})}{d\mathbf{r}^{n-k}} \right], \tag{7.25}$$

which is equivalent to (7.21). This is a surprising result. Namely that Taylor expansion of the unknown electric field $\mathbf{E}(\mathbf{r}')$ about a local position $\mathbf{r}$ gives a non-local response $\mathbf{J}(\mathbf{r})$

identical to one obtained by a Taylor expansion of the conductivity tensor $\sigma_{ij}(\mathbf{r}, \mathbf{k}')$ about a local wave-mode($\mathbf{k}_0$). An explanation for this lies again in the spatial representation. As we are starting from a mixed space description, the dependence of the phase angle on both $\mathbf{r}$ and also on $\mathbf{k}'$ means that there will be an intrinsic symmetry between the differential forms created when we differentiate under the integral sign.

Furthermore, the non-local response is now an operator acting on the *local* electric field rather than convolution integrals over the non-local field. The non-local kernels are now embedded in the electric field operator and so the non-local response leads to ODEs rather than to IDEs. With this in mind we may use (7.25) to write the wave equation (3.1) as follows,

$$\left[\frac{c^2}{\omega^2}\nabla^2 - \frac{c^2}{\omega^2}\nabla\nabla + \delta_{ij} + \sum_{n=0}^{\infty}\frac{(-i)^n}{n!}\frac{\partial^n \chi_{ij}(\mathbf{r}, \mathbf{k}_0)}{\partial \mathbf{k}_0{}^n}\sum_{k=0}^{n}\binom{n}{k}(-i\mathbf{k}_0)^k\frac{d^{n-k}}{d\mathbf{r}^{n-k}}\right] \bullet \mathbf{E}(\mathbf{r}) = 0,$$

or, equivalently,

$$\left[\frac{c^2}{\omega^2}\nabla^2 - \frac{c^2}{\omega^2}\nabla\nabla + \delta_{ij} + \chi_{ij}^{eff}(\mathbf{r}, \mathbf{k}_0)\right] \bullet \mathbf{E}(\mathbf{r}) = 0, \tag{7.26}$$

with

$$\chi_{ij}^{eff}(\mathbf{r}, \mathbf{k}_0) \equiv \sum_{n=0}^{\infty}\frac{(-i)^n}{n!}\frac{\partial^n \chi_{ij}(\mathbf{r}, \mathbf{k}_0)}{\partial \mathbf{k}_0{}^n}\sum_{k=0}^{n}\binom{n}{k}(-i\mathbf{k}_0)^k\frac{d^{n-k}}{d\mathbf{r}^{n-k}}. \tag{7.27}$$

We note that each $i\mathbf{k}_0$ has come from a spatial derivative of the electric field reminiscent of the work of Cairns et al.(1991). We will now apply our wave equation (7.26) to a case of topical interest.

7.2.3 Reduction To ODEs

The simplest hot plasma wave-mode which our IDE can describe is the high frequency($\omega \simeq |\Omega_e|$) ordinary EM mode(O-mode) propagating perpendicularly across the ambient magnetic field, or equivalently along the direction of the magnetic field inhomogeneity, in an isotropic plasma. In this case we set $k_{\parallel} = 0$ and note that only the $\hat{\mathbf{e}}_{zz}$ element of the susceptibility tensor will couple to the O-mode electric field component $E_z(\mathbf{r})$. Furthermore, we may approximate the non-resonant sum by the cold plasma electron susceptibility $\chi_{zz}^{cold} = -\omega_{pe}^2/\omega^2$ since for high frequency waves we may neglect terms of order m_e/m_i. This may be interpreted physically as a sea of electrons intermingling an immobile ion background. In the resonant terms we retain only the contribution from the gyroresonant electrons. If we do all this then the O-mode in the vicinity of the fundamental($l = 1$) gyroresonance is described by,

$$\left(1 - \frac{\omega_{pe}^2}{\omega^2} - \frac{c^2}{\omega^2}\frac{d^2}{dx^2}\right)E_z(x) + \sum_{n=0}^{\infty}\frac{(-i)^n}{n!}\frac{\partial^n \chi_{zz}^R(x, k_0)}{\partial k_0^n}\left[\sum_{k=0}^{n}\binom{n}{k}(-ik_0)^k\frac{d^{n-k}}{dx^{n-k}}\right] \bullet E_z(x) = 0,$$

where the resonant part of the susceptibility is denoted by an R. To 2^{nd} order($n=2$),

$$\left(1-\frac{\omega_{pe}^2}{\omega^2}-\frac{c^2}{\omega^2}\frac{d^2}{dx^2}\right)E_z(x) + \left[\chi_{zz}^R(x,k_0)-k_0\frac{\partial\chi_{zz}^R(x,k_0)}{\partial k_0}+\frac{1}{2}k_0^2\frac{\partial^2\chi_{zz}^R(x,k_0)}{\partial k_0^2}\right]E_z(x) - i\left[\frac{\partial\chi_{zz}^R(x,k_0)}{\partial k_0}-k_0\frac{\partial^2\chi_{zz}^R(x,k_0)}{\partial k_0^2}\right]\frac{dE_z(x)}{dx} - \frac{1}{2}\frac{\partial^2\chi_{zz}^R(x,k_0)}{\partial k_0^2}\frac{d^2E_z(x)}{dx^2}=0. \tag{7.28}$$

The resonant susceptibility from (4.62) is given by,

$$\chi_{zz}^R(x,k_0)=\frac{iL\omega_{pe}^2}{\Omega_{0e}^2}\int_0^\infty dk_1 e^{ik_1x-\frac{1}{4}k_1^2\rho_e^2}I_1(\lambda)e^{-\lambda}, \tag{7.29}$$

with $\lambda=\frac{1}{2}k_0(k_0+k_1)\rho_e^2$. We will also require the first and second derivatives of χ_{zz}^R with respect to k_0. Noting that,

$$\frac{\partial I_1(\lambda)}{\partial k_0}=\frac{dI_1(\lambda)}{d\lambda}\left(k_0+\frac{1}{2}k_1\right)\rho_e^2,$$

then,

$$\frac{\partial\chi_{zz}^R(x,k_0)}{\partial k_0} = \frac{iL\omega_{pe}^2}{\Omega_{0e}^2}\int_0^\infty dk_1 e^{ik_1x-\frac{1}{4}k_1^2\rho_e^2} \times\left\{-\left(k_0+\frac{1}{2}k_1\right)\rho_e^2I_1(\lambda)e^{-\lambda}+\left(k_0+\frac{1}{2}k_1\right)\rho_e^2\frac{dI_1(\lambda)}{d\lambda}e^{-\lambda}\right\},$$

and,

$$\frac{\partial^2\chi_{zz}^R(x,k_0)}{\partial k_0^2} = \frac{iL\omega_{pe}^2}{\Omega_{0e}^2}\int_0^\infty dk_1 e^{ik_1x-\frac{1}{4}k_1^2\rho_e^2} \times\left\{\left[-\rho_e^2+\left(k_0+\frac{1}{2}k_1\right)^2\rho_e^4\right]I_1(\lambda)e^{-\lambda} + \left[\rho_e^2-2\left(k_0+\frac{1}{2}k_1\right)^2\rho_e^4\right]\frac{dI_1(\lambda)}{d\lambda}e^{-\lambda} + \left(k_0+\frac{1}{2}k_1\right)^2\rho_e^4\frac{d^2I_1(\lambda)}{d\lambda^2}e^{-\lambda}\right\}.$$

A first step towards a simplification of this equation is to use the recurrence relation which relates modified Bessel functions to their derivatives,

$$\frac{dI_l(\lambda)}{d\lambda}=I_{l-1}(\lambda)-\frac{l}{\lambda}I_l(\lambda). \tag{7.30}$$

We then have,

$$\frac{dI_1(\lambda)}{d\lambda} = \left(1-\frac{1}{\lambda}\right) I_1(\lambda),$$
$$\frac{d^2 I_1(\lambda)}{d\lambda^2} = \left(1-\frac{2}{\lambda}\right) I_1(\lambda).$$

Substitution of these relations into our expressions for the derivatives of the resonant susceptibilities gives,

$$\frac{\partial \chi^R_{zz}(x,k_0)}{\partial k_0} = -\frac{iL\omega^2_{pe}}{\Omega^2_{0e}} \int_0^\infty dk_1 e^{ik_1 x - \frac{1}{4}k_1^2\rho_e^2} \left[\frac{\left(k_0+\frac{1}{2}k_1\right)\rho_e^2}{\lambda}\right] I_1(\lambda) e^{-\lambda}, \quad (7.31)$$

$$\frac{\partial^2 \chi^R_{zz}(x,k_0)}{\partial k_0^2} = -\frac{iL\omega^2_{pe}}{\Omega^2_{0e}} \int_0^\infty dk_1 e^{ik_1 x - \frac{1}{4}k_1^2\rho_e^2} \left[\frac{\rho_e^2}{\lambda}\right] I_1(\lambda) e^{-\lambda}. \quad (7.32)$$

We may now write out explicitly our 2^{nd} order non-local O-mode using (7.29), (7.31) and (7.32) in (7.28),

$$\left(1-\frac{\omega^2_{pe}}{\omega^2}-\frac{c^2}{\omega^2}\frac{d^2}{dx^2}\right) E_z(x) + \frac{iL\omega^2_{pe}}{\Omega^2_{0e}} \int_0^\infty dk_1 e^{ik_1 x - \frac{1}{4}k_1^2\rho_e^2} \frac{I_1(\lambda)}{\lambda} e^{-\lambda}$$
$$\times \left[2\lambda E_z(x) + \frac{1}{2} ik_1 \rho_e^2 \frac{dE_z(x)}{dx} + \frac{\rho_e^2}{2}\frac{d^2E_z(x)}{dx^2}\right] = 0. \quad (7.33)$$

Notice the appearance of the odd-order derivative of the electric field. We would like to show how we may recover the result obtained by Cairns et al.(1991) in the limit of small gyroradius charged particles where $\lambda \ll 1$. Using λ as a small expansion parameter, we may expand the modified Bessel function to order λ,

$$\frac{I_1(\lambda)}{\lambda} e^{-\lambda} \simeq \frac{1}{2}(1-\lambda) + O\left(\lambda^2\right). \quad (7.34)$$

The O-mode equation is then,

$$\left(1-\frac{\omega^2_{pe}}{\omega^2}-\frac{c^2}{\omega^2}\frac{d^2}{dx^2}\right) E_z(x) + \frac{iL\omega^2_{pe}}{\Omega^2_{0e}} \int_0^\infty dk_1 e^{ik_1 x - \frac{1}{4}k_1^2\rho_e^2} \left[\lambda E_z(x) + \frac{1}{4} ik_1 \rho_e^2 \frac{dE_z(x)}{dx} + \frac{\rho_e^2}{4}\frac{d^2E_z(x)}{dx^2}\right] = 0.$$

Cairns et al.(1991) showed that the integral part of the response gives a plasma dispersion function(Z-function),

$$\int_0^\infty dk_1 e^{ik_1 x - \frac{1}{4}k_1^2\rho^2} = \frac{1}{i\rho} Z\left(\frac{x}{\rho}\right).$$

The wave-numbers k_0's and k_1's may then be associated with differential operators which act on the electric field and the Z-function respectively,

$$ik_0 \equiv \left(\frac{d}{dx}\right)_{E_z}$$
$$ik_1 \equiv \left(\frac{d}{dx}\right)_{Z}.$$

In accordance with this prescription we obtain the ODE,

$$\left(1-\frac{\omega_{pe}^2}{\omega^2}-\frac{c^2}{\omega^2}\frac{d^2}{dx^2}\right)E_z(x)-\frac{L\rho_e}{4}\frac{\omega_{pe}^2}{\Omega_{0e}^2}\left[\frac{d^2E_z(x)}{dx^2}Z\left(\frac{x}{\rho_e}\right)+\frac{dE_z(x)}{dx}\frac{dZ(x/\rho_e)}{dx}\right]=0,$$

which may be written in the following equivalent form for the O-mode at perpendicular incidence to the fundamental gyroresonance in a hot isotropic plasma,

$$\frac{c^2}{\omega^2}\frac{d}{dx}\left\{\left[1-\frac{L\rho_e}{4}\frac{\omega_{pe}^2}{c^2}Z\left(\frac{x}{\rho_e}\right)\right]\frac{dE_z(x)}{dx}\right\}+\left(1-\frac{\omega_{pe}^2}{\omega^2}\right)E_z(x)=0, \qquad (7.35)$$

reproducing exactly equation (44) of Cairns et al.(1991). The extra terms associated with the large gyroradius non-locality have dropped out in the limit of small gyroradius. This gives us a glimpse of how higher order corrections in the effective tensor relate to the inhomogeneity. Particles of high energy have large gyroradii and thus sample the non-local fields over an appreciable layer of the plasma and are therefore more sensitive to the effects of the inhomogeneity. Conversely, low energy particles sample locally and do not see the effects of inhomogeneity. So it is quite natural that the extra corrections due to the inhomogeneity become negligible for low energy particles. The idea of locally-uniform effects in a globally non-uniform theory crops up often in physics. As an example consider the propagation of light near a large mass. According to the general theory of relativity, a large enough mass may cause the light to refract on a global scale although locally the light is seen to propagate linearly. Such gravitational lensing is now an intrinsic part of modern cosmology and astrophysics.

7.3 The Fast Wave ODE

In chapter 1 we described how the fast wave is a suitable EM wave mode for auxiliary heating of a hot Tokamak plasma. It is accessible to the interaction regions subject only to the restraint that the plasma density be sufficiently high(which we have shown to be the case in a JET plasma). We are now in a position to use our non-local wave equation (7.26) to derive an ODE describing the fast wave.

To zeroth order our wave equation(7.26) is,

$$\frac{c^2}{\omega^2}\nabla^2\mathbf{E}(\mathbf{r})-\frac{c^2}{\omega^2}\nabla(\nabla\bullet\mathbf{E}(\mathbf{r}))+\mathbf{E}(\mathbf{r})+\chi_{ij}(\mathbf{r},\mathbf{k}_0)\bullet\mathbf{E}(\mathbf{r})=0. \qquad (7.36)$$

In the ion cyclotron range of frequencies then the electrons have effectively zero inertia in comparison to the ions and so in a characteristic time equal to a few times the inverse of the ion gyrofrequency($\simeq 10^{-8}s$), their motion along the ambient magnetic field results in an electric field due to charge separation. This field shorts out any pre-existing electric field. In our calculation we set $E_z \simeq 0$ allowing us to write down equations for the components E_x and E_y of the wave electric field due to the remaining x,y-manifold. This is most easily done as follows.

Let us assume the following WKB form for the local electric field, which is relevant to EM wave propagation in the $\hat{\mathbf{x}} - \hat{\mathbf{z}}$ plane of a tokamak, with inhomogeneity along the $\hat{\mathbf{x}}$-direction,

$$\mathbf{E}(\mathbf{r}) = \mathbf{E}_0 e^{i\int k_x(x)dx + ik_z z},$$

so that we may identify the operator,

$$\nabla \equiv \left(\frac{d}{dx}, 0, ik_z\right).$$

We may then infer the following,

$$\begin{aligned}
\left(\nabla^2 \mathbf{E}(\mathbf{r})\right)_x &= \frac{d^2 E_x(\mathbf{r})}{dx^2} - k_z^2 E_x(\mathbf{r}), \\
\left(\nabla^2 \mathbf{E}(\mathbf{r})\right)_y &= \frac{d^2 E_y(\mathbf{r})}{dx^2} - k_z^2 E_y(\mathbf{r}), \\
\nabla\left(\nabla \bullet \mathbf{E}(\mathbf{r})\right)_x &= \frac{d^2 E_x(\mathbf{r})}{dx^2}, \\
\nabla\left(\nabla \bullet \mathbf{E}(\mathbf{r})\right)_y &= 0.
\end{aligned}$$

If we recall the definitions of the dielectric tensor and also the refractive index then we have the following wave equations for the wave electric field,

$$\left(\epsilon_{xx}(\mathbf{r}, \mathbf{k}_0) - n_{\|}^2\right) E_x(\mathbf{r}) + \epsilon_{xy}(\mathbf{r}, \mathbf{k}_0) E_y(\mathbf{r}) = 0, \tag{7.37}$$

$$\left(\epsilon_{yy}(\mathbf{r}, \mathbf{k}_0) - n_{\|}^2\right) E_y(\mathbf{r}) + \frac{c^2}{\omega^2}\frac{d^2}{dx^2} E_y(\mathbf{r}) + \epsilon_{yx}(\mathbf{r}, \mathbf{k}_0) E_x(\mathbf{r}) = 0. \tag{7.38}$$

From (7.38) we obtain,

$$E_x(\mathbf{r}) = \frac{-\epsilon_{xy}(\mathbf{r}, \mathbf{k}_0)}{\left(\epsilon_{xx}(\mathbf{r}, \mathbf{k}_0) - n_{\|}^2\right)} E_y(\mathbf{r}), \tag{7.39}$$

which gives the wave polarisation relating transverse and longitudinal components of the field as described in chapter 2. We use this to substitute for E_x in (7.38) giving the following 2^{nd} order ODE for the fast wave electric field,

$$\frac{d^2}{dx^2}E_y(\mathbf{r}) + V(\mathbf{r},\mathbf{k}_0)\,E_y(\mathbf{r}) = 0, \tag{7.40}$$

whose wave potential is defined by,

$$V(\mathbf{r},\mathbf{k}_0) = \frac{\omega^2}{c^2}\{\frac{\left(\epsilon_{xx}(\mathbf{r},\mathbf{k}_0) - n_{\|}^2\right)\left(\epsilon_{yy}(\mathbf{r},\mathbf{k}_0) - n_{\|}^2\right) - \epsilon_{xy}(\mathbf{r},\mathbf{k}_0)\,\epsilon_{yx}(\mathbf{r},\mathbf{k}_0)}{\left(\epsilon_{xx}(\mathbf{r},\mathbf{k}_0) - n_{\|}^2\right)}\}. \tag{7.41}$$

V is the non-local fast wave potential which has folded into it all of the effects of plasma anisotropy and inhomogeneity. Although our neglect of the shear Alfvén wave(the zero e^- inertia approximation), means that we cannot describe the effects of this mode, our approximation does describe the effects of the mode-converted hot plasma mode(the ion hybrid wave) since the fast wave potential is inclusive of the amount of incident energy transferred to this mode. Since it is possible to assign a conservation law to ODEs of the above form, we may adequately describe the transport of energy carried by the fast wave

7.3.1 The Conservation Relation For The Fast Wave

If we neglect the propagation of the shear Alfvén wave as described in the last section we expect that the generalised IDE of (7.1) will have the following general non-local form,

$$\frac{d^2\phi(x)}{dx^2} + \int dx' G(x, x-x')\,\phi(x') = 0. \tag{7.42}$$

The complex conjugate is,

$$\frac{d^2\phi^*(x)}{dx^2} + \int dx' G^*(x, x-x')\,\phi^*(x') = 0. \tag{7.43}$$

We now follow a well understood procedure for determining the conservation equation whereby we calculate $\phi^*\times(7.42)$ $-\phi\times(7.43)$. For ease of notation let us introduce, $\phi(x) = \phi_x$ and $d\phi(x)/dx = D\phi_x$. We then obtain,

$$\phi_x^* D^2\phi_x - \phi_x D^2\phi_x + \int dx' \left[\phi_x^* G(x, x-x')\,\phi_{x'} - \phi_x G^*(x, x-x')\,\phi_{x'}^*\right] = 0.$$

The following identity for differentiation of products,

$$D(\phi_x^* D\phi_x) - D(\phi_x D\phi_x^*) = \phi_x^* D^2\phi_x - \phi_x D^2\phi_x^*,$$

then gives us the complex conservation law for our ODE,

$$D(\phi_x^* D\phi_x - \phi_x D\phi_x^*) + \int dx' \left[\phi_x^* G(x, x-x')\,\phi_{x'} - \phi_x G^*(x, x-x')\,\phi_{x'}^*\right] = 0. \tag{7.44}$$

It may be shown that,

$$Im\left\{D(\phi_x^* D\phi_x - \phi_x D\phi_x^*)\right\} = 2D\left(Im\left\{\phi_x^* D\phi_x\right\}\right),$$

and so the conservation law for the imaginary part of (7.44) is given by,

$$2D\left(Im\left\{\phi_x^* D\phi_x\right\}\right) + Im\int dx'\left[\phi_x^* G\left(x, x-x'\right)\phi_{x'} - \phi_x G^*\left(x, x-x'\right)\phi_{x'}^*\right] = 0. \quad (7.45)$$

If we integrate over all space then we may find the total power absorbed,

$$2\left[Im\left\{\phi_x^* D\phi_x\right\}\right]_{-\infty}^{\infty} + Im\int dx\int dx'\left[\phi_x^* G\left(x, x-x'\right)\phi_{x'} - \phi_x G^*\left(x, x-x'\right)\phi_{x'}^*\right] = 0,$$

and if we interchange x and x' in the second term in the integral then we find,

$$2\left[Im\left\{\phi_x^* D\phi_x\right\}\right]_{-\infty}^{\infty} + Im\int dx\int dx'\left[\phi_x^* G\left(x, x-x'\right)\phi_{x'} - \phi_x^* G^*\left(x-x', x\right)\phi_{x'}\right] = 0.$$

At this point we may introduce a new complex function,

$$H\left(x, x'\right) \equiv G\left(x, x-x'\right) - G^*\left(x-x', x\right),$$

so that,

$$2\left[Im\left\{\phi_x^* D\phi_x\right\}\right]_{-\infty}^{\infty} + Im\int dx\int dx'\left[\phi_x^* H\left(x, x'\right)\phi_{x'}\right] = 0. \quad (7.46)$$

This is the conservation relation for a general second order IDE with a non-local potential term which has the form of an integral over a kernel function. The integral part of (7.46) is the continuous analogue of the more usual quadratic form which is a common feature of such Liouville-Green ODEs.

To check this we will aim to recover the conservation relation obtained by Lashmore-Davies et al.(1993). In (7.18) we obtained an expression for our non-local response tensor. By analogy we may write,

$$G\left(x, x-x'\right) = \int dk' e^{ik'\left(x-x'\right)} G\left(x, k'\right). \quad (7.47)$$

Let us now expand the mixed form about a local wave-mode k_0 so that,

$$G\left(x, k'\right) = \sum_{n=0}^{\infty} \frac{1}{n!}\left(k'-k_0\right)^n \frac{\partial^n}{\partial k_0} G\left(x, k_0\right). \quad (7.48)$$

We follow the familiar road of replacing ik' by ∂_x allowing us to solve the k' integral which becomes a simple delta function,

$$G\left(x, x-x'\right) = \sum_{n=0}^{\infty} \frac{1}{n!}\left(-i\partial_x - k_0\right)^n \frac{\partial^n}{\partial k_0} G\left(x, k_0\right) 2\pi\delta\left(x-x'\right). \quad (7.49)$$

Substitution into (7.45) then gives,

$$2\left(Im\left\{\phi_x^*\phi_x'\right\}\right)' + Im\int dx' \sum_{n=0}^{\infty} \frac{1}{n!}\left[\phi_x^*\left(-i\partial_x - k_0\right)^n \frac{\partial^n}{\partial k_0} G\left(x,k_0\right) 2\pi\delta\left(x-x'\right)\phi_{x'}\right.$$
$$\left. - \phi_x\left(-i\partial_x - k_0\right)^n \frac{\partial^n}{\partial k_0} G^*\left(x,k_0\right) 2\pi\delta\left(x-x'\right)\phi_{x'}^*\right] = 0.$$

The delta functions may be performed and we obtain to zeroth order($n = 0$),

$$2D\left(Im\left\{\phi_x^* D\phi_x\right\}\right) + Im\left\{G\left(x,k_0\right) - G^*\left(x,k_0\right)\right\}\phi_x\phi_x^* = 0.$$

Finally, if we associate the generalised function G with the fast wave potential V and note that,

$$Im\{V - V^*\} \equiv 2Im\{V\},$$

then we find,

$$\frac{d}{dx}\left(Im\left[\phi^*(x)\frac{d\phi(x)}{dx}\right]\right) = -Im\left[V\left(x,k_0\right)\right]\left|\phi(x)\right|^2, \tag{7.50}$$

reproducing exactly the fast wave conservation relation quoted by Lashmore-Davies et al.(1993). In chapter 2 we showed how energy is distributed in the plasma. We showed that the left hand side of the above conservation law represents the time-averaged Poynting flux whereas the right hand side represents the time-averaged work done on the particles by the field. This includes the time-averaged kinetic power flux, resonant particle absorption of energy and loss of energy to another mode through linear mode conversion. The integral of the right hand side gives the absolute power absorbed by the plasma since the kinetic power flux integrates to zero across the whole plasma indicating a conservation of kinetic energy in the plasma. Since our ODE is only of second order, it describes only the fast wave and does not describe the propagation of the mode-converted mode. This means that we are unable to separate, in general, the mode converted energy from the energy absorbed by resonant particles. This limitation is not so important from a practical viewpoint since ultimately energy is transferred to the plasma.

7.3.2 Symmetrisation Of The Fast Wave Approximation

Although the generalised fast wave approximation is energy conserving it would be desirable for the response function to be even with respect to k_0 when describing EM wave propagation phenomena as EM waves may be incident on an interaction region from either side($\pm k_0$). The response function, calculated by the standard fast wave approximation, is not an even function of k_0 and therefore gives a different wave potential (V) depending upon whether or not the wave is incident from the left or the right. This is an unpleasant feature since there are then two different factors to consider. We know,

from the asymmetry of an interaction region in a plasma, that wave propagation characteristics(transmission, reflection and absorption) will also depend upon the direction of wave incidence(whether or not a wave is incident upon a resonance or a cut-off first for example). If, in addition, the wave potential, which houses the physics of the interaction region, is also direction dependent then how are we to be clear about the results? The wave potential has, embedded within it, all the relevant physical make-up of the wave-particle interactions and we seek here a form which is even with respect to the incident wave-vector.

Another motivation for symmetrising the response function is that it may offer a way of including the odd-order derivatives of the electric field without having to evaluate derivatives of the response function which are difficult to calculate numerically. A glimpse back to (7.22) reveals that odd-order derivatives of the electric field are always coupled to odd-order derivatives of the response function in the generalised fast wave theory. We present here a technique, which apart from the desirable feature of producing a plasma response which is symmetric with respect to k_0, also brings about an odd-order derivative of the electric field without the need to evaluate derivatives of the response function.

We begin with the zero-order plasma response which from (7.21) is,

$$\mathbf{J}(x) \simeq \sigma_{ij}(x, k_0) \bullet \mathbf{E}(x). \tag{7.51}$$

We may symmetrise the response function as follows. Let us define,

$$\begin{aligned} \sigma^+(k_0) &= \frac{1}{2}[\sigma(k_0) + \sigma(-k_0)] \equiv \sigma^+(-k_0), \\ \sigma^-(k_0) &= \frac{1}{2}[\sigma(k_0) - \sigma(-k_0)] \equiv -\sigma^-(-k_0). \end{aligned} \tag{7.52}$$

Therefore σ^+ is an even function with respect to k_0 while σ^- is odd. In order to obtain (7.51) we considered a local mode $\mathbf{E}(x) \simeq \mathbf{E}_0 e^{ik_0 x}$. Fourier analysis reveals that $d/dx \equiv ik_0$ and so we may write down the following plasma response in terms of a symmetrised(S) response function which is even with respect to k_0,

$$\mathbf{J}(x) \simeq \sigma^S_{ij}(x, k_0) \bullet \mathbf{E}(x), \tag{7.53}$$

where,

$$\sigma^S(x, k_0) = \sigma^+(x, k_0) + \frac{\sigma^-(x, k_0)}{ik_0}\frac{d}{dx} \equiv \sigma^S(x, -k_0). \tag{7.54}$$

This is the form of the plasma response which needs to be included in Maxwell's equations. It is the second term of this which introduces odd-order derivatives of the electric field. If we neglect electron inertia effects as we did in the last section then we have the following wave equations for the electric field,

$$\left(\epsilon^S_{xx}(x,k_0) - n_{||}^2\right) E_x(x) + \epsilon^S_{xy}(x,k_0) E_y(x) = 0, \quad (7.55)$$

$$\left(\epsilon^S_{yy}(x,k_0) - n_{||}^2\right) E_y(x) + \frac{c^2}{\omega^2}\frac{d^2}{dx^2}E_y(x) + \epsilon^S_{yx}(x,k_0) E_x(x) = 0. \quad (7.56)$$

We now use (7.56) to obtain the wave polarisation which relates E_x and E_y. This may be done by neglecting derivatives acting upon E_x such that,

$$E_x(x) = \frac{-\epsilon^+_{xy}(x,k_0)}{\left(\epsilon^+_{xx}(x,k_0) - n_{||}^2\right)} E_y(x). \quad (7.57)$$

This may be substituted into (7.56) giving the following 2^{nd} order ODE for the fast wave electric field,

$$\frac{d^2}{dx^2}E_y(x) + U(x,k_0)\frac{d}{dx}E_y(x) + V(x,k_0)E_y(x) = 0, \quad (7.58)$$

where,

$$\begin{aligned} U(x,k_0) &= \frac{1}{ik_0}\frac{\omega^2}{c^2}\left\{\epsilon^-_{yy}(x,k_0) - \frac{\epsilon^+_{xy}(x,k_0)\,\epsilon^-_{yx}(x,k_0)}{\left(\epsilon^+_{xx}(x,k_0) - n_{||}^2\right)}\right\}, \\ V(x,k_0) &= \frac{\omega^2}{c^2}\left\{\frac{\left(\epsilon^+_{xx}(x,k_0) - n_{||}^2\right)\left(\epsilon^+_{yy}(x,k_0) - n_{||}^2\right) - \epsilon^+_{xy}(x,k_0)\,\epsilon^+_{yx}(x,k_0)}{\left(\epsilon^+_{xx}(x,k_0) - n_{||}^2\right)}\right\} \end{aligned} \quad (7.59)$$

The symmetrisation procedure described above introduces an odd-order derivative into the fast wave ODE, which is an even function of k_0 and therefore describes equivalently EM waves incident from the left or from the right. Rather than derive a new conservation law for this ODE we may use a suitable integrating factor to transform it into the standard form of the fast wave ODE(7.40) having the conservation relation of (7.50). We will present some numerical solutions of the symmetrised ODE in chapter 8 for the minority heating scenario. It will be shown how this procedure dramatically improves upon the standard fast wave approximation.

In this chapter we have considered several different but connected theoretical concepts relating to solutions of the IDE. Before we move on to discuss the numerical results let us briefly recap.

Summary

The most general wave equation resulting from Maxwell's equations is the full wave IDE of (7.1) which provides the non-local, multi-mode response of the plasma in real space. This involves a double integral even for the simplest case of an isotropic plasma immersed

in a linearly inhomogeneous magnetic field as was shown in section 7.2.1.

The simplest estimate of the amount of energy absorbed from the fast wave by the plasma may be obtained by solving the local dispersion relation(7.6) associated with the Fourier transform of (7.1). In general this still contains a convolution integral and so has no ready analytic solution. Single-mode approximations, like the one used by Beskin et al.(1986) or the fast wave approximation of Kay et al.(1988) and Lashmore-Davies et al.(1988), are able to reduce the convolution integral to an algebraic function. However, as we pointed out in section 7.1, such methods are subject to the restraints of geometrical optics. Furthermore, they do not include effects due to other interacting wave modes and so cannot describe multi-mode processes such as resonant reflection or linear mode-conversion.

Motivated by the numerical difficulties encountered by Sauter et al.(1992) when solving equations like (7.1), we presented in section 7.2.2 a generalisation of the fast wave approximation which included amplitude effects. A pleasing result was that we were able to eliminate one of the integrals by sacrificing information related to the propagation characteristics of mode-converted waves. However, we were able to retain the fraction of energy mode-converted. In addition, our new result(7.21), provides the odd-order derivatives known to be necessary for energy conservation.

In section 7.2.3 we derived the 2^{nd} order fast wave approximation to the exact, electronic O-mode matched in frequency to the fundamental of the electron gyrofrequency and propagating perpendicularly through an isotropic plasma. We showed how, in the limit of small gyroradius electrons, the additional terms related to the non-local, large orbit effects dropped out giving the result obtained by Cairns et al.(1991).

In section 7.3 we presented a novel derivation of the standard fast wave, 2^{nd} order ODE(Lashmore-Davies et al., 1993) and its conservation relation starting from the more general premise of our 2^{nd} order IDE.

Recognising that the non-local response is not symmetric with respect to the direction of wave incidence, we proposed a symmetrisation procedure in section 7.3.2 which provided an odd-order field derivative in the fast wave ODE. Although we have shown that the fast wave ODE is energy conserving, in the next chapter we will see that the symmetrised form resolves a non-physical result which we obtained from the standard fast wave ODE.

Reprint Of Our Recent Large Larmor Radius Non-uniform Theory

PHYSICS OF PLASMAS

Vol. 2, No. 10, October 1995

Wave propagation through cyclotron resonance in the presence of large Larmor radius particles

R. A. Cairns, H. Holt, D. C. McDonald, and M. Taylor
School of Mathematical and Computational Sciences, University of St Andrews, St Andrews, Fife, KY16 9SS, United Kingdom

C. N. Lashmore-Davies
UKAEA Government Division (UKAEA/Euratom Fusion Association), Fusion, Culham, Abingdon Oxon, OX14 3DB, United Kingdom

pp. 3702-3710

Wave propagation through cyclotron resonance in the presence of large Larmor radius particles

R. A. Cairns, H. Holt, D. C. McDonald, and M. Taylor
School of Mathematical and Computational Sciences, University of St. Andrews, St. Andrews, Fife, KY16 9SS, United Kingdom

C. N. Lashmore-Davies
UKAEA Government Division (UKAEA/Euratom Fusion Association), Fusion, Culham, Abingdon, Oxon, OX14 3DB, United Kingdom

(Received 23 February 1995; accepted 19 June 1995)

Absorption of waves propagating across an inhomogenous magnetic field is of crucial importance for cyclotron resonance heating. When the Larmor radius of the resonant particles is small compared to the wavelength then the propagation is described by differential equations, a comparatively simple method for obtaining which has recently been given by Cairns *et al.* [Phys. Fluids B 3, 2953 (1991)]. In a fusion plasma there may, however, be a significant population of ions whose Larmor radius is not small compared to the wavelength. In this case the system is described by integro-differential equations, reflecting the fact that the plasma response at a given position is determined by the wave field over a region of width of the order of the Larmor radius. The simplified method referred to above is adapted to this case and used to obtain various forms of the equations. Methods of simplifying the equations while still retaining information from the non-local response, are discussed and some illustrated numerical results presented.

I. INTRODUCTION

Cyclotron heating of either ions or electrons is of vital importance in various schemes for heating magnetically confined plasmas. The theory of cyclotron absorption requires, as its starting point, the derivation of equations to describe the propagation of waves through a region of cyclotron resonance treating, in the simplest case, a slab geometry in which the gradient of the magnetic field strength is perpendicular to the field. A considerable number of authors have studied this problem for the case when the Larmor radius of a thermal particle is much less than the wavelength, in which case there is a local response of the plasma to the waves, in the sense that the current at a point depends only on the fields and their derivatives at that point, and the system is described by differential equations.[1–5] Some recent work by the present authors[6] has shown how these equations may be obtained in a comparatively simple way. Earlier work using a somewhat similar approach was carried out by Antonsen and Manheimer,[7] though they worked in Fourier transform space and could only obtain a tractable approximation by making an expansion which is equivalent to taking the asymptotic expansion of the plasma dispersion function. We work in real space, where it is possible to obtain much more general results. Our approach begins with the uniform plasma dielectric tensor and then recognises that, in the presence of a magnetic field gradient (with the gradient perpendicular to the direction of the field), the non-uniform response is obtained by evaluating the cyclotron frequency in the resonant denominators at the position of the particle guiding centre. This condition arises automatically in gyrokinetic theory where its importance for cyclotron resonance has been emphasised in Ref. 8. The technique has also been applied to the weakly relativistic problem, which is relevant to electron cyclotron heating.[9]

In the case of ion cyclotron heating, particularly when minority heating is being used or when hot fusion products are present, the assumption of small Larmor radius may not be valid. In this case the response of the plasma to the waves is non-local and the system is described by integro-differential equations. These have been derived by Sauter and Vaclavik[10,11] and by Brambilla.[12] Our purpose here is to show how the simple method referred to above can be used to obtain the governing equations for the large Larmor radius case more easily. The method also provides a convenient way of generating different forms of the equations. The results obtained are completely equivalent to those obtained rigorously by taking a Fourier transform of the wave problem in an inhomogeneous medium.

We then develop Wentzel–Kramers–Brillouin (WKB) and fast wave[13,14] approximations to these equations, which include the full finite Larmor radius effects in a non-uniform magnetic field, but which are computationally much simpler than the full integro-differential equations. In particular, the fast wave approximation, which reduces the problem to a second order ordinary differential equation, should be valuable in allowing simple and rapid numerical modelling of experiments in which fusion plasmas are heated by waves in the ion cyclotron range of frequencies. Some illustrative examples are given of the use of the fast wave approximation for the case of minority ion cyclotron heating.

II. DERIVATION OF THE EQUATIONS FOR A LINEAR FIELD GRADIENT

Initially we shall treat the case of a linear field gradient with $B = B_o(1 - x/L)$, since this relates to our previous work

 1070-664X/95/2(10)/3702/9/$6.00

on the small Larmor radius case and gives rather simpler equations than the more general case in which we allow arbitrary variations, in the direction perpendicular to the field, of the field strength, density and temperature. In the next section we shall discuss this general case, allowing for an arbitrary density, temperature in addition to magnetic field variation. For simplicity we shall discuss only the z-z element of the conductivity tensor, since it serves to illustrate the method. All other elements can be obtained in a similar way. We use the usual coordinate system in which the magnetic field is along the z-direction. Also, we shall consider resonance at the fundamental of the ion cyclotron frequency. Again, the basic method is easily adaptable to any harmonic.

We begin with a standard integration along orbits, for a uniform plasma, which gives

$$\sigma_{zz}=i\epsilon_o\frac{\omega_p^2}{\omega}\int uv_\perp du dv_\perp d\theta\,\frac{\partial f_0}{\partial u}J_1(b)e^{i(b\sin\theta-\theta)}\times\int_{-\infty}^{0}d\tau\,\exp\{-i\tau(\omega-k_\parallel u-\omega_c)\} \tag{1}$$

where the usual cylindrical coordinates in velocity space are being used, with u the parallel velocity, and $b=k_\perp v_\perp/\omega_c$. Now, we recognise that the part of Eq. (1) where the spatial dependence of ω_c is important is in the final resonant integral, and that we can take this into account by putting

$$\omega-\omega_c=\omega_c\left(\frac{x}{L}+\frac{v_\perp}{L\omega_c}\sin\theta\right). \tag{2}$$

Elsewhere we can simply put $\omega\approx\omega_c$. The second term in the bracket in Eq. (2) arises because, as pointed out above, we must evaluate the field at the guiding centre of the particle, not at its final position. This is the gyrokinetic effect discussed by Lashmore-Davies and Dendy.[8]

Since the variable x has already been Fourier transformed in obtaining Eq. (1), the introduction of x here should be regarded as being part of a separation into different length scales, with the $k_\perp$ corresponding to the short scale length of the waves and the x to the long scale length of the equilibrium gradient. This simple procedure gives the same result as orbit integration carried out to first order in x/L in a non-uniform field. We shall take $k_y=0$, but if $k_y\neq 0$ then the drift velocity due to the magnetic field gradient should be taken into account, since it can introduce a term of the same order as the gyrokinetic effect when $k_y\rho\gtrsim 1$ where ρ is the Larmor radius of a resonant particle.

If Eq. (2) is substituted into Eq. (1) and the variable in the τ integral changed to $k=-\omega_c\tau/L$ we obtain

$$\sigma_{zz}=-i\frac{L\omega_p^2}{\omega^2}\int uv_\perp du\,dv_\perp d\theta\,\frac{\partial f_o}{\partial u}J_1(b)e^{i(b\sin\theta-\theta)}\times\int_o^\infty dk\,\exp\left\{ikx-\frac{ikk_\parallel Lu}{\omega_c}+i\frac{kv_\perp}{\omega_c}\sin\theta\right\}.$$

Using

$$\exp\left\{i\frac{(k_\perp+k)}{\omega_c}v_\perp\sin\theta\right\}=\sum_n J_n\left(\frac{(k_\perp+k)}{\omega}v_\perp\right)e^{in\theta},$$

the integrals over velocity can be carried out in the usual way. In terms of $\sigma_{zz}(k_\perp)$, the z-component of the current coming from the z-z component of the conductivity tensor, is, in a uniform plasma,

$$J(x)=\int_{-\infty}^{\infty}dk'E(k')\sigma_{zz}(k')e^{ik'x}.$$

In the non-uniform case, we substitute the expression obtained above for σ_{zz}, depending both on $k_\perp$ and explicitly on x, in this integral to obtain

$$J(x)=\epsilon_o L\frac{\omega_p^2}{\omega^2}\int_{-\infty}^{\infty}dk'E(k')\int_0^\infty dk\times e^{i(k+k')x-(k^2\rho^2/4)-(k_\parallel^2L^2k^2\rho^2/4)}\times I_1\left(\frac{k'(k+k')\rho^2}{2}\right)\times e^{-k'(k+k')(\rho^2/2)}(1-\tfrac{1}{2}k_\parallel^2L^2k^2\rho^2). \tag{3}$$

In this equation ρ is the Larmor radius of a thermal particle, i.e. v_{th}/ω_c where the distribution function has been taken to be proportional to $\exp(-v^2/v_{th}^2)$, and E is the z-component of the electric field. If the Larmor radius is small we may expand the Bessel function and the final exponential function in power series and use the fact that

$$\int_0^\infty dke^{ikx-(k^2\rho^2/4)-(k_\parallel^2L^2k^2\rho^2/4)}=\frac{1}{i\rho(1+k_\parallel^2L^2)^{1/2}}Z\left(\frac{x}{\rho(1+k_\parallel^2L^2)^{1/2}}\right).$$

Powers of k' then produce derivatives of the electric field and powers of k derivatives of the Z function and the integral in Eq. (3) becomes a differential operator acting on E, as discussed in Ref. 6. The procedure described here is a somewhat streamlined version of that given in the earlier paper. Now, however, we wish to consider the large Larmor radius regime where such an expansion is not valid. In this regime we might expect the response of the plasma to the field to be non-local and the current to be given by a term of the form

$$J(x)=\epsilon_0L\frac{\omega_p^2}{\omega^2}\int_{-\infty}^{\infty}E(x')G(x,x')dx'=\epsilon_0L\frac{\omega_p^2}{\omega^2}\int_{-\infty}^{\infty}dk'E(k')\int_{-\infty}^{\infty}dx'e^{ik'_\perp x'}G(x,x'). \tag{4}$$

We now note that Eqs. (3) and (4) will be identical if

$$\int_{-\infty}^{\infty}G(x,x')e^{ik'x'}dx'=\int_0^\infty dk\,e^{i(k+k')x-k^2\rho^2/4-k^2k_\parallel^2L^2\rho^2/4}I_1\left(\frac{k'(k+k')\rho^2}{2}\right)\times e^{-k'(k+k')\rho^2/2}(1-\tfrac{1}{2}k^2k_\parallel^2L^2\rho^2).$$

Since the left hand side of this equation is the Fourier transform of G with respect to x', we can use the Fourier inversion theorem to obtain

$$G(x,x') = \frac{1}{2\pi}\int_{-\infty}^{\infty} dk' e^{-ik'x'} \int_0^{\infty} dk \times e^{i(k+k')x - k^2\rho^2/4 - k^2 k_\parallel^2 L^2 \rho^2/4} \times I_1\left(\frac{k'(k+k')\rho^2}{2}\right) \times e^{-k'(k+k')\rho^2/2}(1-\tfrac{1}{2}k^2 k_\parallel^2 L^2 \rho^2). \quad (5)$$

Equation (5) gives an explicit expression for $G(x,x')$, but as a double integral over an infinite half-plane it is not a very suitable form for numerical calculation or further analysis.

One way of simplifying Eq. (5) to some extent is to use the expression

$$I_1(z) = \frac{1}{\pi}\int_0^{\pi} e^{z\cos\theta}\cos\theta \, d\theta. \quad (6)$$

The integrand then involves the exponential of a quadratic in k and k'. The transformation $k' = K - \frac{1}{2}k$ switches to the principal axes of this quadratic and separates the K and k integrals. Using

$$Z(\zeta) = i\int_0^{\infty} \exp\left(ik\zeta - \frac{k^2}{4}\right)dk, \qquad Z''(\zeta) = -i\int_0^{\infty} k^2 \exp\left(ik\zeta - \frac{k^2}{4}\right)dk \quad (7)$$

we obtain

$$G(x,x') = \frac{\rho}{2^{1/2}\pi^{3/2} i}\int_0^{\pi} d\theta \cos\theta \times e^{-[(x-x')^2/2\rho^2(1-\cos\theta)]}(1-\cos\theta)^{-1/2} \times \left[\frac{1}{a} Z\left(\frac{x+x'}{a\rho}\right) + \frac{k_\parallel^2 L^2}{a^3} Z''\left(\frac{x+x'}{a\rho}\right)\right] \quad (8)$$

with

$$a = (2 + 2\cos\theta + 4k_\parallel^2 L^2)^{1/2}.$$

This reduces G to a single integral over a finite range rather than a double integral over an infinite half-plane. An alternative derivation avoiding the use of Fourier transforms is given in the Appendix.

III. GENERAL GRADIENTS

The previous section deals with linear magnetic field gradients and neglects gradients in density or temperature. Since the resonance condition is determined by the magnetic field, this approximation may be adequate for many purposes. It is, however, of interest to consider the more general case where we show that a comparatively simple calculation can give the results of Brambilla and of Vaclavik and Sauter.[10–12] Again, for the sake of illustration, we restrict our attention to the z-z element of the dielectric tensor, and begin with it in the form

$$\sigma_{zz} = -\epsilon_0 \frac{\omega_p^2}{\omega^2}\int u v_\perp du \, dv_\perp d\theta \, \frac{\partial f_0}{\partial u} \times \frac{J_1(kv_\perp/\omega_c) e^{(ikv_\perp \sin\theta/\omega_c) - i\theta}}{\omega - \omega_c - k_\parallel u}. \quad (9)$$

This is just the standard homogeneous plasma expression, with k the perpendicular wave number. As before we have separated out the resonant contribution for the fundamental resonance.

If we now suppose that the parameters have a slow x-dependence, we can regard this as a dependence on a slowly varying variable x, despite the fact that we have already Fourier transformed over the rapid x variation corresponding to the oscillations of the fields in the wave. However, we must recognise that, as before, the dependence should be on the values of the parameters at the guiding centre, not at the final position of the particle. Thus the spatial dependence comes through the magnetic field, density and temperature being evaluated at

$$x + \frac{v_\perp \sin\theta}{\omega_c}.$$

This can be done by writing

$$\sigma_{zz} = -i\epsilon_0 \int dx'' \frac{\omega_p^2}{\omega}\int u v_\perp \, du \, dv_\perp \, d\theta \, \frac{\partial f_0}{\partial u} \times \frac{J_1(kv_\perp/\omega_c) e^{ikv_\perp \sin\theta/\omega_c - i\theta}}{\omega - \omega_c - k_\parallel u} \delta\left(x'' - x - \frac{v_\perp \sin\theta}{\omega_c}\right). \quad (10)$$

In this integral the density, temperature and magnetic field, in the distribution function or elsewhere are to be taken as functions of x''. For convenience, we have taken the distribution function normalised so that its integral over velocity is one, the density variation being in the plasma frequency.

The contribution to the current from this tensor element is

$$J(x) = \int_{-\infty}^{\infty} dk e^{ikx} \sigma_{zz} E(k), \quad (11)$$

where E is the Fourier transform of the z-component of the field. Again we suppose that this current is given by a nonlocal response of the form

$$J(x) = \int_{-\infty}^{\infty} G(x,x')E(x')dx' = \int_{-\infty}^{\infty} dk \, E(k)\int_{-\infty}^{\infty} dx' \, G(x,x')e^{ikx'}. \quad (12)$$

Comparing (11) and (12) gives

$$\int_{-\infty}^{\infty} dx' \, G(x,x')e^{ikx'} = e^{ikx}\sigma_{zz}$$

and, inverting the Fourier transform, we obtain

$$G(x,x') = -\frac{i\epsilon_0}{2\pi}\int_{-\infty}^{\infty} dk e^{ik(x-x')} \int dx'' \frac{\omega_p^2}{\omega^2} \times \int u v_\perp du dv_\perp d\theta \times \frac{\partial f_0}{\partial u} \frac{J_1(kv_\perp/\omega_c) e^{ikv_\perp \sin\theta/\omega_c - i\theta}}{\omega - \omega_c - k_\parallel u} \times \delta\left(x'' - x - \frac{v_\perp \sin\theta}{\omega_c}\right). \quad (13)$$

Assuming the velocity distribution to be Maxwellian, we can carry out the integral over u, using

$$\int_{-\infty}^{\infty} du \frac{u^2}{\omega - \omega_c - k_\parallel u} e^{-u^2/v_{th}^2} = \frac{v_{th}^2}{k_\parallel} \xi(1 + \xi Z(\xi))$$

where Z is the plasma dispersion function and

$$\xi = \frac{\omega - \omega_c}{k_\parallel v_{th}}.$$

If we now use the formula

$$\delta\left(x' - x - v_\perp \frac{\sin\theta}{\omega_c}\right) = \frac{1}{2\pi}\int_{-\infty}^{\infty} e^{ik'[x' - x - (v_\perp \sin\theta/\omega_c)]} dk'$$

then Eq. (13) is found to contain a factor

$$\int_0^\infty dv_\perp \int_0^{2\pi} d\theta\, v_\perp e^{-v_\perp^2/v_{th}^2} J_1\left(\frac{kv_\perp}{\omega_c}\right) \times \exp\left[\frac{i(k-k')v_\perp}{\omega_c}\sin\theta - i\theta + ik'(x''-x)\right]$$

which can be treated by methods familiar from the derivation of the dielectric tensor in a hot uniform plasma to give

$$e^{ik'(x''-x)} I_1\left(\frac{k(k+k')v_{th}^2}{2\omega_c^2}\right) \exp\left[-\frac{k^2+(k+k')^2}{4\omega_c^2} v_{th}^2\right].$$

This still leaves infinite integrals over k and k' in the expression for G. As in the previous section it is possible to reduce these to a single integral over a finite range by again using the identity of Eq. (6).

The integrals over k and k' then become

$$\int_{-\infty}^{\infty} dk \int_{-\infty}^{\infty} dk' \exp\left\{ik'(x''-x) + ik(x-x') + \frac{k(k+k')\rho^2}{2}\cos\theta - \frac{k^2\rho^2}{4} - \frac{(k+k')^2\rho^2}{4}\right\}$$

which can be integrated using standard techniques to give the final result

$$G(x,x') = \frac{i\epsilon_0}{\pi}\int dx'' \frac{\omega_p^2}{k_\parallel v_{th}\rho^2}\xi(1+\xi Z(\xi)) \int_0^\pi d\theta \cot\theta \exp\left[-\frac{(x-x')^2(1-\cos\theta) + 4(x''-\tfrac{1}{2}x-\tfrac{1}{2}x')^2(1+\cos\theta)}{4\rho^2\sin^2\theta}\right]. \quad (14)$$

In this formula the spatial dependence of the plasma frequency, the Larmor radius ρ, etc., is to be taken into account by regarding them as the appropriate functions of x''. This result is in a form identical to that derived by Sauter and Vaclavik.[11] It is clear from the presence of the final exponential term in Eq. (14) that there is only a significant contribution from values of x, x' and x'' within a few Larmor radii of each other. It is unlikely that smoothing out density and temperature variations over such a scale length, as opposed to taking the local value, will make much difference to absorption calculations. The magnetic field, however, appears in the argument of the Z function which can vary rapidly in the vicinity of a cyclotron resonance. It is in the evaluation of ξ as a function of x'' that the important effects of inhomogeneity occur rather than in ω_p^2, v_{th} or ρ. For the linear magnetic field strength gradient study in Section II we have $\xi = \omega_c x''/Lk_\parallel v_{th}$. If the integral representation of the plasma dispersion function is used once again, the integral over x'' in Eq. (14) can then be carried out analytically and we recover the results of Section II, though it is more straightforward, as there, to introduce the linear magnetic field gradient at an earlier stage in the calculation. This calculation also demonstrates that in the limit as $k_\parallel \to 0$ there is not, as might appear from the form of Eq. (14), any singularity and that the absorption profile remains of finite width as would be expected since the gyrokinetic correction is included.[8]

IV. WKB SOLUTIONS AND REDUCTION TO DIFFERENTIAL EQUATIONS

A WKB approximation, using the integral response calculated in Section II can be obtained as follows. A convenient starting point is provided by combining Eqs. (4) and (5), showing that the plasma current is

$$J(x) = \frac{\varepsilon_0 L}{2\pi}\frac{\omega_p^2}{\omega^2}\int_{-\infty}^{\infty} dx' E(x') \int_{-\infty}^{\infty} dk' e^{-ik'x'} \times \int_0^\infty dk \exp\left\{i(k+k')x - \frac{k^2\rho^2}{4} - \frac{k_\parallel^2 L^2 k^2 \rho^2}{4}\right\} \times (1 - \tfrac{1}{2}k_\parallel^2 L^2 k^2 \rho^2) I_1\left(\frac{k'(k+k')}{2}\right) \times \exp\left\{-\frac{k'(k+k')\rho^2}{2}\right\}. \quad (15)$$

If we take $E(x) = E_0 e^{ik_0 x}$ then the integral over x' in Eq. (15) just involves

$$\int_{-\infty}^{\infty} dx' e^{i(k_o-k')x'} = 2\pi\delta(k_o-k')$$

which, in turn allows us to evaluate the k' integral and leaves us with

$$J(x) = \varepsilon_o L \frac{\omega_p^2}{\omega^2} E_o e^{ik_o x} \int_0^{\infty} dk \times \exp\left\{ ikx - \frac{k^2\rho^2}{4} - \frac{k_\parallel^2 L^2 k^2 \rho^2}{4} \right\} \times (1 - \tfrac{1}{2}k_\parallel^2 L^2 k^2 \rho^2) I_1\left(\frac{k_o(k+k_o)}{2}\right) \times \exp\left\{ -\frac{k_o(k+k_o)\rho^2}{2} \right\}. \quad (16)$$

All the dielectric tensor elements behave similarly, so we can obtain a local dispersion relation in which the coefficients are integrals, which retain the non-local response to the field, rather than the simple polynomials in k_o which would result from a differential equation. The integral of the imaginary part of k_o through the resonance region generally yields a good approximation to the wave transmission coefficient though it does not, of course, give any information on reflection or mode conversion.

A related approximation which can give the reflection coefficient, but does not separate mode conversion from cyclotron damping, is the fast wave approximation,[13,14] which is very similar to the widely used Born approximation in the theory of atomic collisions.[15] This is a perturbative method in which the unknown electric field, which occurs in the kernels of the integrals describing the resonant non-local response (the scattering terms), is approximated by a plane wave $E(x) = E_0 e^{ik_0 x}$ where the wave number k_0 is obtained from the cold plasma dispersion relation. A term of the form

$$H(k_0,x)E_0 e^{ik_0 x} \simeq H(k_0,x)E(x) \quad (17)$$

is obtained in exactly the same way as Eq. (16). The fast wave approximation consists of replacing the full integral by the terms of the form given in Eq. (17), while retaining the derivatives of E which come from the $\nabla\times(\nabla\times\mathbf{E})$ term in the wave equation. In this way a simple differential equation for the electric field is obtained, with the large Larmor radius effect included through the coefficients which are of the form of Eq. (16) and the corresponding terms of a similar nature for the other dielectric tensor elements.

Some preliminary work has been carried out on the application of this technique to minority cyclotron damping. With the usual neglect of the z-component of the electric field, the equations for the other two components become

$$\left(\frac{\omega^2}{c^2} - \frac{\omega}{c^2}\frac{\omega_{pa}^2}{\Omega_a}\left[\frac{r_1}{(r_1^2-1)} + \frac{r_2}{4}\right]\right)E_x(x) - \frac{i\omega}{c^2}\frac{L}{\rho_b}\frac{2\omega_{pb}^2}{v_{Tb}} \times K_{xx}(x)E_x(x) \frac{i\omega}{c^2}\frac{\omega_{pa}^2}{\Omega_a}\left[\frac{r_1^2}{(r_1^2-1)} + \frac{3}{4}r_2\right]E_y(x) + \frac{\omega}{c^2}\frac{L}{\Omega_b}\omega_{pb}^2 K_{xy}(x)E_y(x) = 0 \quad (18)$$

where the subscripts "a" and "b" denote the majority and minority ion species respectively,

$$K_{xx}(k_o,x) = \int_0^{\infty} e^{i\lambda x} e^{-\lambda^2\rho^2/4} e^{-(k_0+\lambda)k_0\rho^2/2} G_{xx}(k_0+\lambda,k_0)d\lambda, \quad (19)$$

$$K_{xy}(k_o,x) = \int_0^{\infty} e^{i\lambda x} e^{-\lambda^2\rho^2/4} e^{-(k_0+\lambda)k_0\rho^2/2} \times G_{xy}(k_0+\lambda,k_0)d\lambda, \quad (20)$$

and

$$G_{xx}(k,k') = \frac{1}{kk'} I_1(kk'\rho^2/2), \quad (21)$$

$$G_{xy}(k,k') = I_1'\left(\frac{kk'\rho^2}{2}\right) - \frac{k'}{k} I_1\left(\frac{kk'\rho^2}{2}\right). \quad (22)$$

We also obtain

$$-\frac{i\omega}{c^2}\frac{\omega_{pa}^2}{\Omega_a}\left[\frac{r_1^2}{(r_1^2-1)} + \frac{3}{4}r_2\right]E_x(x) + \frac{L}{\Omega_b}\frac{\omega}{c^2}\omega_{pb}^2 K_{yx}(k_o,x)E_x(x) - \left(\frac{d^2}{dx^2} + \frac{\omega}{c^2} - \frac{\omega}{c^2}\frac{\omega_{pa}^2}{\Omega_a}\left[\frac{r_1}{(r_1^2-1)} + \frac{r_2}{4}\right]\right)E_y(x) + \frac{iL}{\Omega_b}\frac{\omega}{c^2}\omega_{pb}^2 K_{yy}(k_o,x)E_y(x) = 0 \quad (23)$$

where

$$K_{yx}(k_o,x) = \int_0^{\infty} e^{i\lambda x} e^{-\lambda^2\rho^2/4} e^{-(k_0+\lambda)k_0\rho^2/2} \times G_{yx}(k_0+\lambda,k_0)d\lambda, \quad (24)$$

$$K_{yy}(k_o,x) = \int_0^{\infty} e^{i\lambda x} e^{-\lambda^2\rho^2/4} e^{-(k_0+\lambda)k_0\rho^2/4} \times G_{yy}(k_0+\lambda,k_0)d\lambda, \quad (25)$$

and

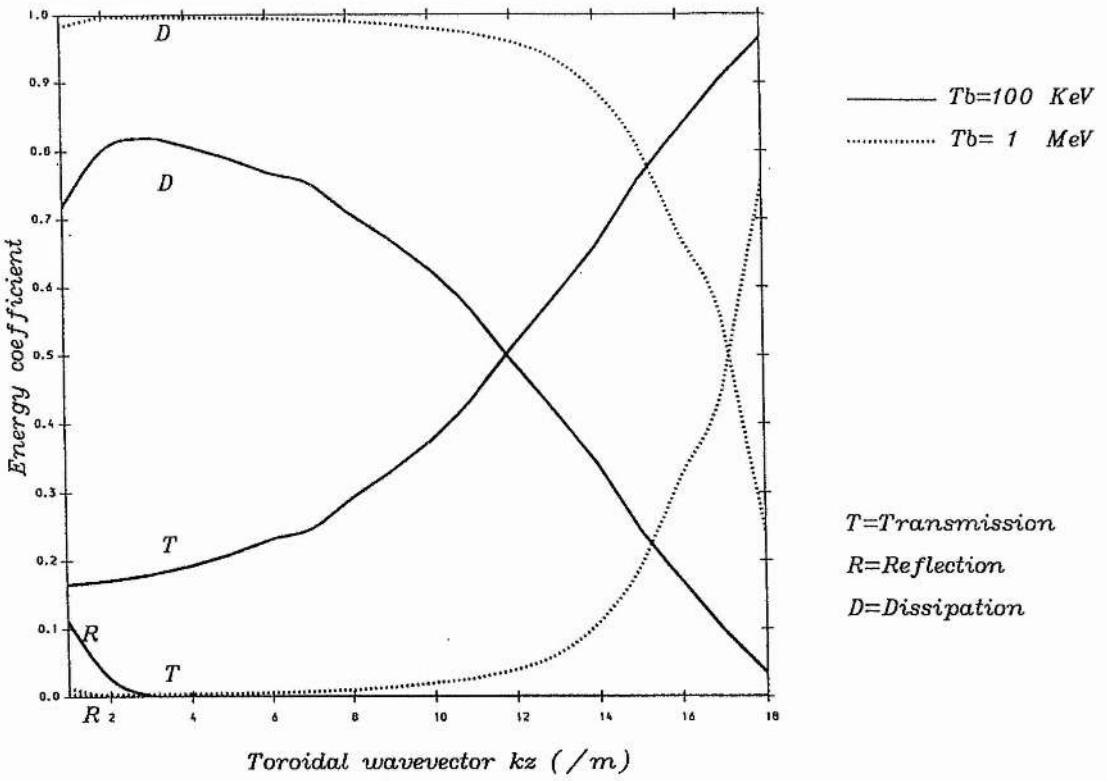

FIG. 1. Non-uniform, large Larmor radius calculation of the transmission (T), absorption (D) and reflection (R) coefficients as a function of the toroidal (parallel) wave number k_z for a fast wave incident on the helium-3 fundamental resonance from the low field side in a plasma where the majority ion species is deuterium. The plasma parameters are $n_e=5\times10^{19}$ m^{-3}, $n_{^3\mathrm{He}}/n_e=0.05$, $B_o=3.4$ T, $L=3.1$ m for helium-3 temperatures of 100 keV (solid line) and 1 MeV (dotted line).

$$G_{yx}(k,k')=I_1'\left(\frac{kk'\rho^2}{2}\right)-\frac{k}{k'}I_1\left(\frac{kk'\rho^2}{2}\right), \tag{26}$$

$$G_{yy}(k,k')=\left(2+\frac{4}{k^2k'^2\rho^4}\right)\frac{kk'\rho^2}{2}I_1\left(\frac{kk'\rho^2}{2}\right)-(k^2+k'^2)\frac{\rho^2}{2}I_1'\left(\frac{kk'\rho^2}{2}\right). \tag{27}$$

The quantities r_1 and r_2 are given by $r_1=\Omega_b/\Omega_a$, $r_2=n_{0b}Z_b/n_{0a}Z_a$ where Z_a, Z_b are the charges of the two ion species and n_{oa} and n_{ob} their equilibrium densities. The fast wave equation can now be obtained from Eqs. (18) and (23) by eliminating $E_x(x)$ in favour of $E_y(x)$, giving

$$\frac{d^2}{dx^2}E_y(x)+V(x)E_y(x)=0 \tag{28}$$

where

$$V(x)=\left[\left\{\frac{\omega^2}{c^2}-\frac{\omega}{c^2}\frac{\omega_{pa}^2}{\Omega_a}\left[\frac{r_1}{(r_1^2-1)}+\frac{r_2}{4}\right]-\frac{iL}{\Omega_b}\frac{\omega}{c^2}\omega_{pb}^2K_{yy}(k_o,x)\right\}\left\{\frac{\omega^2}{c^2}-\frac{\omega}{c^2}\frac{\omega_{pa}^2}{\Omega_a}\left[\frac{r_1}{(r_1^2-1)}+\frac{r_2}{4}\right]-\frac{i\omega}{c^2}\frac{L}{\rho_b}\frac{2\omega_{pb}^2}{v_{Tb}}K_{xx}(k_o,x)\right\}\right.$$

$$\left.+\left\{\frac{i\omega}{c^2}\frac{\omega_{pa}^2}{\Omega_a}\left[\frac{r_1^2}{(r_1^2-1)}+\frac{3}{4}r_2\right]-\frac{L}{\Omega_b}\frac{\omega}{c^2}\omega_{pb}^2K_{yx}(k_o,x)\right\}\left\{\frac{i\omega}{c^2}\frac{\omega_{pa}^2}{\Omega_a}\left[\frac{r_1^2}{(r_1^2-1)}+\frac{3}{4}r_2\right]-\frac{\omega}{c^2}\frac{L}{\Omega_b}\omega_{pb}^2K_{xy}(k_o,x)\right\}\right]$$

$$\times\left[\frac{\omega^2}{c^2}-\frac{\omega}{c^2}\frac{\omega_{pa}^2}{\Omega_a}\left[\frac{r_1}{(r_1^2-1)}+\frac{r_2}{4}\right]-\frac{i\omega}{c^2}\frac{L}{\rho_b}\frac{2\omega_{pb}^2}{v_{Tb}}K_{xx}(k_o,x)\right]^{-1}. \tag{29}$$

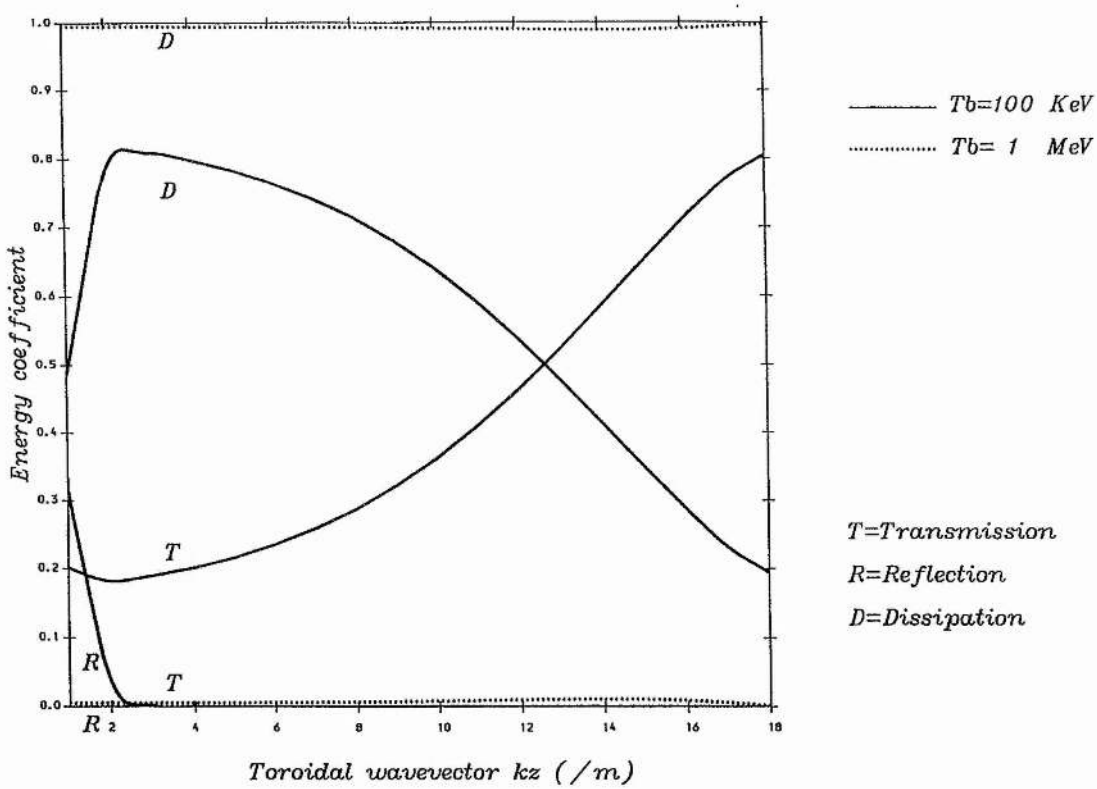

FIG. 2. Locally uniform, large Larmor radius calculation of the transmission, absorption and reflection coefficients for the same parameters as Fig. 1.

The fast wave approximation has therefore allowed us to reduce two coupled integro-differential equations to a second order differential equation. The response of the large Larmor orbit ions in the non-uniform magnetic field is contained in the fast wave potential given in Eq. (29).

We have obtained some preliminary results from a numerical solution of Eq. (28). These results are shown in Fig. 1 which refer to the case of a fast wave incident on a minority, helium-3 fundamental resonance from the low magnetic field side. The majority ion species is deuterium. Two sets of curves are shown in Fig. 1 which correspond to helium-3 temperatures of 100 keV (full line) and 1 MeV (dotted line). The other parameters specified in the calculation are an electron density of 5×10^{19} m^{-3}, a minority ion to electron density ratio of 0.05, a magnetic field of 3.4 T and a magnetic field scale length of 3.1 m.

In the case of the 100 keV minority ions, $k_\perp\rho_b\simeq0.32$ and for the 1 MeV ions, $k_\perp\rho_b\simeq1.02$ where we have taken $k_\perp\simeq\Omega_b/c_A$ giving $k_\perp\rho_b=v_{Tb}/c_A$ with b denoting helium-3. The transmission coefficient for a minority fundamental cyclotron resonance obtained from a locally uniform model with the small Larmor radius approximation yields a value which is independent of the minority temperature.[14] However, Fig. 1 shows a pronounced change in the transmission coefficient between 100 keV and 1 MeV minority ions. Also shown in Fig. 1 is the total absorption which is the sum of the energy dissipated by minority ion cyclotron damping and the energy mode converted to an ion Bernstein wave[14]. The reflection coefficient can be seen to be completely negligible for the higher temperature case and only noticeable for the lower temperature for values of $k_\parallel$ below 2 m^{-1}.

A comparison has been made between these results, obtained from the non-uniform, large Larmor radius theory and the corresponding results obtained from a locally uniform, large Larmor radius model. The results from the locally uniform model are given in Fig. 2. The curves for 100 keV are in reasonable agreement with those obtained from the non-uniform model. The main discrepancies occur for the reflection coefficient for the smaller values of $k_\parallel$ and the transmission and absorption coefficients at the larger values of $k_\parallel$. The locally uniform model predicts more reflection at the lower values of $k_\parallel$ and more absorption for the larger values of $k_\parallel$. The difference between the non-uniform and locally uniform theories is more pronounced at the higher minority ion temperature but only for values of $k_\parallel$ larger than 12 m^{-1}. Notice that the dependence of the transmission coefficient on the minority ion temperature predicted by the non-uniform theory is also given by the locally uniform model. This dependence is evidently due to the inclusion of large Larmor radius effects.

V. CONCLUSIONS

We have shown how the response of an inhomogeneous plasma, with gradients in magnetic field strength, tempera-

ture and density perpendicular to the field direction, can be obtained using a comparatively simple technique. This technique is, in fact, fully equivalent to the Fourier transform of the inhomogeneous problem. For an inhomogeneity described by a linear spatial dependence the Fourier transform can be carried out exactly. The general results of earlier workers[10–12] can be reproduced but, in Section II, we have derived equations for the special case in which the strength of the magnetic field is assumed to have a linear gradient, while other quantities are constant. Since the effect of large Larmor radius ions extends only over a few Larmor radii, we have pointed out that gradients in temperature and density are not likely to be important, but that the magnetic field gradient in the vicinity of cyclotron resonance does lead to rapid variation in the plasma response. The terms which we have calculated for this case have not, so far as we are aware, been given previously in this form. Since they involve one fewer integration than the general forms they are likely to be of some advantage for numerical computations.

We have also shown how a local dispersion relation, which still retains features of the non-local response, can be obtained and how an approach analogous to the Born approximation of scattering theory can yield differential equations in which the coefficients are modified by the non-local response. Some preliminary results of the use of this approximation to describe minority heating are described. Fuller development of the numerical work and comparison of the solutions of the differential equation with those of the full integral equation are planned for the future.

Clearly many different representations of the non-local response of a plasma containing high energy ions are possible. The methods given have provided a relatively easy way of exploring the possibilities, with a view to obtaining forms amenable to numerical calculation. The forms given in Section II for a linear magnetic field gradient include, in our view, the major physical effects of importance and are simpler than the general form used in the numerical analysis of Sauter and Vaclavik.[10] We have also suggested ways in which the problem can be further simplified, at the cost of losing some information on the division between absorbed and mode-converted power. If further study verifies that these techniques, which have been successful in the small Larmor radius regime, are of use here, then a considerable simplification will result. This will make analysis of the important problems of ion cyclotron heating in the presence of a high energy minority tail or α-particle distribution much easier. It is also of relevance to ion cyclotron emission from fusion products and other energetic ions.

ACKNOWLEDGMENTS

This work was partly supported by the U.K. Department of Trade and Industry, Euratom and by Science and Engineering Research Council Grant No. GR/H58162.

APPENDIX: CONFIGURATION-SPACE CALCULATION OF NON-LOCAL REPONSE

For a detailed solution of propagation across a resonance, the equations must be solved numerically in x-space. We have already shown, in Section II, how such equations can be derived from the k-space expressions for the conductivity tensor. Here we offer an alternative approach in which the response is calculated directly in x-space without the need to Fourier transform forwards and backwards.

As usual, we look at the simplest case—that of the ordinary wave propagating perpendicularly through the fundamental—to illustrate the technique. Solving the linearised Vlasov equation by the method of characteristics, gives us the following standard expression for the perturbed current density:

$$J_1(x)=-\frac{q^2}{m}\int d^3v\int_{-\infty}^{0}d\tau \times E_1\left(x+\frac{v_\perp}{\Omega}\{\sin(\Omega\tau-\theta)+\sin\theta\}\right)u\,\frac{\partial f_0}{\partial u}\,e^{-i\omega\tau};$$

E_1 is clearly oscillatory in $\Omega\tau-\theta$ and so we may express it in terms of a Fourier series,

$$E_1(x')=\sum_{n=-\infty}^{\infty}\langle E_1\rangle_n e^{in(\Omega\tau-\theta)}$$

where

$$\langle E_1\rangle_n=\frac{1}{2\pi}\int_0^{2\pi}d\alpha\;E_1\left(x+\frac{v_\perp}{\Omega}\{\sin\alpha+\sin\theta\}\right)e^{-in\alpha},$$

thus enabling us to express the perturbed current density, J_1, in terms of harmonics of $\Omega\tau$. For the fundamental resonance, we need only consider the first ($n=1$) harmonic of E_1, giving,

$$J_1(x)=-\frac{q^2}{2\pi m}\int d^3v\int_{-\infty}^{0}d\tau\int_0^{2\pi}d\alpha \times E_1\left(x+\frac{v_\perp}{\Omega}\{\sin\alpha+\sin\theta\}\right)\times u\,\frac{\partial f_0}{\partial u}\,e^{-i(\alpha+\theta)}e^{-i(\omega-\Omega)\tau}.$$

The gyrokinetic correction is now included by inserting,

$$\omega-\Omega=\frac{\Omega x}{L}+\frac{v_\perp}{L}\sin\theta,$$

in the final exponential, to give,

$$J_1(x)=-\frac{q^2}{2\pi m}\int d^3v\int_{-\infty}^{0}d\tau\int_0^{2\pi}d\alpha \times E_1\left(x+\frac{v_\perp}{\Omega}\{\sin\alpha+\sin\theta\}\right)\times u\,\frac{\partial f_0}{\partial u}\,e^{-i(\alpha+\theta)}e^{-i[(\Omega x/L)+(v_\perp/L)\sin\theta]\tau}.$$

The expression for J_1 now contains five integrals, two of which, u and τ, are reasonably straightforward. The v_x and v_y integrals, however, cannot be performed as they are both arguments of E_1. However, one of these integrals can be made tractable by linearly transforming the velocity coordi-

nates so that only one occurs in E_1. Noting that, $\sin\alpha+\sin\theta=2\sin\frac{1}{2}(\alpha+\theta)\cos\frac{1}{2}(\alpha-\theta)$, we may make the substitution $\alpha'=\frac{1}{2}(\theta+\alpha)$ and $\theta'=\frac{1}{2}(\theta-\alpha)$ (which in Cartesian velocity space gives us the linearly transformed velocities $V_x=v_\perp\cos\theta'$, $V_y=v_\perp\sin\theta'$ and we also take $U=u$), to give,

$$J_1(x)=-\frac{2\varepsilon_0\omega_p^2}{\pi^{5/2}v_t^5}\int d^3V\int_{-\infty}^{0}d\tau\int_0^{2\pi}d\alpha' E_1\left(x+\frac{2V_x}{\Omega}\sin\alpha'\right)$$
$$\times U^2 e^{-V^2/v_t^2}e^{-2i\theta'}$$
$$\times e^{-i[(\Omega x/L)+(V_x\sin\alpha'+V_y\cos\alpha')/L]\tau}.$$

with θ' now having the range $[-\pi,\pi]$. It should also be noted that we have taken a Maxwellian distribution, of the form $f_0=n_0\pi^{-3/2}v_t^{-3}e^{-v^2/v_t^2}$. The U integral is in the form of a gamma function and can be evaluated. The integrand of the V_y integral is quadratic, and can also be evaluated in the form of a gamma function, by completing the square with the substitution $V_y'=V_y/v_t+i\tau v_t\cos\alpha'/2L$. Performing both of these integrals, in this fashion, gives us,

$$J_1(x)=-\frac{\varepsilon_0\omega_p^2}{2\pi^{3/2}v_t}\int_{-\infty}^{\infty}dV_x\int_{-\infty}^{0}d\tau\int_0^{2\pi}d\alpha'$$
$$\times E_1\left(x+\frac{2V_x}{\Omega}\sin\alpha'\right)e^{-V_x^2/v_t^2}e^{-2i\alpha'}$$
$$\times e^{-i[(\Omega x/L)+(V_x\sin\alpha'/L)]\tau-(1/4)(v_t\cos\alpha'/L)^2\tau^2}.$$

The τ integral can also be performed by noting the identity,

$$\int_0^\infty dt\; e^{ixt-(1/4)a^2t^2}=\frac{1}{ia}Z(x/a),\quad \text{where } a>0,$$

giving,

$$J_1(x)=-\frac{i\varepsilon_0\omega_p^2L}{2\pi^{3/2}v_t^2}\int_{-\infty}^{\infty}dV_x\int_0^{2\pi}d\alpha' E_1\left(x+\frac{2V_x}{\Omega}\sin\alpha'\right)$$
$$\times e^{-V_x^2/v_t^2}e^{-2i\alpha'}|\sec\alpha'|Z\left(\frac{x+(V_x/\Omega)\sin\alpha'}{\rho|\cos\alpha'|}\right).$$

Finally, by making the change of variable $V_x=\frac{1}{2}(x-x')\Omega\ \text{cosec}\ \alpha'$ the expression for the perturbed current density becomes,

$$J_1(x)=-\frac{i\varepsilon_0\omega_p^2L}{4\pi^{3/2}\rho v_t}\int_{-\infty}^{\infty}dx'\int_0^{2\pi}d\alpha'|\text{cosec}\alpha'\sec\alpha'|e^{-2i\alpha'}$$
$$\times Z\left(\frac{x+x'}{2\rho|\cos\alpha'|}\right)\exp\left\{-\left(\frac{x-x'}{2\rho\sin\alpha'}\right)^2\right\}E(x').$$

If the change of variable $\theta=2\alpha$ is made, this becomes equivalent to the result of Eq. (7) for the case when $k_\parallel=0$.

[1]P. J. Colestock and R. J. Kashuba, Nucl. Fusion **23**, 763 (1983).
[2]D. G. Swanson, Phys. Fluids **28**, 2645 (1985).
[3]M. Brambilla, Plasma Phys. Controlled Fusion **31**, 723 (1987).
[4]H. A. Romero and J. Scharer, Nucl. Fusion **27**, 363 (1987).
[5]H. A. Romero and G. J. Morales, Phys. Fluids B **1**, 1805 (1989).
[6]R. A. Cairns, C. N. Lashmore-Davies, R. O. Dendy, B. M. Harvey, R. J. Hastie, and H. Holt, Phys. Fluids B **3**, 2953 (1991).
[7]T. M. Antonsen and W. M. Manheimer, Phys. Fluids **21**, 2295 (1978).
[8]C. N. Lashmore-Davies and R. O. Dendy, Phys Fluids B **1**, 1565 (1989).
[9]D. C. McDonald, R. A. Cairns, and C. N. Lashmore-Davies, Phys. Plasmas **1**, 842 (1994).
[10]O. Sauter and J. Vaclavik, in *Theory of Fusion Plasmas*, edited by E. Sindoni, F. Troyon, and J. Vaclavik, *Proceedings of the Joint Varenna–Lausanne International Workshop*, Varenna, 1990 (Editrice Compositori, Societá Italiana di Fisica, Bologna, 1990), p. 403.
[11]O. Sauter and J. Vaclavik, Nucl. Fusion **32**, 1455 (1992).
[12]M. Brambilla, Plasma Phys. Controlled Fusion **33**. 1029 (1991).
[13]A. Kay, R. A. Cairns, and C. N. Lashmore-Davies, Plasma Phys. Controlled Fusion **30**, 471 (1988).
[14]C. N. Lashmore-Davies, V. Fuchs, G. Francis, A. K. Ram, A. Bers, and L. Gauthier, Phys. Fluids **31**, 1614 (1988).
[15]N. F. Mott and H. S. W. Massey, *Theory of Atomic Collisions*, 3rd ed. (Oxford University Press, Oxford, 1965), p. 86.

Chapter 8

Fast Wave Numerics: Heating Of A 2-Ion Species Plasma

Our study of the propagation of the fast wave through a hot Tokamak plasma has so far been of a purely theoretical nature. Let us now solve numerically some of the equations, which we have derived and analysed only qualitatively up until now, with the aim of illustrating the various physical phenomena which we have predicted to occur.

> *When you can measure what you are speaking about, and express it in numbers, you know something about it; but when you cannot measure it, when you cannot express it in numbers, your knowledge is of a meagre and unsatisfactory kind.*
>
> *-Lord Kelvin.*

8.1 Numerical Model Of The Fast Wave

We wish to study wave-particle interactions in a 2-ion species plasma. As an example we will model the $D_1^2(He_2^3)e_{-1}^0$ JET plasma presently under experimental observation at Culham laboratory although other plasma types may be described by the theory presented in chapter 4. In the introduction to this thesis we mentioned that heating in the ICRF may be accomplished by either minority ion heating or by mode conversion heating schemes in a 2-ion species plasma. In what follows we shall consider a predominantly Hydrogen(Deuterium) plasma containing a smaller fraction of Helium ions. Such plasmas form the main constituents of many newly born stars which support themselves against gravitational collapse by the energy released from nuclear fusion reactions. Theoretical and experimental studies of such 2-ion species Tokamak plasmas, it is hoped, will provide clues to the behaviour of $D_1^2(T_1^3)e_{-1}^0$ plasmas which are likely candidates for future, large scale experiments such as ITER.

We will study the minority heating scenario for small concentrations of the minority ion species($\frac{n_{He}}{n_e} \simeq 1\%$) as well as the mode conversion heating scenario for larger concen-

trations of Helium($\frac{n_{He}}{n_e} \simeq 10\%$). Both of these schemes operate most efficiently at the fundamental of the minority gyrofrequency where the wave polarisation is most favourable. In chapter 2, we described how thermal effects are present at each and every harmonic of the gyrofrequency, but that these will provide minor corrections to the salient behaviour of a plasma which may be described by a cold plasma theory. Furthermore, we argued in chapter 5 that, since the gyroresonances are clearly resolved in a Tokamak plasma such as in JET, we need only retain the thermal effects of the resonant harmonic(which may be of the same order as the cold plasma effects from our analysis in chapter 2). By considering the orderings of various terms appearing in the response function, we showed in chapter 2 that the remaining non-resonant terms will have negligible thermal effects in comparison to the resonant term in the sum, providing a justification for keeping only those terms($l = 0, \pm 1$) which asymptotically give the cold plasma behaviour. To model the interaction with the plasma of the fast wave matched to the fundamental of the minority ion gyrofrequency, we retain only the resonant minority term in the sum in (4.62) so that the fast wave manifold of the conductivity tensor(this is the x,y-manifold for the case of zero e^- inertia) may be written as the following resonant(R) susceptibility tensor in terms of the cold plasma wavenumber k_0,

$$\begin{aligned}\chi_{ij}^{R}(x,k_0) &= \frac{iL\omega_p^2}{\Omega_0(0)^2}\int_0^\infty dk_1 e^{ik_1x-\frac{1}{4}k_1^2\rho_\perp^2\left[1+k_\parallel^2L^2\left(\frac{T_\parallel}{T_\perp}\right)\right]-\lambda} \\ &\times \begin{bmatrix} \frac{1}{\lambda}I_1A_1 & i\left[I_1'-\frac{k_0}{k_0+k_1}I_1\right]A_1 \\ -i\left[I_1'-\frac{k_0+k_1}{k_0}I_1\right]A_1 & \left[\left(2\lambda+\frac{1}{\lambda}\right)I_1-\left(2\lambda+\frac{1}{2}k_1^2\rho_\perp^2\right)I_1'\right]A_1 \end{bmatrix}, \quad (8.1)\end{aligned}$$

with,

$$\lambda = \frac{1}{2}k_0(k_0+k_1)\rho_\prime^2, \quad A_1 = 1 + ik_1L\frac{k_\parallel^2u_{T\parallel}^2}{2\Omega_0(x)^2}(1-\frac{T_\perp}{T_\parallel}).$$

The cold plasma expressions for the non-resonant cold(C) dielectric tensor elements are, from (2.6),

$$\begin{aligned}\epsilon_{xx}^C &= \epsilon_{yy}^C = 1 - \frac{\omega_{pD}^2}{\omega^2-\Omega_D^2} - \frac{\omega_{pe}^2}{\omega^2-\Omega_e^2} - \frac{\omega_{pHe^3}^2}{2\omega(\omega+\Omega_{He^3})}, \\ \epsilon_{xy}^C &= -\epsilon_{yx}^C = -\frac{i}{\omega}\left(\frac{\omega_{pD}^2\Omega_D}{\omega^2-\Omega_D^2} + \frac{\omega_{pe}^2\Omega_e}{\omega^2-\Omega_e^2} - \frac{\omega_{pHe^3}^2}{2(\omega+\Omega_{He^3})}\right). \quad (8.2)\end{aligned}$$

Note that we have only included half of the Helium-3 contribution to the non-resonant cold plasma dielectric elements. This is because the other half contribution is housed in the resonant susceptibility tensor elements of (8.1) so that,

$$\epsilon_{ij} \simeq \epsilon_{ij}^C + \chi_{ij}^R.$$

The fast wave potential defined by (7.41) for fundamental gyroresonance in a $D_1^2(He_2^3)e_{-1}^0$ plasma, written in terms of the above expressions is the most amenable form which includes all of the relevant physics. The potential contains the details of the wave-particle dynamics due to magnetic field inhomogeneity, thermal anisotropy and also due to energy-transferral to mode-converted waves. The next step is to solve the full wave equation so as to quantify the energy transport.

8.2 The Fast Wave ODE: Boundary Conditions and WKB Estimates

In the last chapter we obtained a second order ODE describing the fast wave(7.40) and in the last section we specified the wave potential. However, as a second order ODE, the fast wave wave equation requires two boundary conditions. The complex nature of the wave-particle dynamics in the interaction region of the plasma means that it will be difficult to specify accurately the waveforms at boundaries selected in this region. Instead we are guided by the well-understood behaviour of the fast wave in a cold plasma. Far from interaction regions, thermal effects will be negligible and the fast wave will resemble plane waves asymptotically. The spatial inhomogeneity of the magnetic field will inevitably lead to spatial dispersion since the fast wave dispersion relation of (2.9) is dependent upon the spatially varying gyrofrequency $\Omega_0(x)$. A more accurate representation of the fast wave is the WKB waveform,

$$\phi(x) \simeq \frac{C}{k^{1/2}(x)} e^{i\int^x k(x')dx'},$$

derived in appendix B. Fast waves incident on an interaction region with unit amplitude will have a fraction transmitted(T), a fraction reflected(R) while the remainder will be absorbed by the plasma directly or will be convected away in a mode-converted wave as we described in chapter 1. This state of affairs is sketched in figure 8.1 for fast waves incident from the low and high magnetic field sides of the Tokamak. Provided that we choose the boundaries A and B to be far enough away from the interaction region so that the fast wave is effectively only a fluid wave(a cold plasma wave independent of thermal effects), then we may write down the boundary conditions by summing the various combinations of wave modes at each boundary.

These are summed up in the following table,

Wave Incidence	Superposed Waves At A	Superposed Waves At B
High Field Side	$\phi_A = \frac{C}{k_A^{1/2}(x)}\left[e^{i\int^x k_A(x')dx'} + R\frac{C}{k_A^{1/2}(x)}e^{-i\int^x k_A(x')dx'}\right]$	$\phi_B = T\frac{C}{k_B^{1/2}(x)}e^{i\int^x k_B(x')dx'}$
Low Field Side	$\phi_A = T\frac{C}{k_A^{1/2}(x)}e^{-i\int^x k_A(x')dx'}$	$\phi_B = \frac{C}{k_B^{1/2}(x)}\left[e^{-i\int^x k_B(x')dx'} + R\frac{C}{k_B^{1/2}(x)}e^{i\int^x k_B(x')dx'}\right]$

Combinations of these boundary conditions with their derivatives(which we will denote by primes) and normalisation of the incident waves to unity gives the following set of boundary conditions in matrix form,

$$\begin{pmatrix} ik_A + \frac{k'_A}{2k_A} & 1 \\ 0 & 0 \end{pmatrix}\begin{pmatrix} \phi_A \\ \phi'_A \end{pmatrix} + \begin{pmatrix} 0 & 0 \\ ik_B - \frac{k'_B}{2k_B} & -1 \end{pmatrix}\begin{pmatrix} \phi_B \\ \phi'_B \end{pmatrix} = \begin{pmatrix} 2k_A \\ 0 \end{pmatrix}, \tag{8.3}$$

and also the following explicit expressions for the energy transport coefficients,

Wave Incidence	Transmission Coefficient$T$	Reflection Coefficient R
High Field Side	$T = \sqrt{\frac{k_B}{k_A}}\lvert\phi_B\rvert$	$R = \frac{-\left[ik_A + \frac{k'_A}{2k_A}\right]\phi_A + \phi'_A}{2k_A - \frac{ik'_A}{k_A}}$
Low Field Side	$T = \sqrt{\frac{k_A}{k_B}}\lvert\phi_A\rvert$	$R = \frac{\left[ik_B - \frac{k'_B}{2k_B}\right]\phi_B + \phi'_B}{2k_B + \frac{ik'_B}{k_B}}$

The NAG routine will supply us with the waveforms and their derivatives but we must evaluate the derivatives of the wavevectors at the end points. These are most easily estimated by a plane wave treatment. If we consider waveforms which vary as e^{ikx} then the fast wave ODE becomes simply, $k^2(x) = V(x, k_0)$. Implicit differentiation then gives,

$$k'(x) = \frac{V'(x, k_0)}{2k(x)}.$$

We calculate the derivative of the potential at a point by a simple finite difference method whereby we average the local gradients at neighbouring points. Having set up the boundary conditions let us discuss some of the intricacies of our computer code.

8.3 The Numerical Recipe And Self-Consistency

The computer code which we have written to solve the fast wave problem is structured as follows. Our code first of all sets up the physical constants pertaining to the experimental scenario in question and rescales all quantities to a relevant length and time scale which we have chosen to be the minority Larmor radius at the location of its fundamental gyroresonance at the origin and also the inverse of the minority fundamental gyrofrequency. In this way we avoid handling large numbers and the errors they incur. Next, it solves the cold plasma local dispersion relation for the fast wave (2.9) to obtain a value for the cold plasma wavenumber(k_0) which doubles as the asymptotic value of the kinetic model since thermal effects will be negligible away from interaction regions. With this value of k_0 the code steps through the interaction region evaluating the resonant integrals which are present in the conductivity tensor. The quadrature method used to solve the integrals is presented in appendix C. The integrals are constrained to meet a convergence criterion, set by the user(effectively the number of decimal places accuracy) which guarantees that a suitable(in terms of computing time) step size is used and also that there will be a sufficiently large number of data points for an accurate solution of the ODE routine. The fast wave potential is then constructed from the resonant integrals and the non-resonant cold plasma terms and its value at each radial position is stored in a data file. This data file is then read by the ODE routine which interpolates a cubic spline through the data so as to determine its functional form. The ODE solver then solves the boundary value problem using the boundary conditions (8.3) above. Values of the potential are interpolated using the cubic spline at different radial positions selected by the adaptive mesh of the ODE solver which returns an array containing the complex waveform and its derivative at different points on the mesh.

In addition to plotting the fast wave potential, the waveforms and deducing the energy transmission, reflection and inferred absorption coefficients using (8.3) above, we may also check the energy conservation relation for the fast wave presented in (7.50) which is also constructed from the waveforms and the potential. Since the integral of the right hand side of (7.50) is the total power absorbed across the integration interval(physically the slab of plasma being considered), we may compare this value with the deficit from unity of the transmitted plus reflected energy. This provides an excellent check on the self-consistency of our numerics. Indeed a fully energy-conserving system of equations should give unity when we sum the transmitted and reflected energy calculated from the ODE with the power absorbed calculated from the energy conservation law. The results of our numerical experiments presented later in this chapter bear this out beautifully indicating energy conservation to within 1%.

A further check may be made by comparing values of the transmission coefficient calculated from the fast wave potential using a WKB method with values calculated directly from solutions of the ODE. To see how to obtain a WKB estimate of the wave transmission coefficient we take the fast wave ODE of (7.40) and seek a WKB solution of the

form,

$$E_y(x) \simeq E_{0y} e^{i \int^x k(x) dx},$$

such that derivatives of the field produce wavevectors in the manner described in chapter 2. We obtain the simple dispersion relation,

$$k^2(x) = V(x, k_0).$$

We know from (7.8) that the optical depth(τ) of the interaction region is related to the imaginary part of the wavevector and we may write,

$$\tau = \int Im\{\sqrt{V(x, k_0)}\} dx.$$

The transmission coefficient(T) is then simply given by $T = e^{-2\tau}$. So we see that it is straight-forward to obtain an estimate of the transmission simply from the fast wave potential before we even solve the ODE. Furthermore we see clearly that it is the imaginary part of the potential(strictly speaking the square root of the potential) which is responsible for the absorption of energy from the EM wave. We must be clear that energy from the incident wave may be channelled into either the gyroresonant ions or to mode-converted waves and that both of these 'absorptive' effects are folded into the fast wave potential. Of course we are unable to say anything about reflection since that would require the presence of another mode which is beyond the scope of this simple WKB estimate. In the next section we will present the results of our numerical calculations. We present plots of the energy transport coefficients calculated from the ODE and also the transmission coefficient calculated from the same fast wave potential. We find excellent agreement between the ODE and WKB solutions to within 1% in all cases considered.
The fast wave ODE is to be solved as a general two-point boundary value problem with National Algorithms Library(NAG) routine *D02GBF* which uses a deferred correction technique based on an adaptive mesh. We only need to provide the ODE with values of the fast wave potential at different radial positions as well as the boundary conditions which we derived in section 8.2. The fast wave potential $V(x, k_0)$ comprises complex resonance integrals which are time consuming to solve. Rather than calculate V at each value of x used in the adaptive mesh, we calculate the potential separately for a small data set which more densely populates the regions of high curvature around the resonances. We divide the radial distance of the plasma across which we integrate the ODE into three distinctive regimes based on step size as shown in figure 8.2. In chapter 5 our statistical analysis gave us an expression (5.38) for the width of the minority gyroresonance and also the effective thermal width of the 2-ion hybrid resonance due to the minority gyroresonance (5.53). We calculate these widths in our code so that we ensure a high density of data points in these regions. Exterior to these regions we may use a much larger step size. In this way we can increase the efficiency of our code as well as providing a good data set from which to interpolate an accurate cubic spline.

Having obtained a representative data set for the fast wave potential, we fit a cubic spline to the data using NAG routine $E01BAF$. The functional form of the spline is then fed into the ODE routine so as to easily interpolate $V(x, k_0)$ on its adaptive mesh. Due to the highly peaked nature of the potential, particularly around the 2-ion hybrid resonance, we tested the spline routine on an exponential function as shown in figure 8.4. Although this function is not as taxing as our potential, the agreement is excellent even as the exponential function becomes more and more steep at large values of the exponent. This technique using cubic splines was found to accelerate the running of the code.

Let us now look at the results of a series of numerical experiments which were performed to investigate both minority heating and mode-conversion heating scenarios.

8.4 Numerical Experiments

We present here a representative selection of results for a Maxwellian plasma equilibrium subjected to a variety of experimental conditions. We will compare our new nonuniform theory with the existing locally-uniform theory(which we will refer to as uniform theory) presently in use on computer support software at JET. In particular, we will consider the effects of the direction of launch of the fast waves into the plasma either from the high or low magnetic field side. In addition to absorption of energy(which is our primary aim) this will also provide details of the accessibility and mechanisms of the various heating channels. We will see that an unexpected new result from nonuniform theory predicts strong reflection from the low field side of the minority gyroresonance for a plasma containing a high density(20%) of energetic minority ions($0.66MeV$). This may have serious consequences for the accessibility of the minority gyroresonance from the low field side.

8.4.1 Results For The Minority Heating Scheme

In this subsection we present results relevant to small proportions of Helium-3 ions in a reservoir of Deuterium. Our analysis will be restricted to minority density ratios($\frac{n_{He^3}}{n_e}$) less than 10% although pure minority heating is only observed less than about 1%.

Figure 8.5 indicates quite clearly an excellent($\pm 1\%$) agreement between the transmission curves for both the different theories and also for different directions of incidence. Uniform theory appears to overpredict absorption by up to $15 \pm 2\%$ for perpendicular incidence though this discrepancy is rapidly washed out by the effects of Doppler broadening when the toroidal wavevector $\geq 1m^{-1}$. Absorption by the resonant ions falls off with wavevector since it depends critically upon the number of ions in corotation with the left-handed electric fields as we saw in our discussion of wave polarisation in chapter 2. The increased parallel motion due to EM field components along the toroidal direction means that fewer ions are in coresonance(they will in general be moving transiently into

and out of resonance) and so absorption is reduced. The broadening of the gyroresonace also means that it may partially overlap the 2-ion hybrid resonance smoothing its singular profile and hence reducing its reflectivity. Energy conservation then dictates that we see an increasing trend in the transmission. Note also the value of the total energy conservation calculated from the sum of the transmission, the reflection and the integral of the power absorbed from the fast wave potential. We have apparently perfect energy conservation. This will be seen to be the case in every case studied within at most $\pm 1\%$.

In figure 8.6 we consider the effect of having more minority ions present. The result is a drastic difference in predicted absorption by uniform theory over nonuniform theory up to $68 \pm 2\%$ for strongest Doppler broadening. Agreement is generally good between the directions of incidence and, in the JET range of operation of the low field antennae($2 \rightarrow 7m^{-1}$), the two theories are not easily discernible within 2%. However this result is one in support of the need to use the more complex nonuniform theory for larger, future devices like ITER which may launch fast waves with higher toroidal wavenumbers. Since it is the minority ions which are in gyroresonance, it is also they who are responsible for nonlocal effects. The more minority ions which are present, the more strongly will the nonuniform and uniform theories disagree since uniform theory does not adequately take into account nonlocal effects. There is an upper limit to this argument due to the appearance of the 2-ion hybrid resonance at high minority densities which affects the wave polarisation in the gyroresonance region.

Figure 8.7 illustrates another concept. The discrepancy of about $15 \pm 2\%$ between theories for perpendicular incidence is also temperature dependent. At high temperatures the discrepancy is as quoted above but for lower minority temperatures the discrepancy reaches a maximum of $42 \pm 2\%$ at T_{He^3}, tailing off at both higher and lower temperatures. For this particular scenario of a 1% density ratio the effect of nonlocality is greatest at $400 \pm 20KeV$. Why does this deviate from the view that at higher temperatures, the minority gyroradii are longer and therefore more nonlocal and consequently more absorptive? Could it be that rather than be deposited on the resonant ions, energy is channeled elsewhere? Perhaps to cyclotron harmonic waves? This requires further investigation in the future.

Figures 8.8 and 8.9 show the expected single absorption peak at the minority gyroresonance for both theories as well as the expected absorption of the waves at the gyroresonace over a scalelength in direct proportion to the width of the imaginary part of the potential which we know(from our investigation of the energy conservation law) to be responsible for power absorption. In addition to the small difference in the degree of absorption between the theories, the most notable feature is the degree of reflection of the wave power(described by $|E_y|$) which is estimated to be about $30 \pm 5\%$. The standing wave pattern on the low field side is due to the superposition of the incident and reflected fast wave. Reflection is due to the cutoff effect described in chapter 1. The absence of this for high field incidence suggests that wave energy is absorbed by the minority resonant

ions or may be channeled to another unidentified wave mode at the gyroresonace such as a cyclotron harmonic wave. Why the power should have a sinusoidal component is easy to demonstrate. If the superposed waves have the general form,

$$\phi(x) = ae^{ikx} + be^{-ikx},$$

then,

$$\begin{aligned} |\phi(x)^2| &= (ae^{ikx} + be^{-ikx})(a^*e^{-ikx} + b^*e^{ikx}) \\ &= |a|^2 + |b|^2 + ab^*e^{2ikx} + a^*be^{-2ikx}. \end{aligned}$$

The final two terms are oscillatory and we see that the intensity has a sinusoidal component. Furthermore, since the power absorbed(P) is equal to,

$$P(x) = -\int_{-\Delta}^{\Delta} ImV(x, k_0)|\phi(x)|^2 dx$$

then this too will have a sinusoidal component. This brief analysis also yields another idea. The expression above for the power absorbed is sensitive to the sign and magnitude of the imaginary part of the potential and so we are also able to explain the $10 \pm 2\%$ increase in the wave amplitude just before and just after the gyroresonance. This may be traced back to the negative value of the imaginary part of the potential either side of the gyroresonance absorption peak at the origin. This fits in well with the absence of this effect with uniform theory. It appears that only a nonuniform theory is able to produce regions in the plasma where energy flows back from the particles to the wave field. This may be some direct evidence for a definite wave growth event. Integrated over the whole plasma cross-section this effect disappears suggesting that it is in fact a flux of acoustic energy being redistributed around the plasma. This fits in well with negative regions of the absorption coefficient identified by McDonald et al.(1994). The increased reflection with nonuniform theory is presumably due to nonlocal effects. This too requires further study.

Figures 8.10, 8.11 and 8.12 illustrate the transition from predominantly minority heating to predominantly mode conversion heating schemes at high energy and perpendicular incidence as the density of the minority ion is increased. Again there is excellent transmission agreement within $\pm 2\%$. The two theories are indistinguishable for high field incidence but are dramatically different for low field incidence suggesting that the key factor is the development of the cutoff effect with density. In fact we obtained reflection coefficients substantially greater than unity with nonuniform theory whereas uniform theory was well-behaved with little or no reflection. How are we to account for this dramatic(and perhaps theoretically catastrophic) result? We are considering a Maxwellian plasma which has no source of free energy and so we do not expect such unstable behaviour. A logical stance would be to rule out the possibility of an instability. The plots of the waveforms in figures 8.11 and 8.12 echo the energy coefficient values and little is to be learned of the mechanism

from these. However, the fast wave potential is very revealing. The imaginary parts are not widely different and result in almost total absorption at this high minority density. The real part of the fast wave potential, calculated from uniform theory has a single zero crossing which is the standard 2-ion hybrid cutoff. However, nonuniform theory has an additional two cutoffs! One on either side of the minority gyroresonance. Nonlocality has had a dramatic effect on the wave-particle dynamics in this case. I have not come across additional cutoffs in the vicinity of the 2-ion hybrid resonance in the literature and so I am led to believe this is either a real physical effect or is a result of the fast wave approximation being invalidated. This is still to be verified. If it is a real effect then presumably it is a high order finite Larmor radius effect(at least second order as I am unaware of any first order predictions of additional cutoffs). We will see, in the next subsection, that this behaviour is also to be found at much lower minority temperatures($T_{He^3} > 100 \pm 50 KeV$) provided we still have a high minority ion density($\simeq 10\%$). Another interesting point is that we still have excellent power conservation despite the anomalous reflections. We shall show, in the next section, that the symmetric form of the conductivity tensor appears to resolve this difficulty.

Before moving on to look at predominant mode conversion heating, let us consider the effect of Doppler broadening upon this startling effect. For toroidal wavenumbers as small as $kz \simeq 2m^{-1}$, figures 8.13, 8.14 and 8.15 give equivalent results to within $\simeq \pm 2\%$. The wave is smoothly absorbed over a region of some 20 ion Larmor radii with a hint of evidence for group velocity effects with nonuniform theory(although this is hardly visible). The additional cutoffs are absent suggesting that they have their origins in gyrokinetic effects which are swamped by Doppler effects. This provides a shred of evidence that it is indeed the non.local nature of the variation of the magnetic field across the Larmor orbits which is the crucial determining factor at perpendicular incidence, echoing the original claims of Lashmore-Davies and Dendy(1989). An interesting point here is that there appears to be no sinusoidal component to the power absorption. This is attributable to the broadness of the resonance meaning that even these oscillations are critically damped.

8.4.2 Results For The Mode Conversion Scheme

In this subsection we present results relevant to much higher proportions of Helium-3 ions in the Deuterium reservoir. Our analysis will be restricted to minority density ratios($\frac{n_{He^3}}{n_e}$) not less than 5% so that the 2-ion hybrid resonance is not excluded and not more than 20% so that we can observe both resonances.

To dive in at the deep end, let us begin with a critical case. Figures 8.16 through 8.20 consider the controversial high minority density case at perpendicular incidence. It is clear that, although the high field incidence results are well-behaved as was found in figure 8.10, the low field results are divided by the cutoff effect. Reflection again soars above unity at minority temperatures in excess of $100 \pm 50 KeV$ with nonuniform theory but not with, uniform theory. Again, even in this case, we have excellent power conservation.

In figures 8.17 through 8.20, we see that uniform theory still provides only the 2-ion hybrid cutoff even at extreme temperatures of $1.11MeV$ whereas nonuniform theory again reveals multiple cutoffs one on each side of the minority gyroresonance.

The introduction of Doppler broadening with a small toroidal wavenumber($2m^{-1}$) again removes the additional cutoff effects for the possible reasons provided in the discussion of figures 8.13 through 8.15. The asymmetry between low and high field incidence seems to be attributable to the skew of the absorption curve(the imaginary part of the potential) towards the high field side in contrast to the almost perfect symmetry of the potential in figures 8.14 and 8.15. This hypothesis must again be tested.

The occurance of these puzzling effects delayed a study of the effects of thermal anisotropy upon the wave-particle dynamics. The problem is that an anisotropic equilibrium, like the bi-Maxwellian one considered in chapter 4, does have a source of free energy available and, as such, may lead to physically acceptable instabilities. How are we to resolve between genuine instabilities and spurious results due to a possible problem with the fast wave approximation which gives reflections greater than unity for a Maxwellian! In the light of this dilemma and time restrictions, we opted to study only isotropic plasmas with the hope of sorting out the problem of anomalous reflection.

We went back to the drawing board feeling that our fast wave approximation was being violated for some reason. Alan Cairns suggested that there could be a source of the problem in the lack of symmetry of the conductivity tensor with respect to the direction of the incident wavevector. This is not an unfamiliar difficulty(see for example Lashmore-Davies et al., 1993). So it was suggested that we try to somehow symmetrise our conductivity tensor while at the same time trying to validate the fast wave approximation which reduces with ease the order of the exact fourth order IDE problem. We present the preliminary results of our findings in the next section.

8.5 Hope For The Future: The Symmetrised Fast Wave ODE

In chapter 7 we presented two alternative ways of extending the fast wave approximation to introduce additional odd order field derivatives into the fast wave ODE. The generalised fast wave approximation of chapter 7, while succeeding in this goal, adds complexity to the numerics since it is necessary to evaluate derivatives of the conductivity tensor as well as the wave field. Fortunately, the symmetrisation procedure at the end of chapter 7 does not complicate matters much. We have solved the symmetrised fast wave ODE for the most pertinent case of high energy($0.66MeV$), high density($\frac{n_{He^3}}{n_e} = 20\%$) minority ions in a plasma illuminated by perpendicularly propagating fast waves.

Figure 8.24 presents our preliminary findings for the symmetrised nonuniform theory.

We have excellent energy conservation and the reflection coefficient is well-behaved. The real part of the symmetrised fast wave potential(V) shows the characteristic high density cutoffs around the fundamental gyroresonance. They are also present in the first order symmetrised potential(U). The fast waves are seen to be partially transmitted through the minority gyroresonance region despite the multitude of cutoffs before being wholly absorbed at the 2-ion hybrid resonance. The behaviour of the reflection coefficient may be explained as follows. At very low minority temperatures, the ion Larmor radius is insufficiently large to influence the minority gyroresonance. Increasing the temperature simply has the effect that there are more ions contributing to gyroresonance owing to their large Larmor radii overlapping the gyroresonance layer. There is increased absorption taking place over a broader plasma profile. Again, the overlap of the broad gyroresonance with the 2-ion hybrid resonance means that it will become less singular and will have a smaller reflectivity. At a temperature of about $350 \pm 20 KeV$ we have the creation of the additional cutoffs which then result in increased reflection from the low field side which becomes stronger as the cutoffs become more predominant.

All in all there is a possibility that the symmetrisation procedure has solved the problems previously encountered with the fast wave approximation. This will require further trials and tests.

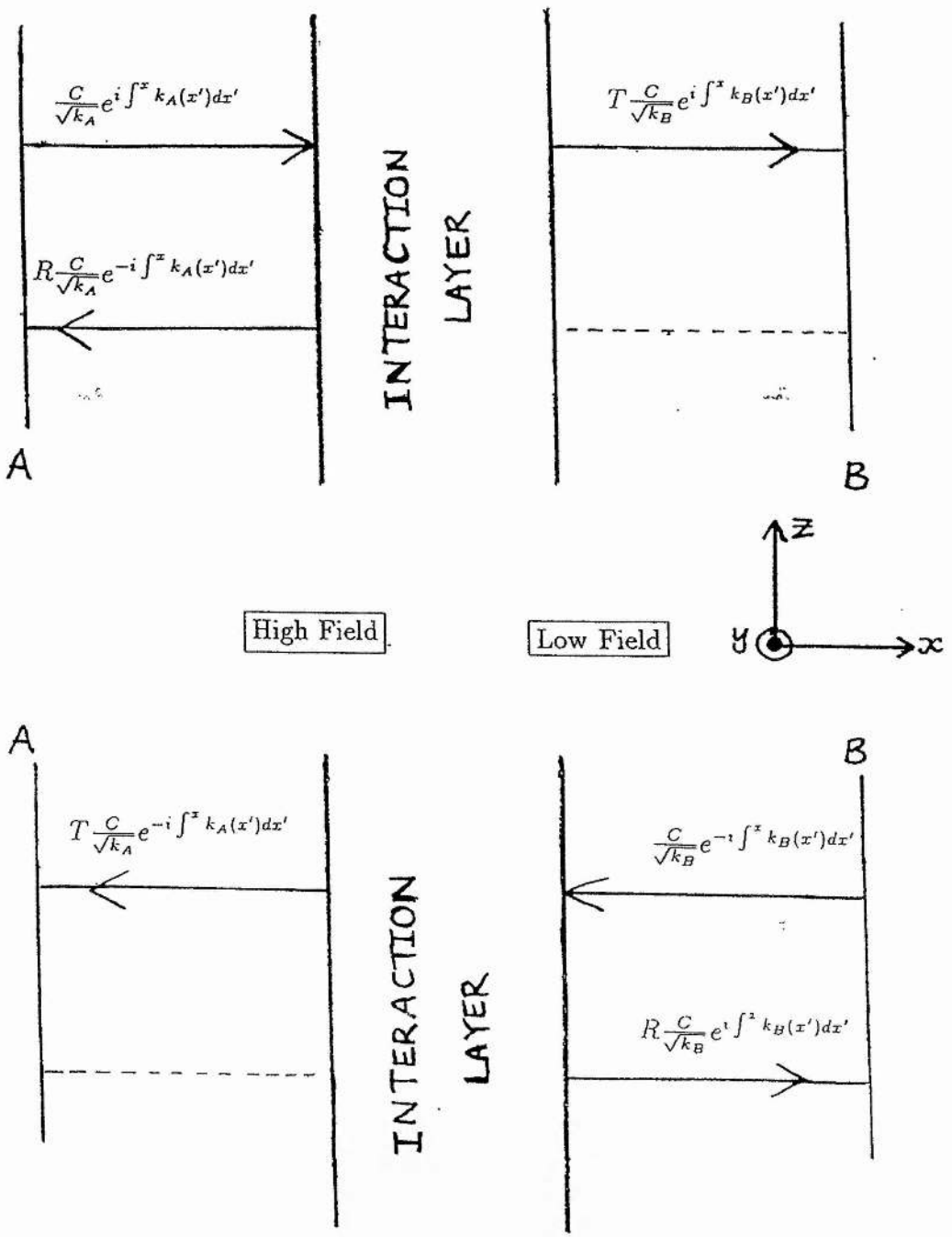

Figure 8.1: A schematic diagram of EM wave interaction with a plasma interaction region for both high(top) and low(bottom) magnetic field incidence. Asymptotically the waves are assumed to have WKB forms and a dotted line indicates a null boundary condition at A or B. The energy transport coefficients are the reflection(R) and transmission(T) in the direction of the wavevector($\pm k$) normalised by a constant(C).

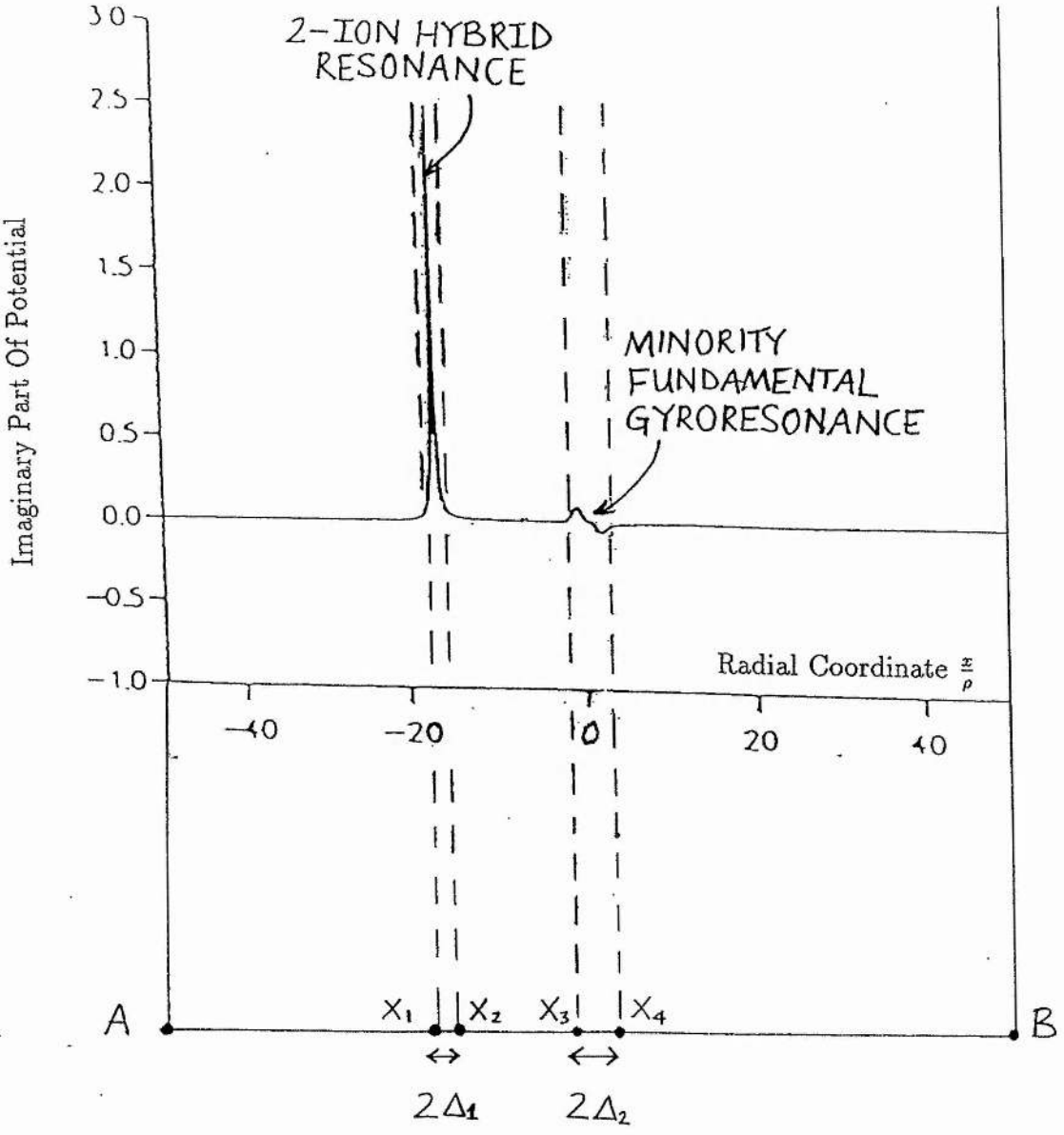

Figure 8.2: A schematic diagram of the integration mesh intervals. Here, Δ_1 and Δ_2 are the thermal widths of the 2-ion hybrid resonance and the minority fundamental gyroresonance respectively.

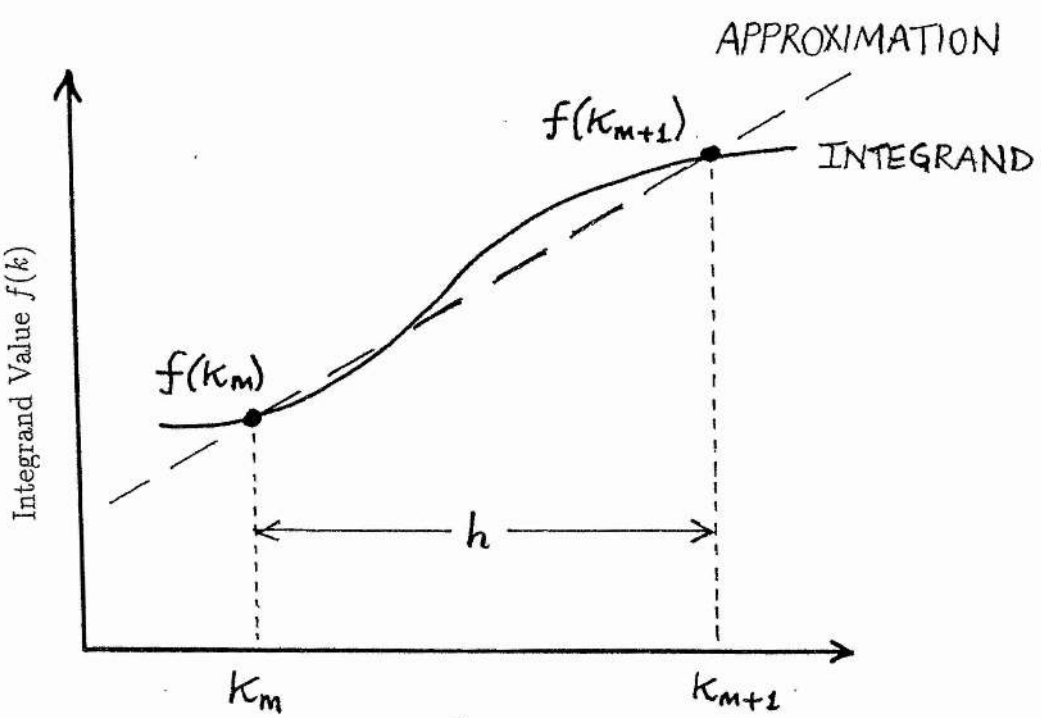

Figure 8.3: A test function and piecewise linear approximation.

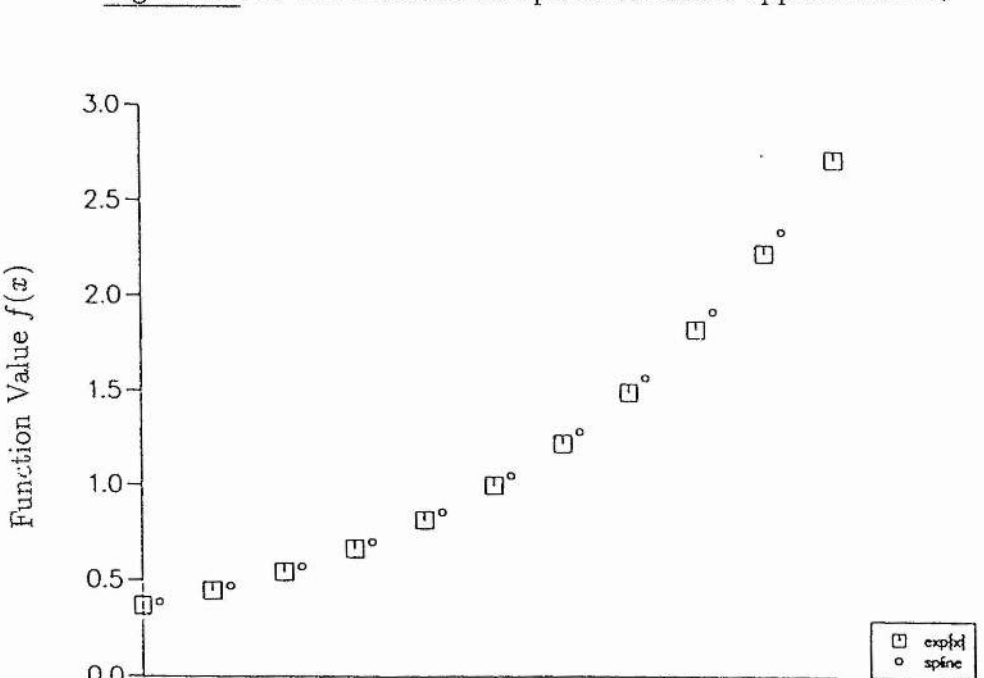

Figure 8.4: A test function and its cubic spline fit.

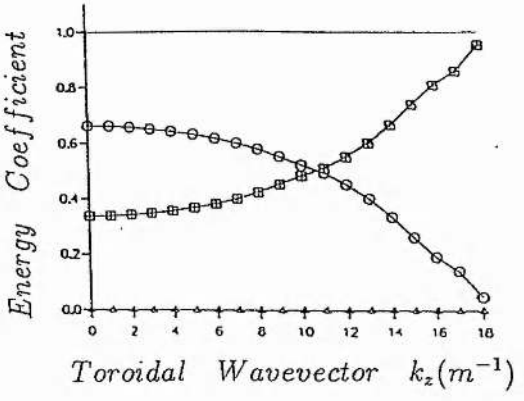

Figure 8.5a: Energy transport as a function of toroidal wavenumber(k_z) for high energy($T_{He^3} = 1MeV$) minority heating($\frac{n_{He^3}}{n_e} = 1\%$), calculated from non-uniform theory with EM waves incident from the high magnetic field side.

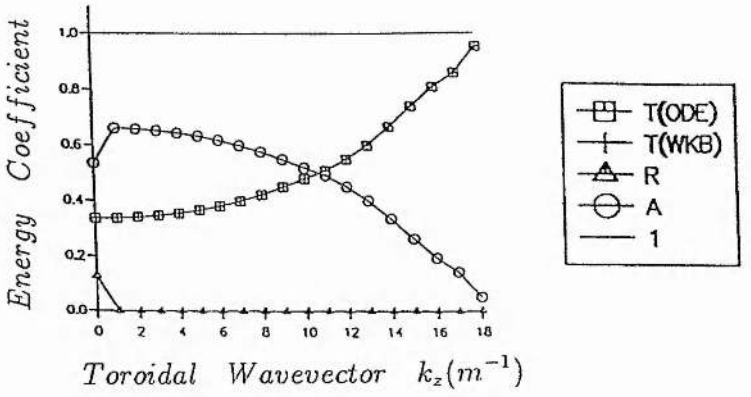

Figure 8.5b: Energy transport as a function of toroidal wavenumber(k_z) for high energy($T_{He^3} = 1MeV$) minority heating($\frac{n_{He^3}}{n_e} = 1\%$), calculated from non-uniform theory with EM waves incident from the low magnetic field side.

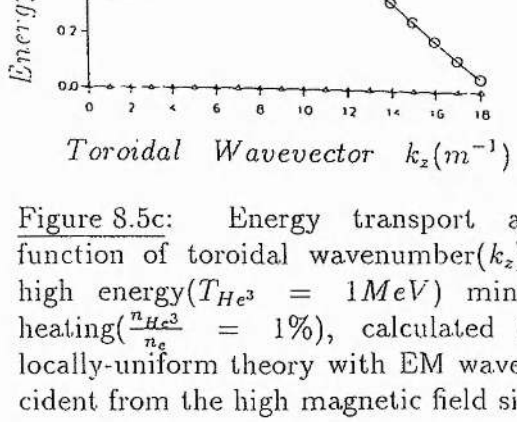

Figure 8.5c: Energy transport as a function of toroidal wavenumber(k_z) for high energy($T_{He^3} = 1MeV$) minority heating($\frac{n_{He^3}}{n_e} = 1\%$), calculated from locally-uniform theory with EM waves incident from the high magnetic field side.

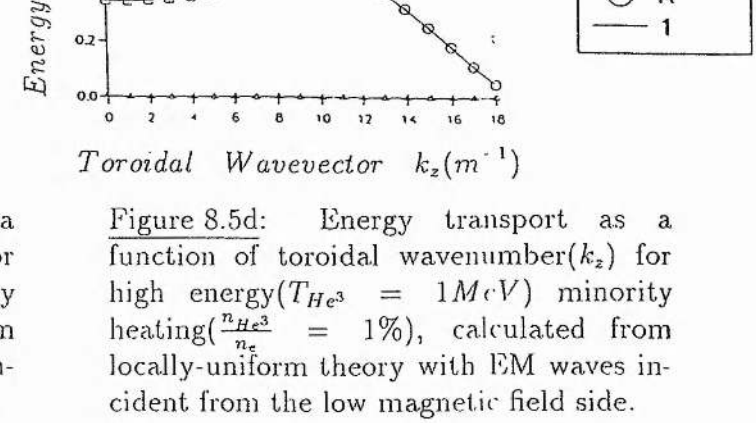

Figure 8.5d: Energy transport as a function of toroidal wavenumber(k_z) for high energy($T_{He^3} = 1MeV$) minority heating($\frac{n_{He^3}}{n_e} = 1\%$), calculated from locally-uniform theory with EM waves incident from the low magnetic field side.

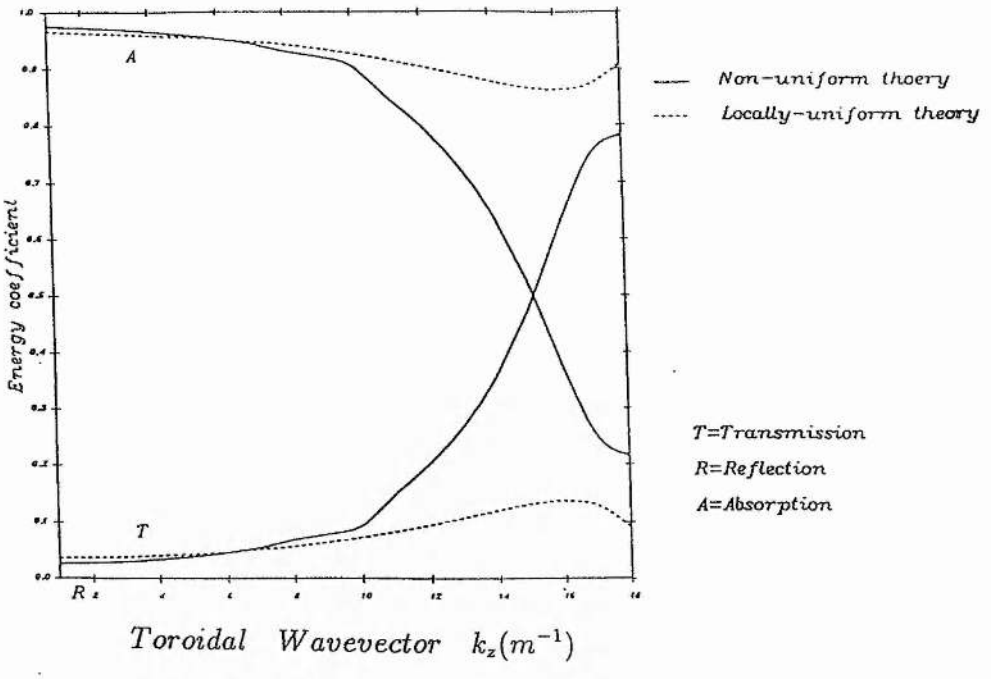

Figure 8.6a: Energy transport as a function of toroidal wavenumber(k_z) for high energy($T_{He^3} = 0.5MeV$) heating($\frac{n_{He^3}}{n_e} = 5\%$), calculated from non-uniform and locally-uniform theories with EM waves incident from the high magnetic field side.

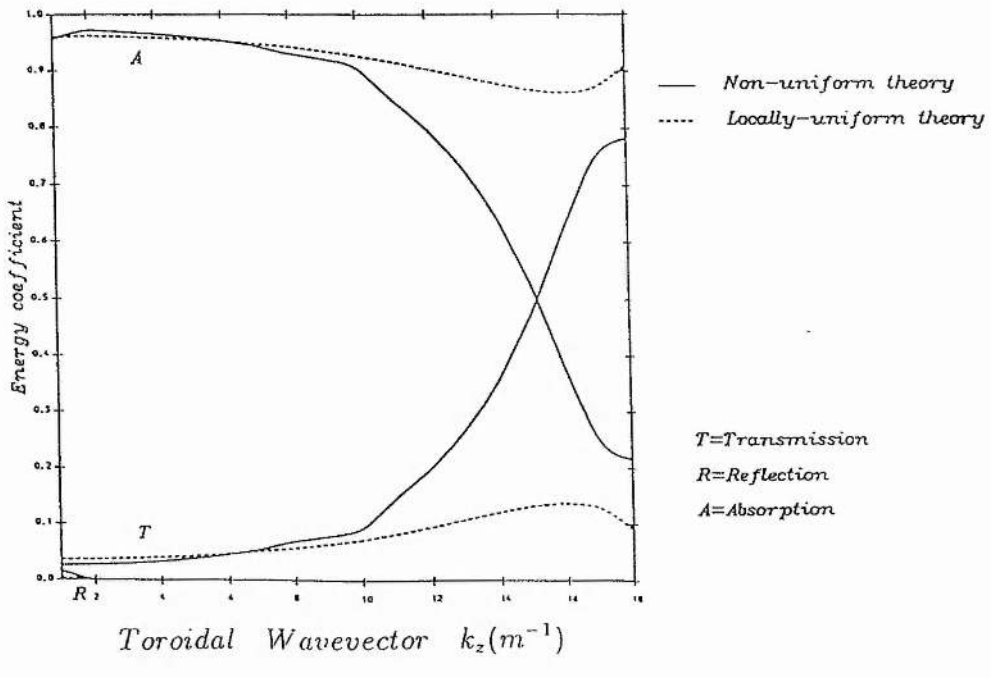

Figure 8.6b: Energy transport as a function of toroidal wavenumber(k_z) for high energy($T_{He^3} = 0.5MeV$) heating($\frac{n_{He^3}}{n_e} = 5\%$), calculated from non-uniform and locally-uniform theories with EM waves incident from the low magnetic field side.

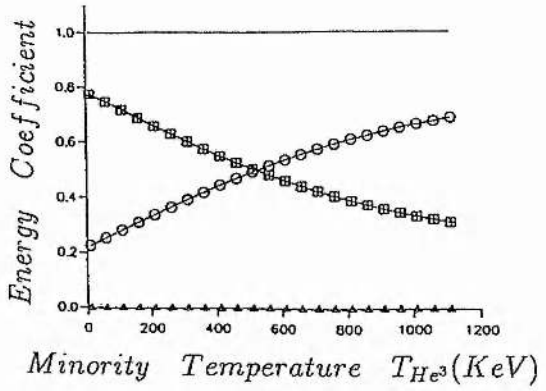

Figure 8.7a: Energy transport as a function of minority temperature(T_{He^3}) for minority heating($\frac{n_{He^3}}{n_e} = 1\%$) at perpendicular incidence($k_z = 0$), calculated from non-uniform theory with EM waves incident from the high magnetic field side.

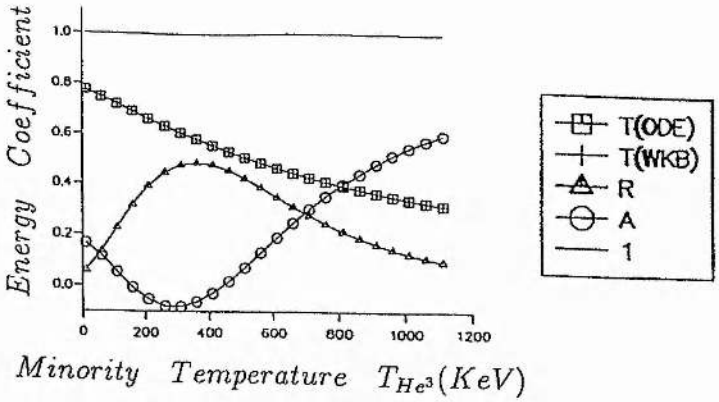

Figure 8.7b: Energy transport as a function of minority temperature(T_{He^3}) for minority heating($\frac{n_{He^3}}{n_e} = 1\%$) at perpendicular incidence($k_z = 0$), calculated from non-uniform theory with EM waves incident from the low magnetic field side.

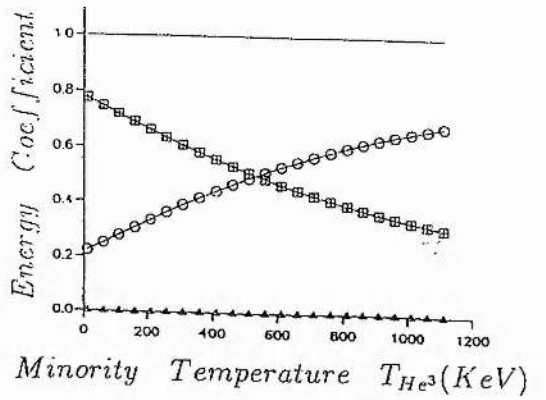

Figure 8.7c: Energy transport as a function of minority temperature(T_{He^3}) for minority heating($\frac{n_{He^3}}{n_e} = 1\%$) at perpendicular incidence($k_z = 0$), calculated from locally-uniform theory with EM waves incident from the high magnetic field side.

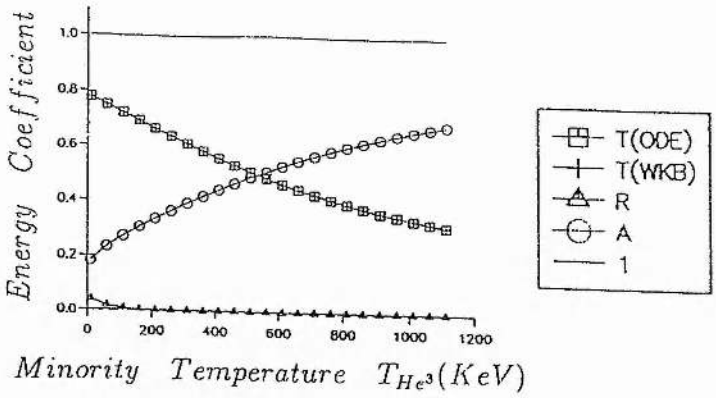

Figure 8.7d: Energy transport as a function of minority temperature(T_{He^3}) for minority heating($\frac{n_{He^3}}{n_e} = 1\%$) at perpendicular incidence($k_z = 0$), calculated from locally-uniform theory with EM waves incident from the low magnetic field side.

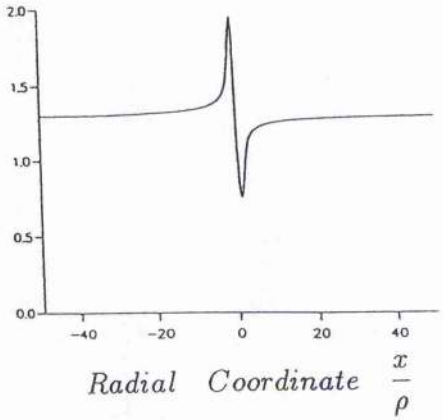

Figure 8.8a: Real part of the fast wave potential pertaining to the parameters of figure 8.7a at $T_{He^3} = 1.11MeV$, calculated from non-uniform theory.

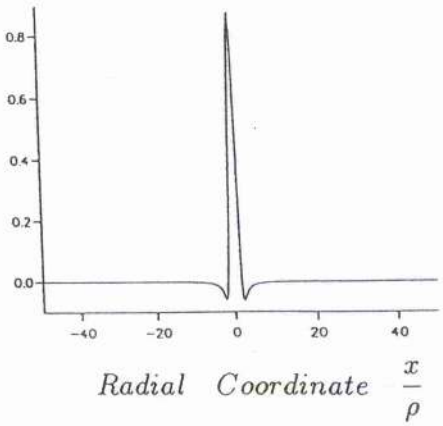

Figure 8.8b: Imaginary part of the fast wave potential pertaining to the parameters of figure 8.7a at $T_{He^3} = 1.11MeV$, calculated from non-uniform theory.

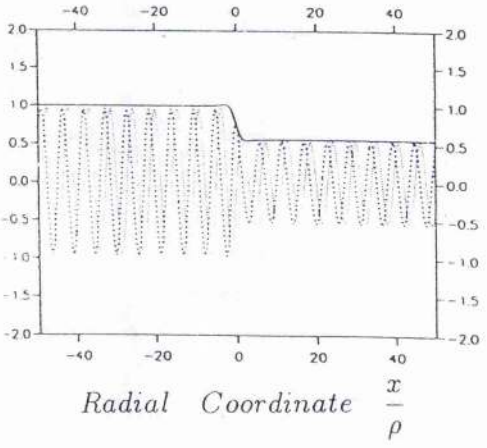

Figure 8.8c: Waveforms for the fast wave electric field(E_y) pertaining to the parameters of figure 8.7a at $T_{He^3} = 1.11MeV$, calculated from non-uniform theory with EM waves incident from the high magnetic field side.

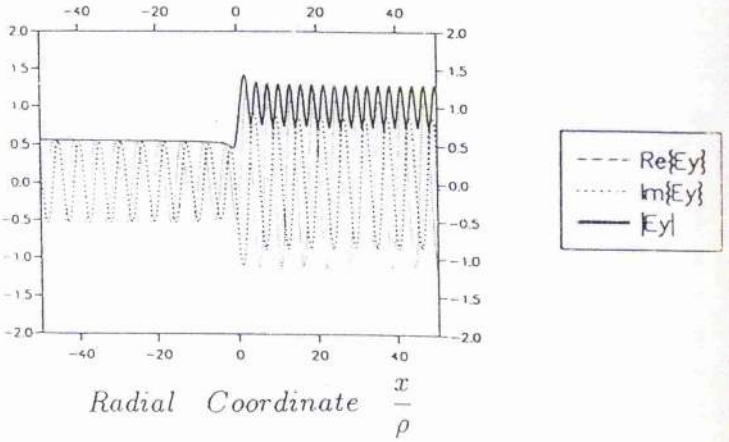

Figure 8.8d: Waveforms for the fast wave electric field(E_y) pertaining to the parameters of figure 8.7a at $T_{He^3} = 1.11MeV$, calculated from non-uniform theory with EM waves incident from the low magnetic field side.

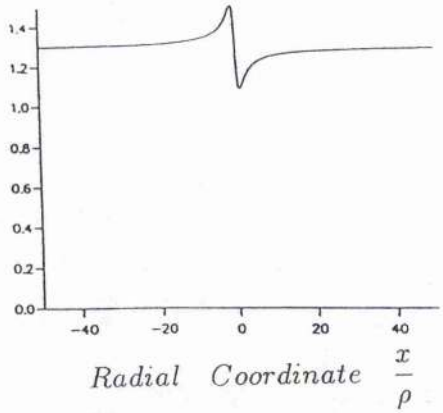

Figure 8.9a: Real part of the fast wave potential pertaining to the parameters of figure 8.7a at $T_{He^3} = 1.11MeV$, calculated from locally-uniform theory.

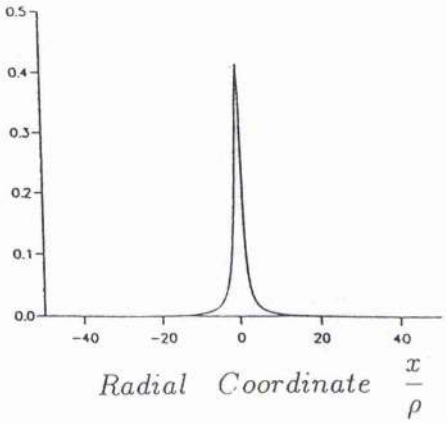

Figure 8.9b: Imaginary part of the fast wave potential pertaining to the parameters of figure 8.7a at $T_{He^3} = 1.11MeV$, calculated from locally-uniform theory.

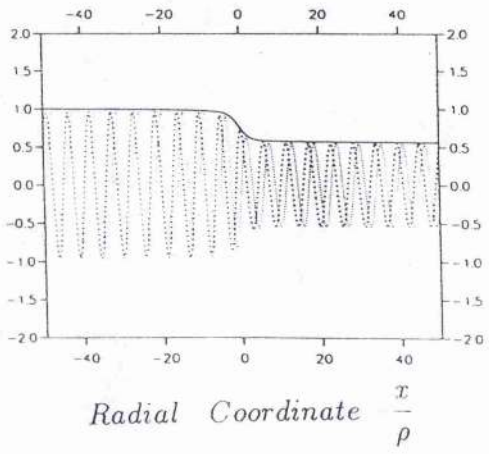

Figure 8.9c: Waveforms for the fast wave electric field(E_y) pertaining to the parameters of figure 8.7a at $T_{He^3} = 1.11MeV$, calculated from locally-uniform theory with EM waves incident from the high magnetic field side.

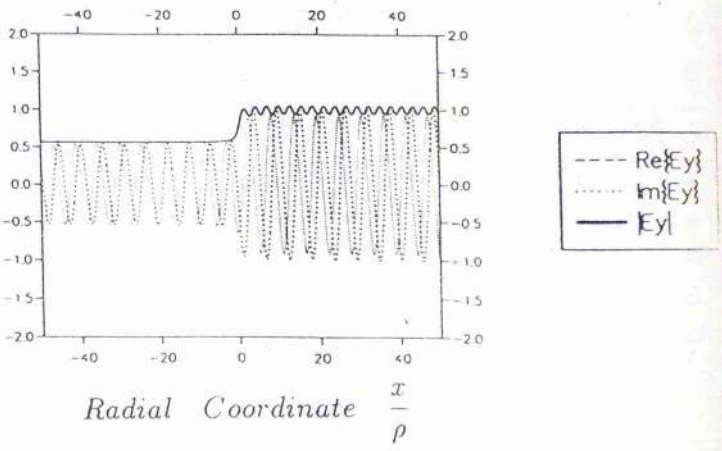

Figure 8.9d: Waveforms for the fast wave electric field(E_y) pertaining to the parameters of figure 8.7a at $T_{He^3} = 1.11MeV$, calculated from locally-uniform theory with EM waves incident from the low magnetic field side.

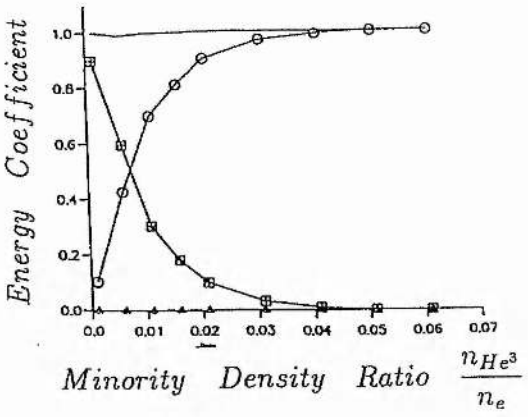

Figure 8.10a: Energy transport as a function of the minority density ratio($\frac{n_{He^3}}{n_e}$) for high energy($T_{He^3} = 1MeV$) heating at perpendicular incidence($k_z = 0$), calculated from non-uniform theory with EM waves incident from the high magnetic field side.

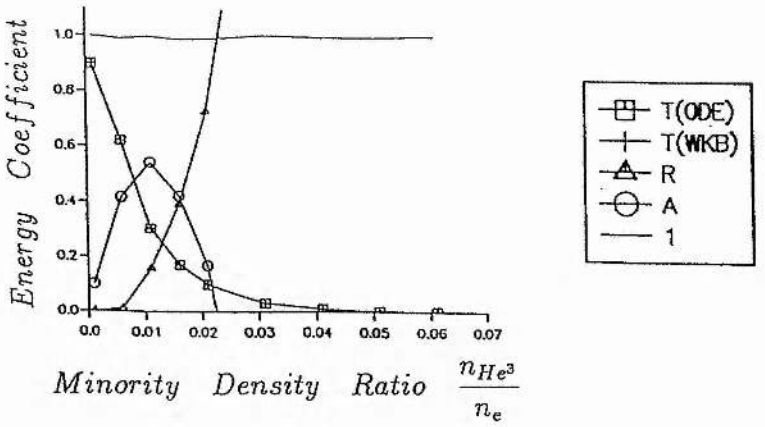

Figure 8.10b: Energy transport as a function of the minority density ratio($\frac{n_{He^3}}{n_e}$) for high energy($T_{He^3} = 1MeV$) heating at perpendicular incidence($k_z = 0$), calculated from non-uniform theory with EM waves incident from the low magnetic field side.

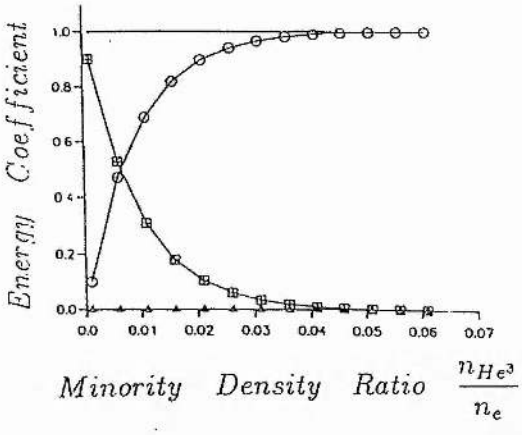

Figure 8.10c: Energy transport as a function of the minority density ratio($\frac{n_{He^3}}{n_e}$) for high energy($T_{He^3} = 1MeV$) heating at perpendicular incidence($k_z = 0$), calculated from locally-uniform theory with EM waves incident from the high magnetic field side.

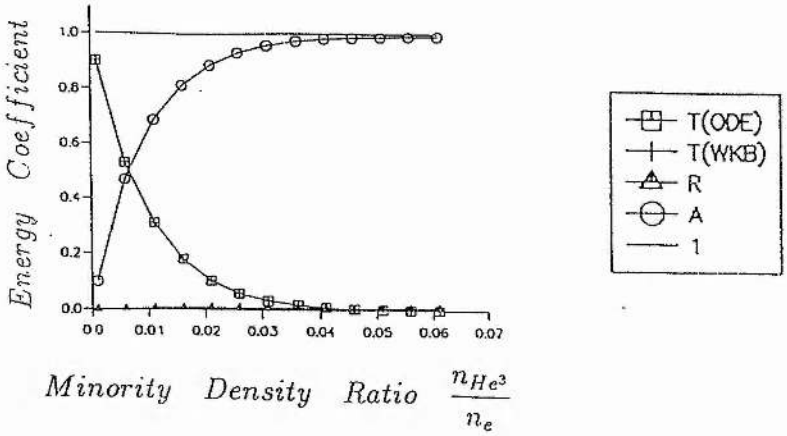

Figure 8.10d: Energy transport as a function of the minority density ratio($\frac{n_{He^3}}{n_e}$) for high energy($T_{He^3} = 1MeV$) heating at perpendicular incidence($k_z = 0$), calculated from locally-uniform theory with EM waves incident from the low magnetic field side.

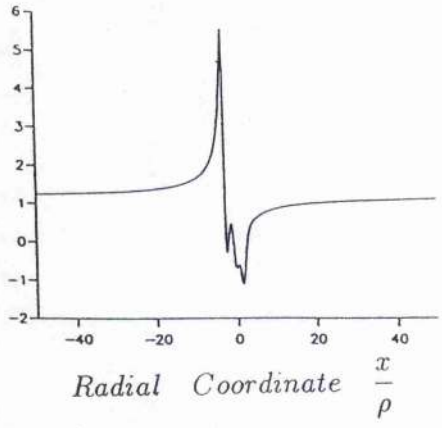

Figure 8.11a: Real part of the fast wave potential pertaining to the parameters of figure 8.10a at $\frac{n_{He^3}}{n_e} = 9.1\%$, calculated from non-uniform theory.

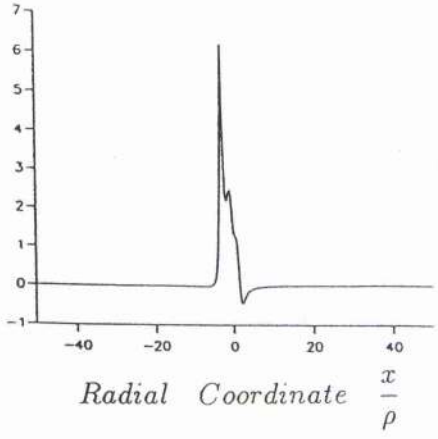

Figure 8.11b: Imaginary part of the fast wave potential pertaining to the parameters of figure 8.10a at $\frac{n_{He^3}}{n_e} = 9.1\%$, calculated from non-uniform theory.

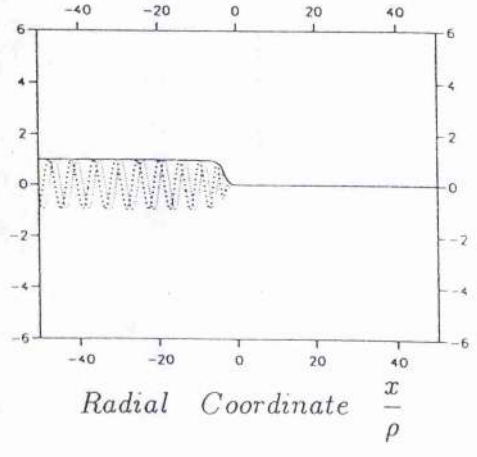

Figure 8.11c: Waveforms for the fast wave electric field(E_y) pertaining to the parameters of figure 8.10a at $\frac{n_{He^3}}{n_e} = 9.1\%$, calculated from non-uniform theory with EM waves incident from the high magnetic field side.

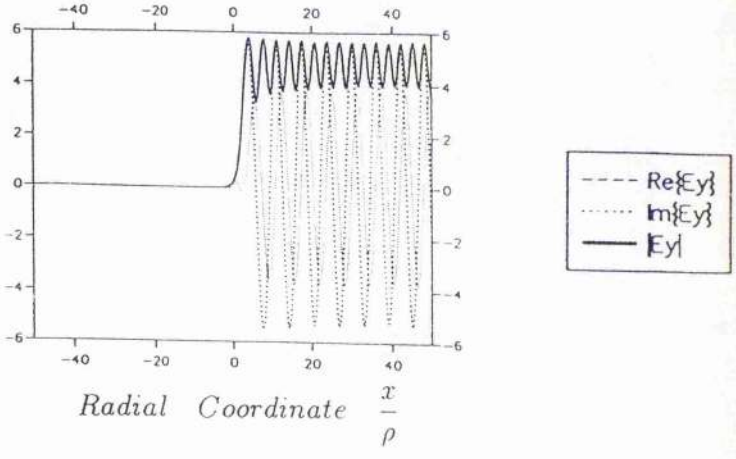

Figure 8.11d: Waveforms for the fast wave electric field(E_y) pertaining to the parameters of figure 8.10a at $\frac{n_{He^3}}{n_e} = 9.1\%$, calculated from non-uniform theory with EM waves incident from the low magnetic field side.

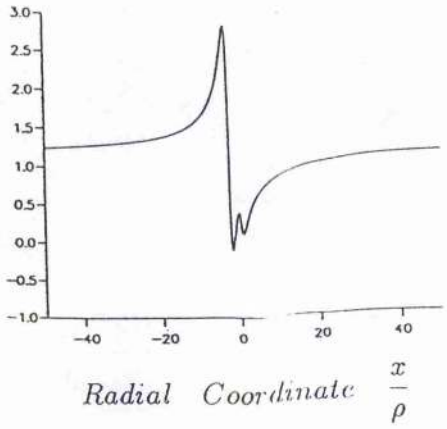

Figure 8.12a: Real part of the fast wave potential pertaining to the parameters of figure 8.10a at $\frac{n_{He^3}}{n_e} = 9.1\%$, calculated from locally-uniform theory.

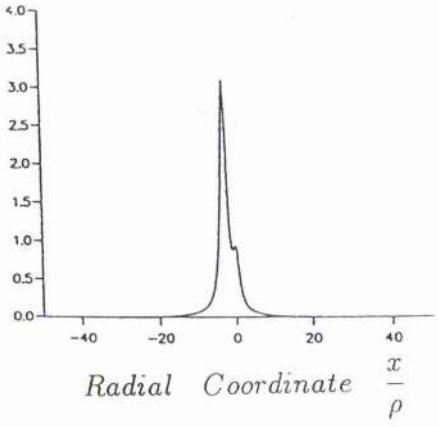

Figure 8.12b: Imaginary part of the fast wave potential pertaining to the parameters of figure 8.10a at $\frac{n_{He^3}}{n_e} = 9.1\%$, calculated from locally-uniform theory.

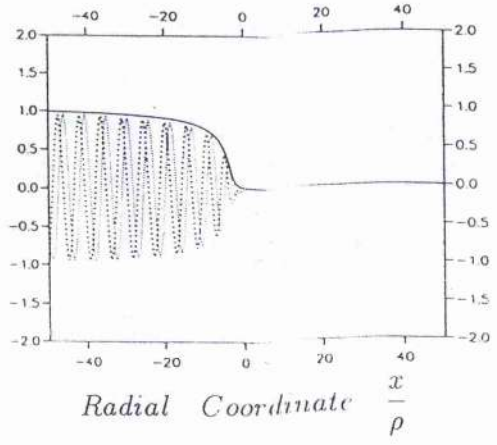

Figure 8.12c: Waveforms for the fast wave electric field(E_y) pertaining to the parameters of figure 8.10a at $\frac{n_{He^3}}{n_e} = 9.1\%$, calculated from locally-uniform theory with EM waves incident from the high magnetic field side.

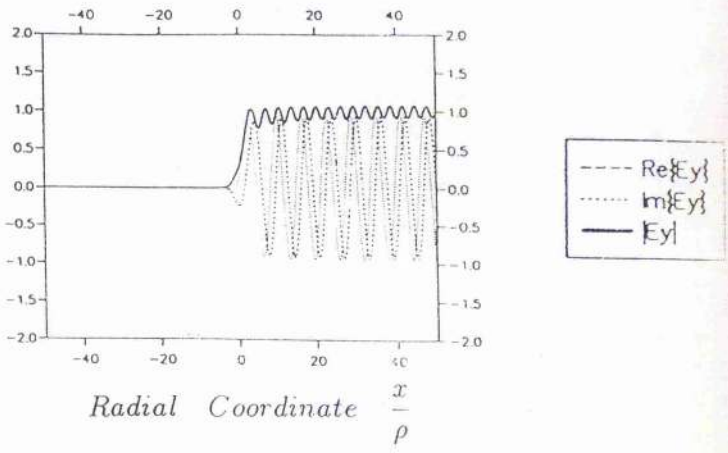

Figure 8.12d: Waveforms for the fast wave electric field(E_y) pertaining to the parameters of figure 8.10a at $\frac{n_{He^3}}{n_e} = 9.1\%$, calculated from locally-uniform theory with EM waves incident from the low magnetic field side.

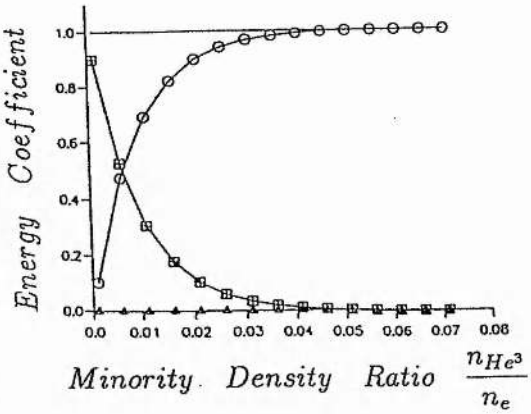

Figure 8.13a: Energy transport as a function of the minority density ratio($\frac{n_{He^3}}{n_e}$) for high energy($T_{He^3} = 1MeV$) heating at oblique incidence($k_z = 2m^{-1}$), calculated from non-uniform theory with EM waves incident from the high magnetic field side.

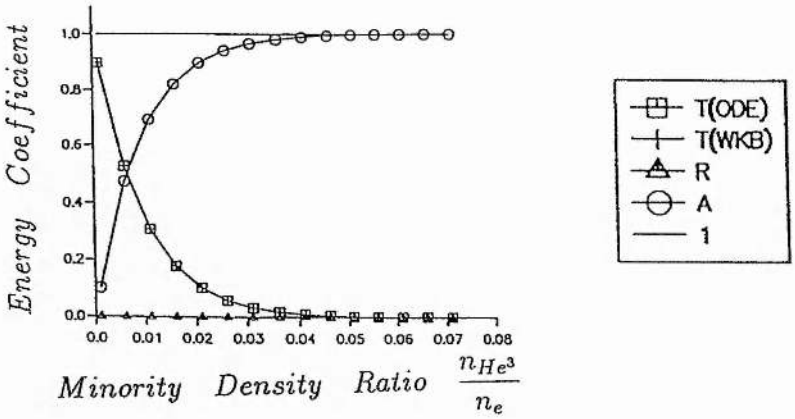

Figure 8.13b: Energy transport as a function of the minority density ratio($\frac{n_{He^3}}{n_e}$) for high energy($T_{He^3} = 1MeV$) heating at oblique incidence($k_z = 2m^{-1}$), calculated from non-uniform theory with EM waves incident from the low magnetic field side.

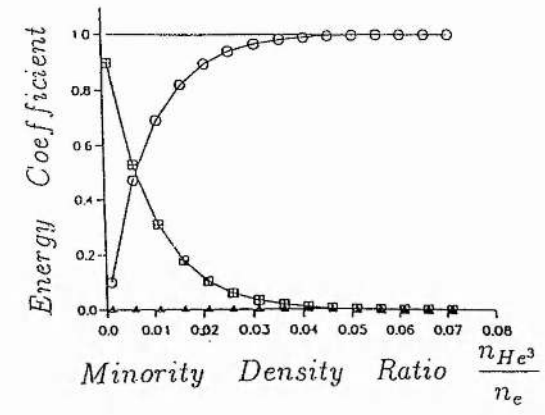

Figure 8.13c: Energy transport as a function of the minority density ratio($\frac{n_{He^3}}{n_e}$) for high energy($T_{He^3} = 1MeV$) heating at oblique incidence($k_z = 2m^{-1}$), calculated from locally-uniform theory with EM waves incident from the high magnetic field side.

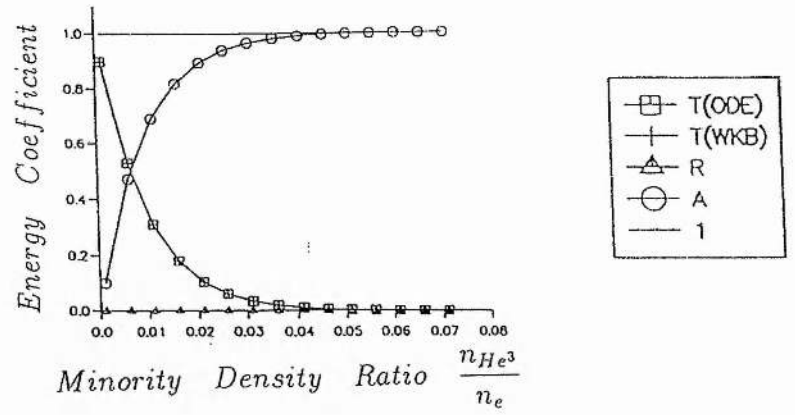

Figure 8.13d: Energy transport as a function of the minority density ratio($\frac{n_{He^3}}{n_e}$) for high energy($T_{He^3} = 1MeV$) heating at oblique incidence($k_z = 2m^{-1}$), calculated from locally-uniform theory with EM waves incident from the low magnetic field side.

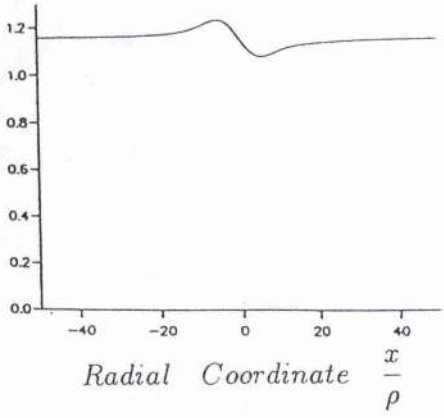

Figure 8.14a: Real part of the fast wave potential pertaining to the parameters of figure 8.13a at $\frac{n_{He^3}}{n_e} = 1.1\%$, calculated from non-uniform theory.

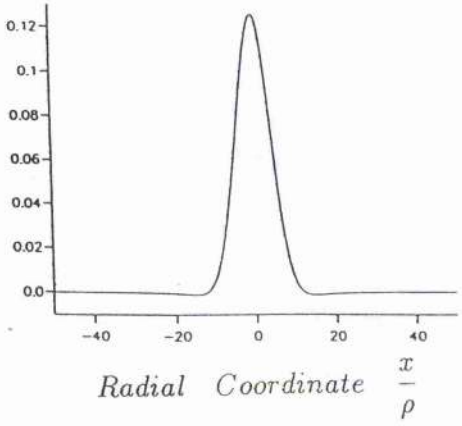

Figure 8.14b: Imaginary part of the fast wave potential pertaining to the parameters of figure 8.13a at $\frac{n_{He^3}}{n_e} = 1.1\%$, calculated from non-uniform theory.

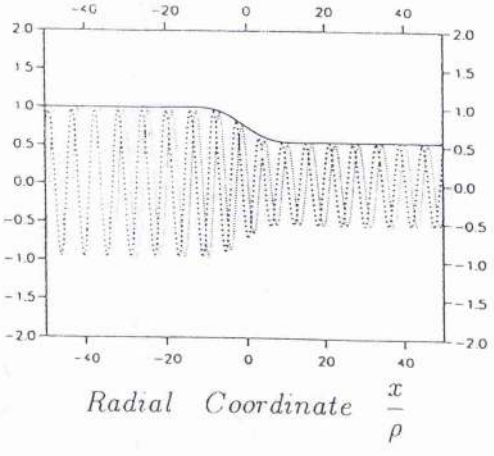

Figure 8.14c: Waveforms for the fast wave electric field(E_y) pertaining to the parameters of figure 8.13a at $\frac{n_{He^3}}{n_e} = 1.1\%$, calculated from non-uniform theory with EM waves incident from the high magnetic field side.

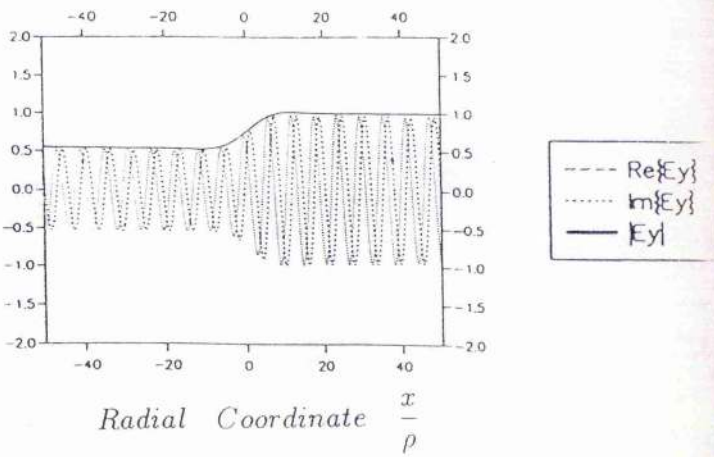

Figure 8.14d: Waveforms for the fast wave electric field(E_y) pertaining to the parameters of figure 8.13a at $\frac{n_{He^3}}{n_e} = 1.1\%$, calculated from non-uniform theory with EM waves incident from the low magnetic field side.

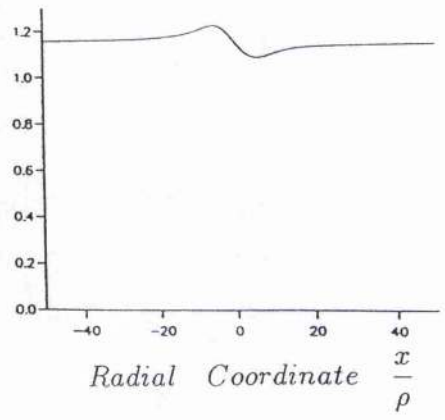

Figure 8.15a: Real part of the fast wave potential pertaining to the parameters of figure 8.13a at $\frac{n_{He^3}}{n_e} = 1.1\%$, calculated from locally-uniform theory.

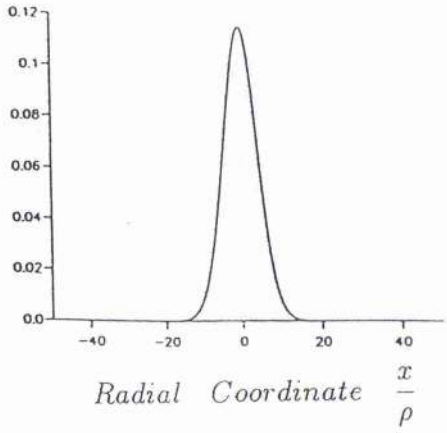

Figure 8.15b: Imaginary part of the fast wave potential pertaining to the parameters of figure 8.13a at $\frac{n_{He^3}}{n_e} = 1.1\%$, calculated from locally-uniform theory.

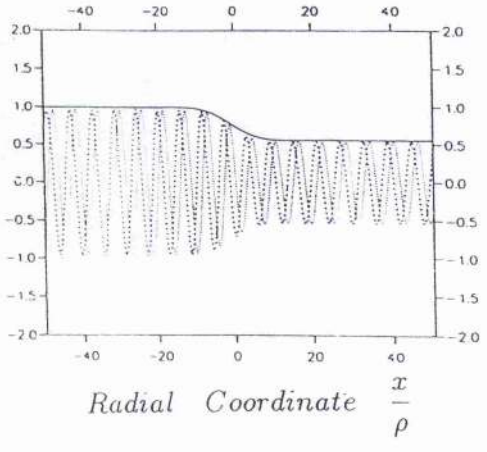

Figure 8.15c: Waveforms for the fast wave electric field(E_y) pertaining to the parameters of figure 8.13a at $\frac{n_{He^3}}{n_e} = 1.1\%$, calculated from locally-uniform theory with EM waves incident from the high magnetic field side.

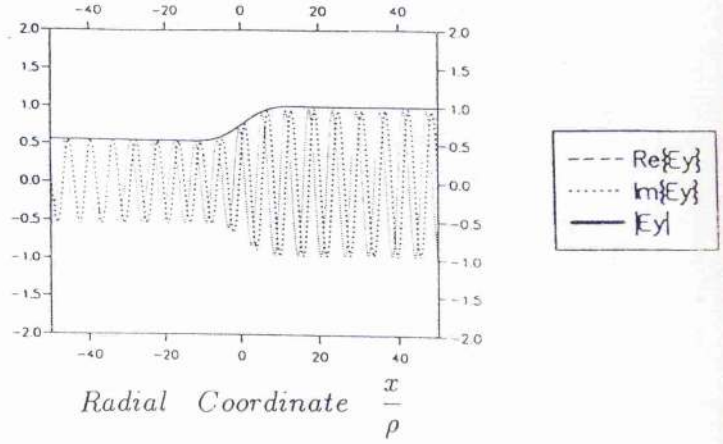

Figure 8.15d: Waveforms for the fast wave electric field(E_y) pertaining to the parameters of figure 8.13a at $\frac{n_{He^3}}{n_e} = 1.1\%$, calculated from locally-uniform theory with EM waves incident from the low magnetic field side.

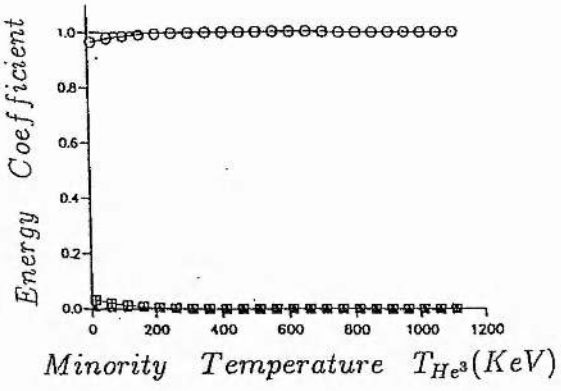

Figure 8.16a: Energy transport as a function of minority temperature(T_{He^3}) for mode conversion heating($\frac{n_{He^3}}{n_e} = 10\%$) at perpendicular incidence($k_z = 0$), calculated from non-uniform theory with EM waves incident from the high magnetic field side.

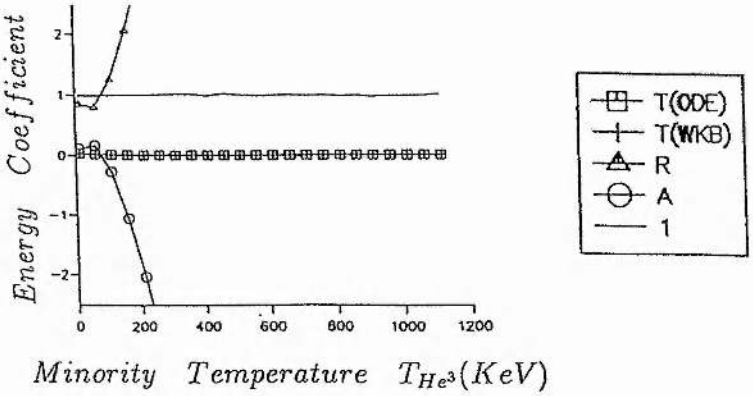

Figure 8.16b: Energy transport as a function of minority temperature(T_{He^3}) for mode conversion heating($\frac{n_{He^3}}{n_e} = 10\%$) at perpendicular incidence($k_z = 0$), calculated from non-uniform theory with EM waves incident from the low magnetic field side.

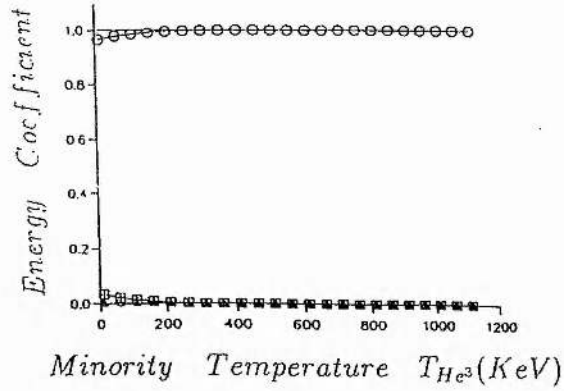

Figure 8.16c: Energy transport as a function of minority temperature(T_{He^3}) for mode conversion heating($\frac{n_{He^3}}{n_e} = 10\%$) at perpendicular incidence($k_z = 0$), calculated from locally-uniform theory with EM waves incident from the high magnetic field side.

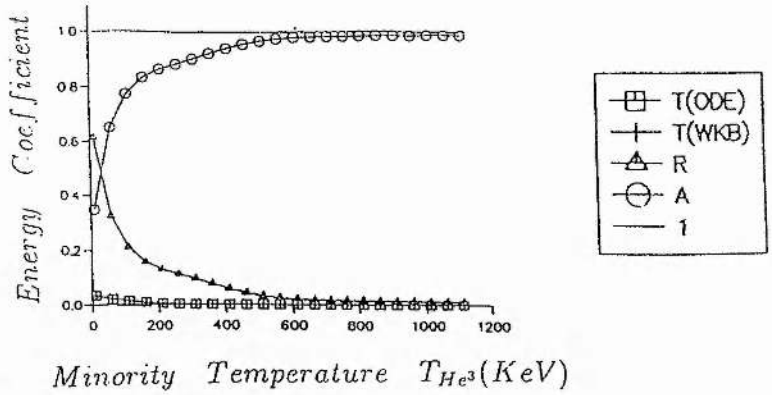

Figure 8.16d: Energy transport as a function of minority temperature(T_{He^3}) for mode conversion heating($\frac{n_{He^3}}{n_e} = 10\%$) at perpendicular incidence($k_z = 0$), calculated from locally-uniform theory with EM waves incident from the low magnetic field side.

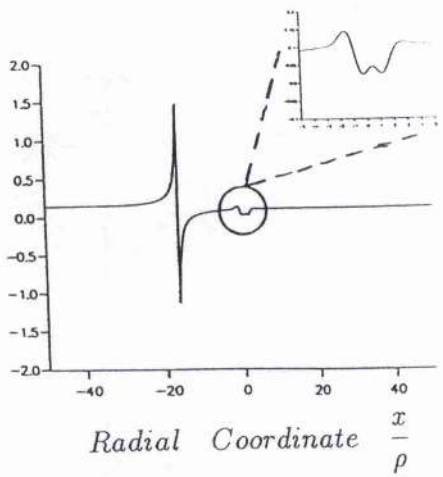

Figure 8.17a: Real part of the fast wave potential pertaining to the parameters of figure 8.16a at $T_{He^3} = 0.11MeV$, calculated from non-uniform theory.

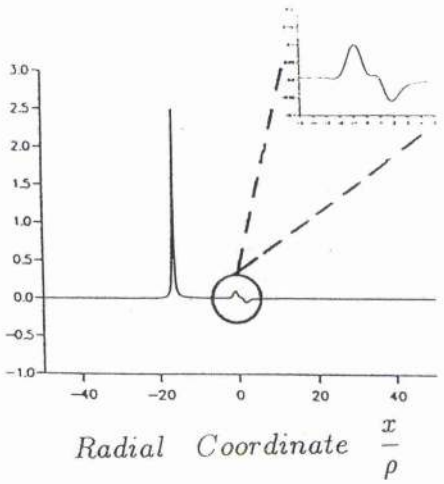

Figure 8.17b: Imaginary part of the fast wave potential pertaining to the parameters of figure 8.16a at $T_{He^3} = 0.11MeV$, calculated from non-uniform theory.

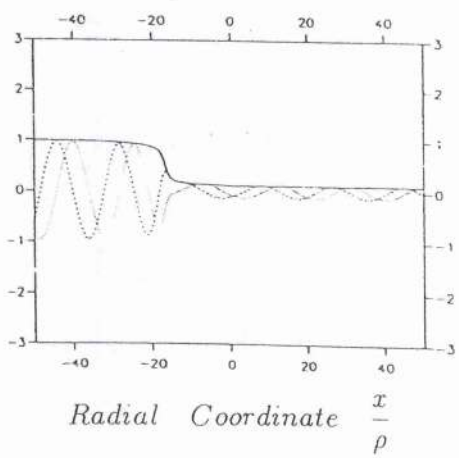

Figure 8.17c: Waveforms for the fast wave electric field(E_y) pertaining to the parameters of figure 8.16a at $T_{He^3} = 0.11MeV$, calculated from non-uniform theory with EM waves incident from the high magnetic field side.

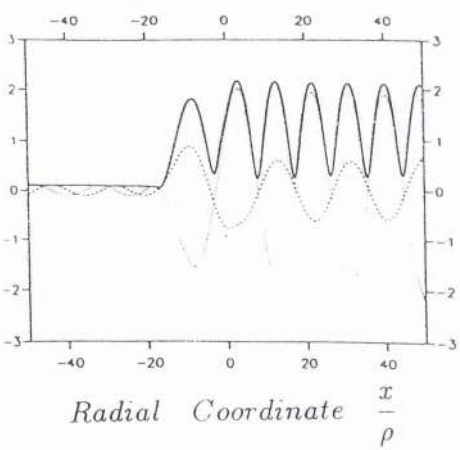

Figure 8.17d: Waveforms for the fast wave electric field(E_y) pertaining to the parameters of figure 8.16a at $T_{He^3} = 0.11MeV$, calculated from non-uniform theory with EM waves incident from the low magnetic field side.

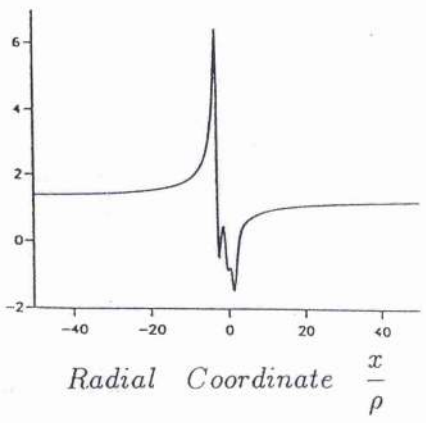

Figure 8.18a: Real part of the fast wave potential pertaining to the parameters of figure 8.16a at $T_{He^3} = 1.11MeV$, calculated from non-uniform theory.

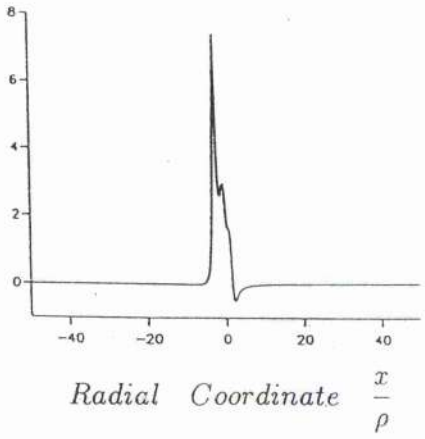

Figure 8.18b: Imaginary part of the fast wave potential pertaining to the parameters of figure 8.16a at $T_{He^3} = 1.11MeV$, calculated from non-uniform theory.

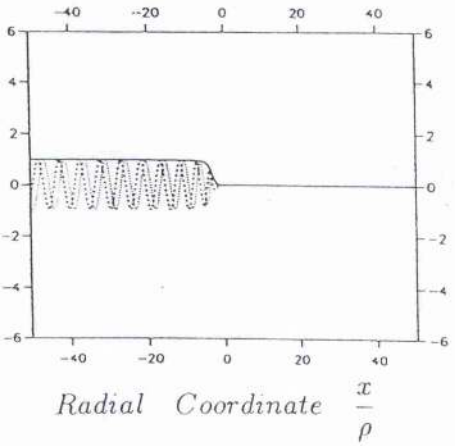

Figure 8.18c: Waveforms for the fast wave electric field(E_y) pertaining to the parameters of figure 8.16a at $T_{He^3} = 1.11MeV$, calculated from non-uniform theory with EM waves incident from the high magnetic field side.

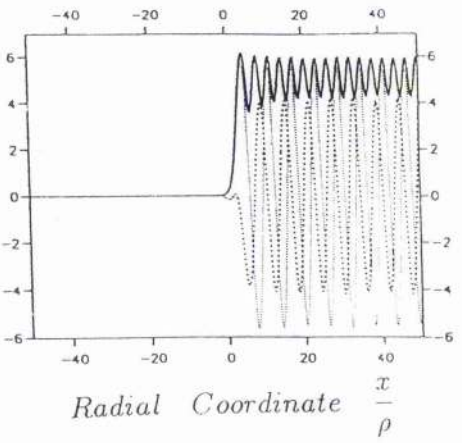

Figure 8.18d: Waveforms for the fast wave electric field(E_y) pertaining to the parameters of figure 8.16a at $T_{He^3} = 1.11MeV$, calculated from non-uniform theory with EM waves incident from the low magnetic field side.

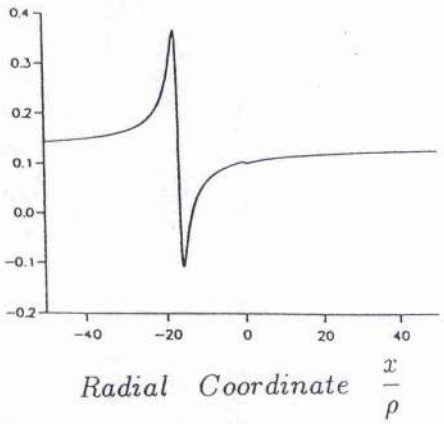

Figure 8.19a: Real part of the fast wave potential pertaining to the parameters of figure 8.16a at $T_{He^3} = 0.11MeV$, calculated from locally-uniform theory.

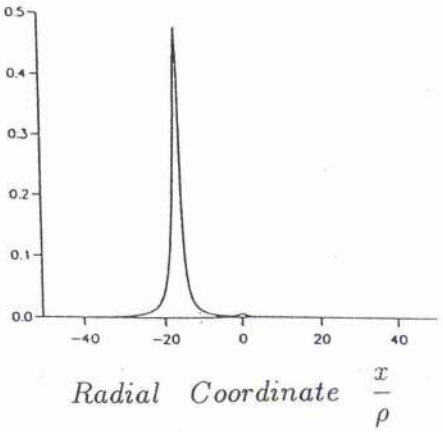

Figure 8.19b: Imaginary part of the fast wave potential pertaining to the parameters of figure 8.16a at $T_{He^3} = 0.11MeV$, calculated from locally-uniform theory.

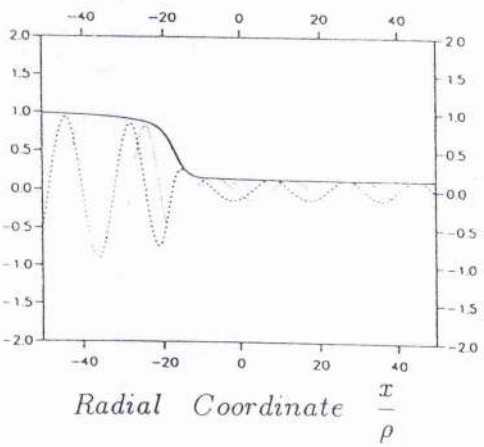

Figure 8.19c: Waveforms for the fast wave electric field(E_y) pertaining to the parameters of figure 8.16a at $T_{He^3} = 0.11MeV$, calculated from locally-uniform theory with EM waves incident from the high magnetic field side.

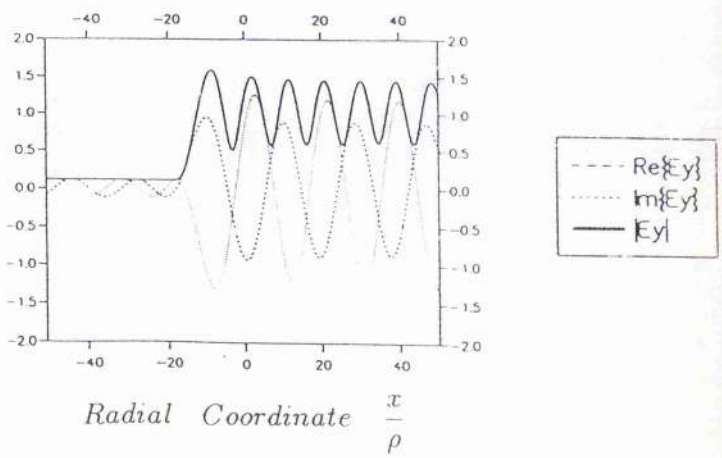

Figure 8.19d: Waveforms for the fast wave electric field(E_y) pertaining to the parameters of figure 8.16a at $T_{He^3} = 0.11MeV$, calculated from locally-uniform theory with EM waves incident from the low magnetic field side.

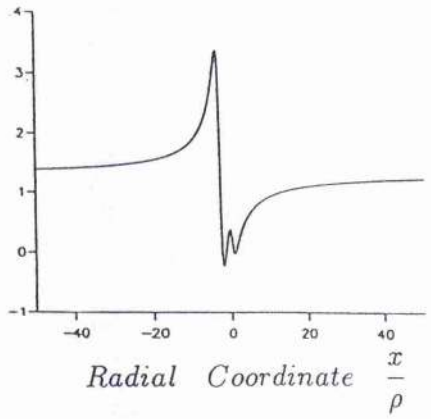

Figure 8.20a: Real part of the fast wave potential pertaining to the parameters of figure 8.16a at $T_{He^3} = 1.11MeV$, calculated from locally-uniform theory.

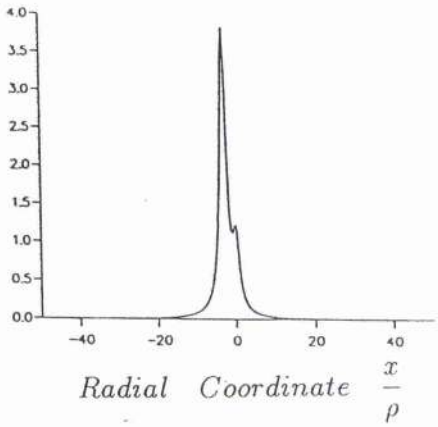

Figure 8.20b: Imaginary part of the fast wave potential pertaining to the parameters of figure 8.16a at $T_{He^3} = 1.11MeV$, calculated from locally-uniform theory.

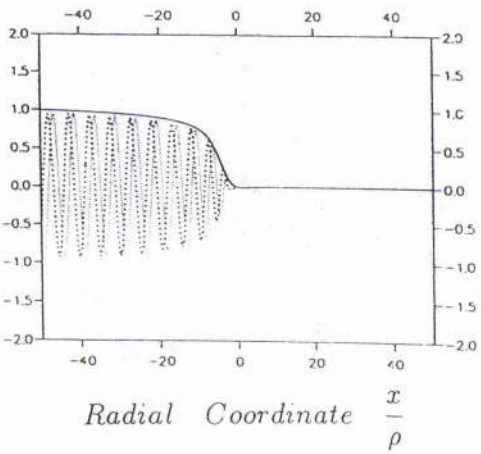

Figure 8.20c: Waveforms for the fast wave electric field(E_y) pertaining to the parameters of figure 8.16a at $T_{He^3} = 1.11MeV$, calculated from locally-uniform theory with EM waves incident from the high magnetic field side.

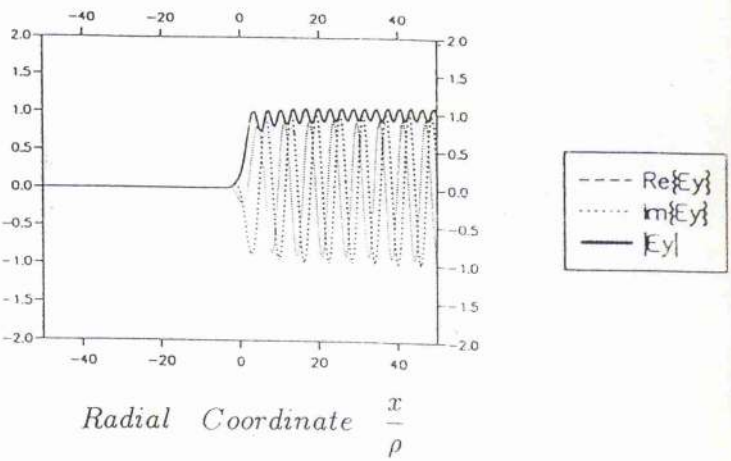

Figure 8.20d: Waveforms for the fast wave electric field(E_y) pertaining to the parameters of figure 8.16a at $T_{He^3} = 1.11MeV$, calculated from locally-uniform theory with EM waves incident from the low magnetic field side.

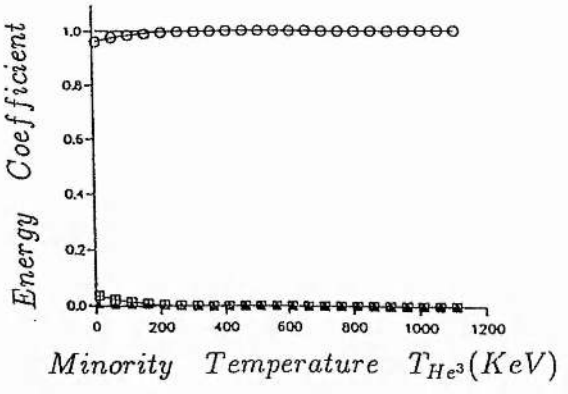

Figure 8.21a: Energy transport as a function of minority temperature(T_{He^3}) for mode conversion heating($\frac{n_{He^3}}{n_e} = 10\%$) at oblique incidence($k_z = 2m^{-1}$), calculated from non-uniform theory with EM waves incident from the high magnetic field side.

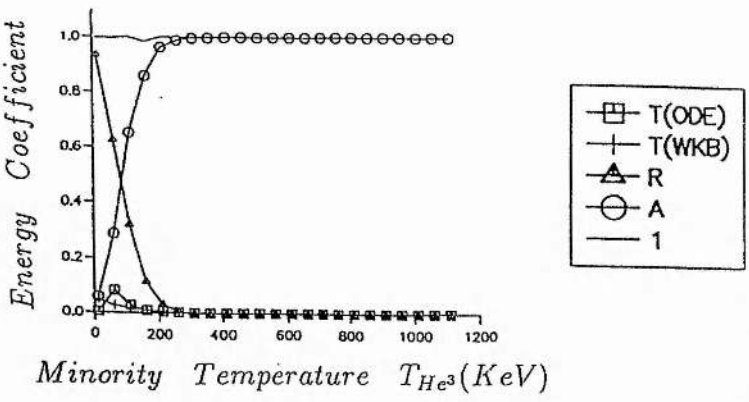

Figure 8.21b: Energy transport as a function of minority temperature(T_{He^3}) for mode conversion heating($\frac{n_{He^3}}{n_e} = 10\%$) at oblique incidence($k_z = 2m^{-1}$), calculated from non-uniform theory with EM waves incident from the low magnetic field side.

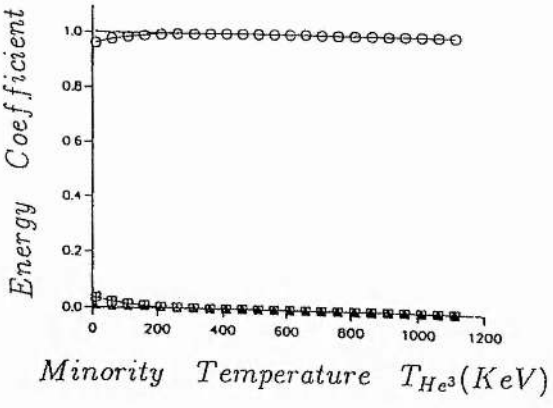

Figure 8.21c: Energy transport as a function of minority temperature(T_{He^3}) for mode conversion heating($\frac{n_{He^3}}{n_e} = 10\%$) at oblique incidence($k_z = 2m^{-1}$), calculated from locally-uniform theory with EM waves incident from the high magnetic field side.

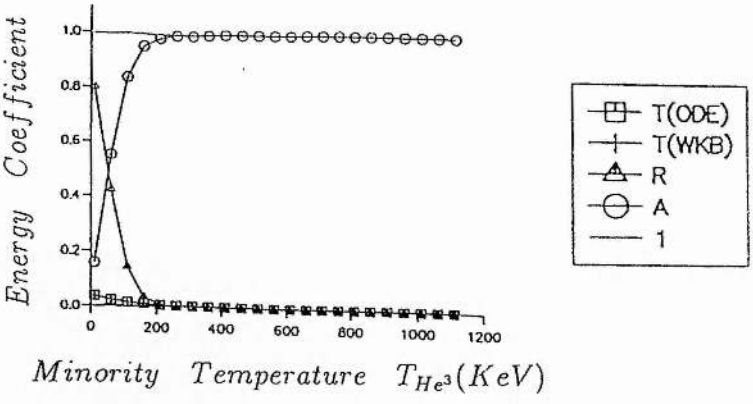

Figure 8.21d: Energy transport as a function of minority temperature(T_{He^3}) for mode conversion heating($\frac{n_{He^3}}{n_e} = 10\%$) at oblique incidence($k_z = 2m^{-1}$), calculated from locally-uniform theory with EM waves incident from the low magnetic field side.

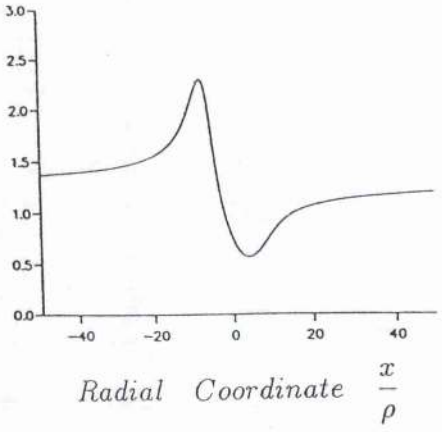

Figure 8.22a: Real part of the fast wave potential pertaining to the parameters of figure 8.21a at $T_{He^3} = 1.11MeV$, calculated from non-uniform theory.

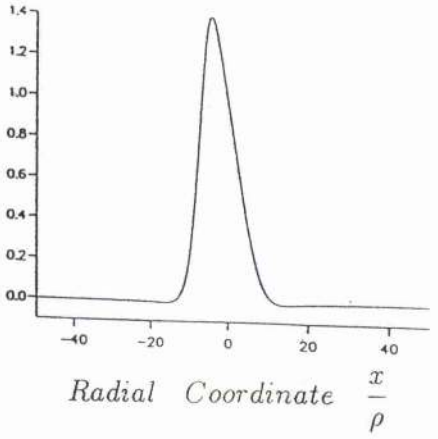

Figure 8.22b: Imaginary part of the fast wave potential pertaining to the parameters of figure 8.21a at $T_{He^3} = 1.11MeV$, calculated from non-uniform theory.

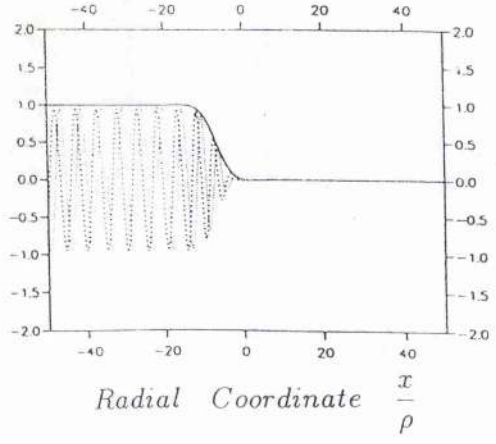

Figure 8.22c: Waveforms for the fast wave electric field(E_y) pertaining to the parameters of figure 8.21a at $T_{He^3} = 1.11MeV$, calculated from non-uniform theory with EM waves incident from the high magnetic field side.

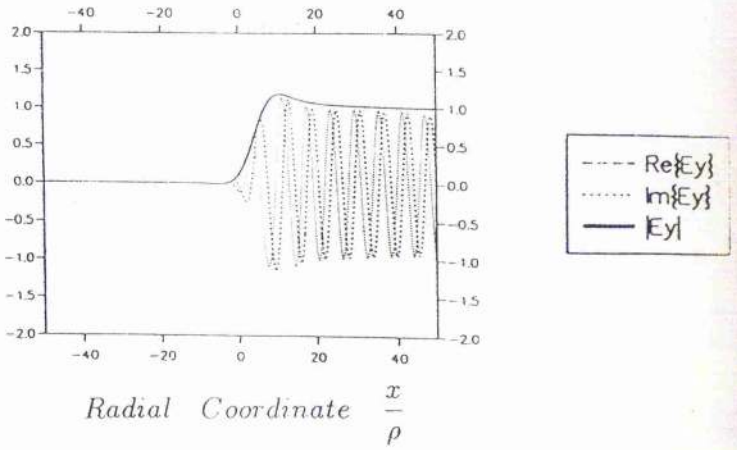

Figure 8.22d: Waveforms for the fast wave electric field(E_y) pertaining to the parameters of figure 8.21a at $T_{He^3} = 1.11MeV$, calculated from non-uniform theory with EM waves incident from the low magnetic field side.

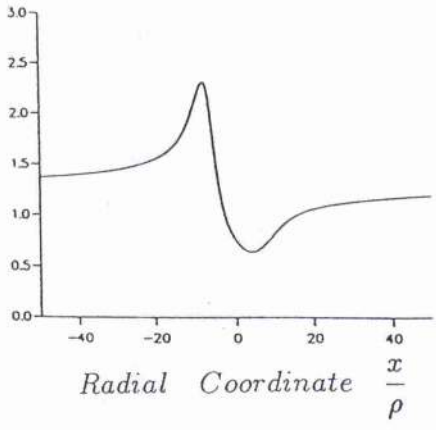

Figure 8.23a: Real part of the fast wave potential pertaining to the parameters of figure 8.21a at $T_{He^3} = 1.11MeV$, calculated from locally-uniform theory.

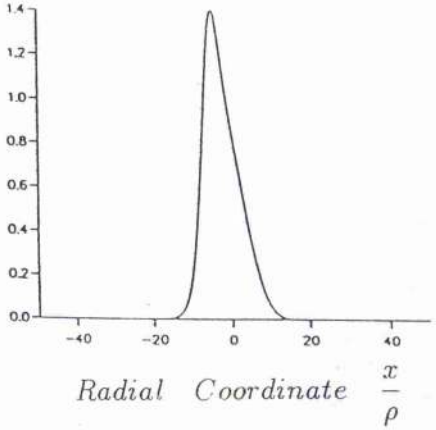

Figure 8.23b: Imaginary part of the fast wave potential pertaining to the parameters of figure 8.21a at $T_{He^3} = 1.11MeV$, calculated from locally-uniform theory.

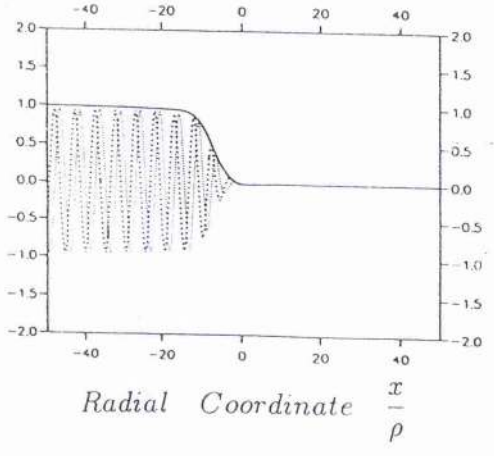

Figure 8.23c: Waveforms for the fast wave electric field(E_y) pertaining to the parameters of figure 8.21a at $T_{He^3} = 1.11MeV$, calculated from locally-uniform theory with EM waves incident from the high magnetic field side.

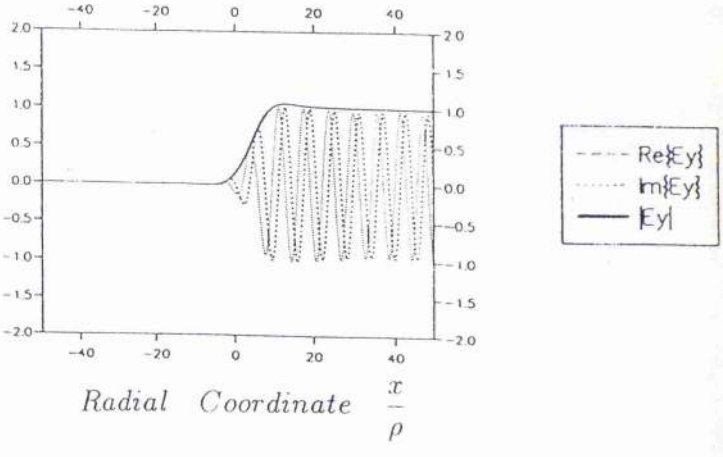

Figure 8.23d: Waveforms for the fast wave electric field(E_y) pertaining to the parameters of figure 8.21a at $T_{He^3} = 1.11MeV$, calculated from locally-uniform theory with EM waves incident from the low magnetic field side.

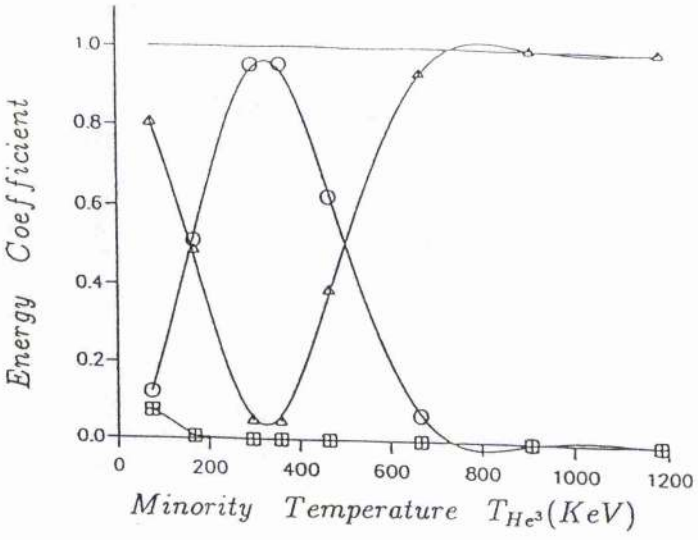

Figure 8.24a: Energy transport as a function of minority temperature(T_{He^3}) for mode conversion heating($\frac{n_{He^3}}{n_e} = 20\%$) at perpendicular incidence($k_z = 0$), calculated from a symmetrised non-uniform theory with EM waves incident from the low magnetic field side.

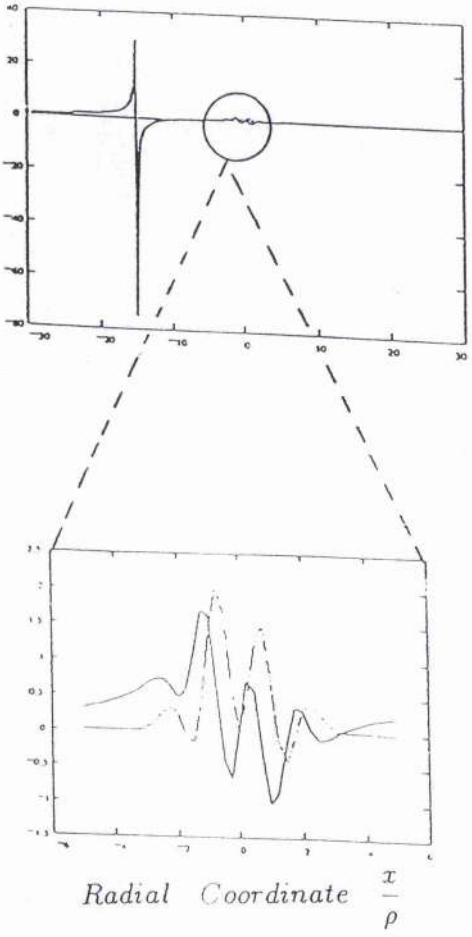

Figure 8.24b: Real part(bold line) and imaginary part(faint line) of the fast wave potential(V) pertaining to the parameters of figure 8.24a at $T_{He^3} = 0.66MeV$, calculated from a symmetrised non-uniform theory.

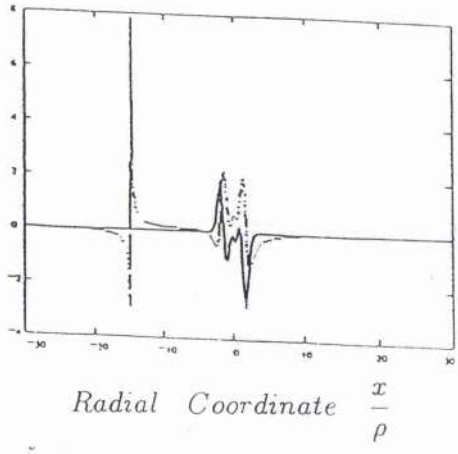

Figure 8.24c: Real part(bold line) and imaginary part(faint line) of the first order potential(U) pertaining to the parameters of figure 8.24a at $T_{He^3} = 0.66MeV$, calculated from a symmetrised non-uniform theory.

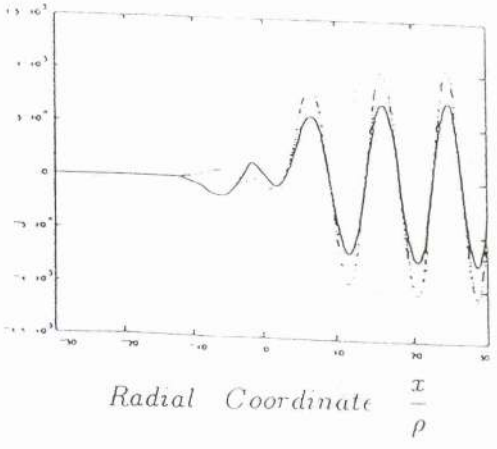

Figure 8.24d: Waveforms for the real part(bold line) and imaginary part(faint line) of the fast wave electric field(E_y) pertaining to the parameters of figure 8.24a at $T_{He^3} = 0.66MeV$, calculated from a symmetrised non-uniform theory with EM waves incident from the low magnetic field side.

Chapter 9

Closing Remarks

As was mentioned in the abstract to this thesis, an outstanding problem in theoretical plasma physics is the precise mechanism by which a hot, magnetically inhomogeneous plasma is heated by radio waves. We hope to have covered some ground on this question, particularly within the scope of kinetic theory.

9.1 General Equilibria

In chapter 3 we have generalised the existing theory available in the literature to allow for a general equilibrium constructed from the linear momentum and the energy which are constants of the motion of charged particles in a magnetic field. We showed in chapter 4 how such an equilibria was not a severe hindrance to the mathematical analysis and indeed we were able to draw several important qualitative conclusions about the effects of a thermally anisotropic equilibria. We found from our statistical analysis of chapter 5 that thermal anisotropy in Tokamaks using combinations of ICRH and NBI(of the type $T_\perp > T_\parallel$) produces resonance localisation. We found also that electron inertial terms in the plasma response are similarly reduced in effect. These are novel features of high ion energy, inhomogeneous plasmas not previously reported. It is hoped that further numerical studies will reveal evidence for temperature driven instabilities in the inhomogeneous plasma.

So as to bring our code more closely online with present Tokamak experiments, the following thought may be worth considering. One of the main obstacles to an inclusion of additional physics is the difficulty encountered in solving the velocity integrals which appear from the Shafranov path integral method outlined in chapter 2. For thermal equilibria these are analytically tractable for a limited class of scenarios, mostly $1D$ slab inhomogeneities. Any realistic equilibria will be unsolvable at the velocity integral stage of the calculation. Progress may be made by performing a quasi-analytic calculation whereby the path integral approach is taken as far as possible until a point in the calculation where the exact form of the equilibria must be specified. These equilibria may

be determined from a function(cubic spline or other) interpolated from empirical measurements of the temperature. This could then be read in by the code in much the same way our ODE solver reads in the cubic spline fit to the fast wave potential. The velocity integrals could then be performed by a standard quadrature method giving a full wave calculation based on real time data.

9.2 General Field Profiles

We have also allowed for a general field profile within the context of a weakly varying magnetic field gradient. This combination, while opening a pandora's box for the study of different Tokamak scenarios, does not allow for drift effects or for the effects of toroidicity. We argued that, provided the Tokamak major radius is about an order of magnitude larger than the minor radius, a $1D$ inhomogeneous slab model is adequate. Any tightening of this condition will need a study in toroidal coordinates. This is one possible avenue for further work. In addition, we argued that since we will only consider fast waves propagating in the $\hat{\mathbf{x}} - \hat{\mathbf{z}}$ plane, the effects of drifts along $\hat{\mathbf{y}}$ were removed from our study. Any $3D$ model of the effects of toroidal magnetic field inhomogeneity must include these drift effects which lead to additional broadening terms. There will then be a $2D$ gyrokinetic effect in the $\hat{\mathbf{x}} - \hat{\mathbf{y}}$ plane. Our study of statistics has shown that it is a powerful tool which may give deep insight into the physics of the resonance process for different distribution functions. A first step in the study of an unfamiliar equilibrium could be a statistical investigation to provide a sound physical basis which may be used to guide the mathematical analysis.

A straightforward extension to our theoretical study of chapter 4 would be the inclusion of weakly inhomogeneous temperature and density profiles. These may be introduced in much the same way as we took into account the spatial variation of the magnetic field using delta functions which allowed us to evaluate all spatially varying quantities at the guiding centre.

9.3 Symmetry Properties

The power of symmetry laws in revealing simple underlying principles in complex systems has attracted scientists for centuries. Although we have managed to show that the response of an inhomogeneous plasma to small amplitude waves satisfies the Onsager reciprocal relations for a thermal plasma, we should try to find utility from such analyses. Although we have generalised the thermodynamic study of Nambu(1995) to include an inhomogeneous magnetic field, it is doubtful that we can utilise this property of the plasma to ease calculational complexity, say. I feel there are important lessons to be learned from the work in chapter 7 related to Beskin's claims about the symmetric form of the dielectric tensor. We should always bear in mind the principle of physical covariance. Our findings in chapter 7 related to the effects of symmetrising the fast wave response tensor seem to

suggest a practical solution to some worrying findings in our numerics. I feel there is an underlying link between Onsager symmetry and the practicality of the symmetrised fast wave tensor. Perhaps a useful future exercise would be to try to coalesce these somewhat unclear concepts.

9.4 Numerics

The code seems to be quite durable and provides excellent energy conservation(to within 1%) in every case investigated. This is further confirmed by the excellent agreement(again within 1%) between transmission coefficients calculated from a WKB analysis of the fast wave potential and separately from the fast wave ODE. We have been able to investigate a range of Tokamak scenarios with varying minority ion temperatures, densities and for different incident wave spectra. Our findings, though not conclusive by any means, have opened a few new doors I feel. For example, the appearance of a new family of cutoffs is worth investigating theoretically perhaps from the easier viewpoint of high order finite Larmor radius theories. See for example Chen and Tsai(1983) or Lashmore-Davies et al.(1988). Hopefully a more thorough study of the symmetrised form of the fast wave response tensor will, in future, provide more credence to the numerical results born out of this thesis. Once a reproducible and consistent category of results is obtained for the study of a thermal plasma, it would be interesting to look at the effects of thermal anisotropy. The code has this theory already built into it and is ready to study these effects once faith in the isotropic plasma results is first established.

All in all, the guiding centre theory of Cairns et al.(1991) allows for a straightforward development of complex physical models as revealed by the work of Holt(1992) and McDonald(1994) before me which considered large Larmor radius ion effects and relativistic electron effects respectively within the context of a Maxwellian plasma immersed in a linearly varying magnetic field gradient. The fast wave approximation and the spinoffs described in this thesis allow complex systems of fourth order IDEs to be reduced to more rapidly solvable and insightful equations. The acid test will be a direct comparison of the fast wave ODE with its associated fourth order brother.

The field of theoretical plasma physics is far from exhausted and it is hoped that this thesis is able to contribute in some small way to the development of the subject and to the international fusion research programme.

Appendix A

Derivation Of The Poynting Theorem

Let U represent the total energy density in the EM field, let $\mathbf{S}$ represent the energy flux in the EM field and let W be the rate at which work is done on matter.

The field energy inside a volume V is,

$$\int_V U dV,$$

and the rate of decrease of the field energy is,

$$-\frac{\partial}{\partial t}\int_V U dV.$$

Similarly the rate of work done on a volume V of the plasma is,

$$\int_V W dV.$$

The flow of field energy out of a volume V is the integral of the normal component of $\mathbf{S}$ over the surface A that encloses V,

$$\int_A \mathbf{S} \bullet \mathbf{n} dA.$$

So if we balance the work done by the field on the plasma in a volume V with the flow of field energy out of the volume and the rate of decrease of the field energy inside the volume we have the energy balance equation,

$$-\frac{\partial}{\partial t}\int_V U dV = \int_A \mathbf{S} \bullet \mathbf{n} dA + \int_V W dV.$$

and since we are integrating over the same volume of plasma(V) then we may equate the expressions within the integrals giving,

$$W = -\frac{\partial U}{\partial t} - \nabla \bullet \mathbf{S}. \tag{A.1}$$

This is the rate of work done by the EM fields on the plasma per unit volume. We may get an intuitive physical picture of this by considering the work done by the EM fields on a particle whose motion is governed by the Lorentz force,

$$\mathbf{F} \bullet \mathbf{v} = q(\mathbf{E} + \mathbf{v} \times \mathbf{B}) \bullet \mathbf{v} \equiv q\mathbf{E} \bullet \mathbf{v}.$$

Since the current density is given by $\mathbf{J} = Nq\mathbf{v}$ for N particles then the loss of energy per unit time and volume from the field is $\mathbf{E} \bullet \mathbf{J}$. In general the exact mathematical form of the work done will depend upon the model used to describe the plasma state. However, the rate of work done is always equivalent to $\mathbf{E} \bullet \mathbf{J}$ with the properties of the plasma housed in the current density response($\mathbf{J}$).

We may use Maxwell's equations to obtain explicit expressions for U and $\mathbf{S}$ in terms of the fields $\mathbf{E}$ and $\mathbf{B}$ and we will see that the above form for the work done arises naturally.

From Ampere's law,

$$\nabla \times \mathbf{B} = \mu_0 \mathbf{J} + \frac{1}{c^2}\frac{\partial \mathbf{E}}{\partial t},$$

then,

$$\mathbf{E} \bullet \mathbf{J} = \frac{1}{\mu_0}\mathbf{E} \bullet (\nabla \times \mathbf{B}) - \epsilon_0 \mathbf{E} \bullet \frac{\partial \mathbf{E}}{\partial t}. \tag{A.2}$$

We now use an identity from vector calculus,

$$\nabla \bullet (\mathbf{a} \times \mathbf{b}) \equiv \mathbf{b} \bullet (\nabla \times \mathbf{a}) - \mathbf{a} \bullet (\nabla \times \mathbf{b}),$$

to write out the second term in (A.2) as,

$$\frac{1}{\mu_0}\mathbf{E} \bullet (\nabla \times \mathbf{B}) = \frac{1}{\mu_0}[\mathbf{B} \bullet (\nabla \times \mathbf{E}) - \nabla \bullet (\mathbf{E} \times \mathbf{B})].$$

Faraday's law,

$$\nabla \times \mathbf{E} = -\frac{\partial \mathbf{B}}{\partial t},$$

then gives,

$$\mathbf{E} \bullet \mathbf{J} = -\nabla \bullet (\frac{\mathbf{E} \times \mathbf{B}}{\mu_0}) - \epsilon_0 \mathbf{E} \bullet \frac{\partial \mathbf{E}}{\partial t} - \frac{1}{\mu_0}\mathbf{B} \bullet \frac{\partial \mathbf{B}}{\partial t}.$$

We may rewrite the time derivative terms as follows. They are of the form,

$$\mathbf{a} \bullet \frac{\partial \mathbf{a}}{\partial t}.$$

Let us write this as,

$$\mathbf{a} \bullet \frac{\partial \mathbf{a}}{\partial t} = \frac{\partial}{\partial t}(A),$$

where,

$$A = \int dt \mathbf{a} \bullet \frac{\partial \mathbf{a}}{\partial t} \equiv \mathbf{a} \bullet \mathbf{a} - \int dt \mathbf{a} \bullet \frac{\partial \mathbf{a}}{\partial t},$$

after performing integration by parts. Therefore $A \equiv \frac{1}{2}\mathbf{a} \bullet \mathbf{a}$ and so,

$$\mathbf{a} \bullet \frac{\partial \mathbf{a}}{\partial t} \equiv \frac{1}{2}\frac{\partial}{\partial t}(\mathbf{a} \bullet \mathbf{a}).$$

The energy balance equation is then,

$$\mathbf{E} \bullet \mathbf{J} = -\nabla \bullet (\frac{\mathbf{E} \times \mathbf{B}}{\mu_0}) - \frac{\partial}{\partial t}[\frac{\epsilon_0}{2}(\mathbf{E} \bullet \mathbf{E}) + \frac{1}{2\mu_0}(\mathbf{B} \bullet \mathbf{B})]. \tag{A.3}$$

Inspection of the conservation law of (A.1) reveals that the first term on the right hand side of (A.3) is the flux of EM energy while the remaining terms give the rate of change of the EM field energy.

Appendix B

Derivation Of The Asymptotic(WKB) Waveforms

Our Governing ODE is,

$$\frac{d^2}{dx^2}\phi(x) + V(x)\phi(x) = 0. \tag{B.1}$$

For an inhomogeneity along $\hat{\mathbf{x}}$ chapter 7 revealed that plane waves will not be the eigenfunctions of (B.1). Instead, a suitable spatially dispersive form is,

$$\phi(x) = \phi_0(x)e^{i\int^x k(x')dx'}, \tag{B.2}$$

with derivatives,

$$\frac{d}{dx}\phi(x) = [\frac{d}{dx}\phi_0(x) + ik(x)\phi_0(x)]e^{i\int^x k(x')dx'}, \tag{B.3}$$

$$\frac{d^2}{dx^2}\phi(x) = [\frac{d^2}{dx^2}\phi_0(x) + 2ik(x)\frac{d}{dx}\phi_0(x) + (i\frac{d}{dx}k(x) - k^2(x))\phi_0(x)]e^{i\int^x k(x')dx'} \tag{B.4}$$

The first order solution of (B.1) is,

$$k^2(x) = V(x), \tag{B.5}$$

so that (B.4) becomes,

$$\frac{d^2}{dx^2}\phi(x) + k^2(x)\phi(x) = [\frac{d^2}{dx^2}\phi_0(x) + 2ik(x)\frac{d}{dx}\phi_0(x) + i\frac{d}{dx}k(x)\phi_0(x)]e^{i\int^x k(x')dx'}. \tag{B.6}$$

The left hand side is zero by virtue of (B.1) and, neglecting the second order derivative term,

$$[2ik(x)\frac{d}{dx}\phi_0(x) + i\frac{d}{dx}k(x)\phi_0(x)]e^{i\int^x k(x')dx'} = 0.$$

This is a separable first order ODE,

$$\frac{\frac{d}{dx}\phi_0(x)}{\phi_0(x)} = -\frac{\frac{d}{dx}k(x)}{2k(x)},$$

with solution,

$$\phi_0(x) = Ck(x)^{-1/2}.$$

Having identified the amplitude function our WKB waveform is, from (B.2),

$$\phi(x) \simeq \frac{C}{k(x)^{1/2}} e^{i\int^x k(x')dx'} \equiv \frac{C}{V(x)^{1/4}} e^{i\int^x V(x')^{1/2}\,dx'}. \tag{B.7}$$

Appendix C

Evaluation Of The Resonance Integrals

The integrals arising in the resonant conductivity tensor must be solved numerically for each value of radial position(x) stepping across the interaction region of the plasma. The integrals are Fourier type integrals over a semi-infinite regime and are of the general form,

$$I(x) = \int_a^b f(k) e^{ikx} dk. \tag{C.1}$$

In each subinterval$[k_m, k_m + h]$ of width h in $[a, b]$, we approximate the integrand $f(k)$ by a linear interpolant as shown in figure 8.3. Between a general value of the integrand $f(k)$ and a subsequent point $f(k_m)$ a distance h away at k_m, the following first order Taylor expansion about(k_m) provides an expression for the linear interpolant,

$$f(k) \simeq f(k_m) + \left[\frac{f(k_m + h) - f(k_m)}{h}\right](k - k_m). \tag{C.2}$$

The contribution to the total integral form this segment of width h is found by substituting (C.2) into (C.1),

$$I_h(x) \simeq \int_{k_m}^{k_m+h} f(k_m) + \left[\frac{f(k_m + h) - f(k_m)}{h}\right](k - k_m) e^{ikx} dk. \tag{C.3}$$

We may straightforwardly perform the integrals by parts to give,

$$\begin{aligned} I_h(x) &= \left[(1 + \frac{k_m}{h})\frac{f(k_m)}{ix} e^{ikx} - (\frac{k_m}{h})\frac{f(k_m + h)}{ix} e^{ikx}\right]_{k_m}^{k_m+h} \\ &+ (\frac{f(k_m + h) - f(k_m)}{h})\left[\frac{1}{ix} e^{ikx}(k - \frac{1}{ix})\right]_{k_m}^{k_m+h}. \end{aligned} \tag{C.4}$$

Evaluation of the limits then provides us with the contribution to the integral from the subinterval$[k_m, k_m + h]$,

$$I_h(x) \simeq \frac{f(k_m)}{ix}\left[-e^{ik_m x} + \frac{1}{ixh}(e^{i(k_m+h)x} - e^{ik_m x})\right] + \frac{f(k_m+h)}{ix}\left[e^{i(k_m+h)x} + \frac{1}{ixh}(-e^{i(k_m+h)x} + e^{ik_m x})\right]. \quad \text{(C.5)}$$

The numerical approximation to the full integral is found by summing over all subintervals in $[a, b]$. Due to the appearance of the position(x) explicitly in the denominator, we ensure that steps near the origin are carefully monitored so as to have small but non-zero values. Our integrals run from $a = 0$ to $b = \infty$.

The integrands are dominated by the linear exponential $e^{ik_1 x}$ for very small values of k_1 such that $k_1\rho_\perp \ll 1$. This effect is swamped by the quadratic exponential term $e^{-\frac{1}{4}k_1^2\rho_\perp^2[1+k_\parallel^2 L^2(\frac{T_\parallel}{T_\perp})/l^2]}$ when $k_1\rho_\perp \geq 1$ ensuring that the integrand is a well-behaved function. It is this dominating behaviour which is responsible for the degree of non-locality of the resonant particles. Their effect is seen to be important over a distance equal to a few times the ion Larmor radius. Highly energy ions, born out of fusion reactions or fuelled by gyroresonance, will have large Larmor radii($> 10cm$) and so this region of non-locality is a substantial proportion of the device scalelength($L \simeq 3.1m$). In the numerical results presented at the end of chapter 8 it is clear that highly non-local behaviour is exhibited by energetic ions.

The integrand is a finite value when $k_1 = 0$ and falls off monotonically to zero in the asymptotic region as $k_1 \to \infty$ which, recalling the definition $k_1 = -\frac{l\Omega_0(0)\tau}{L}$, reflects the fact that there is no response of the plasma at a time $t = 0$ since resonant particles haven't yet moved along their orbits. If we note that for exactly perpendicular wave incidence, the quadratic exponential becomes more simply $e^{-\frac{1}{4}k_1^2\rho_\perp^2}$. When $k_1\rho_\perp \simeq 10$ then the factor $e^{-100} \simeq 10^{-44}$ gives us an adequate value of infinity to use in our code, namely $k_1(\infty) \simeq \frac{10}{\rho_\perp}$.

Bibliography

Publication Type	Abbreviation
Books, Review Articles and Theses	Underlined
Fusion Technology	FT
Journal of Physics(USSR)	JP
Journal of Plasma Physics	JPP
Helvetica Physica Acta	HPA
Nuclear Fusion	NF
Physical Review	PR
Physical Review Letters	PRL
Physica Scripta	PS
Physics of Fluids	PF
Physics Letters	PL
Physics of Plasmas	PP
Physics Reports	PRS
Physics Today	PT
Plasma Physics	PPS
Plasma Physics and Controlled Nuclear Fusion	PPCF
Plasma Physics Note(UKAEA Fusion)	PPN
Proceedings of the Physics Society	PrPS
Proceedings of the Royal Society	PrRS
Reviews of Plasma Physics	RPP
Soviet Physics JETP	SP

ABRAMOWITZ, M., STEGUN, I. A., Handbook of Mathematical Functions, Dover(1972).
ALAVA, M., D.TECH THESIS, Helsinki University of Technology, Espoo, Finland(1993).
ALFVEN, H., ARKHIV. MAT. ASTRON. FYSIK 29B(2)(1942).
ALLIS, BUCHSBAUM, BERS, Waves in Anisotropic Plasmas(1963).
ANTONSEN, T. M., MANHEIMER, W.M., PF 21(12)(1978), 2295.
APPLETON, E. V., J. INST. ELEC. ENGRS. 71(1932), 642.
ARTSIMOVITCH, L. A., NF 12(1972), 215.

BALESCU, R., PF B3(3)(1991), 564.
BARLOW, J., Statistics

BENDER, C. M.M ORSZAG, S. A., Advanced 0 Methods for Scientists and Engineers, McGraw-Hill(1978).
BERGER, J. M., NEWCOMB, W. A., DAWSON, J. M., FRIEMAN, E. A., KULSRUD, R. M., LENARD, A., PF 1(1958), 301.
BERNSTEIN, I. B., PR 109(1958), 10.
BERNSTEIN, I. B., TREHAN, S. K., NF 1(1960), 3.
BERNSTEIN, I. B., TREHAN, S. K., WEENINK, M. P. H., NF 4(1964), 61. BERNSTEIN, I. B., PF 18(3)(1975), 320.
BESKIN, V. S., GUREVICH, A. V., ISTOMIN, Y. N., SP 65(4)(1987), 715.
BHATNAGER, V. P., KOCH, R., MESSIAEN, A. M., WEYNANTS, R. R., NF 22 (1982), 280.
BORNATICI, M., ENGELMANN, F., PP 1(1)(1994), 189.
BORNATICI, CANO, R., DE BARBIERI, O., M., ENGELMANN, F., NF 23(9)(1983), 1153.
BRAMBILLA, M., PPCF 31(1989), 723.
BRAMBILLA, M., PPCF 33(9)(1991), 1029.
BRAVO-ORTEGA, A., GLASSER, A. H., PF B3(3)(1991), 529.
BUCHSBAUM, S. J., PF 3(1960), 418.
BUDDEN, K. G., Radio Waves in the Ionosphere, CUP(1961).

CAIRNS, R. A., Plasma Physics, Blackie(1985).
CAIRNS, R. A., Radio-Frequency Heating of Plasmas, Adam-Hilger(1991).
CAIRNS, R. A., LASHMORE-DAVIES, C. N., PF 25(9)(1982), 1605.
CAIRNS, R. A., HOLT, H., MCDONALD, D. C., TAYLOR, M., LASHMORE-DAVIES, C. N., PP 2(10)(1995), 3702.
CAIRNS, R. A., LASHMORE-DAVIES, C. N., DENDY, R. O., HARVEY, B. M., HASTIE, R. J., HOLT, H., PF B3(11)(1991), 2953.
CALDELA, R. A., SCHNEIDER, R. S., ZIEBELL, L. F., JPP 42(1)(1989), 165.
CALDELA, R. A., SCHNEIDER, R. S., ZIEBELL, L. F., JPP 43(3)(1990), 335.
CHEN, F. F., Introduction to Plasma Physics and Controlled Fusion, Plenum(1984).
CHEN, L., Waves and Instabilities in Plasmas, World Scientific(1987).
CHEN, L., TSAI, S. T., PF 26(1983), 141.
CHOE, W., CHANG, C. S., ONO, M., PP 2(6)(1995), 2044.
CHOW, C., FUCHS, V., BERS, A., PF B2(1990), 1089.
CLEMMOW, P. C., DOUGHERTY, J. P., Electrodynamics of Particles and Plasmas,Addison-Wesley(1969).
COLESTOCK, P., KASHUBA, R. J., NF 23(1983), 763.

DAVIDSON, R. C., GOLDSTON, J., NEILSON, G. H., THOMASSEN, K. I., PP 2(6)(1995), 2417.

ELIEZER, Y. and S., The Fourth State of Matter, Adam-Hilger(1984).
ELLIOT, J., Plasma Physics, Lectures on Physics, UMIST(1991).
EROKHIN, N. S., MOISEEV, S. S., RPP 7(1979), 181.

FEYNMAN, R. P., LEIGHTON, R. B., SANDS, M., Lectures on Physics: Vol. 2,Addison-Wesley(1964).
FRIED, B. D., CONTE, S. D., The Plasma Dispersion Function, Academic(1961).
FUCHS, V., BERS, A., PF 31(12)(1988), 3702.

GORMEZANO, C. AND THE JET TEAM, Proceedings of the 15th International Conference on Plasma Physics and Controlled Nuclear Fusion, IAEA, Vienna, 1(1993), 587.
GRADSHTEYN, I. S., RYZHIK, I. M., Table of Integrals, Series and Products, Academic(1980).

HOLT, H., PHD THESIS, University of St. Andrews, Scotland(1992).

IGNAT, D. W., ONO, M., PP 2(6)(1995), 1899.
ISTOMIN, Y. N., PPCF 36(1994), 1081.

JONAS, P., Energy in Nature, Lectures on Physics, UMIST(1991).

KADOMTSEV, B. B., Plasma Turbulence, Academic(1965).
KAY, A., CAIRNS, R. A., LASHMORE-DAVIES, C. N., PPCF 30(5)(1988), 471.
KRALL, N. A., ROSENBLUTH, M. N., PF 6(2)(1963), 254.
KRALL, N. A., TRIVELPIECE, A. W., Principles of Plasma Physics, McGraw-Hill(1973).
KROMMES, J. A., HU, G., PF B5(11)(1993), 3908.

LAMALLE, P. U., PL(A) 175(1993), 45.
LANDAU, L. D., JP 10(1946), 25.
LASHMORE-DAVIES, C. N., Private Communication(1995).
LASHMORE-DAVIES, C. N., DENDY, R. O., PF B1(8)(1989), 1565.
LASHMORE-DAVIES, C. N., DENDY, R. O., PF B4(3)(1992), 493.
LASHMORE-DAVIES, C. N., DENDY, R. O., KAM, K. F., PPCF 35(1993), 1529.
LASHMORE-DAVIES, C. N., FUCHS, V., DENDY, R. O., PF B5(1)(1993), 3.
LASHMORE-DAVIES, C. N., FUCHS, V., FRANCIS, G., RAM, A. K., BERS, A., GAU-

THIER, L., PF 31(6)(1988), 1614.
LASHMORE-DAVIES, C. N., FUCHS, V., RAM, A. K., PPN 95/9.1(1995).
LAWSON, J. D., PrPS 70B(1957), 6.
LITTLEJOHN, R. G., FLYNN, W. G., PRL 70(1993), 1799.

MAROLI, C., PETRILLO, V., LAMPIS, G., ENGELMANN, F., PPCF 28(1986), 615.
MAROLI, C., PETRILLO, V., LAMPIS, G., PPCF 30(12)(1988), 1723.
MARTIN, T. H., VACLAVIK, J., HPA 60(1987), 471.
MCDONALD, D. C., PHD THESIS, University of St. Andrews, Scotland(1994).
MCDONALD, D. C., CAIRNS, R. A., LASHMORE-DAVIES, C. N., PP 1(4)(1994), 842.
MCDONALD, S. W., PRS 158(6)(1988), 337.
MCGUIRE, K. M. AND TFTR TEAM, PP 2(6)(1995), 2176.
MICHABELI, G. Z., PPCF 33(1991), 1227.
MIKHAILOVSKII, A. B., RPP 3(1967), 159.

NAMBU, M., PPCF 31(1989), 143.
NAMBU, M., PP 2(6)(1995), 1846.

ONSAGER, L., PR 38(1931), 2265.

PERKINS, F. W., NF 17(1977), 1197.
PHILLIPS, C. K. AND THE TFTR TEAM, PP 2(6)(1995), 2427.
PILIYA, A. D., SAVELIEV, A. N., PPCF 36(1994), 2059.
PLEMELJ, J., MONA. MATH. PHYSIK 19(1908), 205.
POST, D. E., Proceedings of the 13th International Conference on Plasma Physics and Controlled Nuclear Fusion, IAEA, Vienna, 3(1991), 239.

RAE, A. I. M., Quantum Mechanics, Adam Hilger(1985).
ROMERO, H., SHARER, J., NF 27(1987), 363.
RUSBRIDGE, M. G., Fusion Physics, Lectures on Physics, UMIST(1992).
RUSBRIDGE, M. G., Human Uses of Energy, Lectures on Physics, UMIST(1992).
RUTHERFORD, P. H., FRIEMAN, E. A., PF 11(1968), 569.

SAUTER, O., VACLAVIK, J., SKIFF, F., PF B2(3)(1990), 475.
SAUTER, O., PHD THESIS, Ecole Polytechnique de Lausanne, Switzerland, Report LRP 457/92(1992).
SAUTER, O., VACLAVIK, J., NF 32(8)(1992), 1455.

SCHUMACHER, E. F., Small is Beautiful, Blond and Briggs(1973).
SHAFRANOV, V. D., RPP 3(1967), 1.
SHKAROFSKY, I. P., PF 9(1966), 561.
STIX, T. H., NF 15(1975), 737.
STIX, T. H., Waves in Plasmas, American Institute of Physics(1992).
SWANSON, D. G., PF 28(9)(1985), 2645.
SWANSON, D. G., Plasma Waves,Academic(1989).

TAYLOR, J. B., HASTIE, R. J., PPS 10(1968), 479.
TROTSKY, L., Dialectical Materialism and Science, Address to the Mendeleyev Congress(1925), YSP(1973).

VAN ESTER, D., JPP 54(1995), 31.
VLASOV, A. A., JP 9(1945), 25.

WANG, C. Y., BATCHELOR, D. B., JAEGER, E. F., PP 2(7)(1995), 2863.
WATSON, G. N., A Treatise on the Theory of Bessel Funtions, CUP (1922).
WEINHOLD, F., PT 29(3)(1976), 23.
WESSON, J., Tokamaks,Clarendon(1987).
WHITE, R. B., Theory of Tokamak Plasmas, North-Holland(1989).